Gold Catalysts for the Hydrochlorination of Acetylene

Thesis submitted in accordance with the requirements of Cardiff University for the degree of Doctor of Philosophy

Catherine Davies

2012

DECLARATION

This work has not been submitted in substance for any other degree or award at this or any other university or place of learning, nor is being submitted concurrently in candidature for any degree or other award.

Signed …… (candidate) Date ……

STATEMENT 1

This thesis is being submitted in partial fulfillment of the requirements for the degree of ……(insert MCh, MD, MPhil, PhD etc, as appropriate)

Signed …… (candidate) Date ……

STATEMENT 2

This thesis is the result of my own independent work/investigation, except where otherwise stated.
Other sources are acknowledged by explicit references. The views expressed are my own.

Signed …… (candidate) Date ……

STATEMENT 3

I hereby give consent for my thesis, if accepted, to be available for photocopying and for inter-library loan, and for the title and summary to be made available to outside organisations.

Signed …… (candidate) Date ……

STATEMENT 4: PREVIOUSLY APPROVED BAR ON ACCESS

I hereby give consent for my thesis, if accepted, to be available for photocopying and for inter-library loans **after expiry of a bar on access previously approved by the Academic Standards & Quality Committee.**

Signed …… (candidate) Date ……

Acknowledgements

First of all I would like to thank my supervisors, in particular Graham Hutchings for allowing me to undertake this project. Thanks also to Albert Carley, Tony Lopez and Marco Conte for all their help and support. I would also like to thank my industrial supervisor Peter Johnston, also Nick Carthey at Johnson Matthey for advice regarding running the reactor.

Special thanks must go to the technicians, without whom I literally wouldn't have been able to do this project: Alun Davies and Steve Morris. Their kindness and both willingness and ability to help is greatly appreciated.

I would also like to thank the many friends I have made during my time in the research group, for making the experience enjoyable. In particular the crossword team, who have provided daily lunchtime entertainment. A special mention must go to Pete Miedziak, for his support I am eternally grateful.

Finally I would like to thank everyone else who has supported and encouraged me throughout my time in Cardiff, especially my family.

Abstract

The direct, gas-phase hydrochlorination of acetylene is a method by which vinyl chloride monomer (VCM) is produced industrially. VCM is polymerised to produce poly-vinyl chloride (PVC), one of the world's most widely used plastics. Although other methods, using oil-derived ethene, are now more widely used, hydrochlorination of acetylene, which is coal-derived, is still the preferred method in areas where coal is a cheap and widely available resource. However, there are numerous problems associated with the mercury based catalysts which are traditionally used for this process, largely for environmental reasons, and therefore a new catalyst is desirable. Gold based catalysts have been shown to be active and particularly selective for this reaction, but deactivation with use is still an issue restricting commercial application.

Previously it has been demonstrated that Au^{3+} is likely to be the active site for acetylene hydrochlorination by Au/C catalysts, and that deactivation of the catalysts during reaction above 120°C is due to reduction of this species to Au^{0}. Therefore Au/C catalysts have been investigated in detail, in order to investigate the true importance of the Au^{3+} species. Catalysts were prepared with numerous variations in the method used, including the acid used for impregnation and the drying temperature, and subjected to oxidation and reduction treatments.

Characterisation was carried out by temperature programmed reduction (TPR) in addition to XPS which has been typically used to identify the surface species of such catalysts. TPR was found to be a technique which is able to provide an extensive amount of information about both the gold and the carbon support and enabled it to be shown that whilst Au^{3+} is important for catalytic activity, its presence alone is not sufficient and the reducibility of this species is a key factor.

Contents

1 Introduction

1.1 Project Background: VCM production

Vinyl Chloride Monomer (VCM) is the monomer from which poly vinyl chloride (PVC) is made (see figure 1.1). PVC is one of the most commonly used plastics and has a wide range of applications, for example in packaging, construction materials, medical devices and clothing. This is largely due to the ability to modify the properties of the substance using additives, for example to alter its rigidity. As a result there is a high demand for the plastic, with over 35 million tonnes of PVC produced every year[1], leading to VCM being a very valuable chemical. The vast majority of VCM (around 90%) is used in the manufacture of PVC, with its alternative use being in the manufacture of chlorinated solvents.

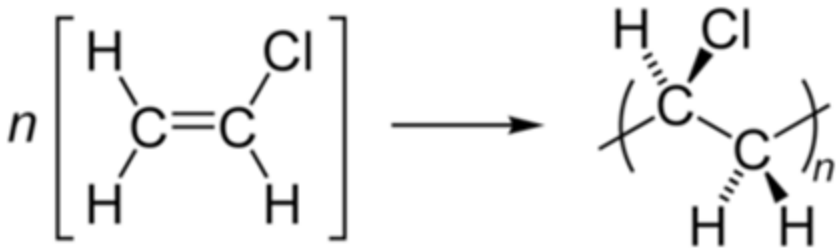

Figure 1.1: Vinyl Chloride Monomer (VCM) is polymerised to polyvinylchloride (PVC).

There are a number of routes by which VCM may be produced industrially, depending on the starting material used. The most commonly used process is the balance process, a combination of chlorination and oxychlorination reactions using ethene, which is oil-derived, as the starting material. Another, simpler method is the direct hydrochlorination of acetylene, which is a coal-derived starting material, and this reaction is traditionally catalysed by carbon-supported mercury chloride. These methods are described in further detail below.

1.1.1 The Balance Process

The balance process is a multi-step process involving the chlorination of ethene to dichloroethene, oxychlorination of ethene and thermal cracking of the product of these, 1,2-dichloroethane, to produce VCM. This is shown in the equations below:

$C_2H_4 + Cl_2 \rightarrow CH_2ClCH_2Cl$ (chlorination)

$C_2H_4 + 2HCl + O_2 \rightarrow 2\ CH_2ClCH_2Cl + 2H_2O$ (oxychlorination)

$CH_2ClCH_2Cl \rightarrow CH_2CHCl + HCl$ (cracking)

This is currently the most commonly used method of producing VCM in the western world, due to its use of ethene, which is an oil-derived feedstock and is a more readily available resource than coal.

1.1.2 Direct Hydrochlorination of Acetylene

Historically, the direct hydrochlorination of acetylene was the primary route used industrially to produce VCM. It is a one-step process (figure 1.2) and typically this reaction is carried out in the gas phase, over a catalyst comprising mercury chloride supported on activated carbon.

$$C_2H_2 + HCl \longrightarrow CH_2{=}CHCl$$

Figure 1.2: Direct hydrochlorination of acetylene to produce VCM.

Although routes to VCM using oil derived starting materials, such as the balance process described above, are now more commonly used in Europe, in countries such as China where coal is still a relatively cheap and available resource, new technologies using calcium carbide mean that acetylene is more readily available than oil derived ethene and therefore acetylene hydrochlorination remains the preferred method.

However, there are a number of issues with the use of mercury based catalysts. The mercury has a tendency to leach from the catalyst, due to its large vapour pressure at temperatures greater than 160°C which leads to thermal desorption of the mercuric chloride from the surface[2]. This not only causes degradation of the catalyst but can lead to pollution of the environment. Therefore a new catalyst for this reaction is desirable.

1.2 Gold Catalysis

1.2.1 Background

While supported metal catalysts have been used in industrial processes for a number of decades, the potential use of gold in such catalysts is a more recent development. Around a similar time, in the 1980s, two key discoveries were made which led to the now vast amounts of research being carried out in this field. Hutchings *et al.* predicted and subsequently confirmed that based on electrode potentials, gold should be the most active metal for the hydrochlorination of acetylene, catalysed by carbon-supported metal chloride catalysts[3, 4]. Meanwhile Haruta *et al.* demonstrated that gold nanoparticles supported on transition metal oxides, e.g. Fe_2O_3, are active for the catalytic oxidation of CO at low temperatures[5]. Previously, gold had largely been considered unreactive, although the use of gold catalysts had been reported for oxidations of ethylene and propylene[6] and reductions of olefins[7]. However, these new findings illustrated the potential use of gold as a catalyst when present in nanoparticle

form. Since then, research into gold catalysis has increased virtually exponentially, leading to the publication of the first book on this subject in 2006[8].

1.2.2 Reactions

1.2.2.1 Heterogeneous Catalysis

In recent years, it has been demonstrated that gold as supported nanoparticles can be active as a catalyst for a vast range of reactions, including hydrogenations[9-11], reductions of NO_x - for example with hydrogen[12], CO[13] and hydrocarbons such as propene[14], methanol synthesis[15] and a wide range of oxidations. These include the direct synthesis of hydrogen peroxide from oxygen and hydrogen[16], epoxidation of propene[17], selective oxidation of alcohols such as glycerol and other polyols[18-20] and CO oxidation as demonstrated by Haruta but also including the water-gas shift reaction[21] and preferential oxidation of CO in the presence of hydrogen (PROX)[22]. As a result of this, gold catalysts have the potential for use in a range of commercial applications, including pollution and emission control, sensors and chemicals processing[23]. The extensive research that has been carried out into CO oxidation over gold catalysts has led to the commercial use of gold catalysts for air purification. Gold based catalysts are also now used in the commercial production of vinyl acetate monomer (VAM)[8].

1.2.2.2 Homogeneous Catalysis

In addition to its use in heterogeneous catalysis, gold has also recently been discovered to be a successful homogeneous catalyst for a number of synthesis reactions. The first instance of a gold catalyst having a significantly higher activity than other catalysts was reported by Teles *et al.* in 1998, where cationic phosphanegold(I) complexes were used for the addition of alcohols to alkynes[24]. Thomas *et al.* had previously reported the oxidation of alkynes using tetrachloroauric acid in aqueous

methanol[25]; however it was not recognised that the gold was acting as a catalyst rather than a stoichiometric oxidising agent[26]. Further uses of homogeneous gold catalysts for reactions of alkynes have since been published, including hydrogenations[27] and hydrations[28]. Catalytic addition of water to alkynes is an effective method of synthesising carbonyl compounds; similarly to the heterogeneous hydrochlorination of acetylene that is the subject of this project, mercury based catalysts were used for this reaction but due to its toxicity a new catalyst was desirable. $HAuCl_4$ and $NaAuCl_4$ were shown to be active catalysts for this reaction, and since then other Au(III) catalysts have been further developed[29]. Homogeneous gold catalysts have also been shown to be active for hydrohalogenations of alkynes[29]; Akana *et al.* used electrophilic Au(I) complexes in the synthesis of fluoroalkenes[30], providing a new, versatile and selective method of producing such compounds. The gold complexes used, containing N-heterocyclic carbene ligands, formed a complex with the internal alkyne bond of 1-phenyl-1-propyne and with a source of HF led to trans-hydrofluorination of the alkyne at room temperature (figure 1.3).

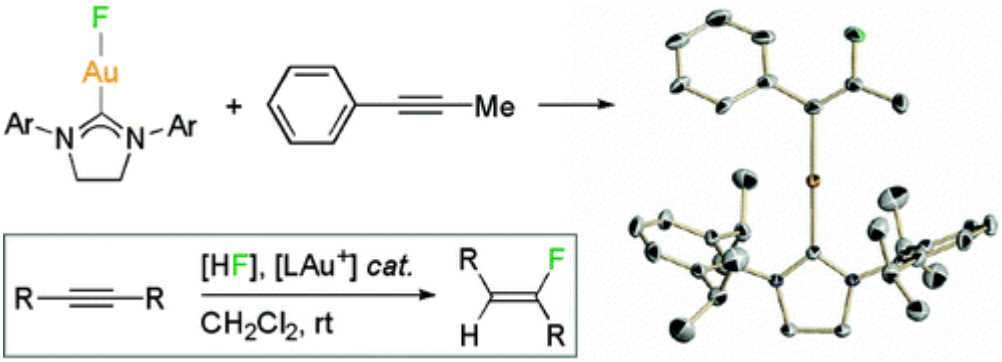

Figure 1.3: Trans-hydrofluorination of alkynes using Au(I) complexes[30].

Gorske *et al.* carried out similar work[31], developing the reaction further by using a range of directing groups on the alkyne substrate in order to enhance the regioselectivity of the HF addition. They found that troc-carbamates were the most successful directing group for stability under reaction conditions and generating the product with the desired regioselectivity – this was suggested to be due to the ability

of the gold catalyst to form a complex with both the carbonyl of the directing group and the alkyne, which is illustrated in the mechanistic hypothesis shown in figure 1.4.

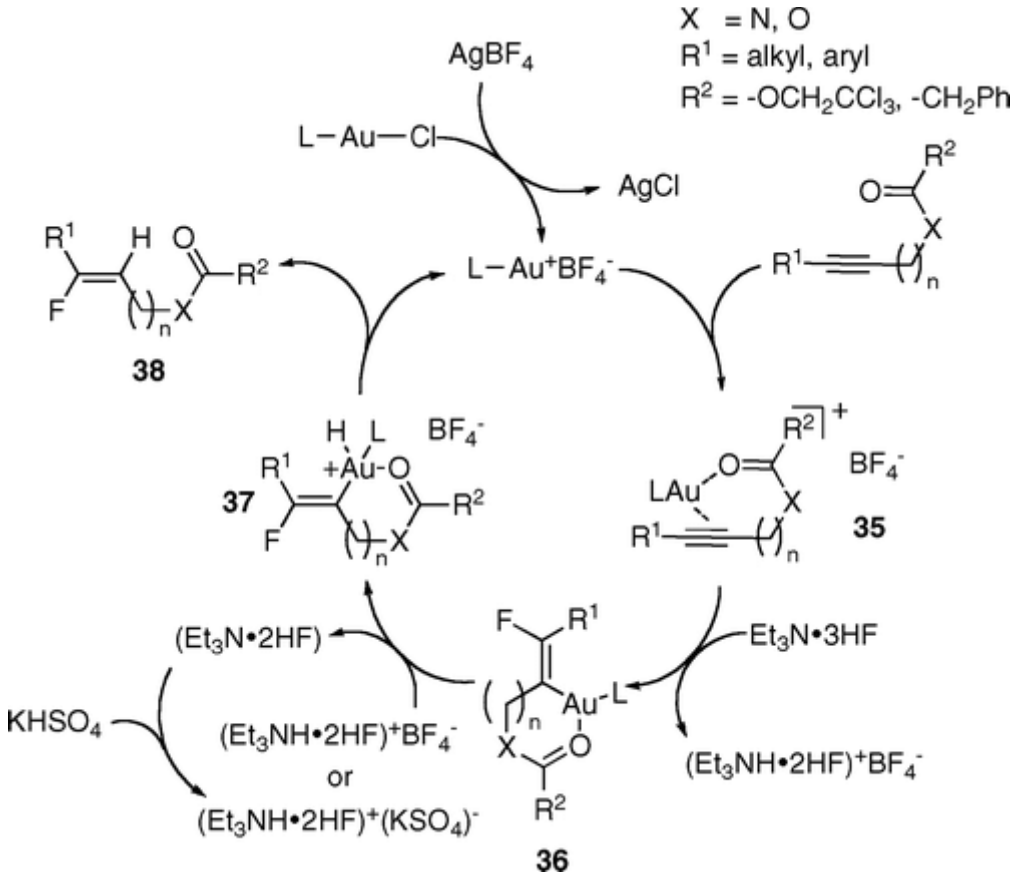

Figure 1.4: Mechanistic hypothesis for hydrofluorination of alkynes by Au(I) catalyst[31].

It has also been demonstrated that gold is able to catalyse carbon-oxygen, carbon-nitrogen and carbon-carbon bond formation reactions[32], all of which are important in the synthesis of organic molecules. In the case of C-O and C-N bond forming, such reactions are often intramolecular and involve molecules containing an alkyne bond forming aromatic heterocycles. For example, cyclisations of propargyl and allyl ketones can be catalysed using $AuCl_3$ in acetonitrile to produce furans[33], which may also result from intramolecular reaction between an alkyne and an epoxide, using the same catalyst[34]. $NaAuCl_4$ in acetonitrile or THF is able to catalyse cyclisation reactions of alkynylamines[35], whilst in ethanol it catalyses intermolecular cyclisation to form indoles from anilines[36]. A number of C-C bond formations have been found to be

successfully catalysed by gold, the first example of this being the asymmetric aldol condensation, which was developed by Ito *et al.* in 1986. This process used a $[Au(CyNC)_2]BF_4$ catalyst (Au(I)) with a chiral ligand to produce the *E*-oxazole product in enantiomeric excess of up to 97%[37]. Simpler gold containing species, for example $NaAuCl_4$ and $AuCl_3$, are also able to act as catalysts for C-C bond forming reactions; it was shown that using $AuCl_3$, Au(III) is the most active catalyst of a number of transition metals for the transformation of a furyl alkynyl to a phenol[33], and $NaAuCl_4$ catalyses the reaction of allyl silanes with propargylic alcohols, with different major products depending on the solvent used[38]. The use of gold based catalysts enables a number of significant reactions to be carried out under mild conditions, typically at lower (often ambient) temperatures and neutral pH. Such reactions include the thermal cyclization of ketones onto akynes, hydroarylation between alkynes and alkenes and reaction of α,β-unsaturated ketones with arenes[8].

1.2.3 Preparation Methods

Supported gold catalysts may be prepared *via* a number of methods, some of the most commonly used being impregnation, deposition-precipitation, co-precipitation and sol-immobilisation. Due to the desire to produce nanoparticles tailored for a particular use, variations of and modifications to these methods are frequently reported, since variables within each method have been shown to significantly affect the activity of the resulting catalyst for a given reaction. These methods are described in more detail below, to illustrate how properties of a catalyst such as particle size, morphology and dispersion may be determined by the way in which it is produced.

Other, less commonly used and more recently developed methods which have been reported for producing supported gold nanoparticles include magnetron sputtering[39], direct anionic exchange[40], cationic adsorption[41] and ultrasonication[42]. In addition chloride-free synthesis of gold catalysts is of great interest; this may be done using alternative gold precursors such as gold acetate $(Au(OAc)_3)$[43], potassium aurocyanide $(KAu^{I}(CN)_2)$[44] and gold phosphine complexes $([Au(PPh_3)]^{+})$[45]. However, the

tetrachloroaurate salt ($HAuCl_4$) tends to be commonly used due to its relatively low cost compared to other gold compounds.

1.2.3.1 Impregnation

Impregnation is by far the simplest method of preparing supported metal catalysts, and can be used with any support. The metal precursor (usually a water soluble salt, in the case of gold catalysts $HAuCl_4$ is commonly used) is made into a solution, which is then mixed with the support to be used. Metal particles form on the surface of the support and the sample is filtered and dried in order to remove the excess solvent. Catalysts prepared by impregnation methods tend to have the largest metal particle sizes (>10nm), which is likely to be in part due to their high chloride content which may cause sintering of the gold; although these catalysts have been shown to be active for reactions including benzyl alcohol oxidation[46] and hydrogen peroxide synthesis[47], they are some of the poorest for CO oxidation[48].

There are numerous variations of the impregnation process, for example in incipient wetness impregnation the minimum amount of solvent to fill the pores of the support is used. This method is favoured industrially due to the minimised waste. The solvent used for impregnation may also be varied – water is by far the most common, but others, e.g. *aqua regia*, have been used[4]. Organic solvents such as acetone are used in the case of some alternative gold precursors, for example gold phosphine complexes[49]. An incipient wetness, double impregnation was described by Bowker *et al.* which used a secondary impregnation of a base to precipitate out gold hydroxide, resulting in removal of chloride with washing[50]. This led to a Au/TiO_2 catalyst with higher activity than a typical incipient wetness catalyst for CO oxidation, with the increase in activity being related to the removal of chloride species as detected by XPS analysis.

Some of the earliest examples of gold catalysts were prepared by impregnation; for example Cant and Hall[6] and Bond *et al.*[7] each describe impregnation of a silica support

using a solution of $HAuCl_4 \cdot 3H_2O$, while the early work concerning Au/C catalysts for acetylene hydrochlorination uses an impregnation method with *aqua regia* as a solvent[4, 51, 52]. This method has remained the most popular for catalysts for this reaction, due to the presence of significant amounts of Au^{3+} on the surface of the resulting catalyst, which is considered to be the active site and is thought to be stabilised by the excess chloride provided by the solvent.

1.2.3.2 Deposition precipitation

Deposition precipitation (DP) is a method of producing smaller supported metal particles than afforded by impregnation and involves the modification of the pH of a stirred mixture of the support in a solution of the metal precursor ($HAuCl_4$ is usually used for gold) in order to form the desired species (the metal hydroxide), which precipitates onto the support. This technique has been successfully used to produce gold catalysts on a range of supports; most often these are metal oxides such as magnesia, titania, alumina, zirconia and ceria[8]. Catalysts prepared *via* this method are often found to be more active than those prepared *via* impregnation for various reactions; for example this has been attributed to smaller metal particle size in the case of Au/titania catalysts for CO oxidation[53] and higher dispersion of gold in ceria supported Au-Cu catalysts for water gas shift[54]. In addition, Bamwenda *et al.* relate the difference in activity of Au/TiO_2 catalysts for CO oxidation to the morphology of the supported gold particles, noting that preparation *via* impregnation resulted in spherical gold particles whereas deposition-precipitation led to hemispherical particles, increasing the interaction of the gold with the support and leading to an enhanced activity[55].

There are a number of variables within the DP preparation procedure which may affect a catalyst's activity, for example the pH of the mixture, the base used and the temperature the preparation is carried out at. Perhaps the most significant of these for gold catalysts is the effect of the pH and this has been investigated in detail: Wolf & Schuth[56] investigated the effect of pH on the activity of catalysts prepared using

deposition-precipitation, on a range of supports, and found that the optimum pH for catalysts using a titania support was in the region 7.8 – 8.8, since catalysts prepared using these pH values were active at lower temperatures. Characterisation of the catalysts by XRD and TEM showed that increasing pH leads to a decrease in particle size, which was responsible for the higher activity. Moreau *et al.* also investigated the effect of pH during preparation of Au/TiO_2 catalysts by the deposition-precipitation method[57]. The concentrations of various gold species in solution were measured as a function of pH; the results are shown in figure 1.5. Catalysts were prepared with a range of initial pH values of a $HAuCl_4$ solution, varied by addition of NaOH. It was found that the optimum pH for high catalytic activity for CO oxidation was pH 9 – this corresponds to a high concentration of $Au(OH)_4^-$ in the solution, whereas at lower pH values the gold complexes contained more chlorine. It was also found that the gold particle size was smaller at higher pH. It was shown that it is during the latter stages of the preparation that the pH of the solution is critical to the activity of the catalyst.

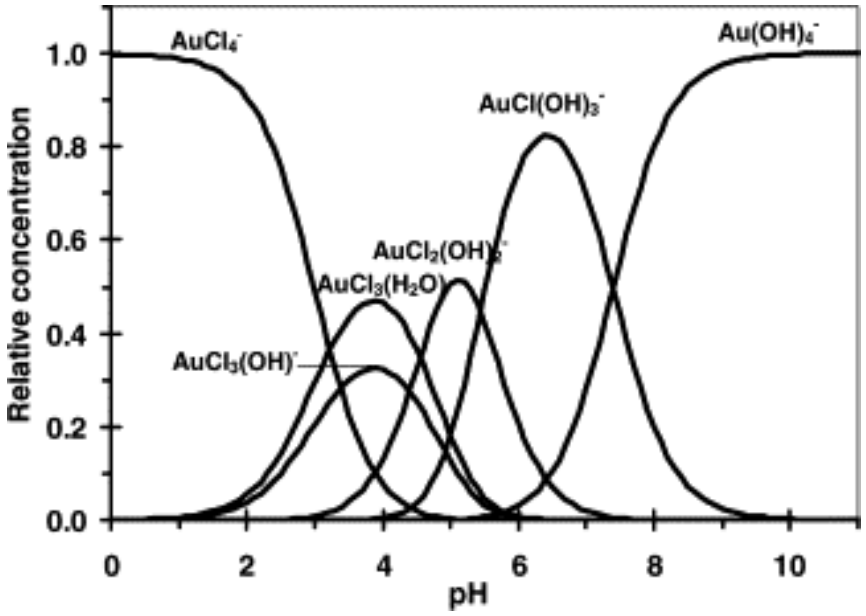

Figure 1.5: Concentration of gold species in aqueous $HAuCl_4$ solution as a function of pH[57].

Yang *et al.* investigated the effect of pH in the preparation of Au/Al_2O_3 catalysts by deposition precipitation and also found that catalysts prepared at a higher pH were more active for CO oxidation[58]. They describe the importance of the pH in terms of

minimising the amount of chloride on the catalyst, which acts as a poison for this reaction and causes the gold to sinter into large particles upon calcinations. Catalysts were also prepared with small particles and a high chloride content, these had a low activity and so it was suggested that the chloride also blocks active sites, by preventing the gold from reacting with oxygen.

1.2.3.3 Co-precipitation

In co-precipitation, the metal particles and the support are formed at the same time. This is a method commonly used for metal oxide supported catalysts, such as Au/Fe_2O_3, and was the method used by Haruta in the early work on gold catalysts for low temperature CO oxidation[5]. For gold catalysts, an aqueous solution of $HAuCl_4$ is typically mixed with a solution of the corresponding nitrate to the desired support (*e.g.* iron nitrate for an iron oxide support) and then the pH is adjusted by addition of a precipitating agent such as sodium carbonate, so that precipitation of the desired product occurs. The mixture is then filtered, washed, dried and may be calcined.

A benefit of using this method is that good dispersion of small metal particles (<10nm) within the support can be achieved[59]. Important variables in this method that can affect the activity of catalysts are the precipitating agent used[60], the speed at which precipitation is carried out and the aging time[61], all of which can affect the gold loading, particle size and residual chloride content .

However, whilst co-precipitation enables active catalysts to be prepared, a disadvantage is that it uses nitrates, which can have a negative impact on the environment when they are released as a waste product.

1.2.3.4 Sol Immobilisation

The sol immobilisation method was first described by Prati *et al.* in 1999, as a new way of forming sufficiently small particles of gold on a carbon support[62]. Whilst sol immobilisation is one of the most complex and sensitive methods used for preparation of catalysts, it has the unique advantage that the size of the metal particles that are being prepared may be strictly controlled. The method involves first making a sol of metallic gold particles, which is done by adding a stabilising ligand, such as poly vinyl alcohol (PVA), and then a reducing agent, usually $NaBH_4$, to a dilute solution of $HAuCl_4$ in water. By adjusting variables such as the ligand that is used and the ratio of ligand to metal, different sizes of metal particles are produced. The support is then added to the sol, to immobilise the metal particles on it. It is important that the metal particles bind to the support, so the pH of the mixture may be adjusted in order to encourage this, by addition of small amounts of acid or base. The pH used is dependent on the iso-electric point of the support being used, in order to encourage interactions between the support and the metal particles. For example, when using a carbon support a small amount of concentrated H_2SO_4 is added to reduce the pH to approximately 2.

In a number of cases it has been demonstrated that catalysts prepared using sol immobilisation techniques are more active than those prepared by other methods, such as impregnation and deposition precipitation. For example, Miedziak *et al.* prepared Au-Pd/TiO_2 catalysts by impregnation, deposition-precipitation and sol immobilisation methods and tested them for benzyl alcohol oxidation[63]. The sol immobilisation catalysts were found to be the most active, and the major factor was considered to be the particle size distribution, with both a smaller particle size and narrower range occurring for the sol immobilisation catalyst compared to those prepared *via* the other methods. Similarly the enhanced activity of Au-Pd catalysts for the oxidation of 1,2-propanediol and hydrogen peroxide synthesis prepared by sol-immobilisation compared to those prepared by impregnation is considered to be due to a smaller particle size[64, 65].

Recently, investigations have been focussed on removal of the stabilising ligands from catalysts prepared *via* sol immobilisation, in order to enhance the activity by greater exposure of the gold surface. This has been shown to be possible, by subjecting to thermal treatment in order to decompose the ligands[66], or by refluxing in water, since many of the ligands used, such as PVA, are water soluble[67].

1.2.3.5 Thermal Treatments

After drying, catalysts are often subjected to thermal treatments in order to enhance their activity. The duration, temperature and atmosphere of these treatments are all important in determining the effectiveness of the treatment. In some cases, thermal treatment such as calcinations are carried out on a catalyst as it results in a greater interaction between the catalyst and the support, which leads to a greater activity being observed. Tsubota *et al.* investigated the effect of various thermal treatments on Au/TiO_2 catalysts prepared by DP for low temperature CO oxidation[68]. They report that treatment in a reducing atmosphere such as H_2 and CO results in smaller gold particles than calcinations in air, also that increasing the calcination temperature leads to both larger particle sizes and an increased interaction with the support. In addition, thermal treatments may enhance a catalyst by removal of species from the surface that lessen the activity (such as the ligands on catalysts prepared by sol immobilisation, as mentioned previously), and may modify the structure of the catalyst support. For example, Kozlov *et al.* prepared iron oxide supported gold catalysts using a gold phosphine precursor for impregnation of an as-precipitated iron hydroxide support[49]. The temperature of the calcination affected the iron oxide phase that was formed, this is illustrated in figure 1.6, and it was suggested that such recrystallisations may lead to metal-support interactions at the interface.

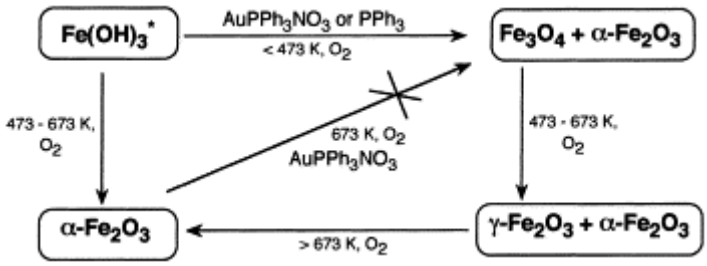

Figure 1.6: Transformations of $Fe(OH)_3$ with calcination, in the presence and absence of gold phosphine complexes or phosphine[49].

However, in other cases calcination is found to be detrimental to catalyst activity, for example as reported for Au/Fe_2O_3 catalysts for CO oxidation[69] and Au/MgO catalysts for selective oxidations of alcohols and aldehydes[70]. In the latter of these, Choudhary *et al.* investigated the effect of calcination temperature and found that maximum activity occurred after calcination at a temperature of 400°C, but with increase in temperature above this point there was a decrease in activity. This was considered to be due to the sintering of gold particles (lower activity after calcinations below this temperature were thought to arise from incomplete decomposition of the gold precursor or residual moisture). For gold catalysts prepared using the $HAuCl_4$ precursor the effect of higher calcination temperatures leading to less active, larger metal particle sizes is generally considered to be due to the effect of residual chloride, which aids mobilisation of the gold particles across the surface of the support and causes them to sinter.

1.2.4 The effect of particle size and morphology

For gold catalysts, as with many other catalysts, it is often found that a decrease in the particle size leads to an increase in the observed activity, as mentioned in the previous discussion of catalyst preparation methods. The simple explanation for this is that the metal surface area has increased, making reactions more likely to occur. However, to be more specific, with smaller particles there is also an increase in the number of sites where the support meets the particle, which has been seen to be important in some

cases, and an increase in the number of atoms with smaller co-ordination numbers which may be more reactive. Steps and edges are often found to be adsorption centres for gases on metal surfaces, and the numbers of such sites are increased on smaller particles. As described above, the size of supported gold particles is dependent upon the method by which the catalyst is prepared, and any subsequent thermal treatments. Guczi *et al.*[71] discussed the effect of particle size of gold catalysts on their activity for various substrates and concluded that generally, catalysts with the smallest gold particle sizes are the most active, due to the preferred adsorption of small molecules such as CO, NO and O_2 on small nanoparticles or rough Au (111) surfaces. However, it should be noted that larger particles are not completely inactive since activation of larger molecules occurs on Au (111) single crystals and gold films; for example cross coupling reactions of phenylacetylene and iodobenzene have been observed to occur.

For similar reasons to the particle size, *i.e.* the number of step and edge sites and the interaction of the particle with the support, the particle morphology can be important in determining a catalyst's activity. As mentioned previously, hemispherical particles of gold supported on titania have been shown to be more active than spherical ones for CO oxidation, which was considered to be due to the greater number of sites where interaction between the metal and the support was able to occur[55].

1.2.5 Support effects

There are a large variety of supports that are used for gold catalysts, although these can be broken down into a few broad categories: metal oxides, carbons, silicas and zeolites. These different supports have different properties that make them suitable for different reactions; for example, gas phase oxidation reactions, the most common of these being CO oxidation, are commonly found to be carried out over catalysts using a metal oxide support, in particular where the metal used is a reducible transition metal. Examples of these include titania (TiO_2), alumina (Al_2O_3) and iron oxide (Fe_2O_3), which have all been shown to be highly active supports for gold

catalysts for CO oxidation. Differences in the metal oxide support used can affect the activity of otherwise similar catalysts for a given reaction. Choudhary *et al.* investigated the effect of the catalyst support on gold catalysts for benzyl alcohol oxidation[20] and found that ZrO_2 was the most active of a wide range of metal oxide supports, in terms of turnover frequency (TOF), having a value significantly larger than any other. In addition to activity, the catalyst support can also affect the selectivity of a reaction. Brett *et al.* investigated the oxidative esterification of 1,2-propanediol over Au catalysts on a range of supports[72] and found that while a ceria-supported catalyst was not the most active, it gave a far higher selectivity to the desired product, methyl lactate, than the other supports which were tested: iron oxide (Fe_2O_3), titania, silica and carbon. Carbon supports generally have a very low activity for CO oxidation, yet have been found to be the preferred support for other types of reaction, for example acetylene hydrochlorination, and carbon supported gold catalysts have been demonstrated to be highly active and selective for a number of liquid phase oxidations. Silica supports have been used for a number of reactions, including CO oxidation (although the activity of these catalysts tends to be lower than for many other supports[8]), the dehydrogenation of propane using bimetallic Au-Ni catalysts[73] and oxidation of VOCs over Au-Co catalysts[74]. Some of the earliest examples of gold catalysts used a silica support and were used for hydrogenation[7] and alkene oxidations[6]. Zeolites also have a variety of uses, in addition to activity of supported gold catalysts for a number of reactions including CO oxidation[75], selective reduction of NO with propene[76] and synthesis of glycerol carbonate[77] it has been shown for aldehyde oxidations over Au/zeolite catalyst that their uniform structure may be used for selective reaction based on the size of the substrates[78].

The interaction of the gold with the support can be important, as different supports can lead to gold particles with different shapes. For example, Tiruvalam *et al.* used aberration corrected STEM to characterise bimetallic Au-Pd catalysts supported on carbon and titania prepared by sol immobilisation, for oxidations of benzyl alcohol and hydrogen peroxide[79]. They observed that the metal particles on carbon were spherical whereas on titania there is a greater wetting and hemispherical particles are formed

with a greater contact area between the metal and the support. For CO oxidation, the interaction with the support may go as far as the support being involved in the reaction in a Mars van Krevelen style mechanism; it has been suggested that once the substrate is adsorbed on the catalyst surface, the source of the oxygen for its oxidation is the support, then this oxygen vacancy is replaced by the molecular oxygen added as a reactant. This explains the high activity of catalysts on metal oxide supports, particularly those of reducible transition metals, in contrast with the low activity of carbon supports – this could be considered to be due to the lack of available oxygen from the surface of the support.

1.2.6 Active Sites

For catalysed reactions in general there is great interest in determining the active site, since this allows the development of improved catalysts. CO oxidation is one of the most widely studied reactions catalysed by gold and there has been some debate as to whether the active site is metallic or cationic gold species. Hutchings *et al.* tested a range of Au/α-Fe_2O_3 catalysts for CO oxidation at 298K and concluded that although metallic and cationic gold were present in the samples it was the presence of a significant fraction of cationic gold that was necessary for high catalytic activity[80]. Similar results have been obtained recently for Au/CeO_2 and Au/SiO_2 catalysts for low temperature CO oxidation: metallic gold exhibited a worse catalytic performance on both supports and achievement of the highest CO conversion at the lowest temperature was attributed to the presence of non-metallic gold. The higher activity of the ceria supported catalyst is thought to be due to stabilization of the cationic gold by the support[81]. The presence of both metallic and cationic species was detected on supported gold clusters on MgO which were active for CO oxidation[82]. However, in preparing a catalyst for preferential oxidation of CO in the presence of hydrogen, Landon *et al.* concluded that in order to obtain high selectivity it was necessary to remove the cationic gold so as to prevent the reverse water-gas shift reaction producing CO[83]. CO conversions of >99.5% were still obtained by a catalyst with relatively large (>5nm), purely metallic gold nanoparticles. In contrast to this, Wang *et*

al. investigated the active site for the water gas shift reaction over Au/TiO_2 catalysts using FTIR and determined that metallic corner Au atoms were the dominant active site[84].

Cationic gold species, Au(I) and Au(III), have also been found to be important for a number of other reactions. Most notable of these is acetylene hydrochlorination, for which it has been reported that Au^{3+} is the active site for the reaction and Au^0 is unreactive – as the subject of this project this will be discussed in more detail later in this chapter. The presence of cationic gold on the surface of Au/CeO_2 catalysts for oxidative esterification of 1,2-propanediol was determined to be responsible for the lower activity, but higher selectivity to the desired product[72]. Presence of cationic gold was considered to be important in determining the activity of zeolite-supported gold catalysts for intramolecular cycloisomerization of gamma-acetylenic carboxylic acids[85], and Carrettin *et al.* demonstrated that cationic gold on the surface of Au/CeO_2 was active for heterogeneously catalysed phenol synthesis[86].

1.2.7 Alkene/alkyne selectivity

In both homogeneous and heterogeneous catalysis a unique selectivity of gold catalysts to reactions of alkynes is observed. Garcia-Mota *et al.* investigated this phenomenon and concluded that in homogeneous catalysis the effect is due to kinetics, whereas for heterogeneous catalysis the origin of the selectivity is thermodynamic[87]. DFT modelling was used to compare the adsorption of alkenes and alkynes on different gold species and the results indicated that for Au_{10} and Au_{19} nanoparticles the selectivity is due to the selective adsorption and activation of C-C triple bonds – this does not occur for double bonds. Mascavage *et al.* investigated intra-molecular selectivity by investigating the addition of HCl to vinyl acetylene – the simplest molecule to contain both double and triple carbon-carbon bonds[88]. Mixtures of HCl and vinylacetylene in IR cells were monitored and the major products were both butadienes. They describe the reaction as being catalysed by water adsorbed on

the walls of the cell and cite computational studies[89, 90] which found that a π-complex of HCl is more stable with the triple bond than the double bond.

The selectivity of gold to reactions with alkynes is also demonstrated in its use for partial hydrogenation reactions, to give the alkene product. Segura *et al.* describe DFT studies which show the better adsorption of C-C triple bonds to Au nanoparticle edges than C-C double bonds and confirm this by testing of Au/CeO_2 catalysts for hydrogen of propyne/propylene mixtures, where selectivities of up to 95% were obtained[91]. This is supported by Lopez *et al.*[92], who reported that for selective hydrogenation of acetylene the use of gold catalysts gives the same results as addition of CO to palladium catalysts in order to enhance the selectivity to the alkene product – the effect of the CO is thought to be the weakening of the adsorption of alkene bonds to the catalyst surface.

1.3 Acetylene Hydrochlorination

The industrial catalyst used for this process is traditionally mercury chloride, supported on activated carbon. However, the deactivation of such catalysts, which was being investigated in some detail in the mid-1980s[2, 93, 94], is a significant problem and in addition to the decrease in activity, leaching of the mercury from the catalyst can be problematic due to its toxic nature. The resultant environmental issues with using mercury and the continued use of this process in areas where coal is a cheap and available resource, such as China, mean that a new catalyst is desirable.

A study by Shinoda[95] investigated the activity of a wide range of carbon supported metal chloride catalysts for acetylene hydrochlorination and correlated the activity with the electron affinity of the metal cation, divided by the metal valence. The correlation consisted of two straight lines and is shown in figure 1.7.

Subsequently, considering that the reaction is most likely a two-electron process whereas electron affinity concerns a one-electron process, a study by Hutchings *et al.*

instead correlated the activity of supported metal chloride catalysts with their standard electrode potential[3] and obtained a curve, shown in figure 1.8. Based on this curve it was suggested that since its standard electrode potential has a greater value than those metals investigated, gold should be the most active metal for this reaction; this was later confirmed[4, 52] and is illustrated in figure 1.9.

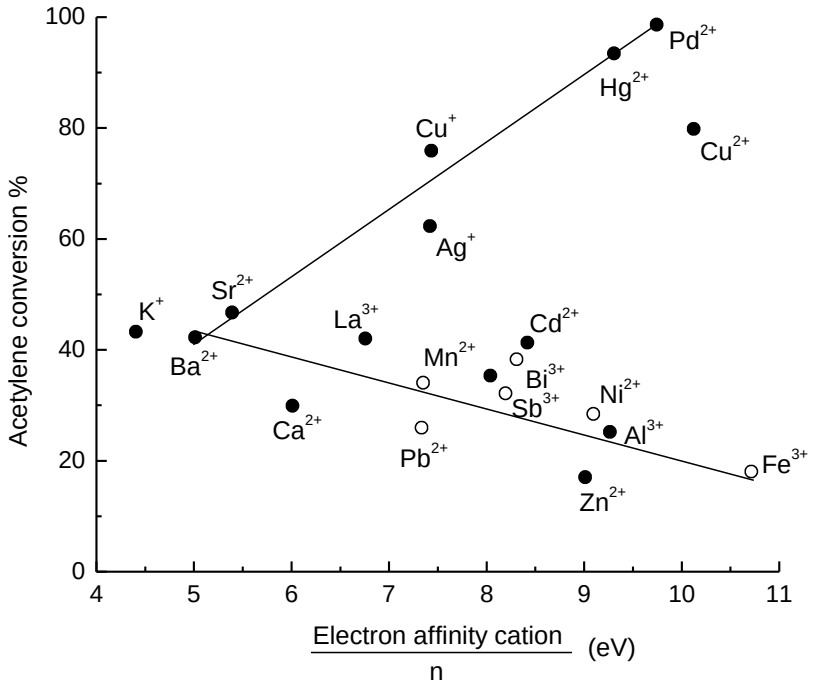

Figure 1.7: Correlation of activity for acetylene hydrochlorination with electron affinity/metal valence for a range of carbon supported metal chlorides[95, 96].

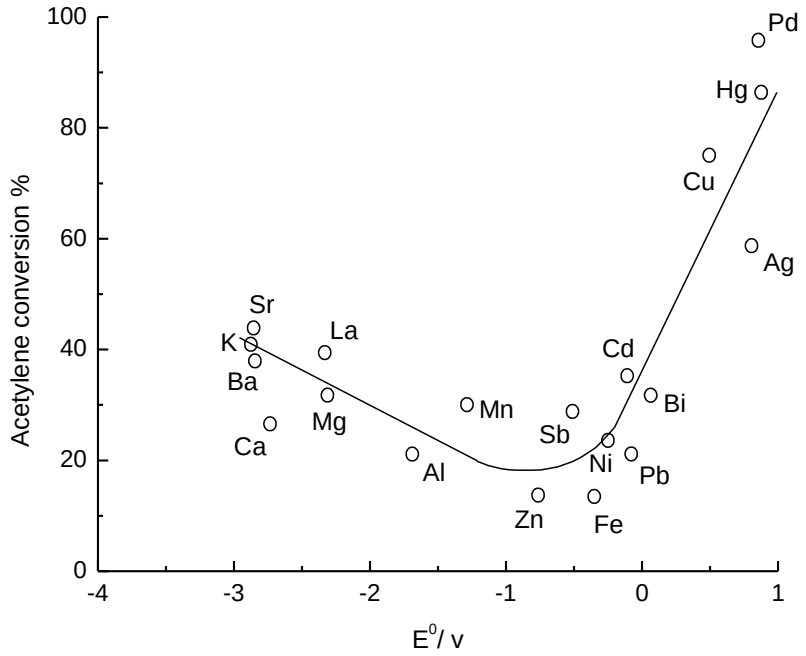

Figure 1.8: Correlation of activity for acetylene hydrochlorination of carbon supported metal chloride catalysts with the standard electrode potential of the metal, $M^{n+} + ne^- \rightarrow M$ [3, 96].

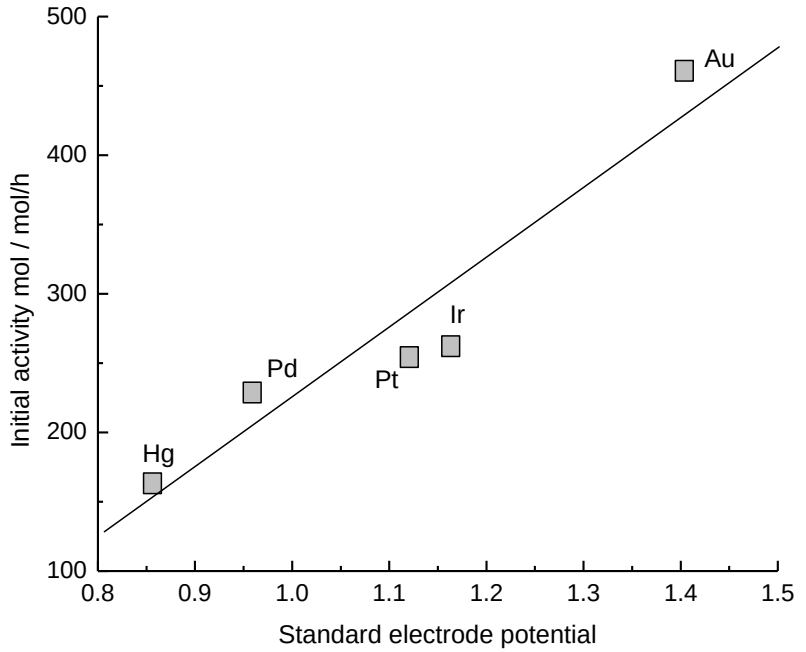

Figure 1.9: Correlation of initial acetylene hydrochlorination activity with standard electrode potential for supported metal chlorides including Au [4, 96].

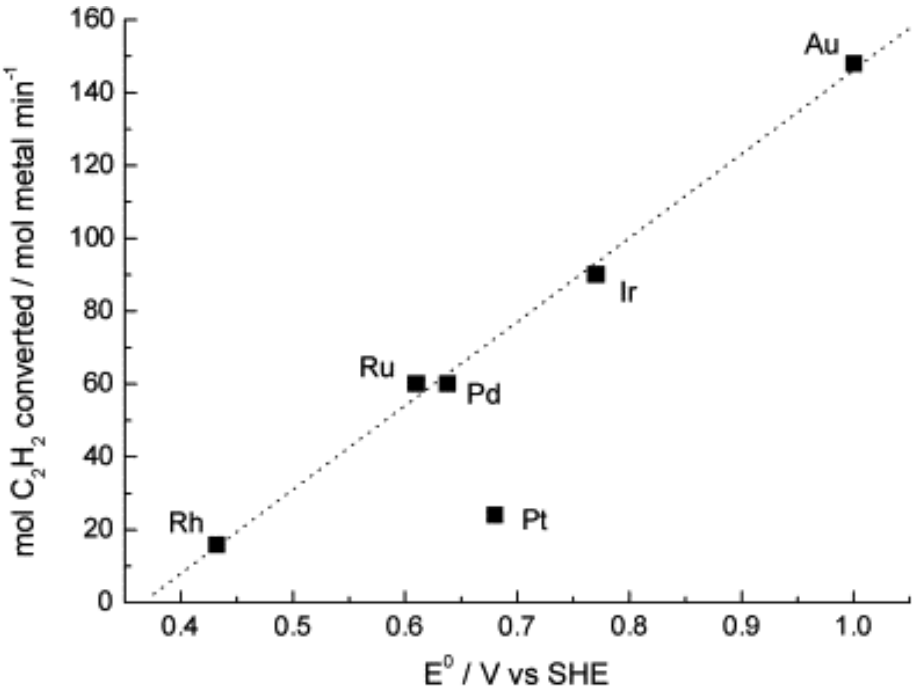

Figure 1.10: Correlation of initial acetylene hydrochlorination activity of supported metal chloride catalysts with the standard electrode potential of metal chloride salts: $(RhCl_6)^{3-}$, $(RuCl_5)^{2-}$, $PdCl_2$, $(PtCl_6)^{2-}$, $(IrCl_6)^{3-}$ and $(AuCl_4)^-$ for the corresponding metals[97].

This correlation was further developed by Conte *et al.*[97] where the standard electrode potential of the metal chloride salt was used, this is shown in figure 1.10.

This further confirms the correlation of catalyst activity with standard electrode potential, although in this case the platinum is an anomalous point. This has previously been explained in terms of the extremely fast deactivation of platinum catalysts and the 4+ oxidation state of the platinum, which is unlikely to form complexes with alkynes[96].

In addition to the highest activity being observed from gold catalysts, another advantage is that they are found to have a much higher selectivity to the desired VCM, greater than 99.5%, whereas a secondary hydrochlorination reaction leading to the production of dichloroethane often occurs with other metals. Deactivation of gold catalysts is, however, still a problem and this was investigated in a study by Nkosi *et al.*[52]. It was determined that whilst leaching of the metal chloride from the support was the main contributor to loss of activity for a number of metals, this was not the

case for gold catalysts. The effect of reaction temperature on deactivation rate was investigated; it was observed that a minimum deactivation rate occurred at 100°C, indicating that two different deactivation mechanisms were occurring (figure 1.11). At temperatures of 60 – 100°C the deactivation was found to be due to deposition of carbonaceous residues on the catalyst surface, likely caused by polymerisation reactions, whereas at temperatures of 120 – 180°C it is attributed to the reduction of cationic gold species (Au^{3+} and Au^{+}) to Au^{0}. Although this suggests that 100°C may be the optimum reaction temperature, the activity at this temperature is considered to be too low and so a temperature of around 180°C continues to be used for catalyst testing.

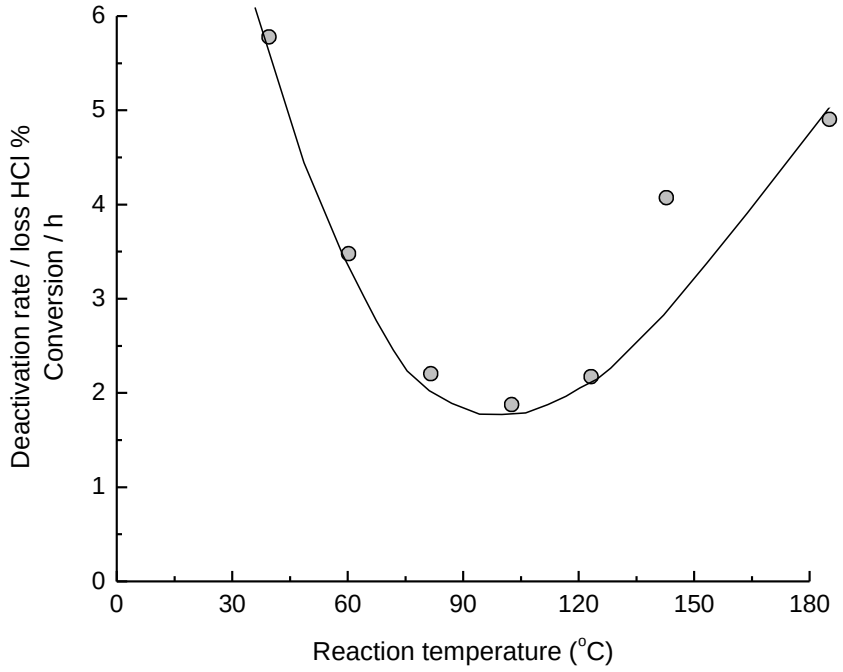

Figure 1.11: The effect of reaction temperature on the deactivation rate of Au/C catalysts for acetylene hydrochlorination [52, 96].

A number of treatments were subsequently demonstrated to be able to regenerate the activity of catalysts which deactivated during testing at the higher temperature range (180°C) by re-oxidation of the gold[51]. Cl_2, NO and N_2O were all found to be effective in restoring catalyst activity, while previously it had also been shown that treatment with HCl could be used for catalyst reactivation[98]. The re-oxidation of the

gold to its cationic state in order to regenerate the catalytic activity is also supported by more recent work, where it was found by Conte *et al.* that treatment of a deactivated catalyst outside the reactor, by boiling in *aqua regia*, was able to do the same[99]. XPS and Mossbauer spectroscopy were used to identify the presence of Au^{3+} on the catalyst surface and correlate this with the observed activity.

Investigation into bimetallic gold based catalysts for this reaction has also been carried out. A further study by Conte *et al.* investigated the effect of addition of a range of precious metals to the gold and while in some cases an enhanced initial catalyst activity was observed, it was concluded that the Au only catalyst was still the best option, largely due to the greater selectivity to the desired product that was obtained[97]. More recently, studies have reported high activity and selectivity from bimetallic catalysts, with copper[100] and lanthanum[101] the metals added to the gold. The conditions were optimised for the Au-Cu/C catalyst and both conversion and selectivity of greater than 99.5% were obtained; however, this used an extremely low gas hourly space velocity (GHSV) of 50 h^{-1}, compared to the GHSVs of 870 h^{-1} used in the studies of the monometallic gold catalysts[102]. For the Au-La/C catalyst a similarly high conversion and selectivity were obtained, also using a lower (but to a lesser extent) space velocity of 360h^{-1}. In this case it was determined that the addition of the lanthanum stabilised the active Au^{3+} species, increasing the lifetime of the catalyst.

The interest in the need for a new catalyst for acetylene hydrochlorination has also led to alternatives to gold based catalysts being reported. These include mechanically activated K_2PdCl_4, K_2PtCl_6 and K_2PtCl_4 salts[103-105], ionic liquids[106], Pt(II) complex solutions[107], palladium based catalysts[108] and a liquid phase rhodium catalyst[109].

1.3.1 Mechanism of acetylene hydrochlorination

Kinetic studies of acetylene hydrochlorination found that the reaction is first order with respect to both acetylene and HCl[51], and formation of a C_2H_2/Au/HCl complex has been suggested. Previous work has also suggested that the reaction may proceed *via* a

redox cycle involving the cationic gold species, although until recently little had been done to determine the mechanism of the reaction. Conte *et al.* now have, however, carried out a detailed investigation into the mechanism of the reaction[102]. Considering that catalyst deactivation occurs due to reduction of cationic gold species to the metallic state, the effects of the individual reactants on the catalyst were investigated since acetylene is known to be a reducing agent. A series of experiments involving sequential exposure of catalyst to the individual reactants both prior to and during reaction found that exposure to HCl enhanced the activity, whereas exposure to acetylene led to catalyst deactivation. This is illustrated in figure 1.12. In addition it was found that the activity of the catalyst increases upon increasing the $HCl:C_2H_2$ ration in the reactant gas feed.

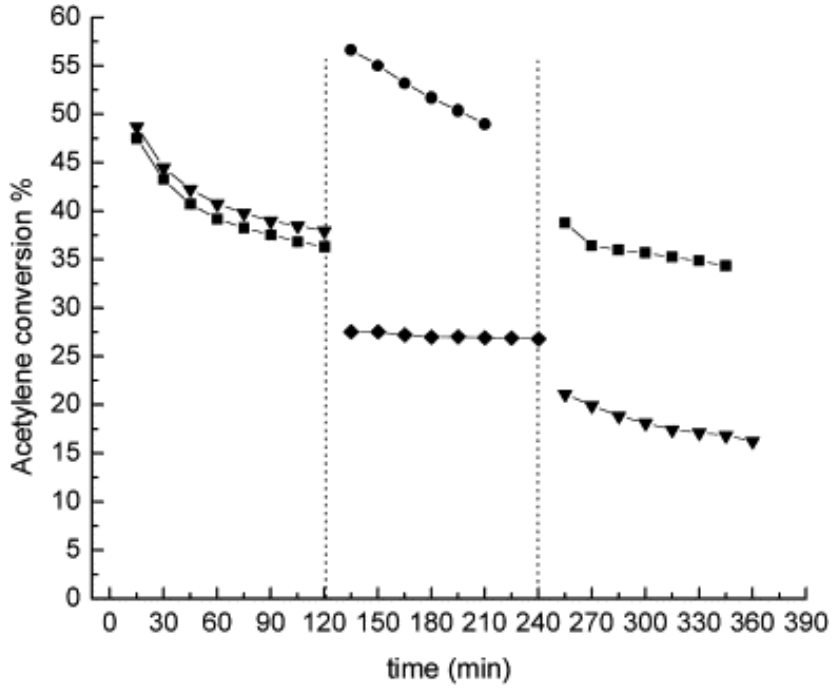

Figure 1.12: Sequential flow experiments to evaluate the effect of each reactant for acetylene hydrochlorination over Au/C catalyst. Experiment A (■): C_2H_2/HCl (2h) → He/Cl (2h) → C_2H_2/HCl (2h); Experiment B (●): He/HCl (2h) → C_2H_2/HCl (2h) → He/HCl (2h); Experiment C (▼):C_2H_2/HCl (2h) → He/C_2H_2 (2h) → C_2H_2/HCl (2h) and Experiment D (◆): C_2H_2/He (2h) → C_2H_2/HCl (2h) → C_2H_2/He (2h)[102].

Due to the symmetric nature of acetylene, mechanistic data is unobtainable since each possible product (*syn*- and *anti*- addition and Markovnikov and *anti*-Markovnikov products) is identical. For this reason, experiments with substituted alkynes were carried out. It was found that activity was affected by steric hindrance of the substrates, with the observed trend in activity of acetylene (40%) > hex-1-yne (10%) > phenylacetylene (7%) > hex-2-yne (2%). These substrates are shown in figure 1.13. Further investigation of these reactions using deuterated substrates (DCl) led to the conclusion that the reaction proceeds *via anti*-addition of HCl across the carbon-carbon triple bond.

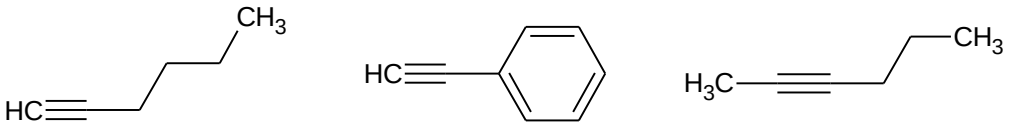

1 2 3

Figure 1.13: Substituted alkyne substrates used to investigate the mechanism of addition of HCl across the alkyne bond: 1) hex-1-yne, 2) phenylacetylene, 3) hex-2-yne.

This result is important as it means that a typical Eley-Rideal mechanism, where only the acetylene is adsorbed on the gold surface and the HCl reacts with it directly from the gas phase, may be eliminated, since this would result in *syn*-addition. A reaction scheme in which a C_2H_2/Au/HCl complex is formed has therefore been suggested, using $[AuCl_4]^-$ as the active site on the catalyst surface (figure 1.14).

DFT calculations were carried out using C_2H_2, HCl and $AuCl_3$ as the active site. It was found that the simultaneous coordination of C_2H_2 and HCl to the Au^{3+} centre was unlikely due to the instability of a pentacoordinated gold atom and it was suggested instead that the acetylene coordinates to the gold centre first then sequential addition of the chlorine and hydrogen occurs, from a HCl molecule that is hydrogen-bonded to a Cl ligand of the Au centre. The reaction pathway is shown in figure 1.15.

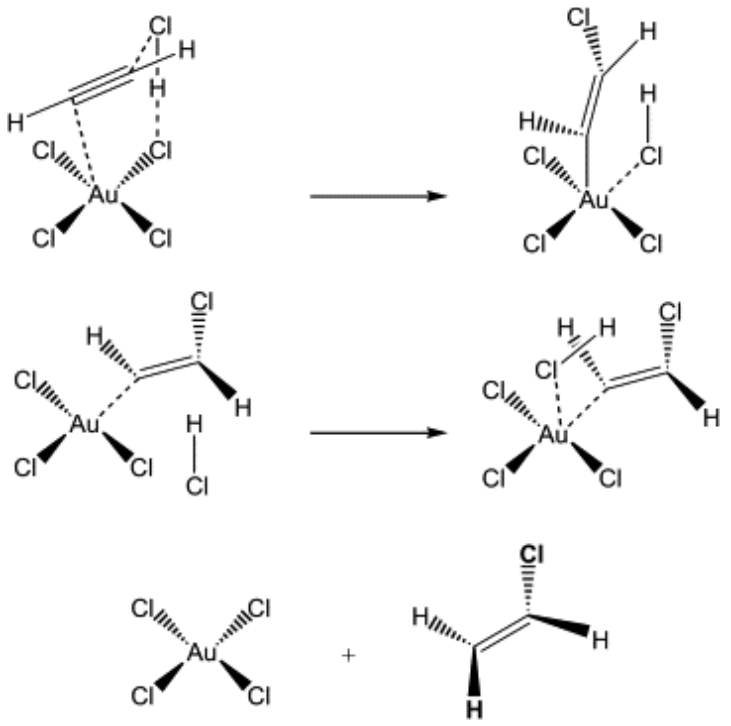

Figure 1.14: Proposed model for acetylene hydrochlorination over an Au/C catalyst involving formation of a C_2H_2/Au/HCl complex[102].

The mechanism of acetylene hydrochlorination catalysed at room temperature by the mechanically activated platinum and palladium salts is described by Mitchenko *et al.*[110]. The first step is π-coordination of the carbon-carbon triple bond to the metal, then nucleophilic attack may occur from either the chlorine ligand of the complex or the HCl, leading to the *cis*- and *trans*- products respectively after protodemetalation. In this case they determine the catalytic active sites to be platinum (IV) complexes with a coordination vacancy, [$PtCl_5$*], for the K_2PtCl_6 and platinum (II) acetylene π-complexes for the K_2PtCl_4 salt. In both cases the rate determining step is considered to be acetylene chloroplatination, involving a HCl molecule. This mechanism is similar to that proposed for the reaction over gold catalysts, in that they both involve coordination of the alkyne to the active site followed by interaction with a chloride species.

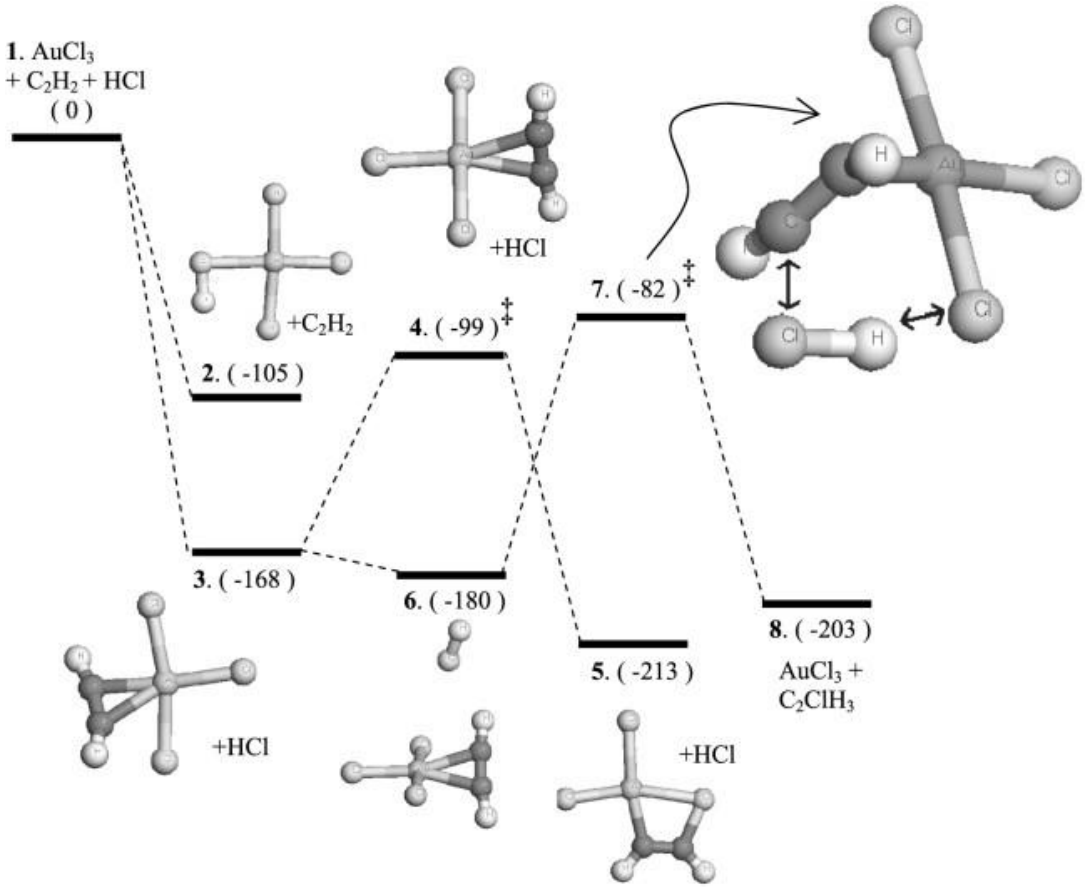

Figure 1.15: Reaction energy profile for acetylene hydrochlorination over Au/C catalyst, assuming active sites to be $AuCl_3$ centres on catalyst surface. Energies are in $kJmol^{-1}$ and transition states are denoted by ‡[102].

1.4 Project Aims

Whilst a new catalyst for the reaction is desirable, studies so far have shown that monometallic gold based catalysts are the most promising due to their high activity and unique selectivity to VCM. Therefore in order to develop a suitable commercial catalyst, the aims of this project are:

- to further understand the source of the activity of such catalysts
- to investigate methods of producing such catalysts in order to increase gold dispersion and cationic gold stability
- to investigate methods of minimising the deactivation of such catalysts.

1.5 References

1. http://www.pvc.org/en/p/how-is-pvc-used.
2. J. B. Agnew and H. S. Shankar, *Ind. Eng. Chem. Prod. R.D.*, 1986, **25**, 19-22.
3. G. J. Hutchings, *J. Catal.*, 1985, **96**, 292-295.
4. B. Nkosi, N. J. Coville and G. J. Hutchings, *Appl. Catal.*, 1988, **43**, 33-39.
5. M. Haruta, T. Kobayashi, H. Sano and N. Yamada, *Chem. Lett.*, 1987, 405-408.
6. N. Cant, *J. Phys. Chem.*, 1971, **75**, 2914.
7. G. C. Bond, P. A. Sermon, G. Webb, D. A. Buchanan and P. B. Wells, *J. Chem. Soc., Chem. Commun.*, 1973, 444b-445.
8. G. C. Bond, C. Louis and D. T. Thompson, *Catalysis by Gold*, Imperial College Press, 2006.
9. Z.-P. Liu, C.-M. Wang and K.-N. Fan, *Angew. Chem. Int. Ed.*, 2006, **45**, 6865-6868.
10. E. Castillejos, E. Gallegos-Suarez, B. Bachiller-Baeza, R. Bacsa, P. Serp, A. Guerrero-Ruiz and I. Rodriguez-Ramos, *Catal. Commun.*, 2012, **22**, 79-82.
11. T. V. Choudhary, C. Sivadinarayana, A. K. Datye, D. Kumar and D. W. Goodman, *Catal. Lett.*, 2003, **86**, 1-8.
12. T. M. Salama, R. Ohnishi and M. Ichikawa, *Chem. Commun.*, 1997, 105-106.
13. N. W. Cant and N. J. Ossipoff, *Catal. Today*, 1997, **36**, 125-133.
14. J. Guo, M. Jia, Z. Bao and Y. Shen, *Rare Metal Mat. Eng.*, 2011, **40**, 1192-1197.
15. H. Sakurai and M. Haruta, *Catal. Today*, 1996, **29**, 361-365.
16. P. Landon, P. J. Collier, A. F. Carley, D. Chadwick, A. J. Papworth, A. Burrows, C. J. Kiely and G. J. Hutchings, *Phys. Chem. Chem. Phys.*, 2003, **5**, 1917-1923.
17. T. A. Nijhuis, B. J. Huizinga, M. Makkee and J. A. Moulijn, *Ind. Eng. Chem. Res.*, 1999, **38**, 884-891.
18. L. Prati and M. Rossi, in *3rd World Congress on Oxidation Catalysis*, eds. R. K. Grasselli, S. T. Oyama, A. M. Gaffney and J. E. Lyons, Elsevier Science Publ B V, Amsterdam, Editon edn., 1997, vol. 110, pp. 509-516.
19. S. Carrettin, P. McMorn, P. Johnston, K. Griffin and G. J. Hutchings, *Chem. Commun.*, 2002, 696-697.
20. V. R. Choudhary, A. Dhar, P. Jana, R. Jha and B. S. Uphade, *Green Chem.*, 2005, **7**, 768-770.
21. D. Andreeva, V. Idakiev, T. Tabakova, A. Andreev and R. Giovanoli, *Appl. Catal. A-Gen.*, 1996, **134**, 275-283.
22. X. Li, S. S. S. Fang, J. Teo, Y. L. Foo, A. Borgna, M. Lin and Z. Y. Zhong, *ACS Catal.*, 2012, **2**, 360-369.
23. D. Thompson, *Top. Catal.*, 2006, **38**, 231-240.
24. J. H. Teles, S. Brode and M. Chabanas, *Angew. Chem. Int. Ed.*, 1998, **37**, 1415-1418.
25. R. O. C. Norman, W. J. E. Parr and C. B. Thomas, *J. Chem. Soc.-Perkin Trans. 1*, 1976, 1983-1987.
26. A. S. K. Hashmi and G. J. Hutchings, *Angew. Chem. Int. Ed.*, 2006, **45**, 7896-7936.
27. C. Gonzalez-Arellano, A. Corma, M. Iglesias and F. Sanchez, *Chem. Commun.*, 2005, 3451-3453.

28. P. Roembke, H. Schmidbaur, S. Cronje and H. Raubenheimer, *J. Mol. Catal. A: Chem.*, 2004, **212**, 35-42.
29. A. Arcadi, *Chem. Rev.*, 2008, **108**, 3266-3325.
30. J. A. Akana, K. X. Bhattacharyya, P. Mueller and J. P. Sadighi, *J. Am. Chem. Soc.*, 2007, **129**, 7736-+.
31. B. C. Gorske, C. T. Mbofana and S. J. Miller, *Org. Lett.*, 2009, **11**, 4318-4321.
32. A. Stephen and K. Hashmi, *Gold Bull.*, 2004, **37**, 51-65.
33. A. S. K. Hashmi, T. M. Frost and J. W. Bats, *J. Am. Chem. Soc.*, 2000, **122**, 11553-11554.
34. A. S. K. Hashmi and P. Sinha, *Adv. Synth. Catal.*, 2004, **346**, 432-438.
35. Y. Fukuda, K. Utimoto and H. Nozaki, *Heterocycles*, 1987, **25**, 297-300.
36. A. Arcadi, G. Bianchi and F. Marinelli, *Synthesis-Stuttgart*, 2004, 610-618.
37. Y. Ito, M. Sawamura and T. Hayashi, *J. Am. Chem. Soc.*, 1986, **108**, 6405-6406.
38. M. Georgy, V. Boucard and J. M. Campagne, *J. Am. Chem. Soc.*, 2005, **127**, 14180-14181.
39. G. M. Veith, A. Villa, L. Prati, A. R. Lupini, S. J. Pennycook and N. J. Dudney, *Gold Bull.*, 2005, **38**, 133-133.
40. S. Ivanova, C. Petit and V. Pitchon, *Appl. Catal. A-Gen.*, 2004, **267**, 191-201.
41. P. A. Pyryaev, B. L. Moroz, D. A. Zyuzin, A. V. Nartova and V. I. Bukhtiyarov, *Kinet. Catal.*, 2010, **51**, 885-892.
42. S. A. C. Carabineiro, N. Bogdanchikova, A. Pestryakov, P. B. Tavares, L. S. G. Fernandes and J. L. Figueiredo, *Nanoscale Res. Lett.*, 2011, **6**.
43. H. S. Oh, J. H. Yang, C. K. Costello, Y. M. Wang, S. R. Bare, H. H. Kung and M. C. Kung, *J. Catal.*, 2002, **210**, 375-386.
44. S. Galvagno and G. Parravano, *J. Catal.*, 1978, **55**, 178-190.
45. Y. Yuan, K. Asakura, H. Wan, K. Tsai and Y. Iwasawa, *Catal. Lett.*, 1996, **42**, 15-20.
46. D. I. Enache, J. K. Edwards, P. Landon, B. Solsona-Espriu, A. F. Carley, A. A. Herzing, M. Watanabe, C. J. Kiely, D. W. Knight and G. J. Hutchings, *Science*, 2006, **311**, 362-365.
47. J. K. Edwards, B. E. Solsona, P. Landon, A. F. Carley, A. Herzing, C. J. Kiely and G. J. Hutchings, *J. Catal.*, 2005, **236**, 69-79.
48. G. C. Bond and D. T. Thompson, *Catal. Rev.-Sci. Eng.*, 1999, **41**, 319-388.
49. A. I. Kozlov, A. P. Kozlova, H. C. Liu and Y. Iwasawa, *Appl. Catal. A-Gen.*, 1999, **182**, 9-28.
50. M. Bowker, A. Nuhu and J. Soares, *Catal. Today*, 2007, **122**, 245-247.
51. B. Nkosi, M. D. Adams, N. J. Coville and G. J. Hutchings, *J. Catal.*, 1991, **128**, 378-386.
52. B. Nkosi, N. J. Coville, G. J. Hutchings, M. D. Adams, J. Friedl and F. E. Wagner, *J. Catal.*, 1991, **128**, 366-377.
53. S. Shimada, T. Takei, T. Akita, S. Takeda and M. Haruta, in *Scientific Bases for the Preparation of Heterogeneous Catalysts: Proceedings of the 10th International Symposium*, eds. E. M. Gaigneaux, M. Devillers, S. Hermans, P. A. Jacobs, J. A. Martens and P. Ruiz, Elsevier Science Bv, Amsterdam, Editon edn., 2010, vol. 175, pp. 843-847.
54. N. K. Gamboa-Rosales, J. L. Ayastuy, M. P. Gonzalez-Marcos and M. A. Gutierrez-Ortiz, *Int. J. Hydrog. Energy*, 2012, **37**, 7005-7016.

55. G. R. Bamwenda, S. Tsubota, T. Nakamura and M. Haruta, *Catal. Lett.*, 1997, **44**, 83-87.
56. A. Wolf and F. Schuth, *Appl. Catal. A-Gen.*, 2002, **226**, 1-13.
57. F. Moreau, G. C. Bond and A. O. Taylor, *J. Catal.*, 2005, **231**, 105-114.
58. J. H. Yang, J. D. Henao, C. Costello, M. C. Kung, H. H. Kung, J. T. Miller, A. J. Kropf, J. G. Kim, J. R. Regalbuto, M. T. Bore, H. N. Pham, A. K. Datye, J. D. Laeger and K. Kharas, *Appl. Catal. A-Gen.*, 2005, **291**, 73-84.
59. M. Haruta, N. Yamada, T. Kobayashi and S. Iijima, *J. Catal.*, 1989, **115**, 301-309.
60. J. Hua, Q. Zheng, K. Wei and X. Lin, *Chin. J. Catal.*, 2006, **27**, 1012-1018.
61. A. Jain, X. Zhao, S. Kjergaard and S. M. Stagg-Williams, *Catal. Lett.*, 2005, **104**, 191-197.
62. L. Prati and G. Martra, *Gold Bull.*, 1999, **32**, 96-101.
63. P. Miedziak, M. Sankar, N. Dimitratos, J. A. Lopez-Sanchez, A. F. Carley, D. W. Knight, S. H. Taylor, C. J. Kiely and G. J. Hutchings, *Catal. Today*, 2011, **164**, 315-319.
64. N. Dimitratos, J. A. Lopez-Sanchez, S. Meenakshisundaram, J. M. Anthonykutty, G. Brett, A. F. Carley, S. H. Taylor, D. W. Knight and G. J. Hutchings, *Green Chem.*, 2009, **11**, 1209-1216.
65. J. A. Lopez-Sanchez, N. Dimitratos, P. Miedziak, E. Ntainjua, J. K. Edwards, D. Morgan, A. F. Carley, R. Tiruvalam, C. J. Kiely and G. J. Hutchings, *Phys. Chem. Chem. Phys.*, 2008, **10**, 1921-1930.
66. G. Hutchings, *Cat. Sci. Tech.*, 2012.
67. J. A. Lopez-Sanchez, N. Dimitratos, C. Hammond, G. L. Brett, L. Kesavan, S. White, P. Miedziak, R. Tiruvalam, R. L. Jenkins, A. F. Carley, D. Knight, C. J. Kiely and G. J. Hutchings, *Nat. Chem.*, 2011, **3**, 551-556.
68. S. Tsubota, D. A. H. Cunningham, Y. Bando and M. Haruta, *Preparation of nanometer gold strongly interacted with TiO2 and the structure sensitivity in low-temperature oxidation of CO*, Elsevier Science Publ B V, Amsterdam, 1995.
69. A. Visco, A. Donato, C. Milone and S. Galvagno, *React. Kinet. Catal. Lett.*, 1997, **61**, 219-226.
70. V. R. Choudhary and D. K. Dumbre, *Catal. Commun.*, 2011, **13**, 82-86.
71. L. Guczi, A. Beck and Z. Paszti, *Catal. Today*, 2012, **181**, 26-32.
72. G. L. Brett, P. J. Miedziak, N. Dimitratos, J. A. Lopez-Sanchez, N. F. Dummer, R. Tiruvalam, C. J. Kiely, D. W. Knight, S. H. Taylor, D. J. Morgan, A. F. Carley and G. J. Hutchings, *Cat. Sci. Tech.*, 2012, **2**, 97-104.
73. Z. Yan and D. W. Goodman, *Catal. Lett.*, 2012, **142**, 517-520.
74. B. Solsona, M. Perez-Cabero, I. Vazquez, A. Dejoz, T. Garcia, J. Alvarez-Rodriguez, J. El-Haskouri, D. Beltran and P. Amoros, *Chem. Eng. J.*, 2012, **187**, 391-400.
75. Q. Ye, D. H. Li, J. Zhao, J. S. Zhao, T. F. Kang and S. Y. Cheng, *Front. Environ. Sci. Eng. China*, 2011, **5**, 497-504.
76. I. Sobczak, K. Musialska, H. Pawlowski and M. Ziolek, *Catal. Today*, 2011, **176**, 393-398.
77. C. Hammond, J. A. Lopez-Sanchez, M. H. Ab Rahim, N. Dimitratos, R. L. Jenkins, A. F. Carley, Q. He, C. J. Kiely, D. W. Knight and G. J. Hutchings, *Dalton Trans.*, 2011, **40**, 3927-3937.

78. K. T. Hojholt, A. B. Laursen, S. Kegnaes and C. H. Christensen, *Top. Catal.*, 2011, **54**, 1026-1033.
79. R. C. Tiruvalam, J. C. Pritchard, N. Dimitratos, J. A. Lopez-Sanchez, J. K. Edwards, A. F. Carley, G. J. Hutchings and C. J. Kiely, *Faraday Discussions*, 2011, **152**, 63-86.
80. G. J. Hutchings, M. S. Hall, A. F. Carley, P. Landon, B. E. Solsona, C. J. Kiely, A. Herzing, M. Makkee, J. A. Moulijn, A. Overweg, J. C. Fierro-Gonzalez, J. Guzman and B. C. Gates, *J. Catal.*, 2006, **242**, 71-81.
81. M. P. Casaletto, A. Longo, A. M. Venezia, A. Martorana and A. Prestianni, *Appl. Catal. A-Gen.*, 2006, **302**, 309-316.
82. J. Guzman and B. C. Gates, *J. Phys. Chem. B*, 2002, **106**, 7659-7665.
83. P. Landon, J. Ferguson, B. E. Solsona, T. Garcia, A. F. Carley, A. A. Herzing, C. J. Kiely, S. E. Golunski and G. J. Hutchings, *Chem. Commun.*, 2005, 3385-3387.
84. J. Wang, V. F. Kispersky, W. N. Delgass and F. H. Ribeiro, *J. Catal.*, 2012, **289**, 171-178.
85. F. Neatu, Z. Li, R. Richards, P. Y. Toullec, J. P. Genet, K. Dumbuya, J. M. Gottfried, H. P. Steinruck, V. I. Parvulescu and V. Michelet, *Chem.-Eur. J.*, 2008, **14**, 9412-9418.
86. S. Carrettin, M. C. Blanco, A. Corma and A. S. K. Hashmi, *Adv. Synth. Catal.*, 2006, **348**, 1283-1288.
87. M. Garcia-Mota, N. Cabello, F. Maseras, A. M. Echavarren, J. Perez-Ramirez and N. Lopez, *Chemphyschem*, 2008, **9**, 1624-1629.
88. L. M. Mascavage, F. Zhang-Plasket, P. E. Sonnet and D. R. Dalton, *Tetrahedron*, 2008, **64**, 9357-9367.
89. Z. Kisiel, P. W. Fowler, A. C. Legon, D. Devanne and P. Dixneuf, *J. Chem. Phys.*, 1990, **93**, 6249-6255.
90. T.-H. Tang and Y.-P. Cui, *Can. J. Chem.*, 1996, **74**, 1162-1170.
91. Y. Segura, N. Lopez and J. Perez-Ramirez, *J. Catal.*, 2007, **247**, 383-386.
92. N. Lopez, B. Bridier and J. Perez-Ramirez, *J. Phys. Chem. C*, 2008, **112**, 9346-9350.
93. H. Bremer and H. Lieske, *Appl. Catal.*, 1985, **18**, 191-203.
94. G. J. Hutchings and D. T. Grady, *Appl. Catal.*, 1985, **17**, 155-160.
95. K. Shinoda, *Chem. Lett.*, 1975, 219-220.
96. M. Conte and G. J. Hutchings, in *Modern Gold Catalyzed Synthesis*, eds. F. D. Toste and A. S. K. Hashmi, Wiley VCH Verlag GmbH, Editon edn., 2011.
97. M. Conte, A. F. Carley, G. Attard, A. A. Herzing, C. J. Kiely and G. J. Hutchings, *J. Catal.*, 2008, **257**, 190-198.
98. B. Nkosi, N. J. Coville and G. J. Hutchings, *J. Chem. Soc.-Chem. Commun.*, 1988, 71-72.
99. M. Conte, A. F. Carley and G. J. Hutchings, *Catal. Lett.*, 2008, **124**, 165-167.
100. S. J. Wang, B. X. Shen and Q. L. Song, *Catal. Lett.*, 2010, **134**, 102-109.
101. H. Zhang, B. Dai, X. Wang, L. Xu and M. Zhu, *J. Ind. Eng. Chem.*, 2012, **18**, 49-54.
102. M. Conte, A. F. Carley, C. Heirene, D. J. Willock, P. Johnston, A. A. Herzing, C. J. Kiely and G. J. Hutchings, *J. Catal.*, 2007, **250**, 231-239.
103. S. A. Mitchenko, E. V. Khomutov, A. A. Shubin and Y. M. Shul'ga, *J. Mol. Catal. A: Chem.*, 2004, **212**, 345-352.

104. S. A. Mitchenko, T. V. Krasnyakova, R. S. Mitchenko and A. N. Korduban, *J. Mol. Catal. A: Chem.*, 2007, **275**, 101-108.
105. S. A. Mitchenko, T. V. Krasnyakova and I. V. Zhikharev, *Theor. Exp. Chem.*, 2008, **44**, 316-319.
106. G. Qin, Y. H. Song, R. Jin, J. Shi, Z. Y. Yu and S. K. Cao, *Green Chem.*, 2011, **13**, 1495-1498.
107. L. A. Sil'chenko, S. A. Panova, G. K. Shestakov and O. N. Temkin, *Kinet. Catal.*, 1997, **38**, 790-794.
108. Q. L. Song, S. J. Wang, B. X. Shen and J. G. Zhao, *Pet. Sci. Technol.*, 2010, **28**, 1825-1833.
109. S. A. Panova, G. K. Shestakov and O. N. Temkin, *J. Chem. Soc.-Chem. Commun.*, 1994, 977-977.
110. S. A. Mitchenko, T. V. Krasnyakova and I. V. Zhikharev, *Kinet. Catal.*, 2009, **50**, 734-740.

2 Experimental Techniques

2.1 Introduction

This chapter will describe the techniques used in this project for catalyst preparation, characterisation and testing. These are as follows:

- Preparation
    - Wet Impregnation
    - Deposition Precipitation
    - Sol Immobilisation
    - Acid Impregnation
- Characterisation
    - X-ray Photoelectron Spectroscopy (XPS)
    - X-ray Diffraction (XRD)
    - Temperature Programmed Desorption/Reduction/Oxidation (TPD/R/O)
    - Raman Spectroscopy
    - Titrations
- Testing
    - Reactor Conditions
    - Product Analysis
        - Gas Chromatography

2.2 Catalyst Preparation

A series of 1% Au/C catalysts were prepared via a range of methods, as described below. In all cases the carbon support used is Norit ROX 0.8, an activated carbon extrudate of 0.8mm diameter, provided by Johnson Matthey.

2.2.1 Wet Impregnation

$HAuCl_4.3H_2O$ (Aldrich, 5g) was dissolved in distilled water (250 mL). The resulting solution (2.2mL) was added to the activated carbon support (1.98g), sufficient water added to just cover the support, then the mixture was stirred at ambient temperature for 10 minutes. The sample was dried overnight (16h) at 110°C.

2.2.2 Deposition precipitation (DP)

$HAuCl_4.3H_2O$ (Aldrich, 5g) was dissolved in distilled water (250 mL). A portion of the resulting solution (2.2mL) was made up to a volume of 10 mL with distilled water. Activated carbon (1.98g) was added, and the pH adjusted to pH9.2 via dropwise addition of a saturated solution of Na_2CO_3 (Fisher) in distilled water. The mixture was stirred at ambient temperature for 1h and the pH maintained at 9.2, then it was filtered, washed with distilled water and dried overnight (16h) at 110°C.

2.2.3 Sol Immoblisation

$HAuCl_4.3H_2O$ (Alfa Aesar, 25g) was dissolved in distilled water (1L). The resulting solution (1.632 mL) was added to double-distilled water (394mL) with stirring. PVA (Aldrich, 0.1g) was dissolved in distilled water (10mL) and the resulting solution (1.3mL) was added. Subsequently $NaBH_4$ (Aldrich, 0.38g) was dissolved in distilled water (10mL) and the resulting solution (5mL) added. The solution was then stirred for 30 minutes. The carbon support (1.98g) was added and the mixture was acidified to pH 2 using concentrated H_2SO_4. The mixture was stirred at ambient temperature for 1h, then filtered, washed with distilled water (1.5L) and dried overnight (16h) at 110°C.

However, it should be noted that the carbon support was first ground to a powder before use in the sol immobilisation preparation. The method was attempted on the carbon extrudate but when the catalyst was filtered it was clear that the gold colloid

had not attached to the support surface as the filtrate was still red in colour. However, the sol immobilisation method has been used with other, powder carbon supports before e.g. Darco G60[1], graphite[2] so it was decided to try grinding the extrudate to a powder (by hand, using a pestle and mortar), which proved successful.

2.2.4 Acid Impregnation

$HAuCl_4.xH_2O$ (Alfa Aesar, 99.9% (metals basis), Au 49%, 40mg) was dissolved in aqua regia (3:1 HCl (Fisher, 32%):HNO_3 (Fisher, 70%) by volume, 5.4ml) and the solution added dropwise with stirring to the activated carbon support (1.98g). Stirring was continued at ambient temperature until NO_x production subsided, approximately 10 minutes. The sample was dried overnight (16h) at 110°C.
A number of variations on this method have been used, these are described in further detail in chapter 3, concerning the chemistry of aqua regia and its effect on catalyst preparation.

2.3 Catalyst Characterisation

2.3.1 X-ray photoelectron spectroscopy (XPS)

XPS is a surface-sensitive characterisation technique, used to analyse the chemical composition at the surface of a sample, and is therefore a frequently used technique for analysis of heterogeneous catalysts. It can not only reveal which elements are present, but also the oxidation state they are in. To carry out XPS analysis, a sample is irradiated with monochromatic X-rays under ultra high vacuum (UHV) conditions. This results in the emission of electrons (known as photoelectrons) from core energy levels of atoms; however only those from atoms at the surface are able to be detected as the mean free path of the electrons through the solid is comparable to only a few atomic distances (ca. 1-2 nm)[3]. Since the energy of the X-rays used is known, from the

measured kinetic energy of these detected electrons the binding energy of the atoms can be calculated using the following equation:

$$E_{kinetic} = h\nu - E_{binding} - \Phi \qquad \textbf{Equation 2.1}$$

Where $h\nu$ is the energy of the incident X-rays (h = Planck's constant, ν = frequency) and Φ is the work function of the spectrometer. This is the energy required to release the electron from the highest energy level, the Fermi level of the atom, and is the difference between the vacuum energy level and the Fermi energy level. This is illustrated in figure 2.1.

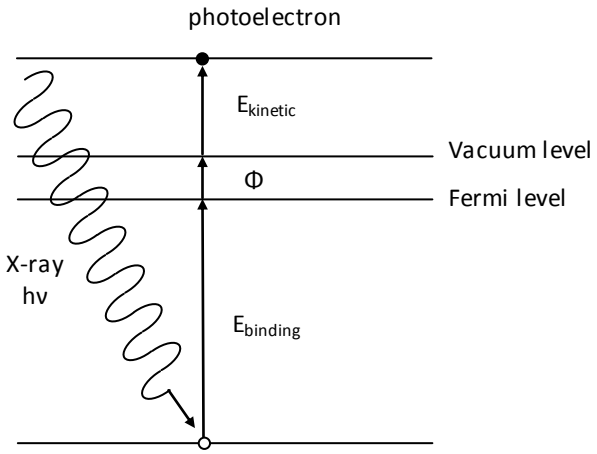

Figure 2.1: Diagram to illustrate photoemission

Binding energies are unique to atoms of a particular element in a particular oxidation state and therefore its chemical environment. In turn this allows the species present on a sample's surface to be identified.

XPS spectra are usually presented as a plot of intensity (i.e. number of electron counts) against binding energy, with peaks occurring at binding energies characteristic of species present on the surface. These peaks are labelled according to quantum numbers of the level from which the electrons are emitted, *e.g.* the commonly used peaks for analysis of Au species are the Au 4f. Quantum number n refers to the core energy level, and is an integer ≥ 1. The orbital momentum l = 0,1,2,3... is denoted as

s,p,d,f... and for each level with l≥1 the spin momentum s may be either +1/2 or -1/2 (up or down), resulting in 2 sub-levels since the total momentum j = l+s. This leads to the presence of a doublet in the spectrum for electrons from such levels, again using Au as an example these are the Au $4f_{5/2}$ and $4f_{7/2}$ peaks, a typical XPS spectrum for this region can be seen in Figure 2.2 (this is a spectra of a 1% Au/C catalyst after a reduction treatment). Characteristic binding energies for these levels of metallic Au are 87.7eV and 84eV respectively.

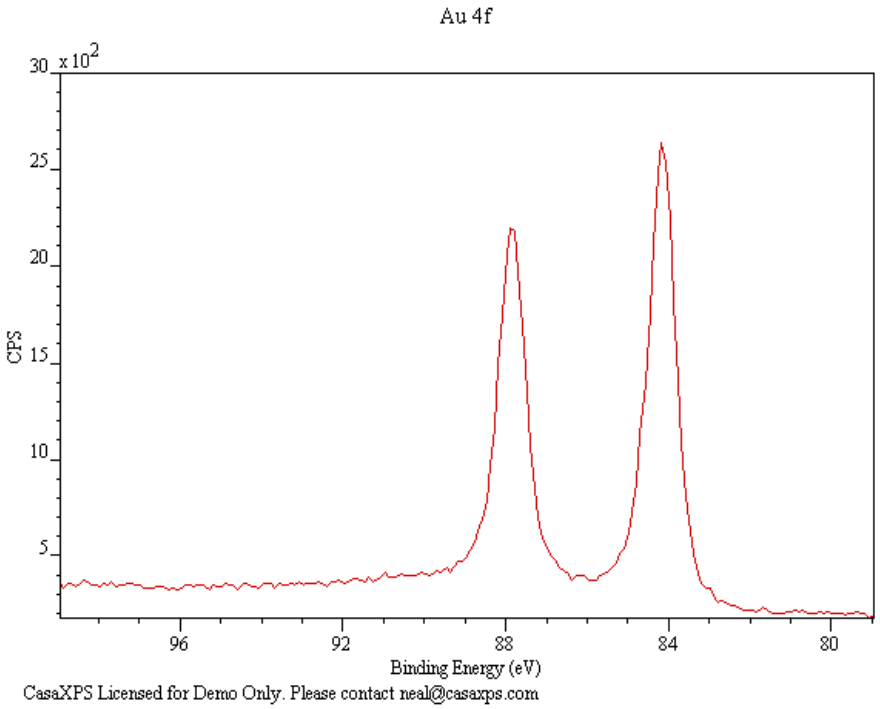

Figure 2.2: XPS spectrum of the Au 4f region of metallic gold.

X-ray photoelectron spectroscopy (XPS) was performed using a Kratos Axis Ultra-DLD photoelectron spectrometer. Samples were mounted in batches of 9 using 6mm diameter stainless steel stubs *via* doubled sided adhesive tape. Analysis was performed at a typical base pressure of $1x10^{-9}$ Torr, using a monochromatic Aluminium X-ray source, operating at 120 W power (10 mA emission, 12 kV anode potential).

Survey scans were acquired at a pass energy of 160 eV and high resolution scans at 40 eV. All spectra were collected in Hybrid mode of operation, which utilises both electrostatic and magnetic lenses to increase sensitivity. Charge compensation was achieved using the Kratos patented immersion lens system, which typically resulted in a shift of 2-3 eV lower energy for the photoelectron peak, therefore all spectra were calibrated to the C(1s) line for adventitious carbon at 284.7 eV.

Data analysis was carried out using CasaXPS software. For quantification of Au^{3+}/Au^{0} species the Au 4f region was used, with two doublets of peaks fitted. The second peak of each doublet was constrained to have the same full width half maximum (FWHM) as the first, but have an area ¾ of the value and a position 3.7 eV higher, as this is typical of the Au 4f doublet. This peak fitting is illustrated in figure 2.3, which shows the spectrum of a 1% Au/C catalyst prepared by impregnation in aqua regia and dried at 110°C. The software then calculates the % contribution of each component from its peak area.

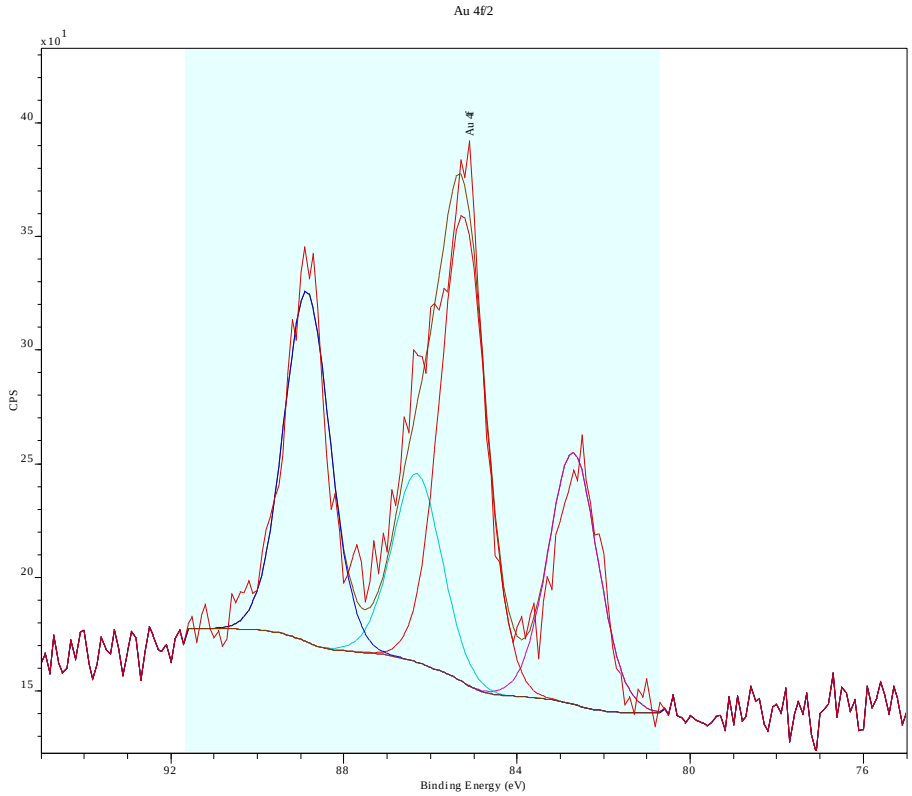

Figure 2.3: XPS spectrum of the Au 4f region of a Au/C catalyst prepared by impregnation in aqua regia and dried at 110°C.

2.3.2 X-ray Diffraction (XRD)

X-Ray Diffraction (XRD) is a non-destructive technique for analysis of the crystal structure of the bulk of a material. XRD can identify the crystallinity of a material, and also give information on the size of microcrystallites and the d-spacings and unit cell dimensions of a crystalline material. Since the wavelength of x-ray radiation is comparable to the periodic spacings in a crystal lattice, diffraction occurs as the x-rays are reflected by the crystal planes, which produces an interference pattern providing structural information about the sample[4].

XRD may be carried out on single crystals or powders. Of these, powder XRD is the most commonly used in the study of heterogeneous catalysts. It can be used to produce a fingerprint of a crystalline phase, of which there are large databases available that results can be compared to for identification, and is also useful for monitoring structural changes of a solid during a reaction, and providing information on particle size. Although powder XRD is less accurate in the determination of lattice parameters, it has the advantage that randomly distributed crystallites may be analysed, without the need for a single crystal. In contrast, single crystal XRD is more suitable for complete crystal structure determination, however this does require a crystal of sufficient size and quality which is difficult to obtain for heterogeneous catalysts intended for industrial application.

XRD analysis is carried out by exposing the sample to a monochromatic x-ray source and detecting the resulting reflected (i.e. diffracted) x-rays. In powder XRD the sample is also rotated, to increase the probability that the reflected x-rays are detected. A diffractogram is a plot of intensity against the angle (2θ) at which constructive interference of x-rays is detected. A fundamental of XRD is the Bragg equation:

$$n\lambda = 2d \sin\theta \qquad \textbf{Equation 2.2}$$

Where n is an integer, λ is the wavelength of the radiation, d is the periodic spacing between planes of the crystal structure and θ is the incident angle of the radiation[5]. This equation is derived from the idea that constructive interference of reflected x-rays will occur when they are in phase with each other - in order for this situation to arise the difference in the path lengths of waves reflected by adjacent planes must be a whole number of wavelengths – i.e. nλ. This is shown in figure 2.3.

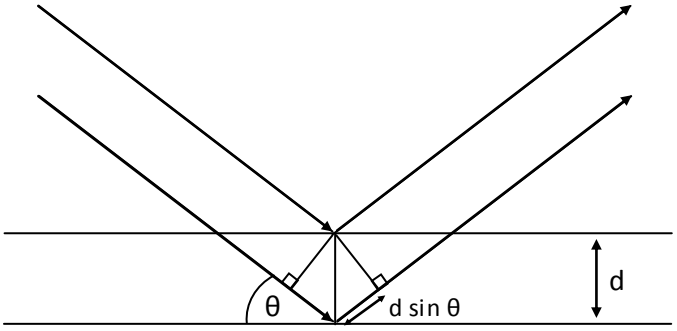

Figure 2.3: Diagram to illustrate Bragg's law – the difference in path length between the two rays is 2dsinθ, which for constructive interference to occur must be equal to an integer multiple of the wavelength of the x-ray.

Perfect crystals give XRD reflections that are very sharp, however as crystallite size decreases below 100 nm, line broadening occurs. Line width is related to crystallite size by the Scherrer equation (equation 2.3), and this can be used to determine crystallite size from a diffractogram[3].

$$L = \frac{K\lambda}{\beta \cos\theta}$$ **Equation 2.3**

L is a measure of particle size (perpendicular to the reflecting plane), λ is the x-ray wavelength, β is the peak width (measured at half the height of the peak maximum and known as the full width half maximum, FWHM), θ is the angle between the beam and the normal on the reflecting plane and K is a constant (usually taken as 1) which is related to the shape of the crystallite.

XRD was used for comparison of the size of the supported Au particles in Au/C catalysts prepared via different methods; reflections due to metallic gold are present at angles of 38 (111), 44 (200), 64 (220) and 78 (311) 2θ. The reflection due to the (111) plane, at 38 2θ, was used in the Scherrer equation to estimate the size of the metallic gold particles, since this was the most intense reflection.

XRD analysis was performed on a (θ-θ) PANalytical X'pert Pro powder diffractometer using a Cu K_α radiation source operating at 40 keV and 40 mA.

2.3.3 Temperature programmed desorption/reduction/oxidation (TPD/R/O)

Temperature programmed desorption/reduction/oxidation (TPD/R/O) encompasses a range of temperature programmed techniques, which monitor a chemical reaction as temperature changes. TPD is used to investigate desorption of gases from a sample's surface, which can be used to investigate features of a catalyst surface, for example the presence of acidic/basic sites, or the surface coverage of a particular gas of interest. The sample may be heated in an inert atmosphere and the desorption products detected, or the sample may first be subjected to treatment by a suitable gas, for example ammonia for investigating acidic sites on a surface, and then the desorption of this gas monitored.

TPO/TPR is used to investigate the redox properties of a sample. In order to do this the sample is heated under a flow of the appropriate gas (oxygen for oxidation, hydrogen for reduction, usually *ca.* 10% in an inert gas), and the signal at a thermal conductivity detector (TCD) recorded. These work by measuring the thermal conductivity of two gas streams, the gas to be analysed and a reference (in this case the gas after it has passed the sample, and the original gas feed). Since the gases being analysed, i.e. oxygen and hydrogen, typically have different thermal conductivity to the inert gas (Ar), any change in their concentration will lead to a change in thermal

conductivity, which is detected and presented as an electrical signal. This shows the uptake of oxygen/hydrogen respectively, and therefore at what temperatures oxidation/reduction processes occur. TPR profiles are usually presented as a plot of detector signal against temperature, with peaks representing individual oxidation/reduction processes[6].

A vast amount of information may be obtained from TPO/R, for example in addition to the position of the peak maxima telling you about the thermodynamics of the reaction, the slope of the peaks tells you about the kinetics of the reaction, and the area under the peak directly relates to the amount of oxidised/reduced species.

It is also possible to determine the kinetic parameters of these reactions. For example, the activation energy for a reduction reaction may be obtained from TPR analysis, from the shift of the temperature of the peak maximum (T_{max}) that occurs when a sample is heated at different ramp rates. The relationship between T_{max} and the heating ramp rate (β) is given by the Kissinger equation (equation 2.4); the activation energy (and pre-exponential factor, A) can therefore be determined by plotting $\ln(\beta/T_{max}^2)$ against $1/T_{max}$, which gives a straight line with gradient $-E_a/R$ and intercept $\ln(AR/E_a)$[7].

$$\ln \frac{\beta}{T_{max}^2} = \ln \frac{AR}{E_a} - \frac{E_a}{R\,T_{max}} \qquad \textbf{Equation 2.4}$$

TPR was extensively used in this thesis for analysis of the Au^{3+} content of Au/C catalysts and for the determination of kinetic parameters - the Kissinger method as described above was used to find the activation energies and pre-exponential factors for the reduction of Au^{3+} in a hydrogen atmosphere for a series of 1% Au/C catalysts which contain cationic gold species (see chapter 4, section 4.4). TPD was also used, for analysis of the surface functional groups present on acid-treated carbons.

TPR analysis was carried out on a Thermo TPD/R/O 1100 Series. The sample (0.1 g) was heated up to 800°C at a ramp rate of 5 °C/min, under a flow of Hydrogen (10%/Ar, 20 ml/min). For activation energy determination, heating ramp rates of 10, 15 and 20 °C/min were also used. TPD analysis of the carbon catalyst support was carried out by heating the sample (0.1 g) up to 800 °C at a ramp rate of 5 °C/min, under a flow of helium (20 ml/min).

2.3.4 Raman Spectroscopy

Raman Spectroscopy uses the inelastic scattering of photons to investigate vibrations of chemical bonds in a sample. Vibrations are only Raman active if they change the polarisability of the sample, which usually means that the shape of the sample's structure is changed. The technique involves exposure of the sample to a monochromatic light source, usually provided by a laser. The frequency of the scattered photons is measured and any change in frequency corresponds to a difference in energy between the vibrational energy levels of a sample, so can be used for identification of the bond vibrations taking place and therefore aid in structure determination[3].

There are a number of possible outcomes from the scattering of the radiation, depending on the vibrational energy levels involved. These are known as the Stokes, Rayleigh and Anti-Stokes bands and these are illustrated in figure 2.4.

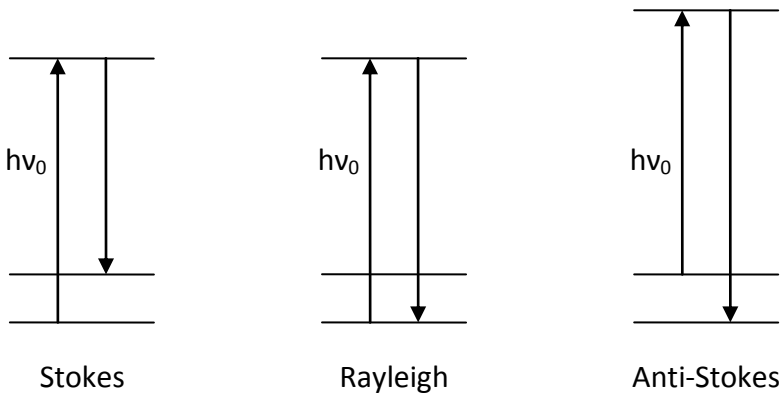

Figure 2.4: Diagram of scattering that leads to the Stokes, Rayleigh and Anti-Stokes bands.

Rayleigh scattering is elastic, since the incident and detected photons are of the same energy, however the Stokes and Anti-Stokes scattering are inelastic, since the energy of the detected photons is either greater (Anti-Stokes) or less than (Stokes) that of the incident photons. The Rayleigh band in a spectrum is around 3 orders of magnitude larger than the stokes and anti-stokes bands, but does not provide any information about the sample.

Raman spectroscopy is often used for analysis of oxides, since the frequencies of metal-oxygen vibrations tend to be in a suitable range[3]. This makes it suitable as an analytical technique in catalysis, since many industrial catalysts consist of oxides, or metal supported on oxides. However, Raman is also commonly used for structure determination of carbon materials, e.g. carbon nanotubes, and it is for this reason it has been used in this thesis.

Raman Spectroscopy was used to investigate the structure of the activated carbon support of 1% Au/C catalysts. It was carried out on a Renishaw inVia Raman Microscope, using a laser of wavelength 514 nm at 100% intensity.

2.3.5 Titrations

Titrations may be used to investigate the acidic and basic features of the surface of activated carbons. There are a number of methods which can be used; for example the Boehm method, which involves reacting the carbon with different bases known to react with different surface functional groups (i.e. NaOH will neutralise carboxyls, lactones and phenols, Na_2CO_3 carboxyls and lactones and $NaHCO_3$ only carboxyls), then back titrating these basic solutions to find the change in concentration and therefore the amount of functional groups on the surface[8]. A more straightforward potentiometric titration may also be used, where the carbon is suspended in water and titrated with acid or base (HCl or NaOH). From the plot of pH against amount of acid/base added, the pKa of functional groups may be determined and therefore the functional groups identified. The amount of these groups present may also be calculated. This is done by differentiation of the plot, the peaks in this derivative plot then correspond to the end point of the titration with each functional group – the volume of titrant added at this point is known, so the number of moles and therefore the number of functional groups may be calculated.

The methods used for titrations and analysis of the data will be discussed in more detail in the relevant results chapter (chapter 4). Typically, the sample to be analysed (0.1g) was suspended in deionised water (10ml) with stirring, and dilute (0.02M) HCl or NaOH as appropriate added step-wise (0.2ml) and the pH measured after a stabilisation time (e.g. 1 minute) after each addition. A plot of pH against volume of titrant added was then used to determine the end-point of each titration with a surface functional group (for quantification) and the pKa of the functional groups being titrated (for identification). Functional groups can be identified from titrations as fitting into 3 categories as determined by Boehm: carboxylic (pKa<6.37), lactonic (6.37<pKa<10.25) or (phenolic pKa>10.25).

2.4 Catalyst Testing

2.4.1 Reactor Design

The design for the reactor used for this project was provided by Johnson Matthey, a schematic diagram of the reactor being shown in figure 2.5, with a photograph in figure 2.6.

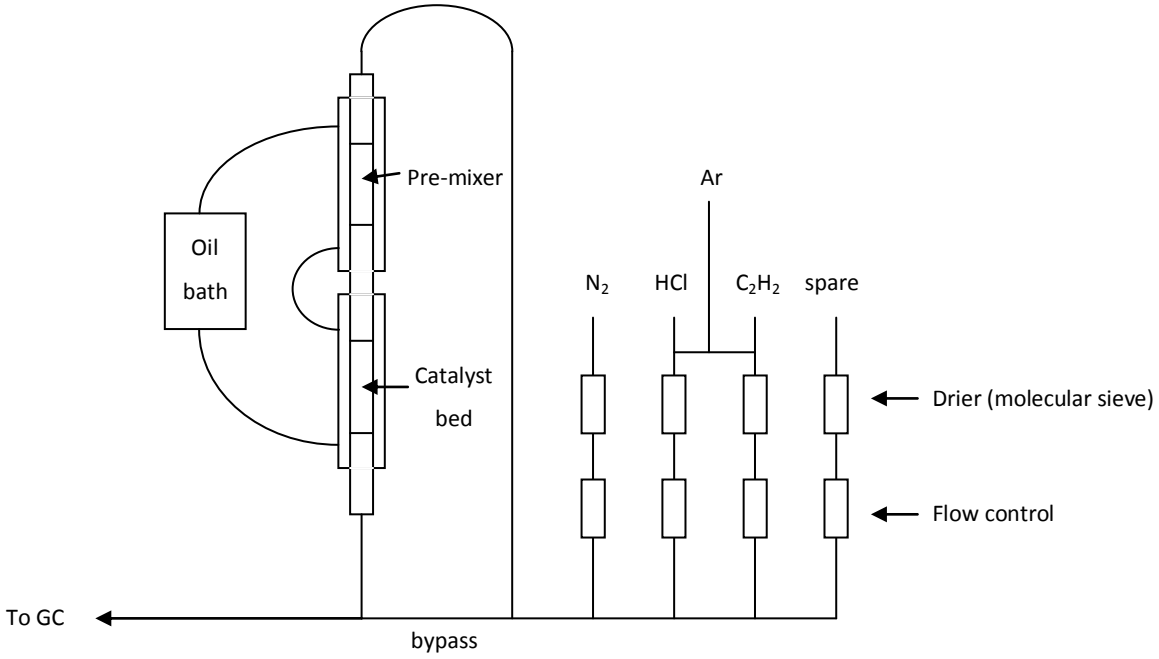

Figure 2.5: Schematic diagram of the hydrochlorination reactor.

The main body of the reactor which contained the catalyst bed was made of a modified glass reflux condenser (i.d. 6mm, length approx. 150mm), heated by circulating oil which was controlled by a Julabo ME-4 circulating oil bath. Prior to the catalyst bed there was a pre-mixer/heater in order to enhance the mixing of the reactant gas stream; this was made from a similarly modified reflux condenser, packed with 2mm glass beads which were supported by quartz wool. PTFE tubing was used at the reactor inlet and outlet, due to its inertness. In fact, in previous work where stainless steel tubing was used it was seen that reactions may take place on the reactor walls, for example oligomerisation and polymerisation[9]. In addition it reduces

the number of reactor components that may be damaged due to corrosion caused by the HCl. All of the gas inlet lines are fitted with a stainless steel bomb filled with molecular sieve to act as a drying agent to reduce moisture in the system. Flow control is by electronic mass flow controller, with the exception of the HCl, which uses needle valves and a PTFE rotameter. The HCl and acetylene lines are set up so that they may be purged with Argon.

Figure 2.6: Photograph of the reactor used for acetylene hydrochlorination.

2.4.2 Testing conditions

Catalysts (150 mg) were tested in a fixed bed micro-reactor, as described above, under a flow of 5 ml/min acetylene (0.5 bar), 6 ml/min HCl (1 bar) and 10 ml/min nitrogen (1 bar). The oil bath was set to a temperature of 185°C. SiC (2 x 2.5 g) was used to extend the bed length, above and below the catalyst itself, separated by quartz wool. These conditions, i.e. a gas flow of 21 cm^3/min and catalyst volume of 1.7 cm^3, give a gas hourly space velocity (GHSV) for the catalyst of 740h^{-1}. These are the conditions used for all data reported, unless otherwise stated. The reactor and catalyst were purged before each reaction by pressurising then depressurising the system with argon (1.5 bar) 5 times. Analysis was done by time-on-line gas chromatography, using a Varian 450GC equipped with a flame ionisation detector (FID). The catalytic activity is

described in terms of percentage acetylene conversion (see equation 2.5). To obtain the value for blank acetylene counts, prior to each reaction a number of GC runs were recorded with the reactant gases bypassing the reactor, until a stable value was achieved (usually 3-5 runs were necessary). After reaction the HCl line and reactor were purged with argon overnight.

$$\%\ acetylene\ conversion = \left(\frac{blank\ acetylene\ counts\ -\ measured\ acetylene\ counts}{blank\ acetylene\ counts}\right) \times 100$$

Equation 2.5

2.4.3 Product Analysis

2.4.3.1 Gas Chromatography

Gas Chromatography (GC) is a commonly used technique for analysing gas mixtures, based on separation of the component gases. This is done by passing the mixture to be analysed (the mobile phase) through a stationary phase inside a column, which separates the components of a mixture by the strength of their interactions with the stationary phase. In GC the mobile phase is a gas and the stationary phase can be a solid, a chemically bonded phase or an absorbed liquid film[10]. The sample to be analysed is eluted by a carrier gas (an inert gas, such as helium), which continuously flows through the system. A stronger interaction between a component and the stationary phase will result in it taking longer to pass through the column. The time at which a component is detected is known as its retention time, t_r, and can be used for qualitative analysis, if the retention time of a component is known for certain analysis conditions e.g. column type, temperature and pressure. When a component is detected it appears as a peak in the chromatogram; the area under the peak is proportional to the amount of the component present and so can be used for quantitative analysis.

There are a range of detectors that may be used with GC, for example two of the most commonly used are thermal conductivity detectors (TCDs) and flame ionisation detectors (FIDs). For analysis of the acetylene hydrochlorination reaction, a flame ionisation detector (FID) is used. The working principle of the FID is to burn the components to be detected in a flame (generated by burning hydrogen in air), which is positioned between two electrodes. Since the combustion of these components involves an ionisation process, the current between the electrodes changes when they are present (there is a baseline current resulting from the ionisation of the hydrogen). These changes in current are detected and quantified[11]. In view of this, FIDs are very suitable for use with organic chemicals, since they are easily combustible. There is a proportional relationship between the number of carbon atoms in the flame and the number of ions produced – the detector is mass-sensitive, since the signal output is related to the number of carbon atoms that pass through it[10]. This means that once a detector is calibrated, it may even be used to assist in product identification, since the number of carbon atoms in a molecule can be quantified.

For analysis of the acetylene hydrochlorination reaction, chromatographic separation was carried out using a 6ft x 1/8”stainless steel column, with Porapak N packing. An isothermal temperature programme was used, at an oven temperature of 130°C. Helium was used as a carrier gas, at a column pressure of 18.9psi. Only two major components were observed in the GC trace, acetylene (t_r = 1.3 minutes) and VCM (t_r = 6.4 minutes).

2.5 References

1. J. A. Lopez-Sanchez, N. Dimitratos, P. Miedziak, E. Ntainjua, J. K. Edwards, D. Morgan, A. F. Carley, R. Tiruvalam, C. J. Kiely and G. J. Hutchings, *Phys. Chem. Chem. Phys.*, 2008, **10**, 1921-1930.
2. N. Dimitratos, F. Porta and L. Prati, *Appl. Catal. A-Gen.*, 2005, **291**, 210-214.
3. J. W. Niemantsverdriet, *Spectroscopy in Catalysis*, 3rd edn., Wiley-VCH, 2007.
4. J. Pickworth Glusker and K. N. Trueblood, *Crystal Structure Analysis*, 3rd edn., Oxford University Press, 2010.
5. W. L. Bragg, *Proc. R. soc. Lond. Ser. A-Contain. Pap. Math. Phys. Character*, 1913, **89**, 248-277.
6. *Characterisation of Catalysts*, John Wiley & Sons, 1980.
7. H. E. Kissinger, *Anal. Chem.*, 1957, **29**, 1702-1706.
8. H. P. Boehm, W. Heck, R. Sappok and E. Diehl, *Angewandte Chemie-International Edition*, 1964, **3**, 669-&.
9. M. Conte, Cardiff University, 2006.
10. D. A. Skoog, D. M. West, F. J. Holler and S. R. Crouch, *Fundamentals of Analytical Chemistry*, 8th edn., Thomson Learning, 2004.
11. L. Szepesy, *Gas Chromatography*, Iliffe Books Ltd., 1970.

3 The Effect of Impurities in the Reactant Gas Stream

3.1 Introduction

Acetylene hydrochlorination requires the use of a corrosive reagent *i.e.* HCl in the gas phase and at high temperature. Therefore it is essential that a reactor is constructed that can withstand the problem associated with the use of such a reactant. A reactor was designed and constructed, and this chapter describes the testing that was carried out using this initial set-up.

However, during the course of the project, the reactor used for acetylene hydrochlorination needed to be rebuilt, due to severe damage caused by corrosion of stainless steel components. In order to reduce the likelihood of further damage occurring, the HCl gas was changed from technical grade (N3, 99.9%), as used for reactions described in this chapter, to electronic grade (N5, 99.999%), as used for all reactions described in subsequent chapters, due to its higher purity and, most significantly, reduced moisture content. The effect that changing the quality of this reactant gas had on the results obtained is also reported in this chapter.

3.2 Preliminary Testing

Initial catalytic testing was carried out using a standard catalyst provided by Johnson Matthey (JM), referred to throughout this thesis as Au/C-JM, to evaluate whether the results obtained were comparable to those obtained by analogous tests carried out by JM. The reactor was also used to test a catalyst made and tested according to protocols used in previous work[1] on this reaction to test reproducibility; these results are described in this section.

3.2.1 Benchmarking of JM catalyst

Initially, for comparable conditions to those used in catalyst testing by JM, higher flow rates of the reactant gases and a larger amount of catalyst than those described in chapter 2 were used. These were 60 ml/min of HCl, 50 ml/min of acetylene and 100 ml/min of nitrogen, using 1.5g of catalyst. The reactor was heated to the same temperature of 185°C. The testing results for four reactions using the Au/C-JM catalyst are shown in figure 3.1; although there is some spread in the data it can be seen that the same trend occurs – there is a steady deactivation of the catalyst from around 80% down to around 40% over the 4 hour reaction time. This is consistent with previous work which demonstrates the deactivation of Au^{3+} containing catalysts[2-4], attributed to the reduction of Au^{3+} to Au^{0}, and is the expected result from the catalyst provided.

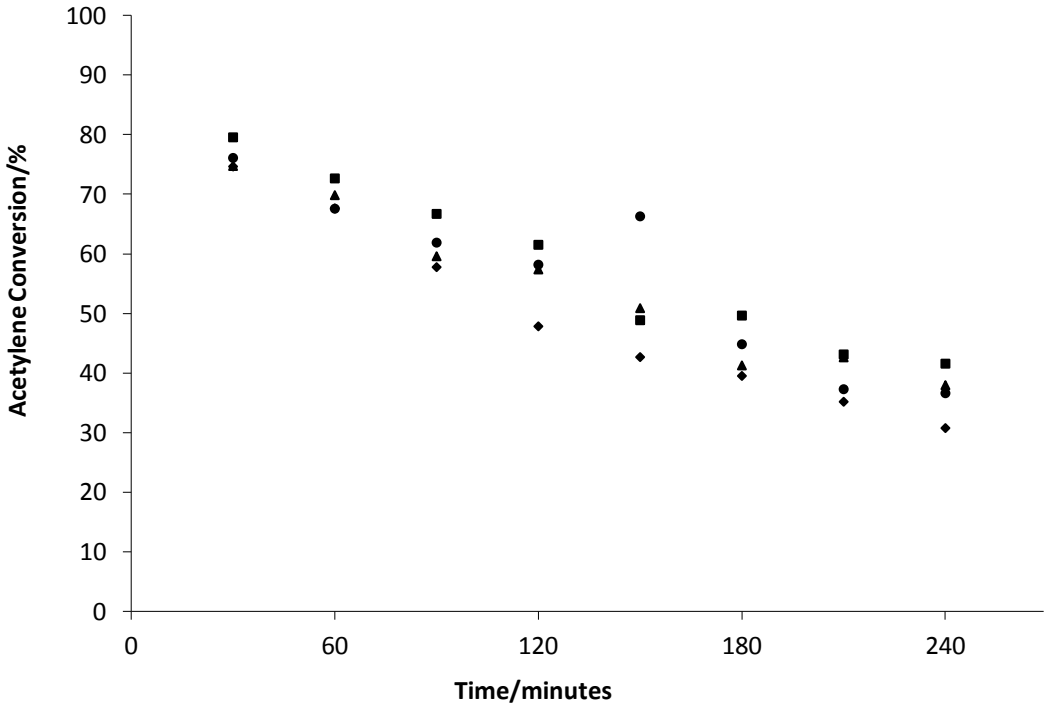

Figure 3.1: Testing of Au/C-JM under high flow rate conditions:60 ml/min HCl, 50 ml/min C_2H_2, 100 ml/min N_2, 1.5g catalyst, 185°C. Each set of data (■, ●, ▲, ◆) is a fresh 1.5g from the same batch of catalyst.

Testing of the same catalyst was then carried out under milder, scaled down conditions – 6 ml/min of HCl, 5 ml/min of acetylene, 10 ml/min of nitrogen and 150 mg of catalyst (the same temperature of 185°C was used). This was primarily for safety reasons, to limit the amount of VCM produced since it is a known carcinogen; however, it is also more economical as it significantly reduces the amount of catalyst that is needed for testing and the amount of the reactant gases used. However, in order to keep the catalyst packing and bed length in the reactor the same, the difference in the bed length was made up by using the carbon support, separated from the catalyst by quartz wool. The results can be seen in figure 3.2 and although the initial activity of the catalyst is slightly lower, at around 70%, overall the data obtained are similar to those obtained under the higher flow rate conditions and are consistent with the steady deactivation seen in previous work. The GHSV for the high- and low-flow testing conditions are calculated to have the same value, of 740 h^{-1}, due to the reduction by the same factor of both the amount of catalyst used and the flow rate of the reactant gases, so the similarity of data observed is to be expected.

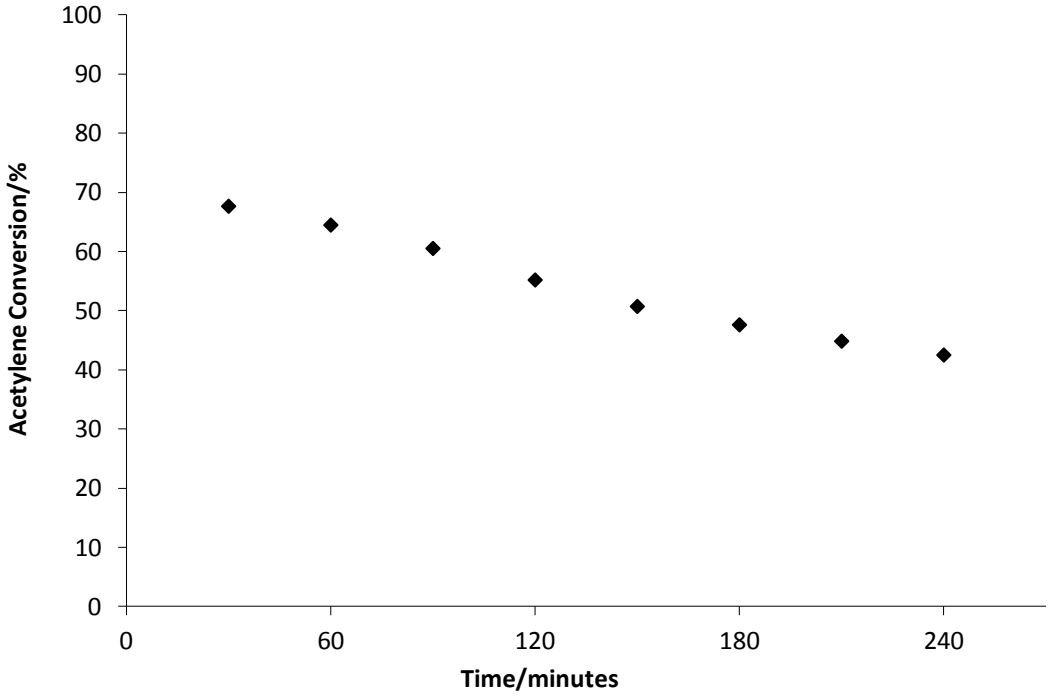

Figure 3.2: Testing of Au/C-JM under standard conditions: 6 ml/min HCl, 5 ml/min C_2H_2, 10 ml/min N_2, 150 mg catalyst, using carbon support to extend the catalyst bed.

The above results, showing consistency with activities seen previously for similar catalysts and being as expected for the Au/C-JM catalyst that was provided, indicated that the reactor was suitable for use and fresh catalysts could be prepared and tested for comparison with this standard catalyst.

3.2.2 Reproduction of catalyst preparation/testing from previous studies

It was decided to make and test a catalyst according to the methods as described in previous work concerning Au catalysts for the hydrochlorination reaction[1], with the aim of reproducing results recently obtained in a similar laboratory setting. A 1% Au/C catalyst was prepared by incipient wetness impregnation of powdered activated carbon (Darco 12-20) with a $HAuCl_4$/Aqua Regia solution. The pore volume of the carbon was first calculated, by adding water dropwise to varying masses of carbon until a paste was formed and measuring the amount of water used, which enabled the correct volume of solvent for the preparation to be used. This value was found to be 1.33 ml/g. $HAuCl_4$ (0.080g) was dissolved in aqua regia (3:1 HCl:HNO_3 by volume, 5.27 ml) and this solution added dropwise with stirring to the carbon support (3.96 g) until a paste was formed. This was then dried overnight (18h, 110°C). The catalyst (200mg) was tested under gas flows of HCl 5ml/min, C_2H_2 5ml/min and N_2 10ml/min at a temperature of 185°C; the results are shown in figure 3.3.

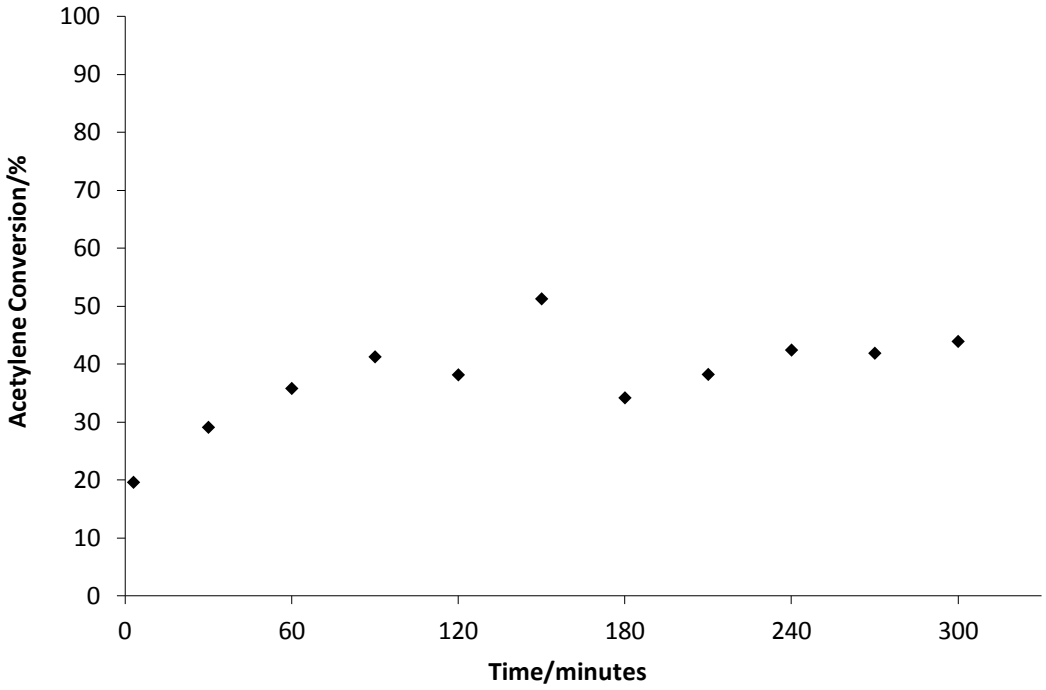

Figure 3.3: Testing data of 1%Au/C catalyst prepared by incipient wetness impregnation on Darco 12-20 carbon support and tested under conditions used in previous work: 5 ml/min HCl, 5 ml/min C_2H_2, 10 ml/min N_2, 200 mg catalyst, 185°C.

A different trend to that expected is observed, however, with an initial increase in activity which then stabilises, contrasting with the steady deactivation which is usually reported for such catalysts. Although there is a clear difference in the activity observed over the course of the reaction, when the initial activity of these catalysts under the same conditions is compared they have a similar initial activity: the catalyst prepared as described above shows 20% acetylene conversion, while in the previous work it is around 25%[1].

This catalyst was characterised by XPS since this is one of the most effective techniques for studying Au/C catalysts, in particular those used for the hydrochlorination reaction, as it provides information on the oxidation state of the gold which has been shown to be an important factor in determining the activity of these catalysts. The spectrum can be seen in figure 3.4 and shows two doublet signals, one for metallic gold at 84 and 87.7 eV and the other for Au^{3+} at 86.5 and 90.2 eV. The

signal at 86.5 and 90.2 eV is much larger, showing that the majority of the gold on the catalyst surface is present in the Au^{3+} form.

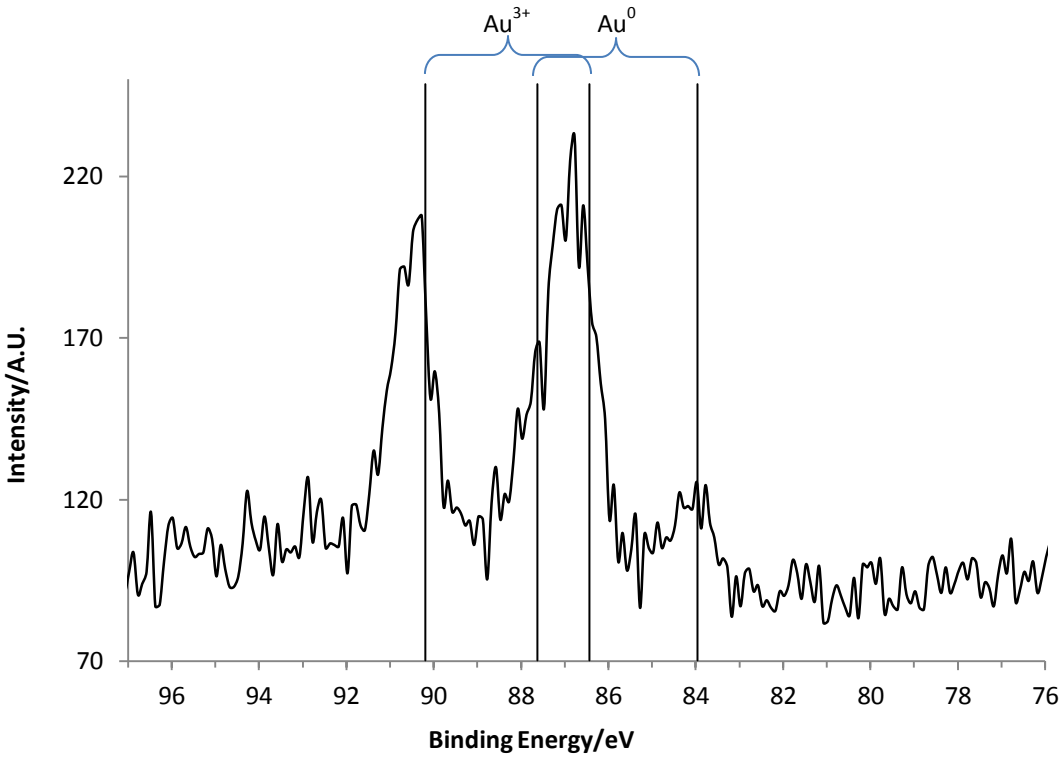

Figure 3.4: Au4f XPS spectrum of 1% Au/C catalyst prepared by incipient wetness impregnation of Darco 12-20 with $HAuCl_4$/aqua regia solution.

This differs from the catalyst from the previous work in that the XPS spectrum of that catalyst showed the majority of the gold was present in the Au^0 form, although the presence of Au^{3+} was indicated.

The XPS of these catalysts shows that they are similar in regards to the oxidation state of the gold present on the surface, in that there is Au^{3+} present in both cases, however there is significantly more Au^{3+} in the catalyst prepared for this project. This could be a determining factor in the differences in activity observed, however, it is a possibility that this is not the only reason. Another contributing factor may be differences in the reactor set-up used. As described in chapter 2, the design for the reactor used for this thesis was provided by JM and is made largely of inert materials *i.e.* the reactor itself is glass and much of the tubing used is PTFE. In contrast, while the reactor used

previously used a quartz tube to contain the catalyst bed, the majority of the rest of the tubing was made almost completely from stainless steel and so it is possible that the reactivity of this may have affected the observed activity for VCM production. For example, reactions on the stainless steel walls are possible which may affect the amount of the reactants that reach the catalyst. In addition, the methods of heating the reactors are different: previously a furnace surrounding the reactor tube was used whereas the reactor built for this project is heated by circulating hot oil around it. The reaction is known to be exothermic (ΔH = -99 kJ/mol^{-1})[5] and therefore the circulating oil may help to reduce the effect of the temperature increase, which may affect the catalyst activity.

Whilst a complete reproduction of previous work was not achieved, results showing similar initial conversion of catalysts were obtained and with the expected results being produced from testing of the industrial catalyst in the reactor which is comparable to that used by the industrial sponsors it was decided that this was sufficient to begin new experiments.

3.3 The Effect of Catalyst preparation method

In the majority of previous work on Au/C catalysts for the acetylene hydrochlorination reaction, a catalyst preparation method involving impregnation in acid has been used[2-4, 6, 7]. It is well known that the preparation method used can have a great effect on a catalyst's structure and therefore its activity, as described in the introduction to this thesis. Therefore it was decided to prepare catalysts by a number of commonly used protocols, namely wet impregnation, deposition precipitation and sol immobilisation, and to test them for acetylene hydrochlorination. These catalysts are referred to as IMP, DP and SI respectively. All catalysts had a theoretical gold loading of 1% by weight. The conditions used were 6 ml/min HCl, 5 ml/min C_2H_2, 10 ml/min N_2 and 150

mg catalyst at a temperature of 185°C. The carbon support was used to extend the catalyst bed, as described above (section 3.2.1).

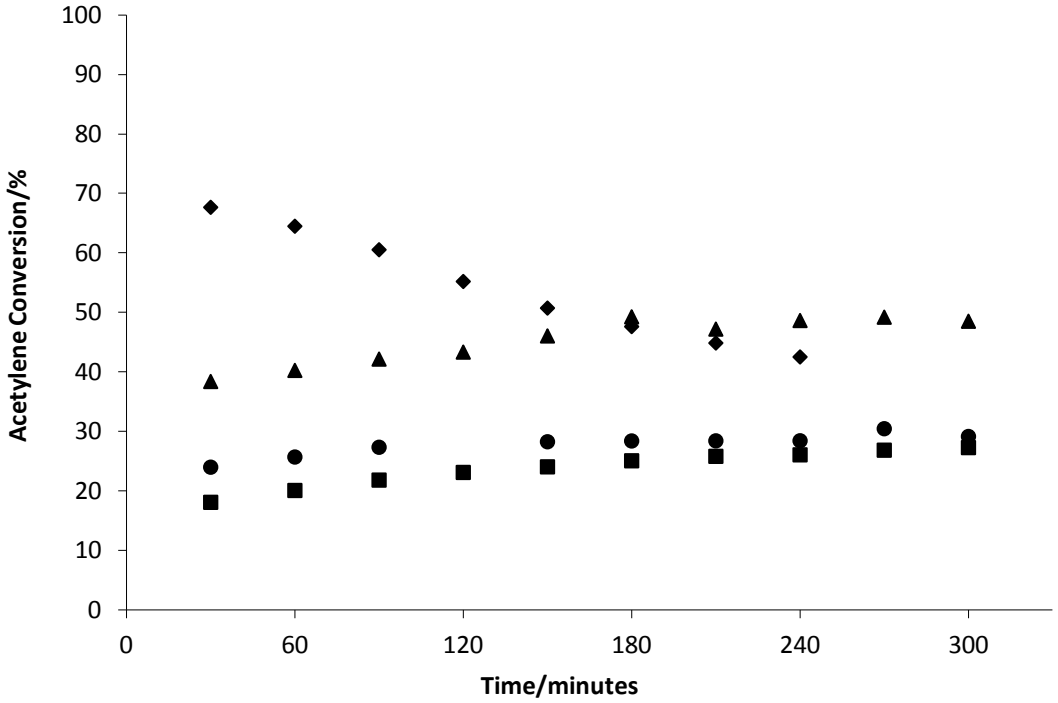

Figure 3.5: Activity of Au/C-JM (◆) and catalysts prepared by IMP (●), DP (■) and SI (▲).

Figure 3.5 shows the activity of each of these catalysts, as well as that of the Au/C-JM catalyst. In contrast to Au/C-JM, which deactivates steadily over the course of the reaction, the other three catalysts show a different activity profile, with acetylene conversion actually increasing over the first 3 hours and then stabilising. This is similar to that seen for the incipient wetness catalyst discussed earlier in this chapter, however these results should not be directly compared due to the difference in the testing conditions used. Initially, the IMP and DP catalysts have the lowest activity, of around 20% conversion, whilst the SI catalyst has around 40%. These are much lower than Au/C-JM, the initial activity of which is around 70%, however it is important to note that after 3 hours reaction time, the activity of the SI catalyst is actually greater than that of Au/C-JM.

Characterisation of these catalysts was carried out by XPS and XRD, in order to obtain information about the oxidation state and particle size of the gold. The XPS spectra for each of the four catalysts are shown in figure 3.6.

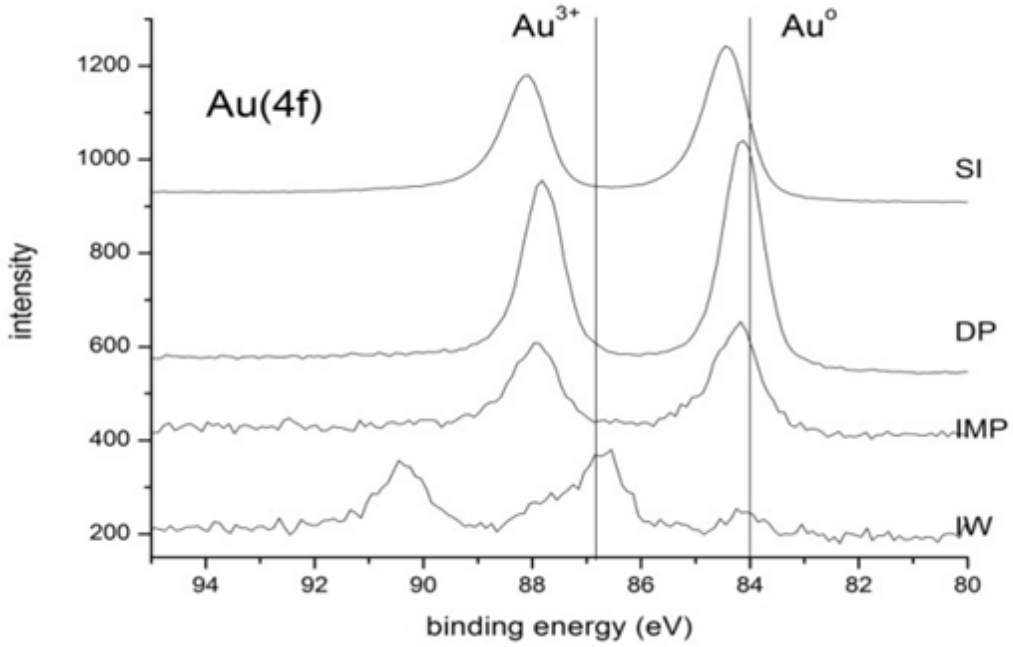

Figure 3.6: XPS spectra of catalysts prepared *via* different methods.

These results indicate that for catalysts prepared by wet impregnation, deposition precipitation and sol immobilisation methods, only metallic gold is present since there is just one doublet present, at the characteristic Au 4f binding energies for metallic gold of 84 and 87.7 eV. However, for the Au/C-JM catalyst there are two doublets present in the spectrum, one at the same Au^0 position and another, larger one at higher Au4f binding energies of approximately 86.5 and 90.2 eV, typical of Au^{3+}. This shows that the majority of the gold is in the 3+ oxidation state; this has been quantified as 59%. Since the Au/C-JM catalyst is the most active of all the catalysts at the start of the reaction, this is consistent with previous work which has attributed deactivation of Au/C catalysts for the acetylene hydrochlorination reaction at the temperature used (185°C) to the reduction of Au^{3+} to Au^0 [4]. However, there is a small

shift towards higher binding energy in the Au^0 peak position for the sol immobilisation sample. This is likely to be due to particle size effects, since the sol immobilisation method is known to give gold particle sizes in the range <10 nm, in fact 1% Au/C catalysts prepared in a similar way to the SI catalyst were shown by TEM to have a Au particle size of 3.5 +/- 1.6 nm[8]. At this range shifts in binding energy may be observed[9], with the positive shift observed for Au/C attributed to a final state effect, caused by charging of the particle during analysis[10].

XRD results are shown in figure 3.7 for all four catalysts, and for the carbon support as provided by JM. Reflections due to gold are present at 38, 44, 64 and 78° 2θ. However, these reflections can be seen only for the catalysts prepared by IMP, DP and SI methods and not for Au/C-JM, whose XRD pattern is comparable to that of the carbon support alone. This is to be expected since it is known from the XPS that very little metallic gold is present, so it is unlikely that the long range order necessary to produce a reflection will occur. It also suggests that if there are particles of metallic gold, they are very small (approximately 1-5nm, less than those prepared *via* the sol immobilisation method, since reflections are still visible in the XRD pattern of the SI catalyst) and highly dispersed.

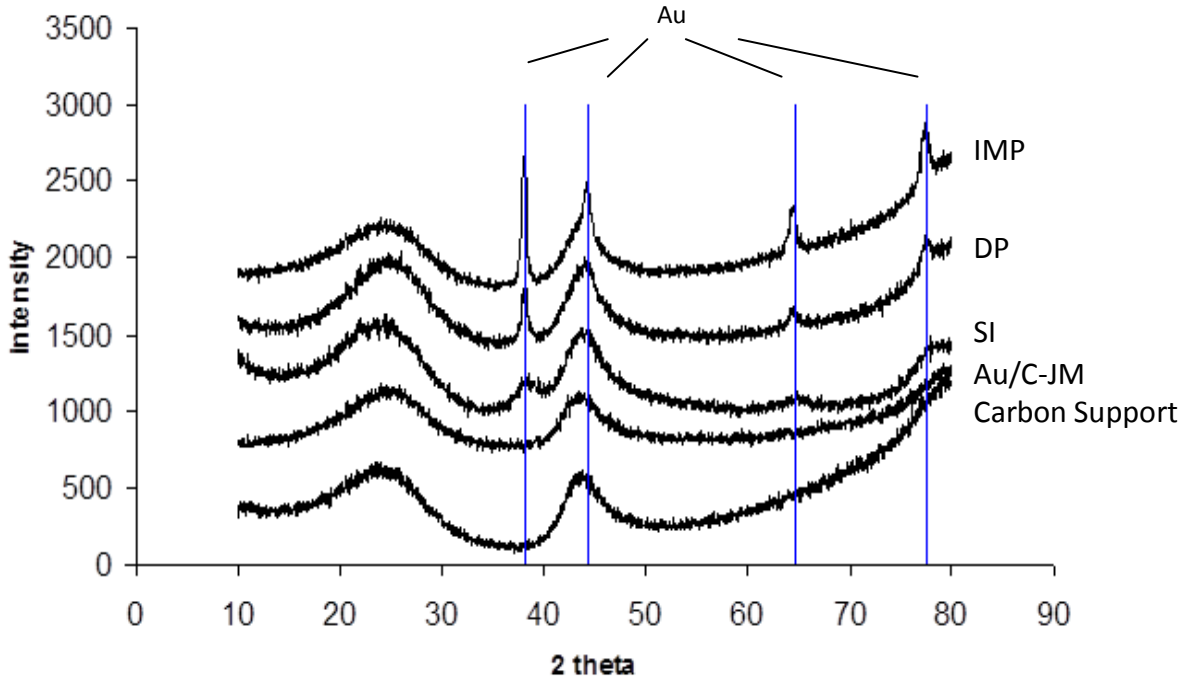

Figure 3.7: XRD patterns for catalysts prepared *via* different methods: impregnation (IMP), deposition precipitation (DP) and sol immobilisation (SI), the Au/C-JM standard catalyst and the carbon support. The vertical lines show the position of reflections due to Au.

From the width of the reflections due to gold on the other samples, it can be seen that the relative size of the gold particles is IMP>DP>SI, since narrower reflections arise from a larger crystallite size. These results are also as expected from literature concerning catalysts made by these methods[11]. Impregnation commonly gives large Au particle sizes due to the residual chloride which aids sintering during the drying process, whereas the high pH used during DP preparation means that more of the chloride is substituted by hydroxide and so when the mixture is washed more of the chloride is removed, minimising this effect[12]. Catalysts prepared by sol immobilisation typically have metal particle sizes of just a few nanometres[13, 14].

The Scherrer equation was used to calculate the size of the gold particles on each of the three catalysts prepared *via* alternative methods. This could not be done for the JM catalyst, however, due to the absence of reflections due to gold. The results are shown in table 3.1.

Sample	FWHM of (111) reflection at 38° 2θ	Calculated particle size/nm
IMP	0.474	22
DP	0.611	17
sol	2.193	10

Table 3.1: Size of gold particles on catalysts prepared *via* different methods, as calculated using the Scherrer equation.

The results from the catalysts prepared by alternative methods to impregnation in acid are of considerable interest, since before reaction they only contain metallic gold, yet still give significant initial activity (albeit lower than for Au^{3+} containing catalysts). This suggests that metallic gold may possibly also be an active site for acetylene hydrochlorination, and that if this is the case there may be particle size dependence, since the initial activity of these catalysts has an inverse correlation with particle size, *i.e.* the smaller the size of the gold particles, the higher the activity. Although this is not strictly observed for the DP and IMP catalysts, they both have a gold particle size which is much larger than the SI catalyst, and both have lower activity – the effect may simply not apply beyond a certain limit or there may be other contributing factors, for example particle morphology. However, it is likely that the mechanism for this reaction involves a redox cycle, as indicated by the correlation of activity with standard electrode potential and has been suggested previously[3]. It is therefore also possible that while the catalysts do not contain any Au^{3+} prior to reaction, the oxidised gold species are created *in-situ* under the reaction conditions - an excess of HCl is used and it has been shown previously that treatment with gaseous HCl is able to regenerate the activity of a deactivated catalyst, thought to be due to formation of oxidised gold[3]. It has also been shown that treatment with HCl prior to reaction leads to enhanced activity[7]. In this case, it could be that the amount of Au^{3+} generated by the excess HCl is sufficient to give the observed activity. This could also be a possible explanation for the initial increase in activity that is observed – as more Au^{3+} is being generated, the activity increases and then stabilises when Au^{3+} generation reaches an equilibrium with the reaction taking place.

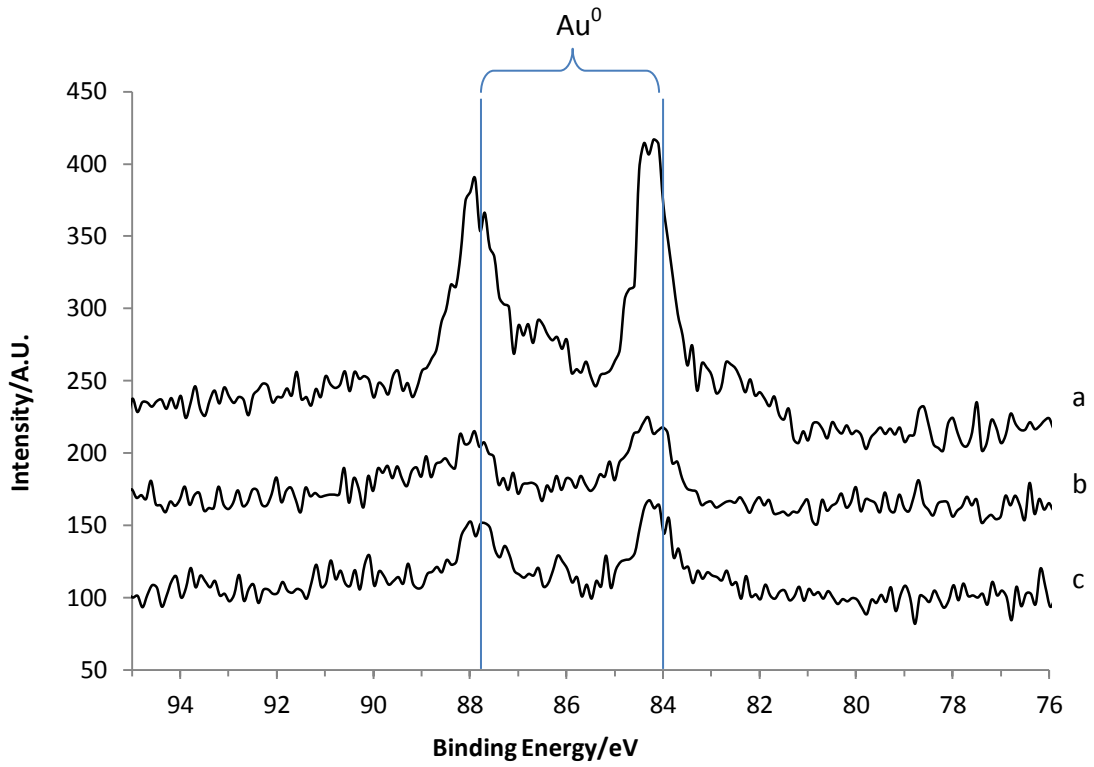

Figure 3.8: XPS spectra of a) SI, b) DP and c) IMP catalysts after use.

Characterisation of catalysts after reaction was also carried out by XPS and XRD. XPS spectra are shown in figure 3.8 and the reduction in intensity of the signal shows a large reduction in the amount of gold present on the surface for catalysts prepared by IMP, DP and SI. This could be due to remaining products on the surface of the gold particles, or polymerisation occurring and covering the gold on the surface, which is known to be a deactivation mechanism of these catalysts[4]. XRD, however, indicates a significant increase in the size of metallic gold particles, which suggests that sintering has occurred during the course of the reaction. This sintering could also lead to a decrease in intensity of XPS signals as observed, since if the same amount of gold is present in larger particles then a smaller amount of that gold is on the surface, and therefore within the detection limits of XPS.

3.4 The Effect of Higher Purity HCl

The results described so far were obtained from catalyst testing using technical grade HCl gas. However, as described at the start of this chapter, due to damage caused by corrosion this was changed to a higher purity electronic grade, in order to reduce the level of moisture in the system. This section describes the effect of using this higher purity gas.

Testing results for Au/C-JM, using electronic grade HCl and carbon support bed extension are shown in figure 3.9, with the technical grade data for comparison. It can be seen that there is a significant difference in the observed activity, perhaps the most interesting point being that there is no deactivation of the catalyst over the reaction time. In addition, the initial activity is greater, at almost 90%.

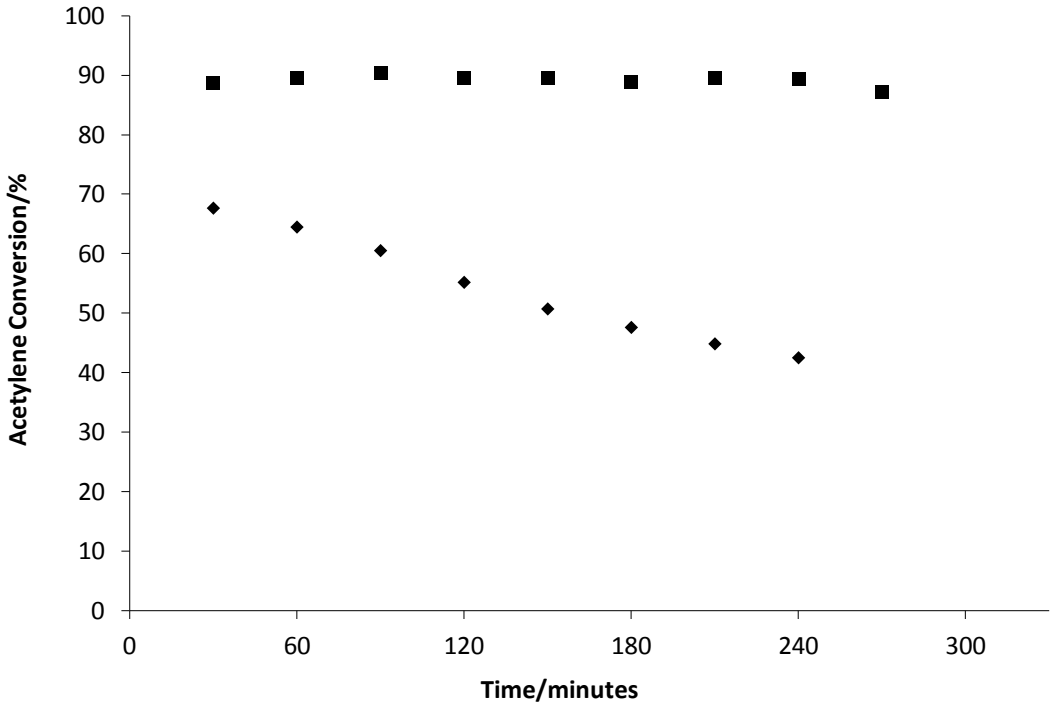

Figure 3.9: Activity of catalyst JM M07565 using electronic grade (■) and technical grade (◆) HCl gas.

The IMP, DP and SI catalysts were also tested using the electronic grade HCl, the results are shown in figure 3.10. As seen for Au/C-JM, there is a change from the activity that was seen previously; the activity is fairly stable, and there is no initial increase in activity observed. The initial activity is also higher than was observed using the technical grade HCl, with all three catalysts giving between 45 – 55% acetylene conversion. To understand the cause of these differences in activity, the impurities present in the technical and electronic grade HCl gases used were compared. These are shown in table 3.2.

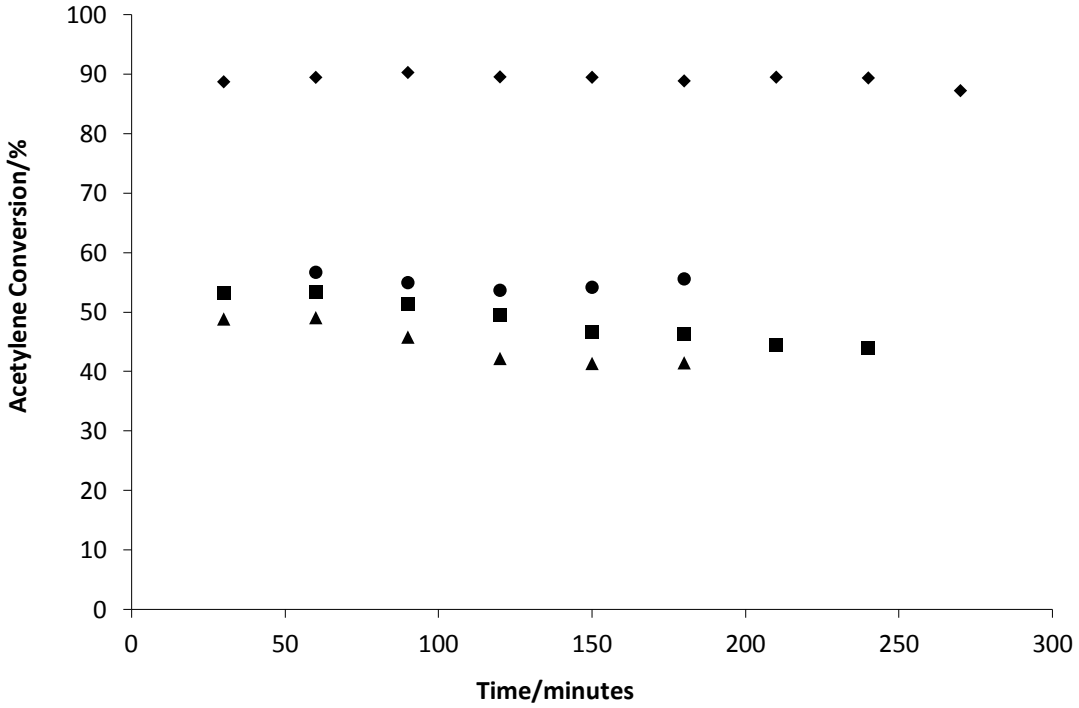

Figure 3.10: Activity of Au/C-JM (◆) and catalysts prepared by IMP (●), DP (■) and SI (▲) using electronic grade HCl.

Whilst there are large differences in the amount of a number of impurities, the most significant difference is the hydrogen impurity, unspecified for electronic grade but 350ppm in technical grade. Although there is a much larger difference in the amount of nitrogen present in the two gases, nitrogen is added to the reaction stream as a diluent, so this can be considered to be of negligible importance. Since hydrogen is a reducing agent and the previous deactivation of the catalyst was attributed to

reduction of the Au^{3+}, it was considered that this could be a key factor in the activity differences. Therefore, it was decided to run a reaction with the addition of hydrogen to the reactant gases, by using a 10% H_2/Ar mixture in place of the nitrogen diluent, the results of which are shown in figure. 3.11.

Impurity	Technical Grade (N3) Concentration/ppm	Electronic Grade (N5) Concentration/ppm
Moisture	10	1.5
O_2	125	1
N_2	500	2
CO_2	15	5
H_2	350	-
THC (Total Hydrocarbon)	-	1

Table 3.2: Impurities in technical and electronic grade HCl.

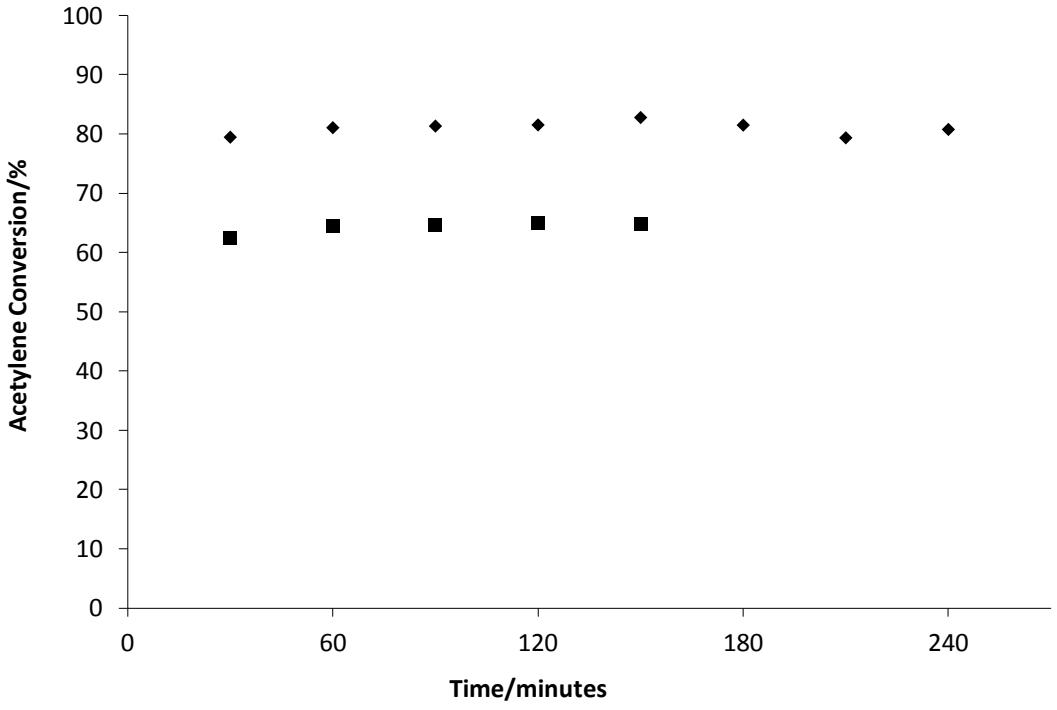

Figure 3.11: Activity of Au/C-JM using electronic grade HCl under standard conditions (◆) and with hydrogen (10%/Ar) added to the gas stream (■).

It can be seen that the activity is lower when hydrogen is added to the reactant gas stream, by around 20% acetylene conversion. However, it would be expected that if the change in activity after using a higher grade HCl was due to the hydrogen impurity, a far more severe drop in activity would be seen since the amount of hydrogen used in the hydrogen addition experiment is in great excess of the hydrogen impurity found in the HCl. Deactivation of the catalyst as seen previously may also be expected, yet does not occur. Therefore the presence of the hydrogen impurity may be a contributing factor to the difference in activity, but cannot be the sole cause. Other impurities that may be responsible are oxygen and moisture. The effect of the moisture cannot be investigated, due to the potential damage to the reactor from corrosion, although it may be possible to investigate the effect of oxygen by using air instead of the nitrogen diluent. However, it has been shown that treatment with air may be used to regenerate the activity of a used catalyst that has deactivated, *via* removal of carbonaceous deposits on the catalyst surface rather than oxidation of the gold[3], which is contradictory to the possibility of a deactivating effect on the catalyst.

3.5 Activity of the Carbon Support

Since under the milder testing conditions the carbon support, which was thought to be inert for the acetylene hydrochlorination reaction, was being used to extend the catalyst bed length, it was necessary to determine if this was in fact the case. This became of particular importance once a number of catalysts with low Au loadings had been tested and found to have significant activity; this section describes the experiments involving the low Au loadings and the subsequent testing of the activated carbon support.

3.5.1 Catalysts with low Au loading

It was decided to investigate the activity for acetylene hydrochlorination of catalysts with a gold loading of lower than 1%, following the attempted sol immobilisation

preparation on carbon extrudate as described in chapter 2 (experimental). As the mixture was still red in colour after the support had been added, the gold sol had not been adsorbed onto the support – the mixture was filtered to recover the extrudate and after drying overnight this was tested as a catalyst. The original reactor set-up, with technical grade HCl, was used and the results are shown in figure 3.12; it can be seen that after 3 hours reaction time the activity has stabilised, with an acetylene conversion of around 20% obtained.

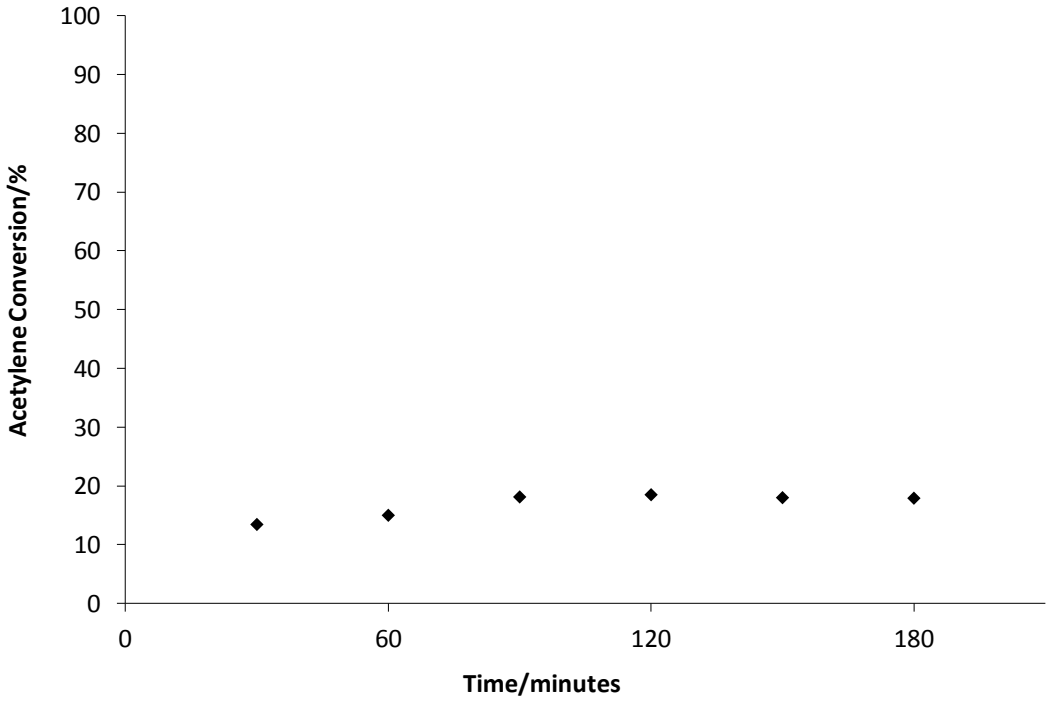

Figure 3.12: Activity of carbon extrudate recovered from an unsuccessful sol immobilisation catalyst preparation. Testing was carried out using the original reactor set-up, with technical grade HCl.

This is comparable to the initial activity of the 1% Au/C DP and IMP catalysts and so it was decided to make some catalysts of very low gold loadings, since if they are active this has a potential benefit to industry due to the lower cost of such a catalyst. Catalysts were prepared by wet impregnation (in H_2O), with calculated gold loadings of 0.1 % and 0.005 %. The testing results are shown in figure 3.13 and were obtained using the original reactor set-up, with technical grade HCl. Each of these catalysts

displays a similar activity, with an initial acetylene conversion of 10% which then slightly increases then stabilises at close to 20% acetylene conversion. The small difference in activity between these catalysts and those with 1% gold, and the significant activity still observed when the Au loading was known to be extremely low, indicates that the Au may not be the only source of activity, and so the activity of the carbon support was investigated.

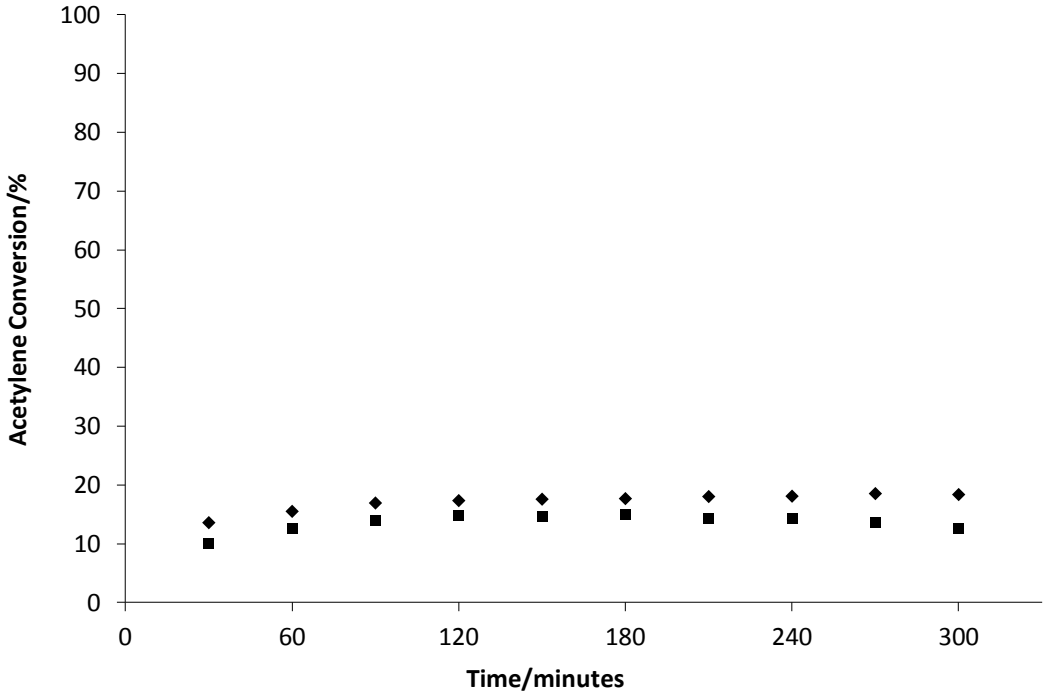

Figure 3.13: Activity of catalysts prepared with low Au loadings: 0.1% (◆) and 0.05% (■).Testing was carried out using the original reactor set-up, with technical grade HCl.

3.5.2 Testing of the carbon support

Following significant acetylene conversions of around 15 - 20% being observed for catalysts prepared with extremely low Au loadings, the carbon support itself was tested, although it should be noted that this was carried out on the new reactor set-up using electronic grade HCl. Figure 3.14 shows testing data for the carbon support alone, using a carbon bed extension; a relatively stable conversion of approximately

45% is seen which confirms the suspected activity of the carbon. This is in fact higher than would be expected given the previous results and shows that the change in the grade of HCl used may enhance the activity of the carbon support as well as that of the gold containing catalysts. This activity is similar to that of the metallic gold containing catalysts under the same conditions (see figure 3.10), and so it was decided to find a different material to extend the catalyst bed length. Silicon carbide (SiC) was tested and found to be inert for the reaction, with no acetylene conversion observed, and so was chosen to be used instead of the carbon support to extend the catalyst bed length for future testing.

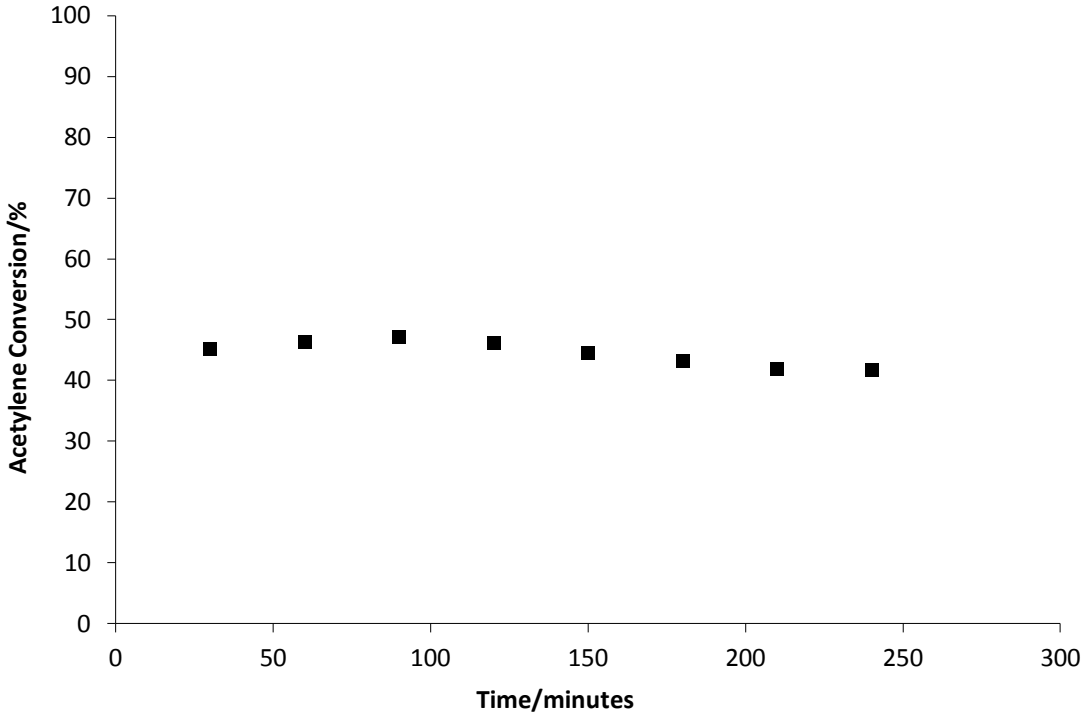

Figure 3.14: Activity of the carbon support, using a carbon bed extension. Testing was carried out using the new reactor set-up, with electronic grade HCl.

Testing data for the carbon support, using a SiC bed extension, is shown in figure 3.15. An activity of around 10% acetylene conversion is observed, which is possibly due to the presence of trace amounts of metals such as aluminium or potassium that are commonly found in carbon materials.

Testing of the four catalysts (Au/C-JM, SI, DP and IMP) was then carried out using SiC instead of the carbon support for the catalyst bed extension; these results are shown below in figure 3.16 and are those used in Chapter 4 for discussion of the effect of catalyst preparation method. The activity for each sample has decreased by at least 10% conversion, showing that the use of the carbon support to extend the bed length in the reactor was indeed affecting the results.

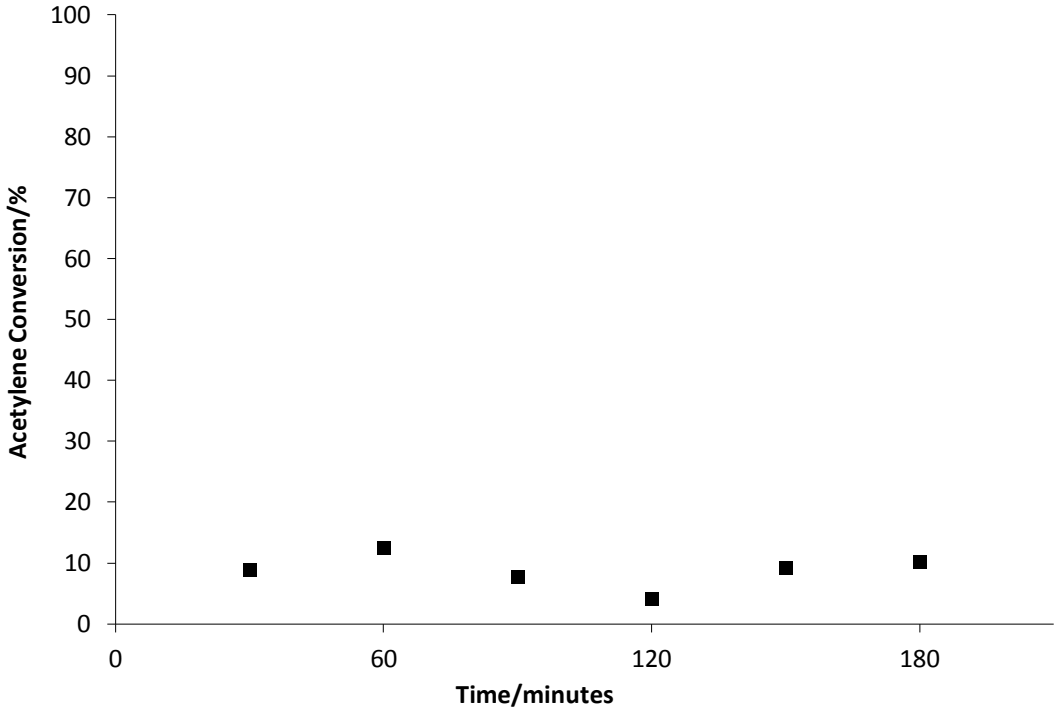

Figure 3.15: Activity of carbon support using SiC bed extension. Testing was carried out using the new reactor set-up, with electronic grade HCl.

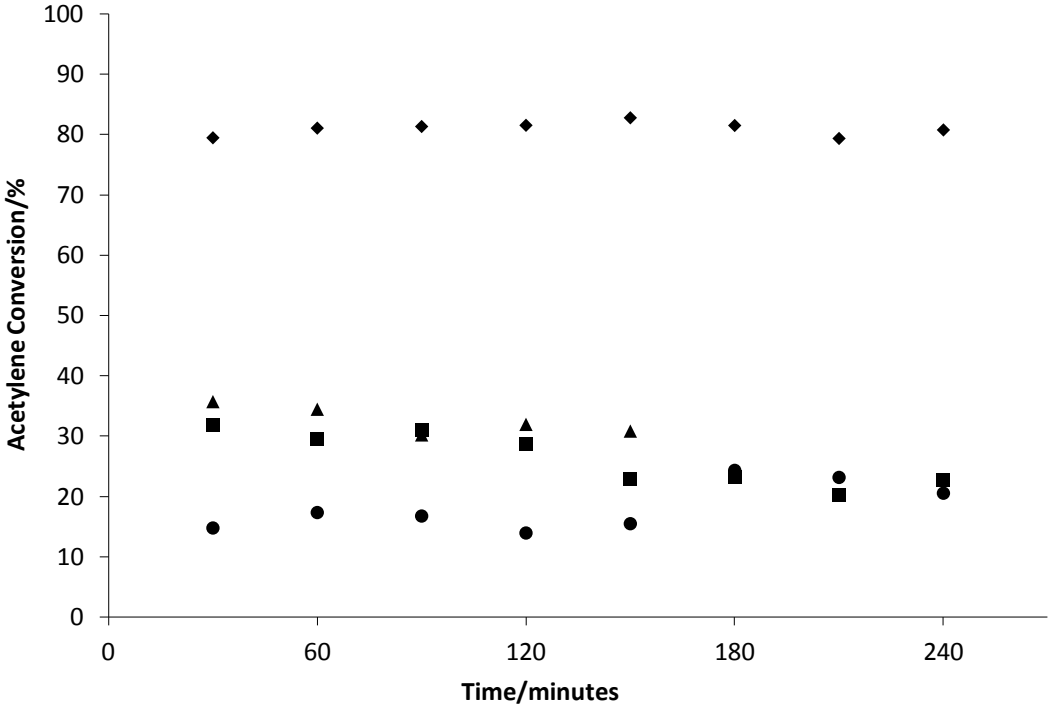

Figure 3.16: Activity of Au/C-JM (◆) and catalysts prepared by IMP (•), DP (■) and SI (▲). Testing was carried out using electronic grade HCl and SiC bed extension.

3.6 Conclusions

This chapter has detailed the initial stage of the project, which involved the building of the reactor for acetylene hydrochlorination and initial experimentation which led to the testing conditions being optimised for the work which the following chapters are based on.

Two key discoveries that were made during this initial testing are the activity of the carbon support and the effect of the purity of the reactant gases used. The activity of the carbon support, although relatively low at around 10 – 15%, is significant in terms of the activity that is observed for 1% Au/C catalysts. It is also important as the carbon support was being used to extend the catalyst bed length in the reactor, which affected the observed activity of the catalysts being tested under these conditions. The cause of this activity is also something that could be investigated further; activated carbon frequently contains metal impurities and it is known that many

metals are able to catalyse the hydrochlorination of acetylene, so it would be of interest to remove these impurities, for example by acid washing, and test if it is the presence of these metals, or perhaps a feature of the carbon itself such as surface functional groups that leads to the activity.

The change from technical grade to electronic grade HCl in order to reduce the damage caused by moisture impurities had the added effects of both increasing the acetylene conversion that was observed and changing the reaction profile, in that steady deactivation of the Au/C-JM catalyst no longer occurred. While the cause of this is as yet uncertain it is likely to be in part due to the lower hydrogen content, since addition of hydrogen to the reaction led to a lower activity, but did not exhibit the severe drop in activity that should be expected if it were solely responsible for the differences that are observed. The other impurities that differ significantly between the two gases are moisture and oxygen, however, whilst investigating the effect of moisture is undesirable due to the aforementioned corrosion problems, the effect of oxygen is something that could be investigated further.

Interesting results were obtained from testing catalysts prepared *via* different methods, with catalysts known to contain only Au^0 showing a different activity profile to any seen previously, initially increasing in activity and then stabilising, while the Au/C-JM catalyst displayed the same steady deactivation as reported previously for such catalysts which are known to contain large amounts of Au^{3+}. Perhaps most significantly after 3h reaction time the catalyst prepared by SI was more active than the standard provided by JM, due to the initial increase in activity of the former and deactivation of the latter.

3.7 References

1. M. Conte, Cardiff University, 2006.
2. M. Conte, A. F. Carley and G. J. Hutchings, *Catal. Lett.*, 2008, **124**, 165-167.
3. B. Nkosi, M. D. Adams, N. J. Coville and G. J. Hutchings, *J. Catal.*, 1991, **128**, 378-386.
4. B. Nkosi, N. J. Coville, G. J. Hutchings, M. D. Adams, J. Friedl and F. E. Wagner, *J. Catal.*, 1991, **128**, 366-377.
5. M. Conte and G. J. Hutchings, in *Modern Gold Catalyzed Synthesis*, eds. F. D. Toste and A. S. K. Hashmi, Wiley VCH Verlag GmbH, Editon edn., 2011.
6. M. Conte, A. F. Carley, G. Attard, A. A. Herzing, C. J. Kiely and G. J. Hutchings, *J. Catal.*, 2008, **257**, 190-198.
7. M. Conte, A. F. Carley, C. Heirene, D. J. Willock, P. Johnston, A. A. Herzing, C. J. Kiely and G. J. Hutchings, *J. Catal.*, 2007, **250**, 231-239.
8. N. Dimitratos, J. A. Lopez-Sanchez, D. Morgan, A. Carley, L. Prati and G. J. Hutchings, *Catal. Today*, 2007, **122**, 317-324.
9. G. C. Bond, C. Louis and D. T. Thompson, *Catalysis by Gold*, Imperial College Press, 2006.
10. R. Meyer, C. Lemire, S. K. Shaikhutdinov and H. Freund, *Gold Bull.*, 2004, **37**, 72.
11. G. C. Bond and D. T. Thompson, *Cat. Rev. - Sci. Eng.*, 1999, **41**, 319-388.
12. F. Moreau, G. C. Bond and A. O. Taylor, *J. Catal.*, 2005, **231**, 105-114.
13. N. Dimitratos, A. Villa, C. L. Bianchi, L. Prati and M. Makkee, *Appl. Catal. A-Gen.*, 2006, **311**, 185-192.
14. F. Porta, L. Prati, M. Rossi, S. Coluccia and G. Martra, *Catal. Today*, 2000, **61**, 165-172.

4 Chemistry of *Aqua Regia* and its effect in the preparation of Au/C catalysts

4.1 Introduction

It has been shown that for acetylene hydrochlorination, the activity of carbon-supported metal chloride catalysts can be correlated with the standard electrode potential of the metal[1] and as a result of this, gold-based catalysts have been shown to be the most active[2]. A further benefit of using gold catalysts for this reaction is that they show a much higher selectivity (>99%) to the desired product, VCM. This was illustrated in a recent study by Conte et.al. where bimetallic catalysts were investigated for acetylene hydrochlorination and the selectivity was found to decrease with addition of increasing amounts of another metal to the gold[3]. For these reasons, monometallic gold catalysts remain the focus of this project. It is known that preparation of 1% Au/C catalysts *via* an impregnation method using $HAuCl_4$ dissolved in *aqua regia* produces catalysts which contain a significant amount of Au^{3+} (*ca.* 30-40%) and have good activity for the gas-phase hydrochlorination of acetylene[1, 4]. It has been shown that this Au^{3+} is key to the activity of the catalysts[5] and that the *aqua regia* could be an important factor in producing this cationic gold, since deactivated catalysts have been treated by boiling in *aqua regia* and regeneration of both Au^{3+} and activity is observed[6]. Therefore a detailed investigation into the preparation of Au/C catalysts and how this affects their activity for the acetylene hydrochlorination reaction was carried out. The effect of the use of *aqua regia* during preparation in particular was investigated in some detail.

All catalyst testing reported from this point onwards was carried out under the standard conditions as described in Chapter 2.

4.2 The Effect of catalyst preparation method

4.2.1 Catalysts prepared by alternative methods

As described in Chapter 3, catalysts were prepared by a number of different methods and tested for acetylene hydrochlorination, for comparison with catalysts made by impregnation in acid as are typically used for this reaction. It was found that catalysts prepared by IMP, DP and SI are less active than Au/C-JM (a catalyst provided by Johnson Matthey of which preparation details are undisclosed due to confidentiality, though it is known to have been prepared by impregnation in acid) although they still have a significant activity, with initial acetylene conversions of around 15%, 30% and 35% respectively (figure 4.1).

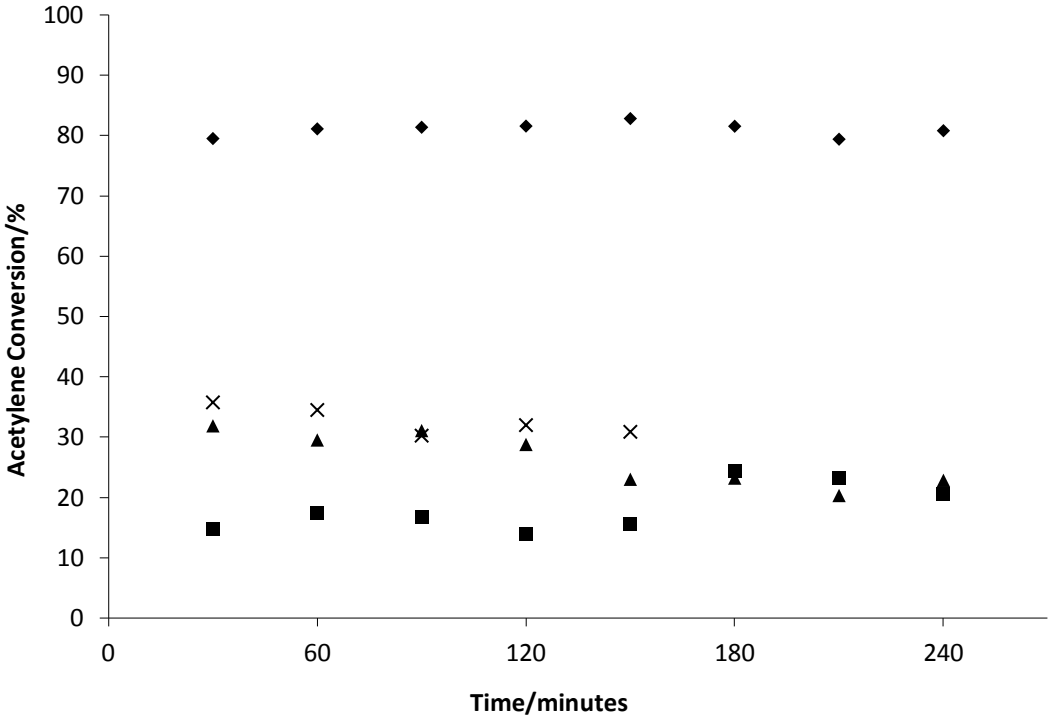

Figure 4.1: time-on-line activity for 1% Au/Catalysts prepared by different methods – SI (×), DP (▲), IMP (■) and Au/C-JM (♦)

Characterisation of these catalysts by XRD and XPS is described in detail in chapter 3 (section 3.3). It was found that the majority of gold on the surface of Au/C-JM is in the 3+ oxidation state, whereas in the IMP, DP and SI catalysts only metallic gold is

observed. The Scherrer equation was used to determine the size of the metallic gold particles on these catalysts from their XRD patterns and as expected the relative gold particle size was IMP>DP>SI. These observations suggest that whilst Au^{3+} has been shown to be responsible for the activity of Au/C catalysts for acetylene hydrochlorination, metallic gold may also be an active site.

4.2.2 Further Investigation of Sol Immobilisation Method

Since the catalyst prepared using the sol immobilisation technique gave the best activity of those not made by impregnation in acid, the preparation method was investigated in a number of ways in order to enhance the activity of this material. A catalyst was prepared omitting the addition of $NaBH_4$, the reducing agent, to see if any Au^{3+} could be obtained on the Au particles and lead to an increase in activity. Also, it has been seen for other reactions using gold catalysts prepared by sol immobilisation that removing the protective PVA ligands can improve catalyst activity[7] and it has been shown that the activity of Au-Pd/C catalysts for benzyl alcohol oxidation and H_2O_2 production can be enhanced by thermal treatment at 200°C, with this being attributed to partial removal of the PVA ligands[8]. A sample of catalyst prepared using the standard sol immobilisation method was therefore calcined (200°C, 3h, ramp rate 10°C/min). In addition, a sol immobilisation catalyst was prepared on a titania support.

The activity of these catalysts is shown in figures 4.2 – 4.4. All of the above catalysts made by sol immobilisation show a similar initial activity of around 20% acetylene conversion, which is lower than that observed for the standard SI catalyst. The calcined catalyst shows an initial decrease in activity, which stabilises at around 15% conversion and then increases again after four hours to reach a similar conversion to its initial activity by the end of the reaction, however, both the catalyst prepared without using $NaBH_4$ and the one prepared on a titania support steadily deactivate during the reaction time, although the deactivation of the titania catalyst is much larger: after 4 ½ hours only around 3% conversion is obtained. This suggests that the interaction of the gold with the support may be an important factor in the catalyst activity.

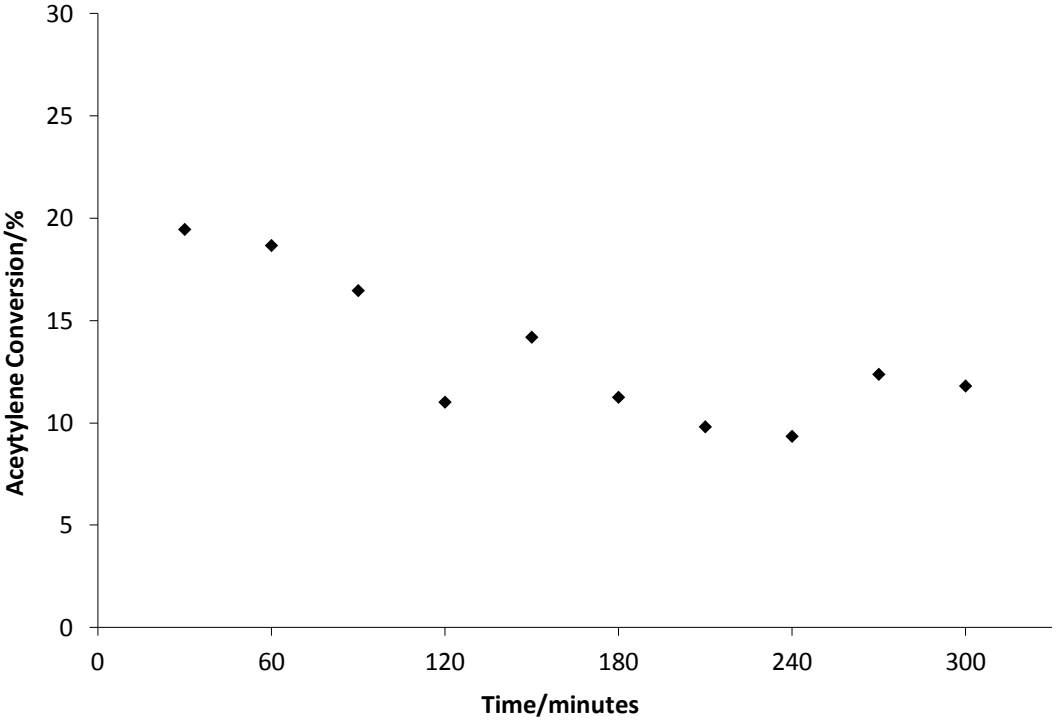

Figure 4.2: Activity of 1% Au/C catalyst prepared using sol immobilisation method, without the addition of $NaBH_4$.

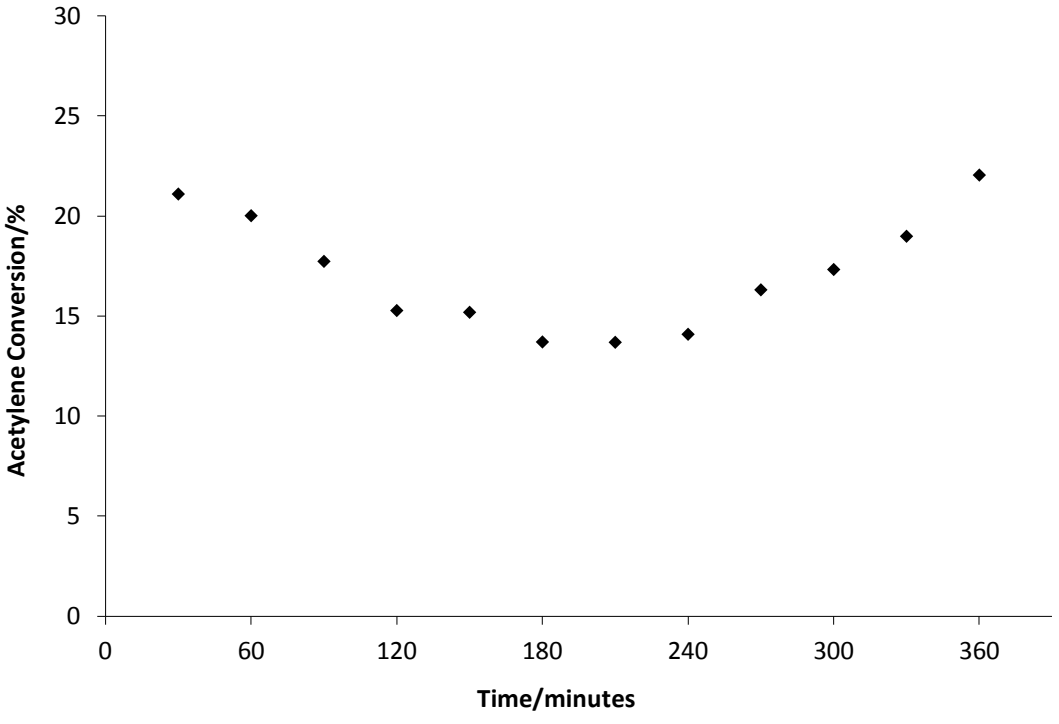

Figure 4.3: Activity of 1% Au/C catalyst prepared by sol immobilisation, calcined for 3h at 200°C.

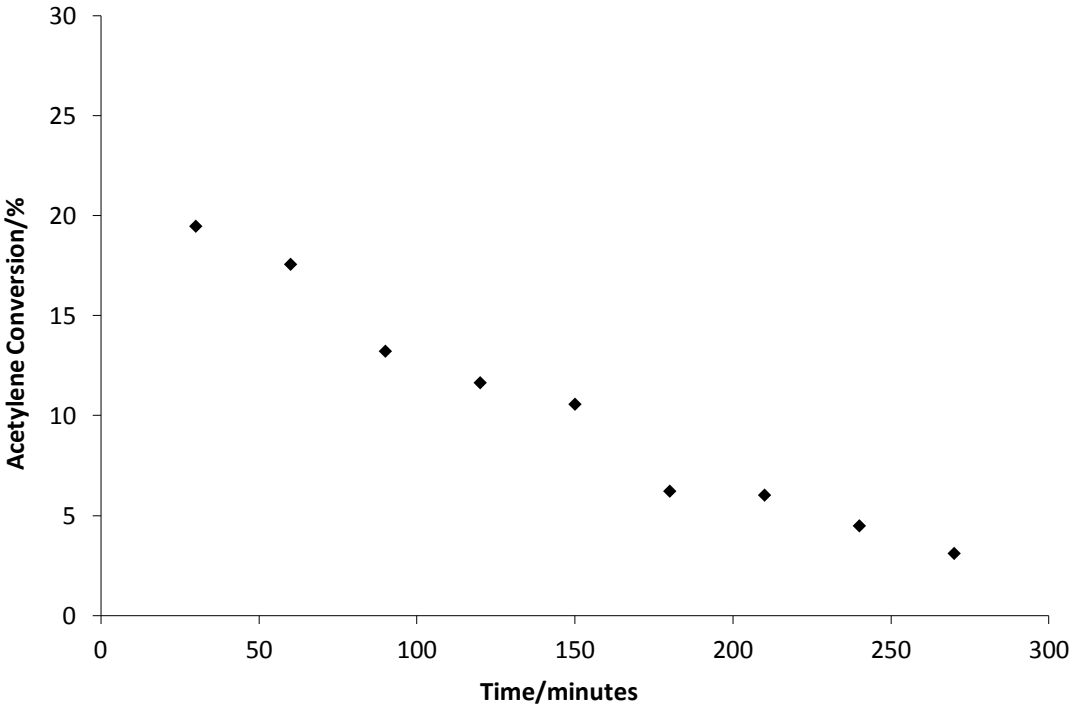

Figure 4.4: Activity of 1% Au/TiO_2 catalyst prepared by sol immobilisation.

It is known that the morphology of gold nanoparticles can vary depending on the support that is used, for example greater wetting being observed for titania than carbon resulting in particles which are less spherical in shape and have a greater area of contact with the support[9]. This difference in shape may affect the activity of the catalysts, for example due to different possible locations of active sites at particle edges or their interaction with the support at the perimeter of the particles. If a small, undetectable amount of Au^{3+} were present on the catalyst, its location and reactivity might therefore be different for the different supports. In addition, the large amounts of oxygen present in titania may react to form gold oxide, quenching the active sites. The activity of the 1% Au/C catalyst prepared by sol immobilisation is not enhanced by either the omission of the $NaBH_4$ during the preparation, or the calcination of the catalyst. This could be due to a number of reasons, for example perhaps without the $NaBH_4$ metallic Au nanoparticles of sufficient size are not formed. Also the removal of the PVA ligands may not have as significant effect as hoped as they could also be vulnerable to attack under the acidic reaction conditions, and therefore removed during reaction anyway.

Although it is of interest that catalysts known to contain very little Au^{3+} do show activity for the acetylene hydrochlorination, by far the highest activity was observed for the catalyst provided by JM, prepared by impregnation in acid, so it was decided to focus on this type of preparation and investigate it further, with a view to catalyst optimisation.

4.3 The effect of variations in the acid impregnation method

As described previously, it is known that preparation of Au/C catalysts by impregnation in acid produces catalysts containing a significant amount of Au^{3+}, which is thought to be the main active site for the acetylene hydrochlorination reaction. In order to gain further understanding of this effect, with the aim of producing higher activity catalysts, a number of experiments were carried out. Catalysts were prepared in the typical way (described in detail in chapter 2), using *aqua regia* as an impregnation solvent for $HAuCl_4$, and the drying temperature was varied. The effect of using the component acids of *aqua regia*, HCl and HNO_3, individually was also investigated, as well as different ratios in the acid mixture.

4.3.1 The effect of drying temperature

Testing of a 1% wt Au/C catalyst prepared *via* impregnation in *aqua regia* and dried at 110°C gave an activity profile different to any seen previously: initial low activity (*ca*. 15%) followed by an increase in activity after around 3 hours' reaction time (figure 4.5). One possible explanation for this was that since the reaction temperature is higher than the catalyst drying temperature, Au nanoparticles may be forming during reaction, and although Au^{3+} is the active site these nanoparticles may also be a contributing factor to activity if, as suspected, a redox cycle is involved. Consequently, 1% Au/C catalysts were made by the same method but dried at a slightly higher temperature of 140°C. An increase in activity was still observed and so a drying temperature of 185°C, equivalent to the reaction temperature, was used. These results are also shown in figure 4.5. An increase in activity during the course of the reaction was again observed, and as yet this activity profile is unexplained. It may be

due to a number of factors, including the formation of nanoparticles, or perhaps *in-situ* oxidation of Au^0 to Au^{3+} over the course of the reaction, due to the excess of HCl present in the reactant gas stream, leading to an increase in activity.

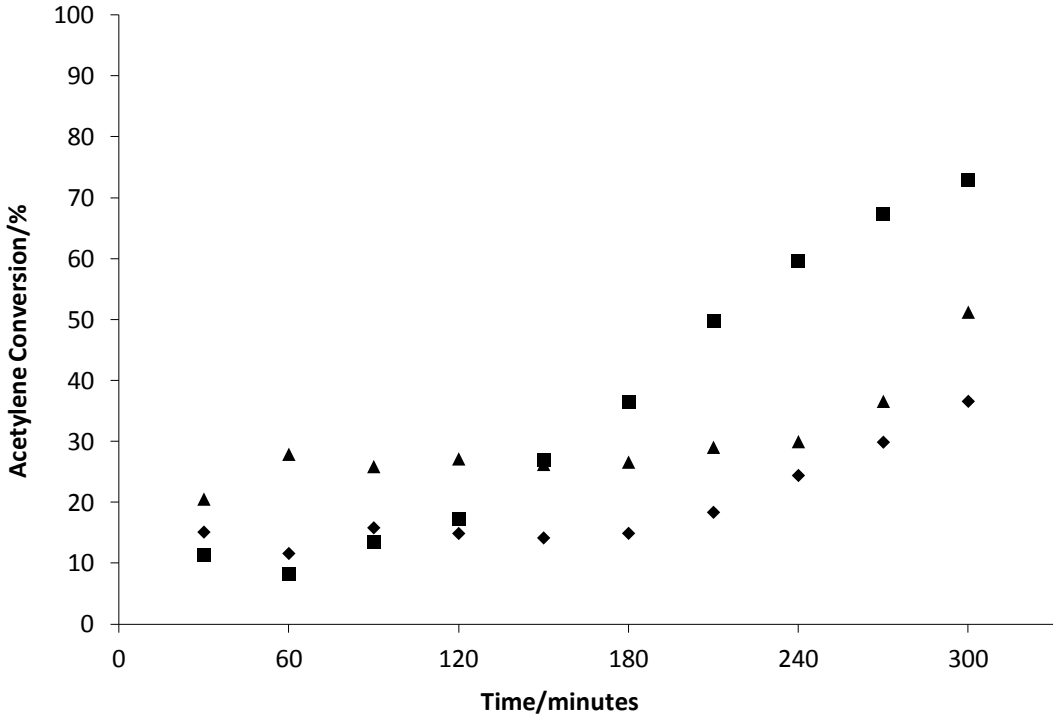

Figure 4.5: Activity of 1% Au/C catalysts prepared by IMP in *aqua regia*, dried at 110°C (◆), 140°C (■) and 185°C (▲).

Of the three drying temperatures used, 140°C gives the catalyst with the highest activity. This could be explained as previously by the formation of nanoparticles at higher temperatures contributing to the activity. However, it has been shown that on heating, activated carbon is able to reduce metal oxides to their metals, for example in the case of cobalt[10] and nickel[11], so it is also likely that it is able to reduce the gold precursor to metallic gold; this competing effect of the reduction of gold by the carbon support, which may be increased at higher temperatures, could reduce the amount of cationic gold present and cause the formation of metallic particles that are too large, leading to the lower activity observed for catalysts dried at 185°C. This would agree with the activity of the catalysts prepared by SI/DP/IMP in water as

reported earlier in this chapter, suggesting there may be a particle size effect if there is activity due to metallic gold particles.

The XPS spectra of these catalysts are shown in figure 4.6. It can be seen that for the catalyst dried at 110°C the majority of the gold is in the 3+ oxidation state, due to the larger signal at the higher binding energies of 86.5 and 90.2 eV. At drying temperatures of 140°C and 185°C, however, the size of this signal is greatly reduced, although still visible, and the size of the signal due to metallic gold, at 84 and 87.7 eV, has increased.

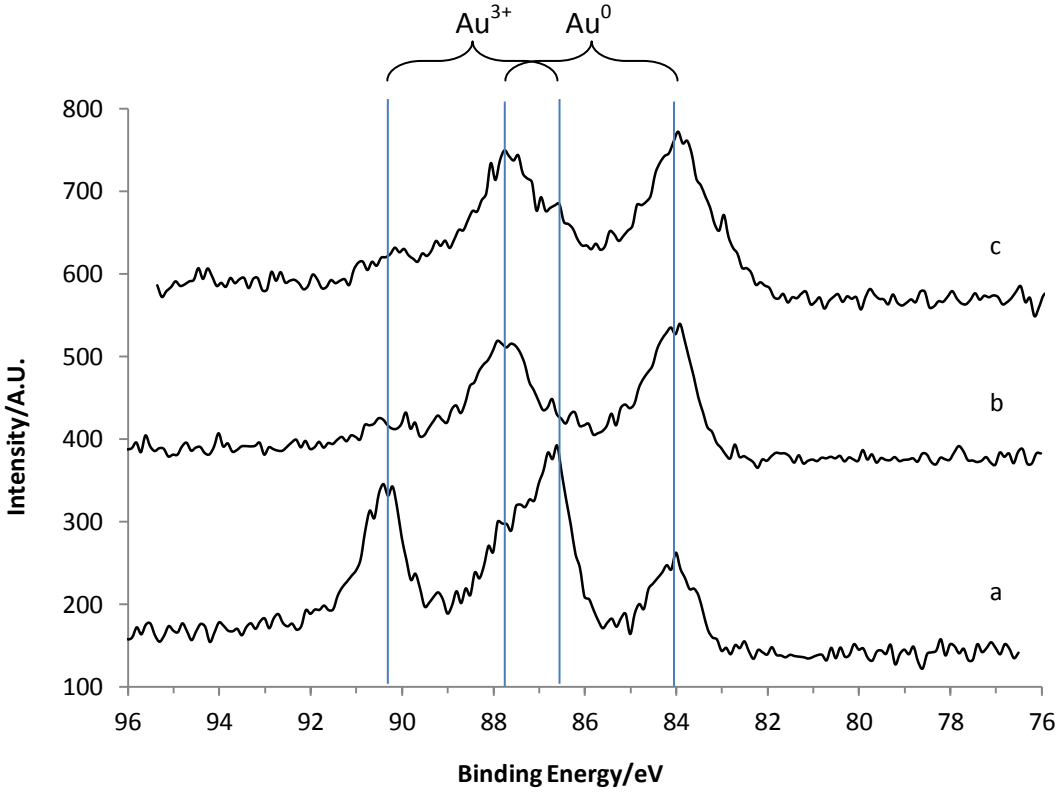

Figure 4.6: XPS Au4f spectra of catalysts prepared by impregnation in *aqua regia* and dried at a) 110°C, b) 140°C and c) 185°C.

4.3.2 The effect of the acid used for impregnation: contribution of HCl and HNO_3

4.3.2.1 Preparation of catalysts using HCl and HNO_3, and the effect of drying temperature

Catalysts were also prepared in concentrated hydrochloric acid (36%) and nitric acid (70%), in order to investigate the effects of the constituent parts of the *aqua regia* solvent. Again samples were made using drying temperatures of 110°C, 140°C and 185°C, for comparison to the results obtained using *aqua regia*. Figures 4.7 - 4.9 compare the activity of the catalysts made in HCl, HNO_3 and *aqua regia*, at each drying temperature.

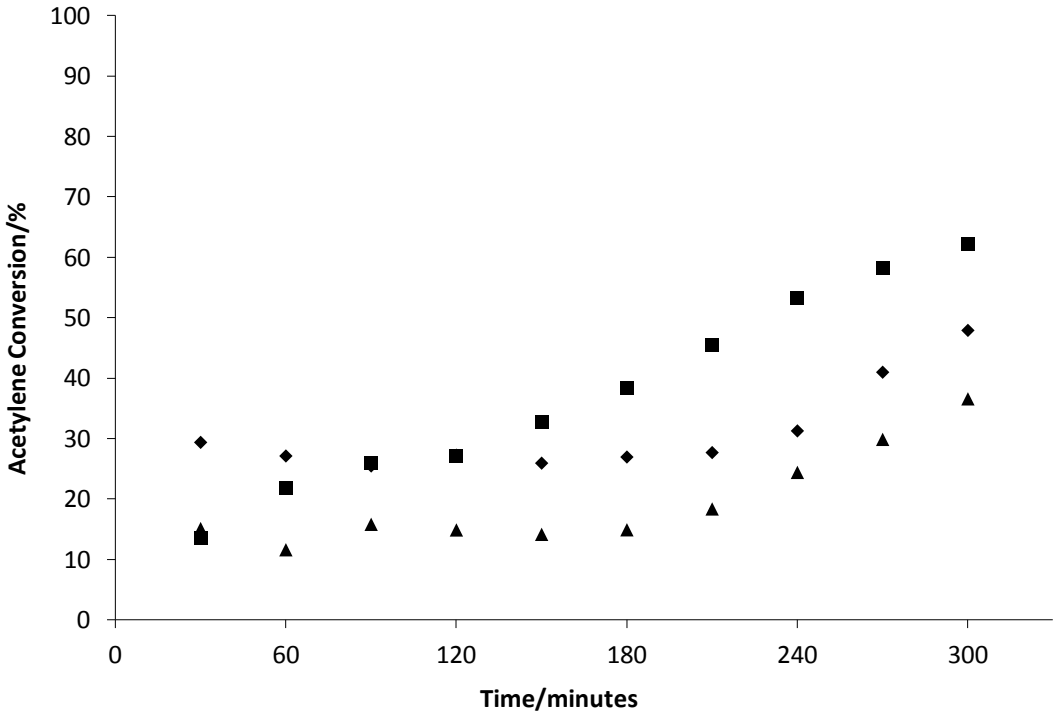

Figure 4.7: Time on-line activity of 1% Au/C catalysts prepared in *Aqua Regia* (▲), HCl (•) and HNO_3 (■) and dried at 110°C.

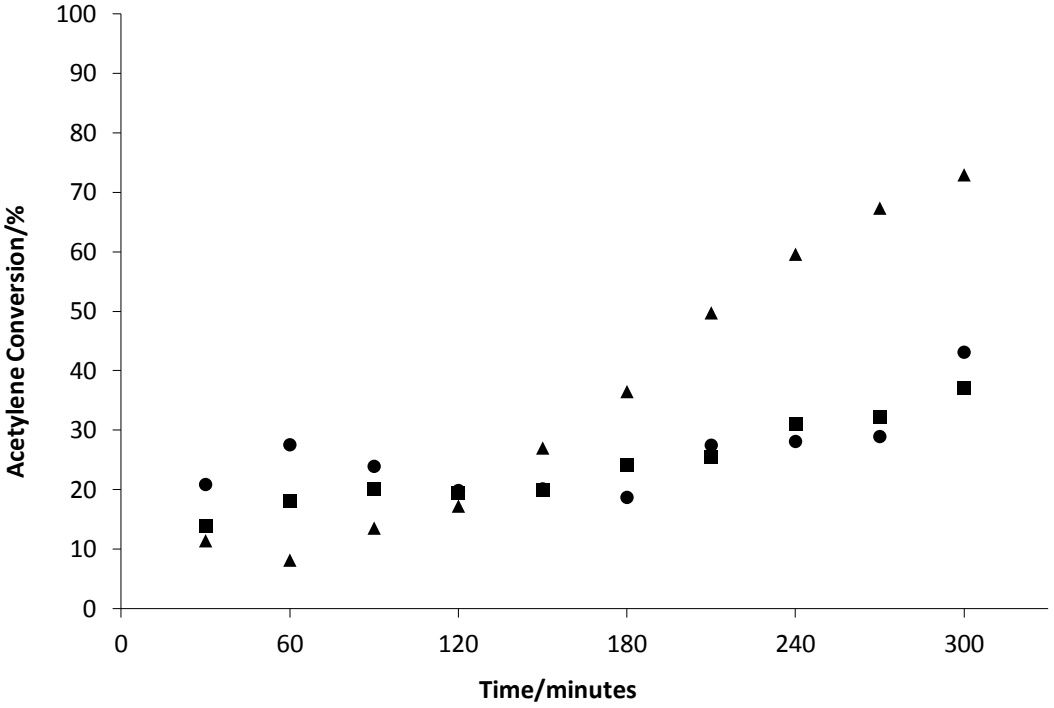

Figure 4.8: Time on-line activity of 1% Au/C catalysts prepared in *Aqua Regia* (▲), HCl (•) and HNO_3 (■) and dried at 140°C.

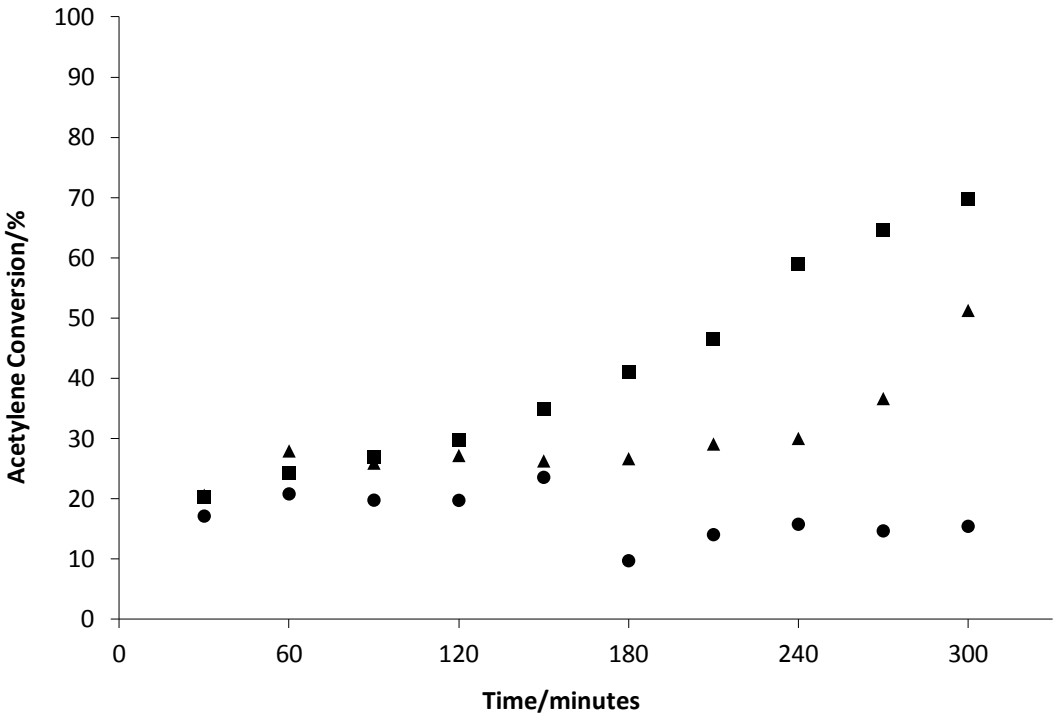

Figure 4.9: Time on-line activity of 1% Au/C catalysts prepared in *Aqua Regia* (▲), HCl (•) and HNO_3 (■) and dried at 185°C.

Of all nine catalysts, the most active was the one prepared in *aqua regia* and dried at 140°C. However at both 110°C and 185°C the catalyst prepared in nitric acid was the most active of the three solvents used. The activity of the catalysts prepared in HCl is lowest at the highest drying temperature, this could be due to the known effect of chlorine aiding mobilisation of Au particles[12], aiding the sintering process.

XRD analysis of the catalysts dried at 140°C was carried out, the results are shown in figure 4.10. It can be seen that the only catalyst for which reflections characteristic of metallic gold are observed is the one prepared in HCl. This again is likely to be due to the presence of a large amount of chlorine, which aids the sintering process of the gold, leading to larger size particles on the catalyst surface. Otherwise, it seems that preparation by impregnation in acid, as seen previously, leads to catalysts with a smaller gold particle size than other methods and the presence of Au^{3+}, both of which contribute to the absence of particles large enough to produce reflections due to metallic gold. These results are consistent with the XRD analysis of the Au/C-JM catalyst, which was prepared by impregnation in acid and does not show any reflections due to gold, with the XPS spectra showing that a significant amount of the Au was present in the 3+ state.

XPS of these catalysts shows the presence of both Au^0 and Au^{3+} species in all samples, however as the drying temperature is increased, the amount of Au^{3+} detected decreases (see figures 4.11 – 13). The catalysts dried at 110°C in fact contain more cationic than metallic gold (in the region of 64 – 68% Au^{3+} for all three acids), whereas for those dried at 140°C and 185°C significantly more metallic than cationic is observed (ranging from 12% Au^{3+} for the HNO_3 catalyst dried at 185°C to 40% for the aqua regia catalyst dried at 140°C). Quantification of the amount of Au^{3+} present is shown in table 4.1.

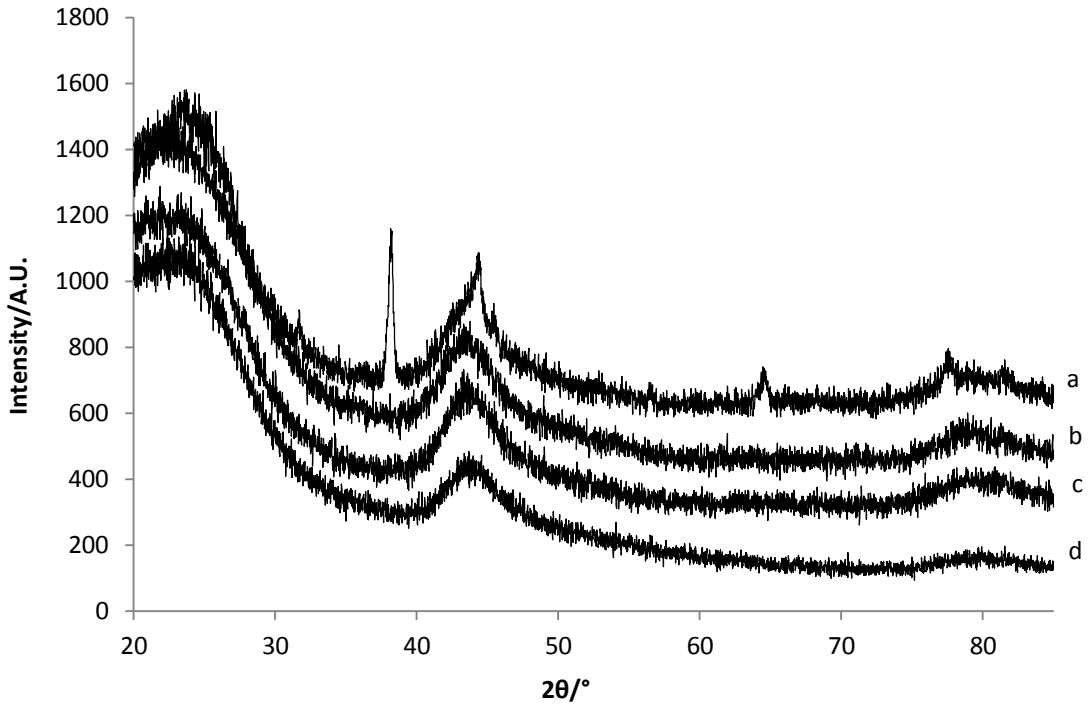

Figure 4.10: XRD patterns of 1% Au/C catalysts prepared in a) HCl, b) HNO_3, c) aqua regia and dried at 140°C and d) Au/C-JM.

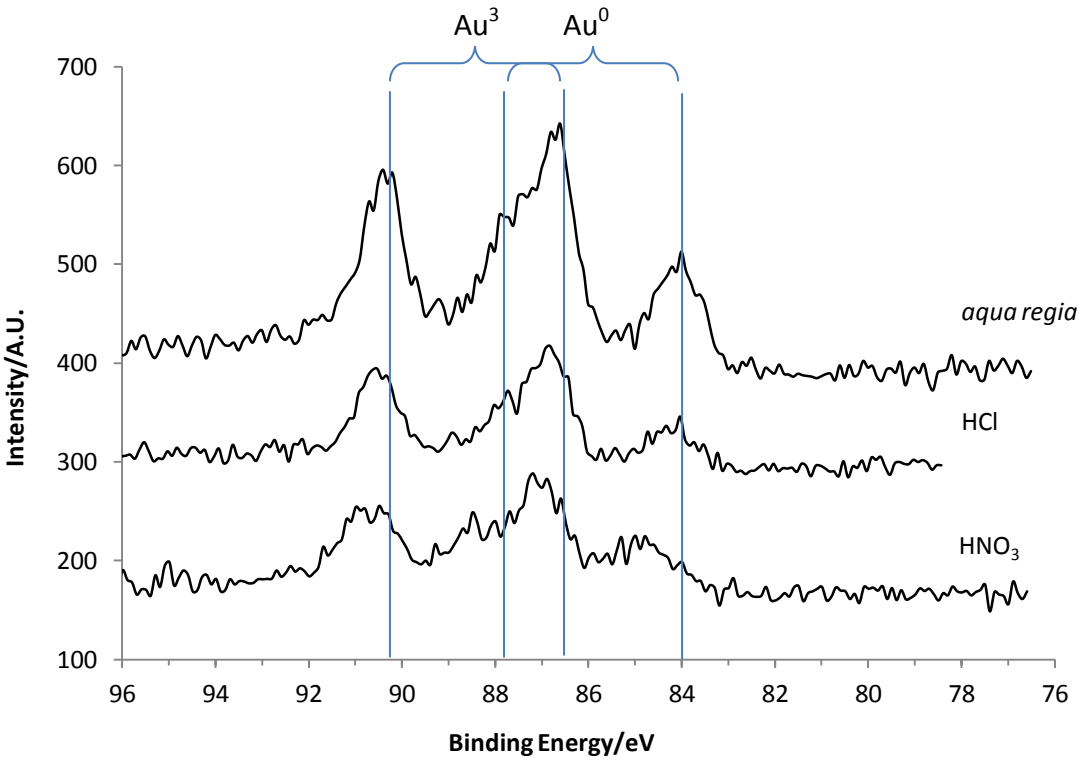

Figure 4.11: Au 4f XPS spectra of catalysts prepared in aqua regia, HCl and HNO_3 and dried at 110°C.

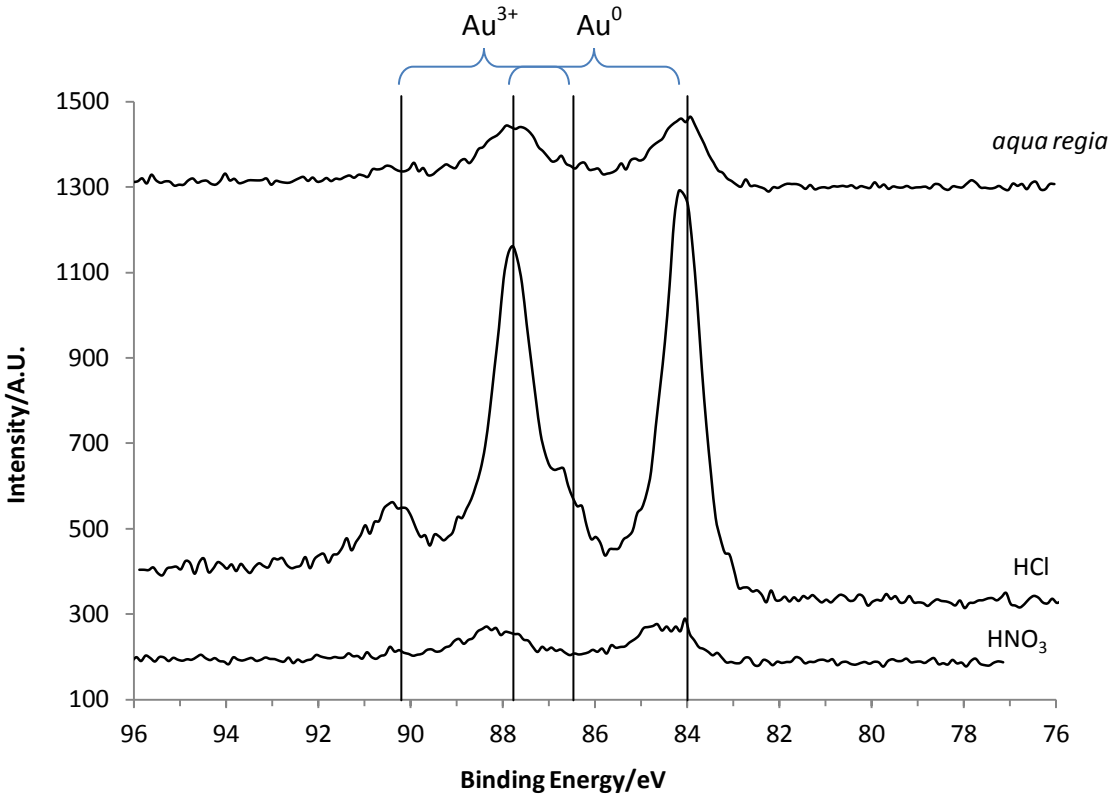

Figure 4.12: Au 4f XPS spectra of catalysts prepared in aqua regia, HCl and HNO_3 and dried at 140¨C.

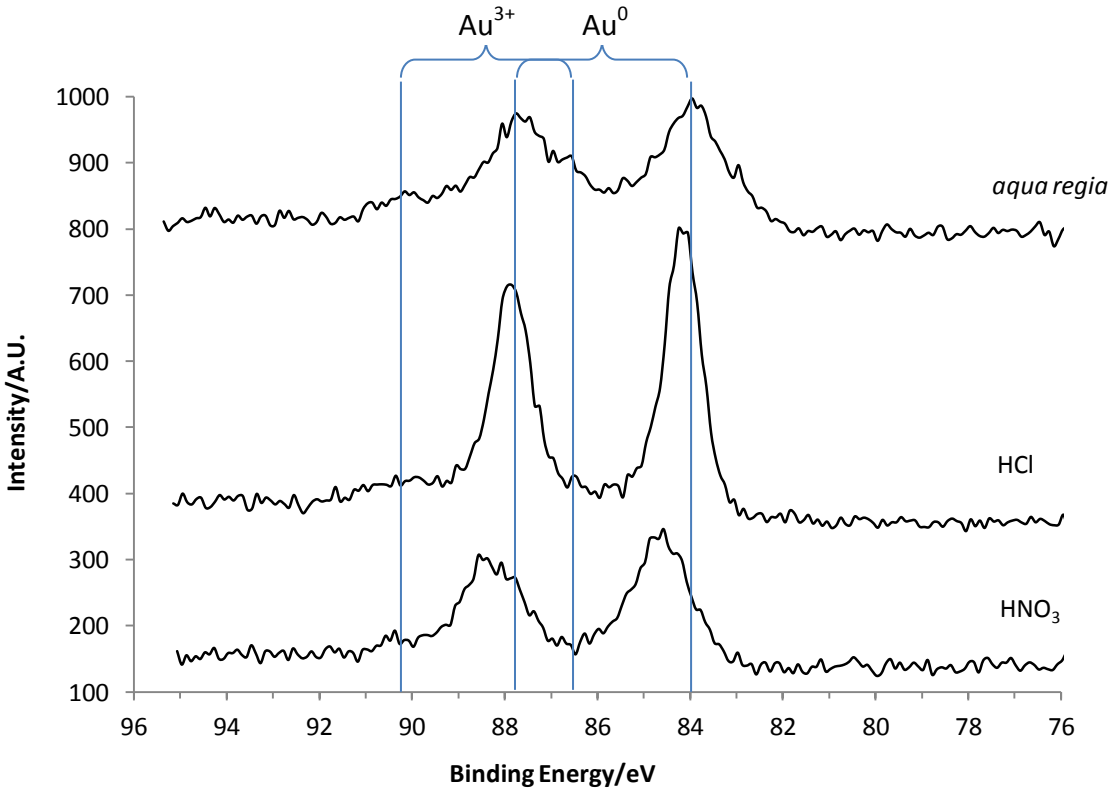

Figure 4.13: Au 4f XPS spectra of catalysts prepared in aqua regia, HCl and HNO_3 and dried at 185°C.

Acid/Drying Temperature	110°C	140°C	185°C
HCl	67.5	28.9	30.3
Aqua Regia	64.7	40.5	21.5
HNO_3	66.2	34.9	12.8

Table 4.1: Quantification of the percentage of the Au detected by XPS which is present in the 3+ oxidation state.

4.3.2.2 The effect of the composition of a HCl/HNO_3 mixture used in catalyst preparation

As described above, at a drying temperature of 140°C, the catalyst prepared using *aqua regia* is more active than those prepared using either individual acid. In view of this, and since *aqua regia* is a mixture of HCl and HNO_3 (with a HCl:HNO_3 ratio by volume of 3:1), a range of catalysts were produced by the acid impregnation method as previously described, using solvents with varying HCl:HNO_3 ratios. These are expressed in terms of HNO_3 volume fraction, having values between 0 and 1. All catalysts showed the same trend of increasing activity with reaction time, the testing results can be seen in figure 4.14 and the conversion at the end of 5 hours reaction time is compared in table 4.2. The catalyst with the highest activity after 5h is still the *aqua regia* (3:1) catalyst, HNO_3 volume fraction 0.25.

It can be seen from table 4.2 and the plot of this data in figure 4.15 that although the catalyst prepared in *aqua regia* leads to the highest activity after 5h (73% conversion), there does not seem to be a clear trend directly relating the composition of the acid mixture used in a catalyst's preparation to its observed activity. For this reason, characterisation of these catalysts was carried out in order to investigate the effect that the acid has on the proposed active sites – Au^{3+} species – for example the amount generated and its redox properties.

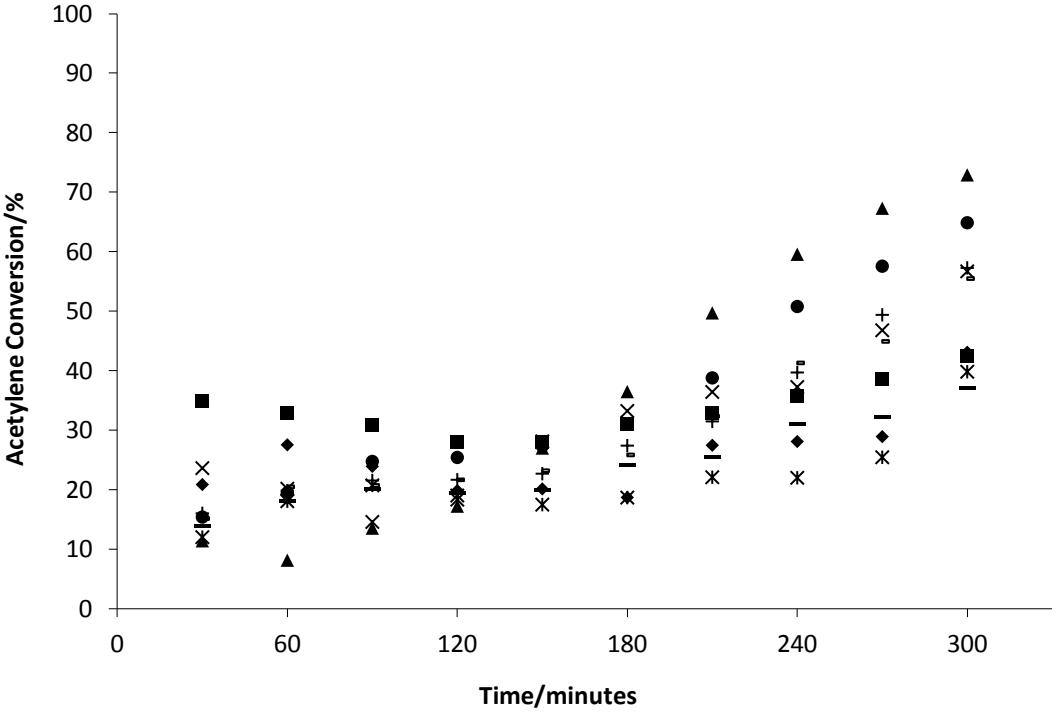

Figure 4.14: activity of catalysts prepared by impregnation in acid mixtures of varying HCl:HNO_3 ratios, described by volume fraction of HNO_3: 0 (◆), 0.1 (■), 0.25 (▲), 0.33 (×), 0.5 (✳), 0.65 (●), 0.75 (+), 0.9 (-), 1 (–).

HNO_3 volume fraction	Final activity: % acetylene conversion after 5h
0	43.1
0.1	42.5
0.25	72.9
0.33	56.7
0.5	39.8
0.65	64.9
0.75	57.3
0.9	55.5
1	37.1

Table 4.2: The activity after 5 hours reaction time of catalysts prepared using different ratios of HCl:HNO_3 as a solvent for impregnation of $HAuCl_4$.

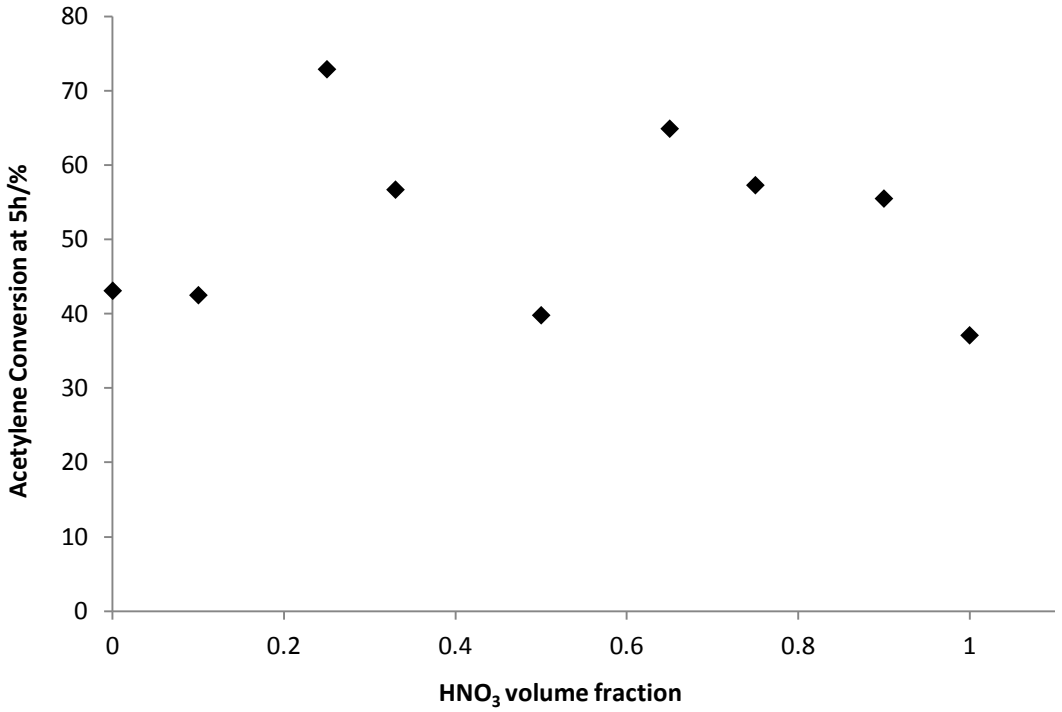

Figure 4.15: Activity of catalysts after 5h with the volume fraction of HNO_3 of the acid mixture used to prepare them.

4.4 TPR analysis of Au/C catalysts

Since it is known that the reduction of Au^{3+} is an important factor in the deactivation of Au/C catalysts such as these, it was decided to use TPR analysis to investigate this process. The samples were heated to a temperature of 800°C at a ramp rate of 5°C/min, under a flow of 10% H_2/Ar (20 ml/min). Two main features can be seen in the TPR, these are reductions at a temperature of around 250-300°C and around 600°C. The lower temperature reduction is attributed to reduction of Au^{3+}, since this feature only occurs for catalysts which are known to contain Au^{3+}, while the higher temperature reduction is thought to be due to oxygen containing functional groups on the surface of the carbon. This is supported by literature in which TPR signals at temperatures greater than 500°C have been attributed to decomposition of oxygen-containing surface functional groups on carbon[13, 14]. TPR profiles of catalysts prepared in HCl, HNO_3 and *aqua regia* and dried at 140°C are shown in figure 4.16.

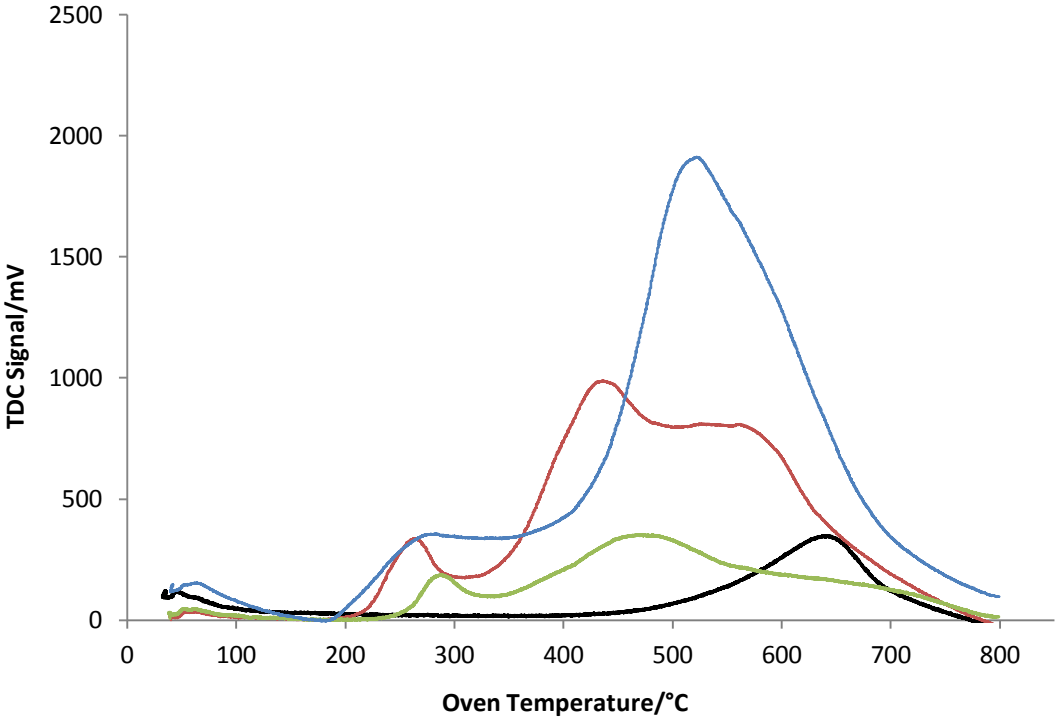

Figure 4.16: TPR profiles of catalysts prepared in HCl (green), HNO_3 (blue) and *aqua regia* (red), dried at 140°C, and the as-provided carbon support (black).

Baatz *et al*. used TPR to investigate a series of 0.3% Au/Al_2O_3 catalyst precursors, prepared by impregnation of $HAuCl_4$ in solvents including water, NaCl and HCl, and reported reduction of gold occurring between 150 and 250°C, depending on the solvent used[15]. The precursor with the highest reduction temperature was that prepared using 2M HCl, with a reduction temperature of 234°C. These results are consistent with our attribution of reductions occurring around 250°C to reduction of Au^{3+}, with the differences in reduction temperature likely to be due to the different species present in the impregnation solutions used, the different supports and the methods used. Gil *et al.* also observed reductions at a similar temperature for Au/C catalysts and attributed them to reduction of Au^{3+} [16].

The reductions at higher temperatures are likely to be due to functional groups on the carbon, since the carbon support as-provided shows one reduction feature, at approximately 650°C. The areas of the reduction peaks observed for the acid-treated carbons are in the order HNO_3>*aqua regia*>HCl, and it would be expected that higher HNO_3 content leads to a greater amount of oxygen containing functional groups, due

to its strong oxidising nature. These reductions also occur at different temperatures where different acids were used, in fact there are two distinct reductions of the *aqua regia* catalyst compared to larger single reductions for the individual HCl and HNO_3 prepared catalysts. This could be due to different functional groups being present on the surface depending on which acid was used; the effect of the acid on the carbon support is described in detail later in this chapter.

TPR analysis was carried out on the series of catalysts prepared using different acid ratios and the Au^{3+} reduction peak was integrated in order to compare the amount of cationic gold present in each case. Figure 4.17 shows the relationship between HNO_3 volume fraction and integration of Au^{3+} reduction, a curve is obtained which shows a maximum amount of Au^{3+} at the 0.65 volume fraction. It is known that HNO_3 is a good oxidiser, so it would be expected that a larger amount of HNO_3 in the preparation would give a higher amount of oxidised gold species. However this is not the case, and so it seems likely that the higher amount of chlorine present from the HCl is able to stabilise the oxidised Au^{3+} species better.

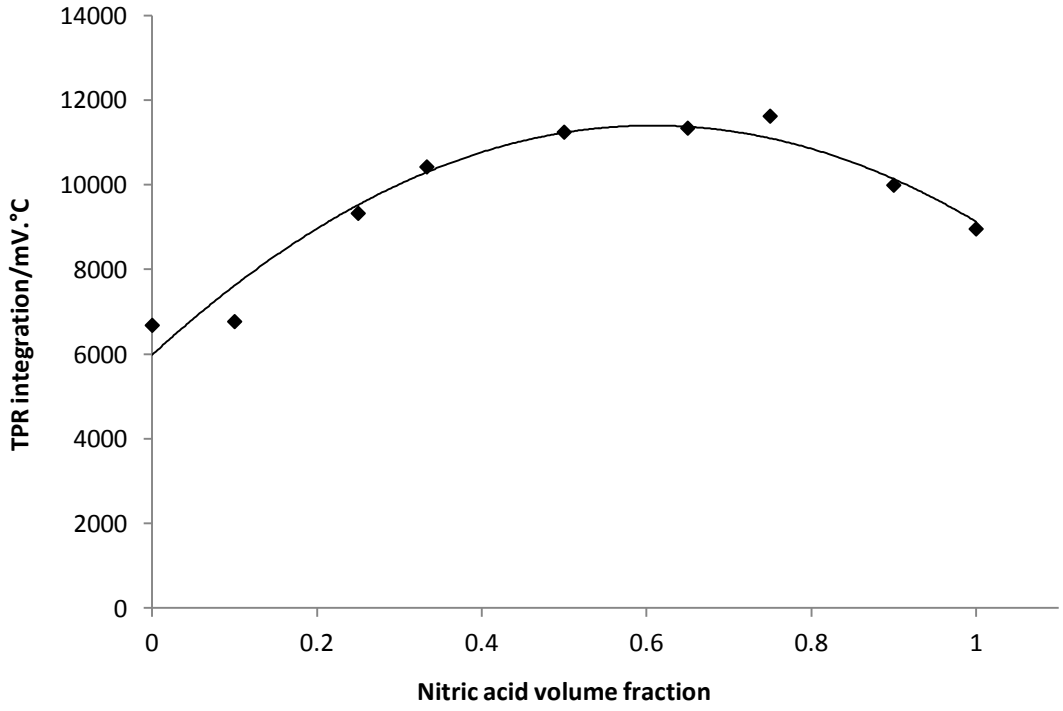

Figure 4.17: Plot of integration of the Au^{3+} reduction in the TPR profile vs. the volume fraction of HNO_3 used in the catalyst preparation.

However, it is important to note that the catalyst containing the most Au^{3+} is not the most active, and a similar curve is not observed when activity is compared to nitric acid volume fraction. This suggests that although the presence of Au^{3+} is known to be an important factor in catalyst activity, there must be other contributions involved. For example, the location of the Au^{3+} could also be important in determining its activity – it may be that for catalysts which are found to contain more cationic gold but are less active than expected, it is not in the right place.

The activity for each of the catalysts after 5h was compared to the temperature at which the Au^{3+} reduction peak in the TPR occurred; this is shown in figure 4.18. The catalyst with the most reducible Au^{3+}, *i.e.* the lowest reduction temperature, is in fact the most active (0.25 HNO_3 volume fraction), showing that not only the presence of Au^{3+} species is important, but the reducibility of these species could be crucial in determining catalyst activity. This may be related to the idea of a redox cycle being involved in the reaction – the transition between oxidation states would be more facile given a more easily reducible Au^{3+} species. There is a general trend that a higher reduction temperature gives lower activity, with the exception of a peak-like shape near the middle of the graph, which occurs where the catalyst had the largest amount of Au^{3+}. To see how the reducibility of the catalyst was related to the composition of the acid used in the preparation, a plot of reduction temperature against volume fraction of nitric acid was produced, this is shown in figure 4.19. A curve is obtained with a minimum at a volume fraction of 0.25, the most active catalyst. This shows that initially, the reducibility of the catalyst increases with the amount of nitric acid used in its preparation, however above a volume fraction of 0.25 this trend is reversed. It could be that the reducibility of the cationic gold species is affected by the functional groups present on the carbon surface, which it is able to interact with if its location is the gold-carbon interface, and which in turn are dependent on the acids used in the catalyst preparation. For example, the presence of surface functional groups may activate the reduction of the gold up to a certain point, beyond which the interaction with the gold becomes too strong and the reduction is inhibited.

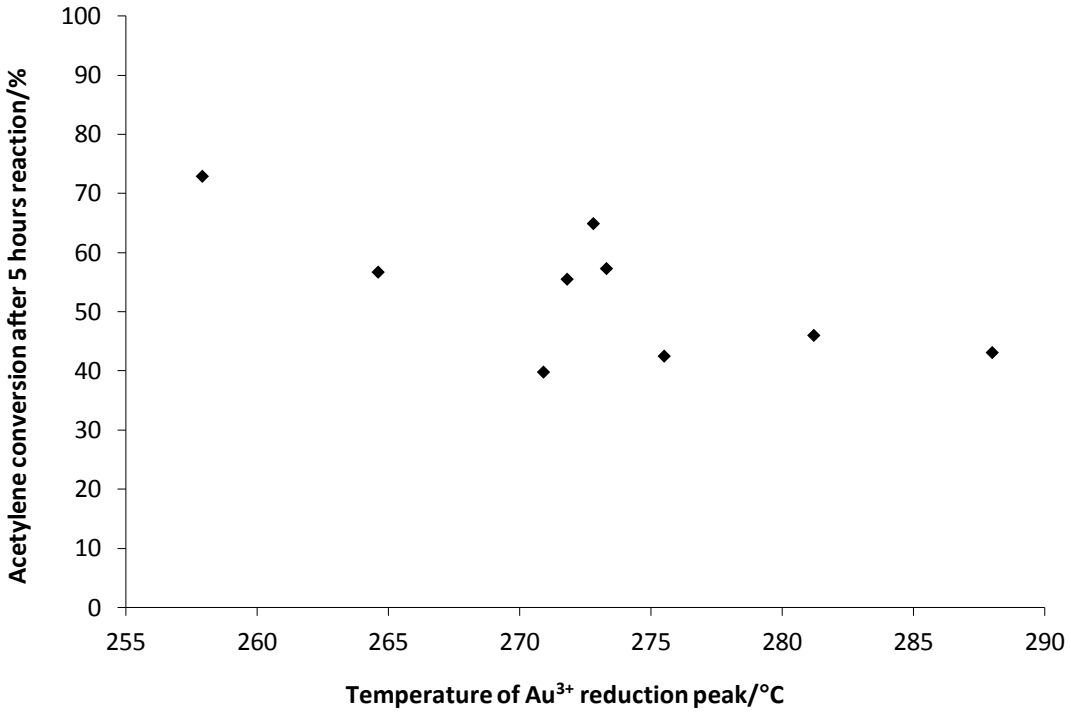

Figure 4.18: final activity of catalysts compared to the temperature at which the peak maximum for the reduction of cationic gold occurs in TPR.

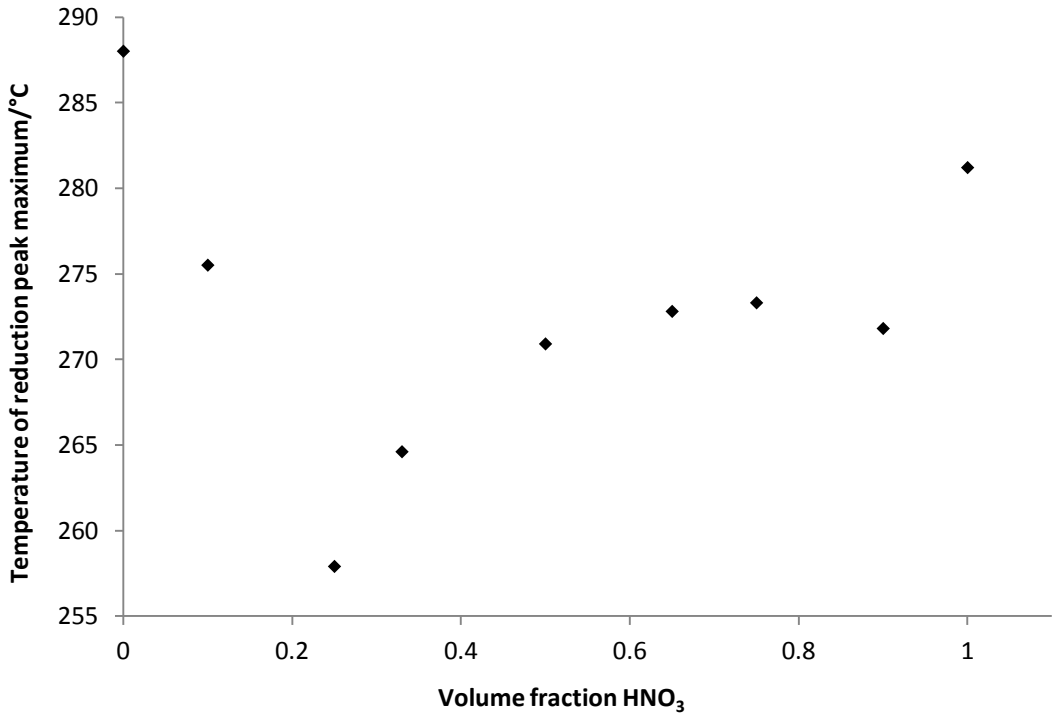

Figure 4.19: Plot of the temperature of the peak maximum for the Au^{3+} reduction from the TPR vs. the volume fraction of HNO_3 used in the catalyst preparation.

Further information can be extracted from TPR analysis; by varying the ramp rate of the heating it is possible to determine the activation energy of a reduction reaction using the Kissinger Equation (as described in experimental chapter 2). The TPR profiles and Kissinger Plot for the Au/C-JM catalyst are shown in figures 4.20 and 4.21. This process was carried out on a number of catalysts: those prepared in HCl, *Aqua Regia* and HNO_3 and dried at 110, 140 and 185°C in addition to Au/C-JM. The TPR profiles, tabulated data, Kissinger plots and calculations for the remainder of these catalysts are contained in Appendix 1, the values obtained for the activation energies and pre-exponential constants are given in table 4.3.

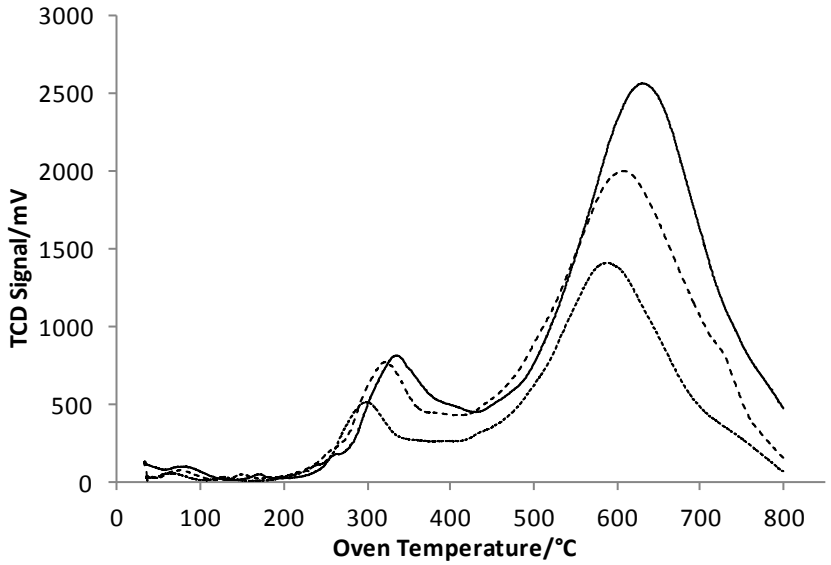

Figure 4.20: TPR profiles of JM catalyst M07565 at heating ramp rates of 10 (short dashes), 15 (long dashes) and 20 (solid line) °C/min.

Ramp Rate (β)	Temperature of Peak Maximum/°C	Temperature of Peak Maximum/K (T)	ln (β/T^2)	1/T ($x10^{-3}$)
10	300	573	-10.4	1.74
15	321	594	-10.1	1.68
20	335	608	-9.82	1.64

Table 4.3: Table of data for Kissinger plot for Au/C-JM.

The activation energy and pre-exponential factor, A, are calculated from the gradient and intercept of the Kissinger plot as follows:

Gradient = -5690.3 = $-E_a/R$ ∴ E_a = 47309 J/mol

Intercept = -0.4734 = ln (AR/E_a) ∴ A = 3544

(R = 8.314 $Jmol^{-1}K^{-1}$).

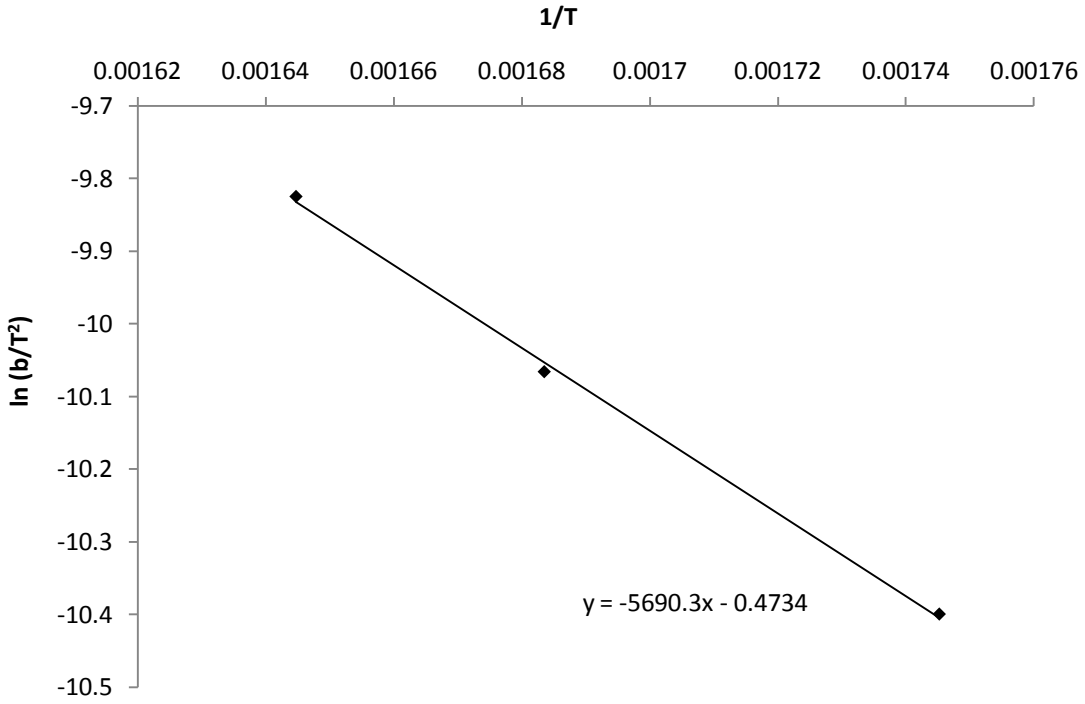

Figure 4.21: Kissinger plot for Au/C-JM.

Sample	Activation Energy, E_a/(kJ/mol)	Pre-exponential Factor (A)
Au/C-JM	47.3	3544
HCl IMP, dried 110°C	43.3	1348
HCl IMP, dried 140°C	53.6	11624
HCl IMP, dried 185°C	71.8	853386
HNO_3 IMP, dried 110°C	43.0	1219
HNO_3 IMP, dried 140°C	54.2	15999
HNO_3 IMP, dried 185°C	45.0	1600
Aqua regia IMP, dried 110°C	56.8	32509
Aqua regia IMP, dried 140°C	50.4	7701
Aqua regia IMP, dried 185°C	39.6	755

Table 4.4: Activation Energy and pre-exponential factor A for the reduction of Au^{3+} in a series of 1% Au/C catalysts.

Comparing the values obtained for the activation energy with the observed activity of the catalysts after 5 hours produces a curve, with maximum activity seen at around 48kJ/mol (figure 3.22). The expected trend would be that the lower the activation energy for Au^{3+} reduction, the more active the catalyst. However, the decline in activity at lower activation energies suggests that there may be a threshold below which the gold is too reducible to be active, *i.e.* it will completely reduce and sinter into large particles rather than perhaps become involved in a redox cycle, which as mentioned previously could be a possible mechanism for this reaction. It should be noted, however, that the conditions differ between the TPR analysis, since this is reduction in H_2, and reaction, where the reactant gases C_2H_2 and HCl are present. While the TPR analysis is therefore not directly applicable to the reaction situation, it does still provide a useful model.

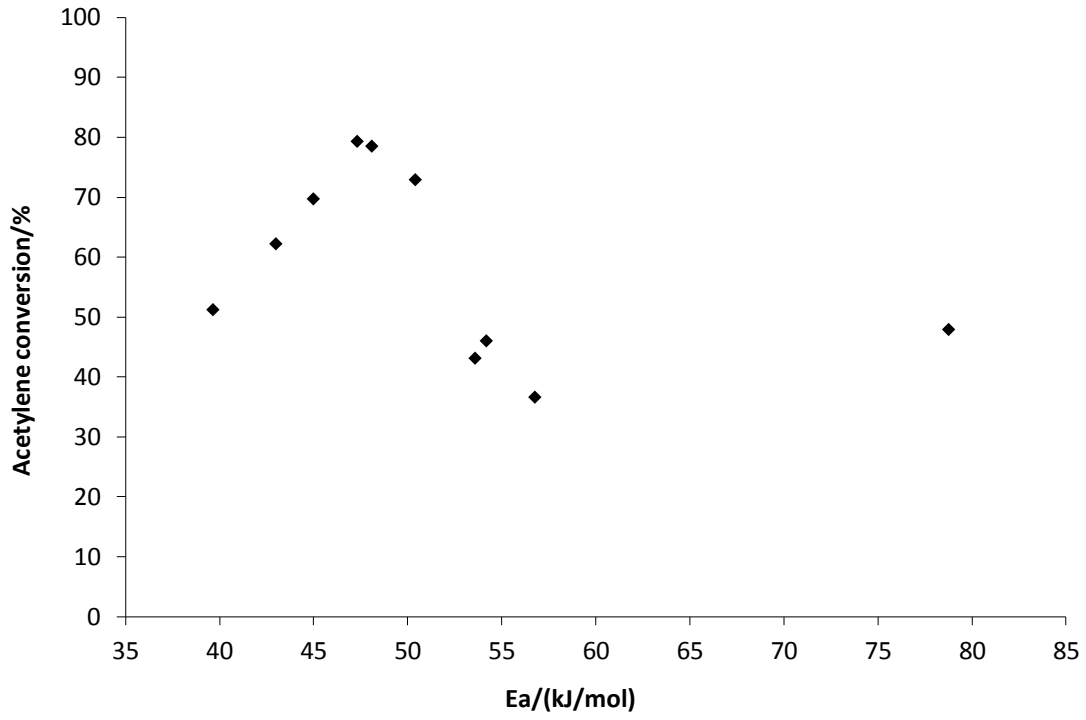

Figure 4.22: Plot of activity after 5h reaction time against activation energy for a series of 1% Au/C catalysts.

As seen above, the pre-exponential factor, A, for the reduction of Au^{3+} to Au^0 has also been determined from the TPR data and resulting Kissinger plots. A plot of lnA vs Ea is known as a 'compensation plot'[17], such a plot for the reaction under investigation is shown in figure 4.23. A straight line is obtained, which shows that compensation does

occur for the reduction of Au^{3+} in hydrogen for these catalysts. This indicates that there is a common factor linking the number of collisions with the activation energy, which is likely to be the amount of Au^{3+} present in the right chemical environment.

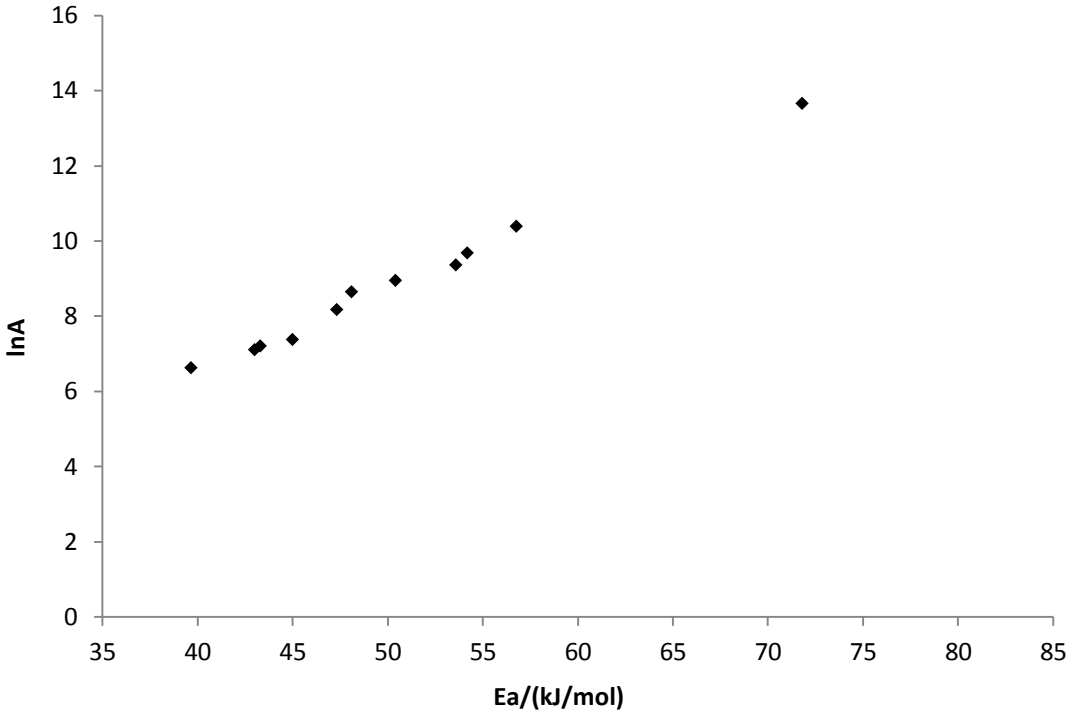

Figure 4.23: Compensation plot for a series of 1% Au/C catalysts.

4.5 The Effect of Alternative Solvents used in Impregnation

In addition to HCl, HNO_3 and *aqua regia*, a number of other solvents were used in the impregnation of $HAuCl_4$ on activated carbon. Other common laboratory acids, sulphuric and acetic acid, were used, as well as a base (NaOH) and an alternative chloride source (bleach, NaOCl). The results are shown in figure 4.24. All catalysts show some activity; however, in all cases it is relatively low (a maximum of around 30% conversion is observed) and fairly stable. The large increase in activity as seen for *aqua regia* and its constituent acids is not observed. This suggests that it is something unique about the particular acids used that leads to the high activity; this is thought to be the strong oxidising nature of HNO_3 and the stabilisation effect of HCl on Au^{3+}.

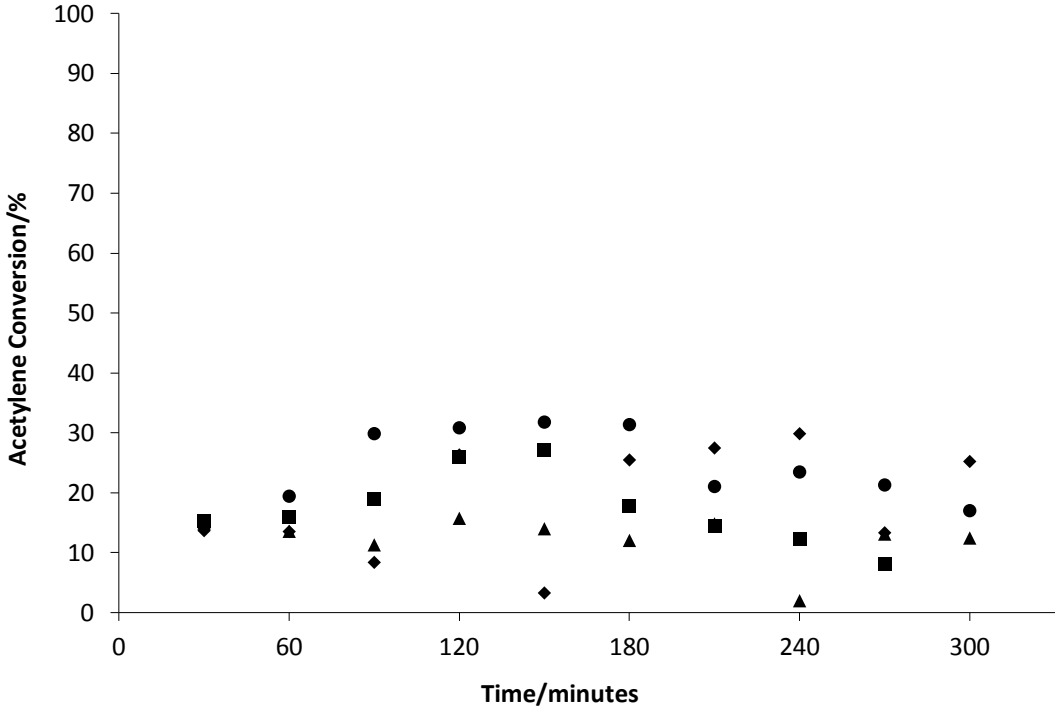

Figure 4.24: Alternative solvents used for impregnation – NaOH (■), NaOCl (◆), sulphuric acid (▲) and acetic acid (●).

4.6 The effect of acid treatment on the carbon support

A number of techniques have been used to investigate the effect of acid treatment on the activated carbon used as the catalyst support, including TPR/TPD, Raman spectroscopy and titrations. It is known that acid treatment of carbons can affect the functional groups present on the surface, for example treatment with concentrated HNO_3 leading to the presence of carboxylic acid groups[18], and it is thought that this may have an influence on the catalyst since these groups could provide nucleation sites for gold nanoparticles[19]. Acid treatment was carried out as follows: The acid (e.g. HCl, 32%, Fisher, 5.4 mL) was added drop-wise with stirring to the carbon extrudate (1.98 g) and the mixture stirred at room temperature for 10 minutes. This mixture was then dried overnight (16 h) at 140°C. This was done to be analogous to the catalysts prepared by impregnation of $HAuCl_4$ using acid as a solvent, *i.e.* equivalent preparation but excluding the source of the gold. Therefore this acid treatment is not considered similar to acid washing treatments that are commonly used for carbon

supports, e.g. by stirring the carbon in a dilute solution of HCl for several hours before filtering and washing thoroughly, in order to remove impurities. Portions of the carbon support as provided were treated using HCl (32%), HNO_3 (70%) and *aqua regia* (3:1 HCl: HNO_3 by volume).

4.6.1 Temperature Programmed Characterisation of Acid Treated Carbons

TPR analysis of the catalysts as described previously shows different TPR profiles at the higher temperature region, *ca.* 600°C, for catalysts prepared in different acids. So TPR of the acid treated carbons was carried out, for comparison to that of the untreated carbon. It can be seen from figure 4.25 that all three acid treatments cause oxidation of the carbon surface, as the area of the reductions that occur in the higher temperature region are larger than for the untreated carbon.

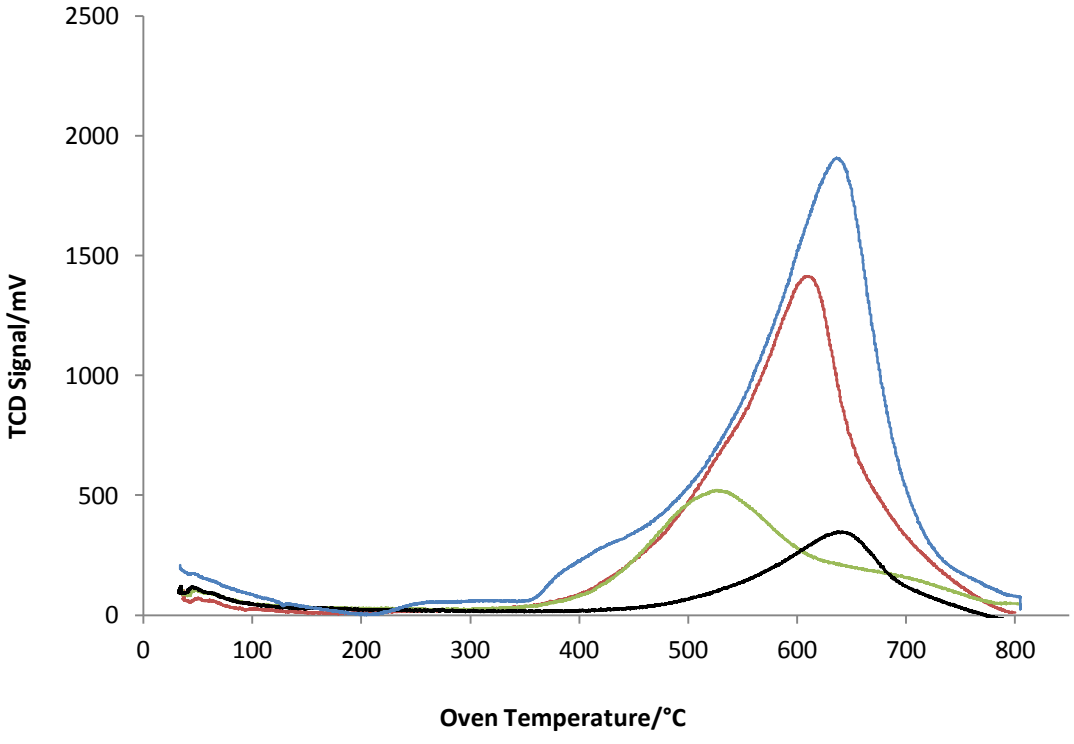

Figure 4.25: TPR profiles of acid treated carbons, using HCl (green), HNO_3 (blue) and *aqua regia* (red), and the untreated carbon (black).

From the size of the reduction peaks it can be seen that the strongest oxidant is HNO_3, then *aqua regia*, then HCl. This is as would be expected due to the strong oxidising nature of HNO_3 – the more that is used, the greater the effect. It is also of note that the reduction peaks for all three acid treated carbons have a similar initial slope, yet the peak maxima occur at different temperature positions. Only the peak maximum for the HNO_3 treated sample is in a similar position to that of the untreated carbon - for the *aqua regia* and HCl the peak maxima occur at lower temperatures. However, the higher temperature reduction features seen for the acid treated carbons are different to those for their corresponding catalysts (as shown earlier in figure 4.16), most noticeably for the *aqua regia* samples, where two distinct reductions are observed. This suggests that the gold may be interacting with one of the species present on the surface and increasing its reducibility.

TPD was also carried out on the acid treated carbons, by heating under a flow of helium and recording the resulting TCD signal. The results can be seen in figure 4.26. Desorption temperatures due to particular functional groups were taken from the literature[20] and are shown in table 4.5.

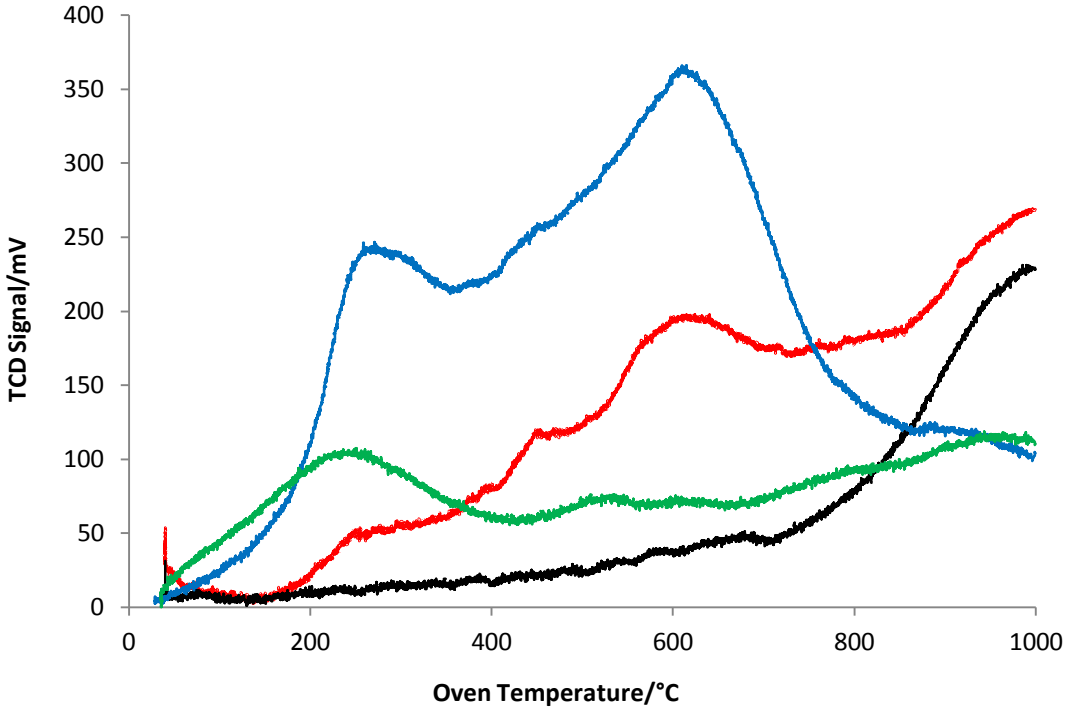

Figure 4.26: TPD profiles of carbon support as provided (black) and after acid treatment with HCl (green), HNO_3 (blue) and *aqua regia* (red).

Temperature range/°C	Functional Group	Decomposition product
100 - 400	Carboxylic acid	CO_2
400 - 450	Carboxylic anhydride	CO, CO_2
500 - 800	Lactones	CO_2
700 - 800	Phenols	CO
900 - 1100	Ethers/carbonyls/quinines	CO

Table 4.5: Temperature of desorption of CO and CO_2 due to carbon surface functional groups.

The TPD shows that all of the acids used lead to an increase in oxygen containing functional groups on the surface of the catalyst. As is seen from the TPR, the TPD also shows that nitric acid treatment leads to the highest amount of oxidised species. From the values taken from the literature, it can be seen from the TPD that the most prominent groups on the carbon surface are carboxylic acid and lactone groups.

4.6.2 Raman Characterisation of Acid Treated Carbons

Raman spectroscopy can be used to analyse the structure of carbon materials[21], and so was used to see if there was any significant difference between the acid treated carbons and the untreated sample. The spectra can be seen in figures 4.27 – 4.30. The spectra of all samples are similar in shape, with features occurring around the same wavenumbers, which unfortunately does not reveal much about the effect of the acids on the carbon. The features at around 1575 cm^{-1} and 1355 cm^{-1} are known as the G-band and D-band respectively[22]; The G-band is due to crystalline graphite type carbon structure, resulting from vibration of sp^2 atoms, while the D-band may be used as a measure of structural disorder, and arises from defects in the graphite structure, for example the edges of planes. The disorder of a carbon material may be quantified using the D/G ratio of peak sizes[23].

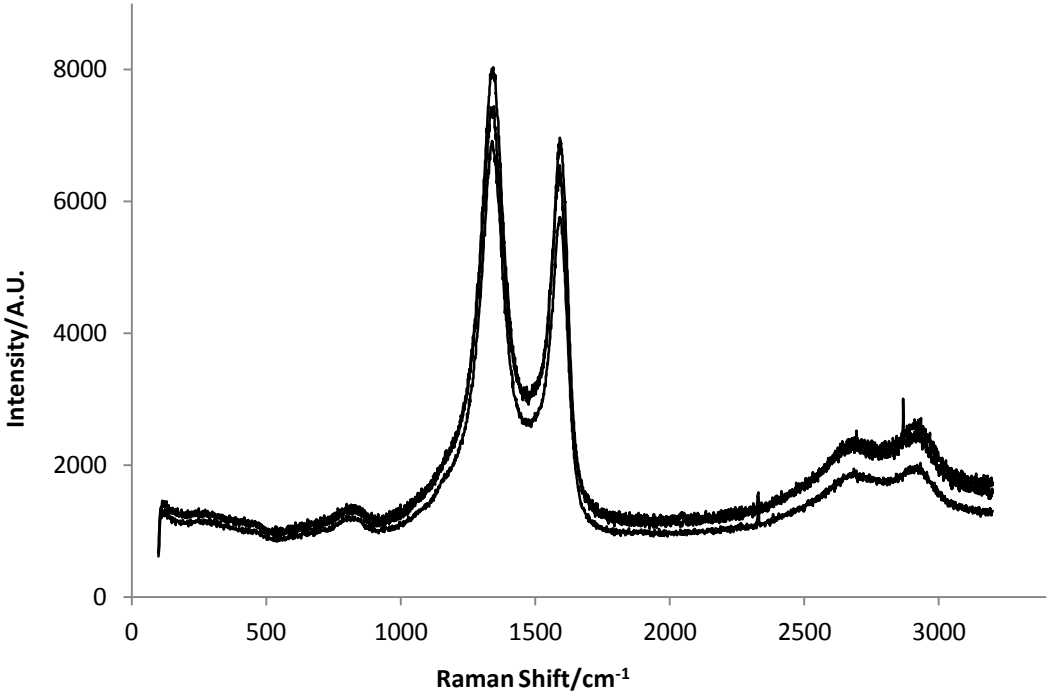

Figure 4.27: Raman spectra of the as-received carbon support.

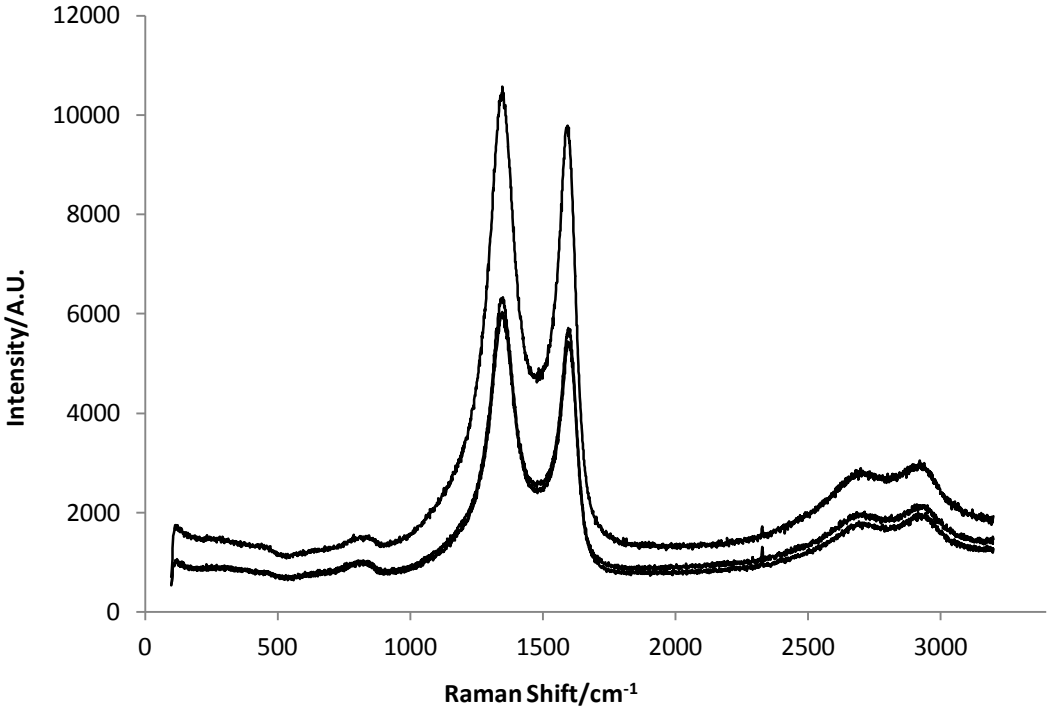

Figure 4.28: Raman spectra of HCl treated carbon.

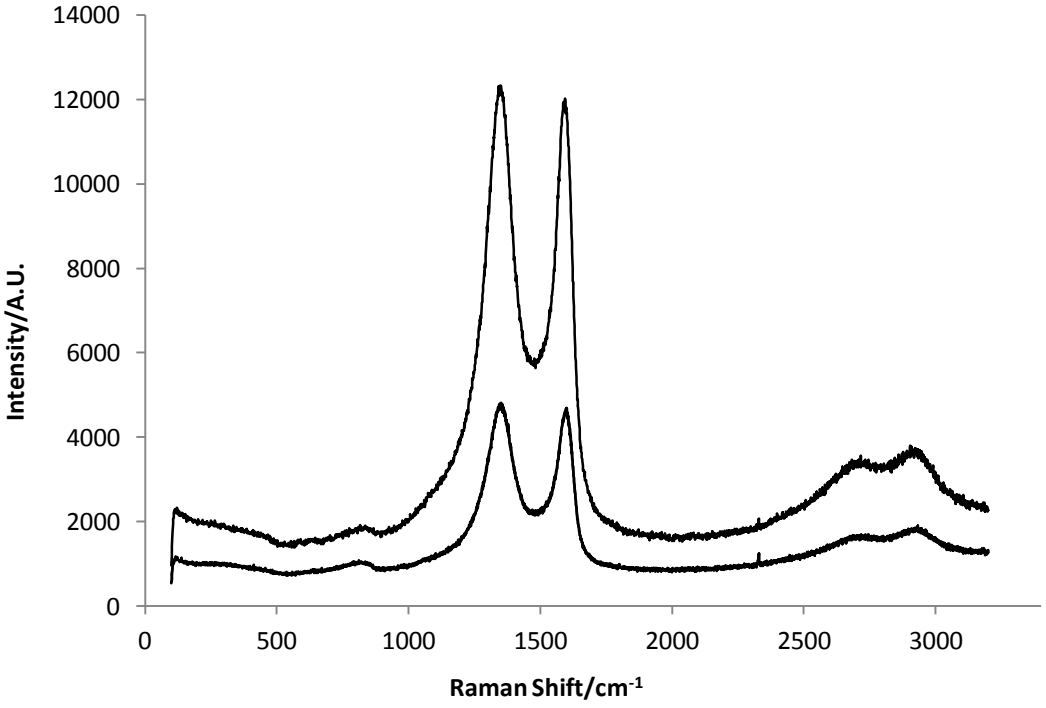

Figure 4.29: Raman spectra of HNO_3 treated carbon.

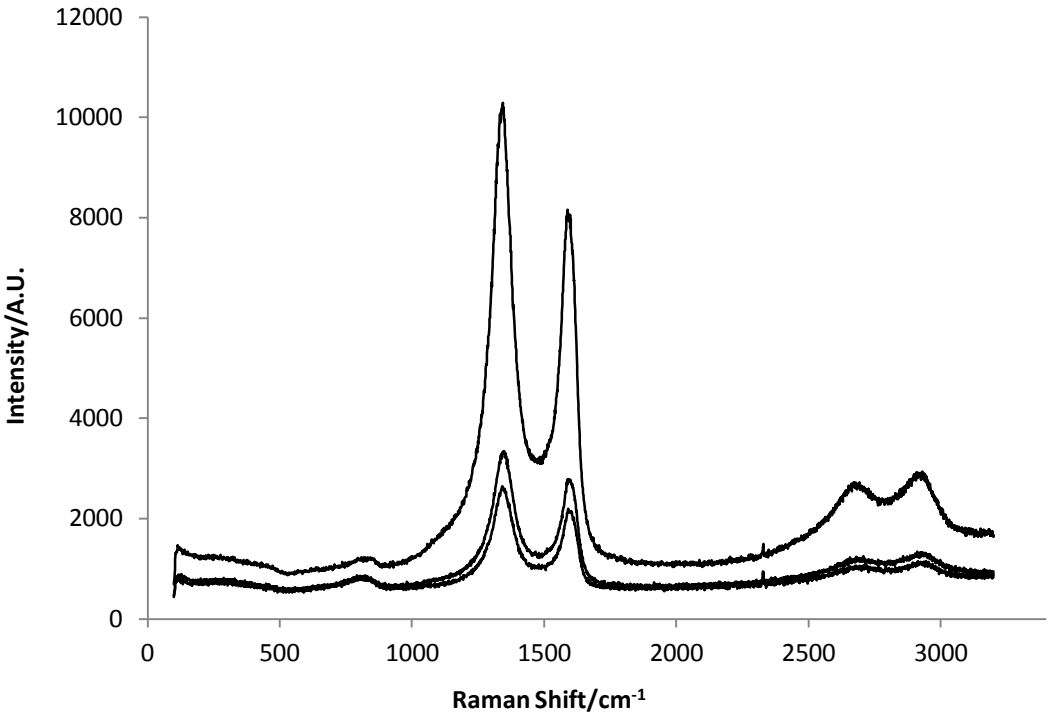

Figure 4.30: Raman spectra of *aqua regia* treated carbon.

It can be seen from the Raman spectra that although intensities of the spectra vary somewhat, even within one sample, all of the carbons analysed show the same features, of the D- and G-bands as described above. The D/G ratio was calculated for all the above spectra, this is shown in table 4.6.

Sample	D/G ratios			Average D/G ratio
JM carbon	2.1	2.14	2.06	2.1
HCl treated carbon	2.11	2.04	2.05	2.07
HNO_3 treated carbon	2.11	2.13	2.18	2.14
Aqua Regia treated carbon	2.03	2.02	2.00	2.02

Table 4.6: D/G ratios for Raman spectra of as-provided and acid-treated carbon supports.

Similar values were obtained for all samples, indicating that the acid treatment of the carbon support does not significantly alter its bulk structure, and the effect of the acid

appears to be purely on the surface. This further enhances the idea of the importance of the functional groups on the catalyst surface.

4.6.3 Acid/Base Titrations of Acid Treated Carbons

Titrations may be used to identify and quantify acidic/basic functional groups present on the surface of activated carbons. Titrations were carried out by suspending the carbon samples in water and measuring the pH, then adding small amounts of dilute HCl/NaOH as appropriate, measuring the pH after a stabilisation time. The results of these titrations for carbons as-provided, and after treatment with each of the three acids (hydrochloric, nitric, *aqua regia*) can be seen in figures 4.31 – 4.34.

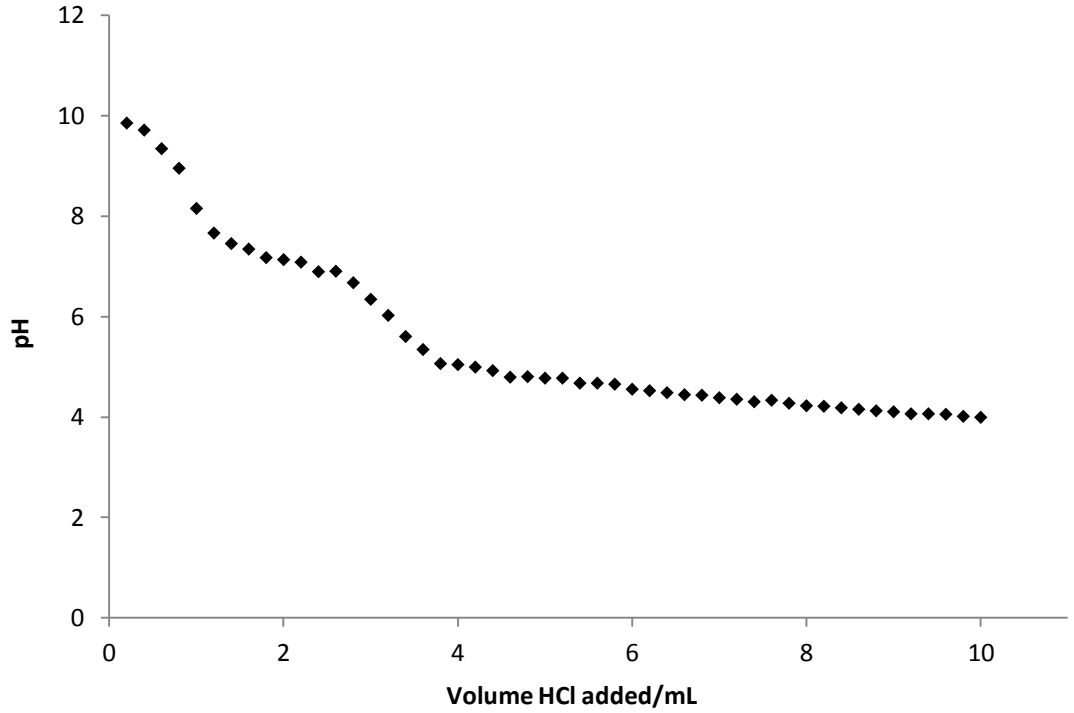

Figure 4.31: Titration of carbon as supplied (0.1 g) with 0.002M HCl, added in 0.2 mL portions, pH measured after 1 minute of stirring.

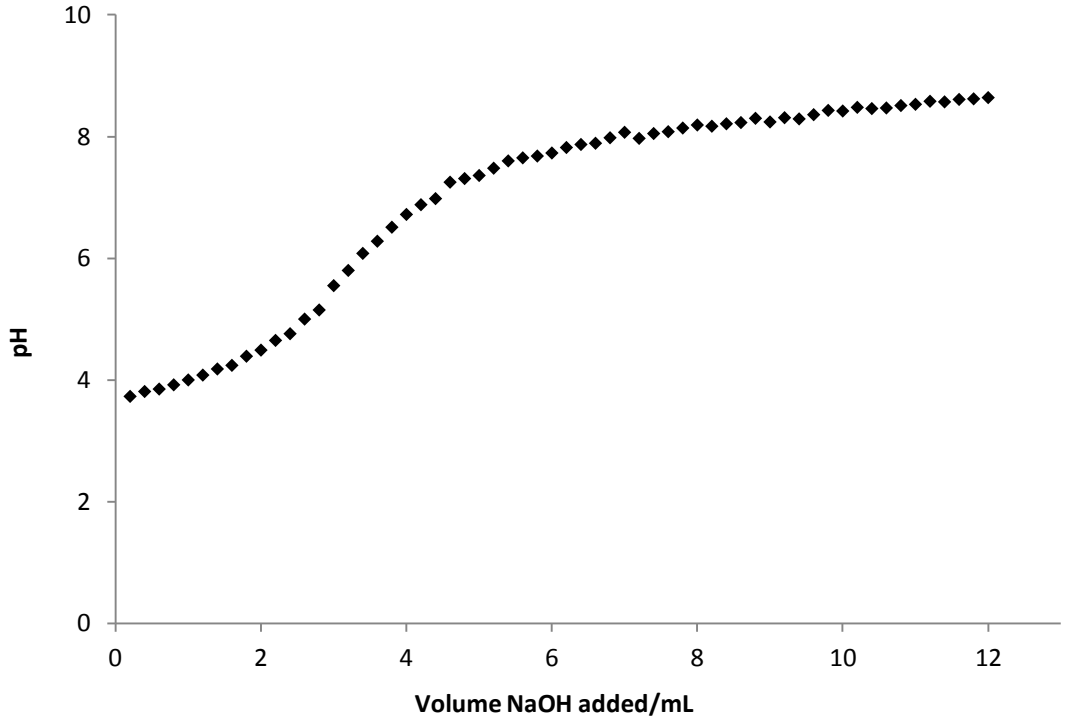

Figure 4.32: Titration of aqua regia treated carbon (0.1 g) with 0.002M NaOH, added in 0.2 mL portions, pH measured after 1 minute of stirring.

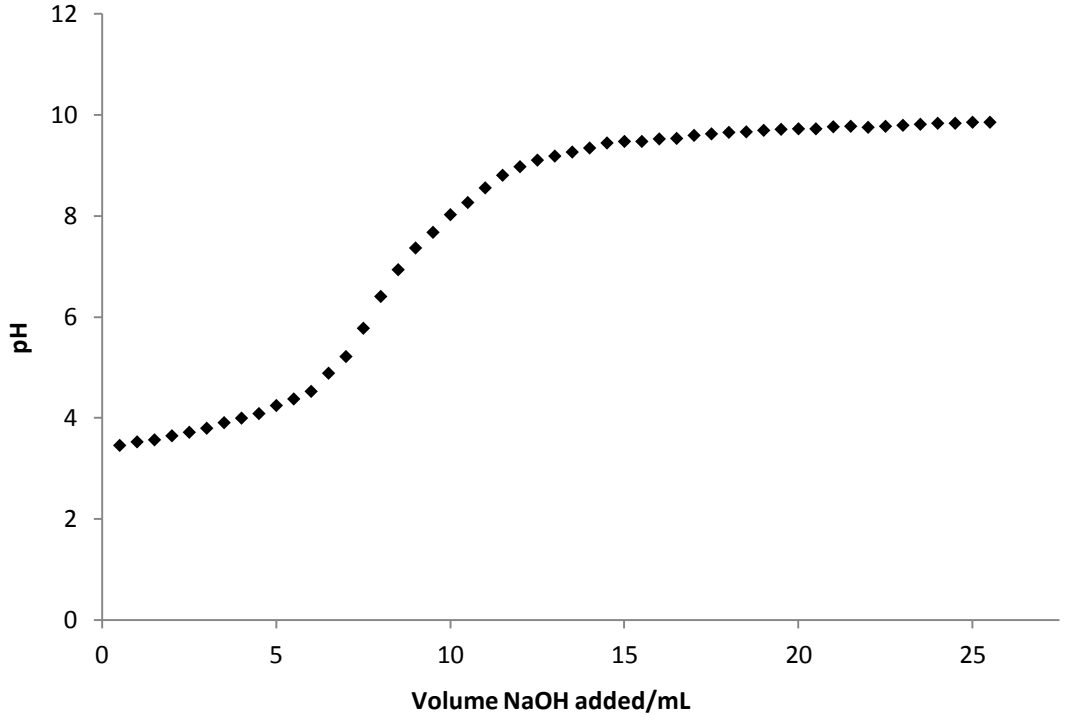

Figure 4.33: Titration of HNO_3 treated carbon (0.1 g) with 0.002M NaOH, added in 0.5 mL portions, pH measured after 1 minute of stirring.

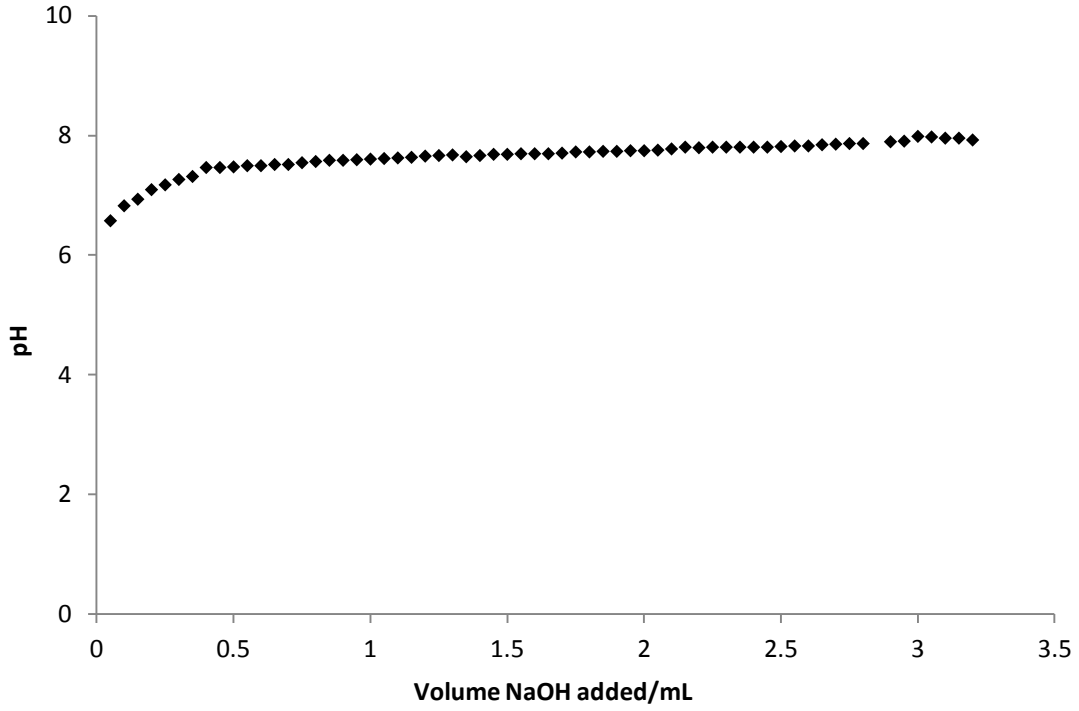

Figure 4.34: Titration of HCl treated carbon (0.1 g) with 0.002M NaOH, added in 0.05 mL portions, pH measured after 1 minute of stirring.

The end points of the titrations can be used to quantify the amount of a particular surface group that is present, whilst the flat sections of the graph are used to determine the pKa of the functional groups, which allows them to be identified. The amount of acid was varied for each sample in order to provide a plot of sufficient number of points to determine end points. As described in Chapter 2, it has been shown that carboxylic groups have pK_as in the range <6.37, lactones 6.37 – 10.25 and phenolic >10.25[24]. Therefore, from the titrations shown above, the functional groups present on the surface of the carbon before and after acid treatments can be identified and quantified to some extent, the results are shown in table 4.7.

It can be seen that the key difference between the untreated and acid treated carbons is that the untreated carbon is in fact basic. Also, there are two visible end points in the titration of the untreated support, but only one clear endpoint can be seen in each of the acid treated samples. However, the titrations for all three samples end at a fairly stable pH which is lower than that of 0.02 M NaOH alone would be

(approximately 12), suggesting that these may also be pK_as of functional groups. These pH values are all in the range 7.5 – 9.5, which is indicative of pK_as of lactone groups. For the nitric acid and aqua regia treated samples, there is initially a very slow increase in pH, which may be due to the presence of functional groups. The pH at this point is around 3.5 – 4, which indicates carboxylic groups. The hydrochloric acid treated sample, however, has a steep curve initially which resembles an end point. Although on the suspension of the carbon in water the lowest pH that was reached was 5.8, the position of this apparent end point is such that it occurs at a similar pH to those for the other acid treated samples. This suggests the possibility of the presence of carboxylic acid groups. The presence of carboxylic and lactone surface functional groups as suggested by titrations of the carbon correlates with the TPD results above, which also suggest that carboxylic and lactone groups are the main functional groups present on the surface of the catalysts.

Sample	pK_a	Functional group	Volume at end point/mL	Amount/(mol/g)
Aqua regia treated	3.8 8.2	Carboxylic Lactone	3.01 -	6.02×10^{-5}
HNO_3 treated	3.5 9.7	Carboxylic Lactone	7.60 -	1.52×10^{-3}
HCl treated	<6.37 7.8	Carboxylic Lactone	- -	-

Table 4.7: Functional groups present on the surface of acid treated carbons, as determined by titrations.

Quantification of functional groups is not feasible for the possible lactone groups, since there is no end point, or for the possible carboxylic groups on the HCl treated sample, since the titration appears to begin during the end point. However quantification of possible carboxylic acid groups on the aqua regia and HNO_3 treated samples is possible and is shown in table 4.7. As illustrated by the TPR/TPD data, these values confirm that the nitric acid treatment generates a larger amount of surface functional groups than the *aqua regia* treatment.

4.7 Acid Treated Carbons as a Support

A series of catalysts were prepared by impregnation in water, on the acid treated carbons. This was done to investigate the interaction of the gold with the surface functional groups created by the acid treatment, and how much of an effect this may have on the catalyst activity, since they may be possible nucleation sites for gold nanoparticles on the carbon surface. The testing results are shown in figures 4.35 – 4.37, compared with the activity of the corresponding catalysts prepared in acid (dried at 110°C).

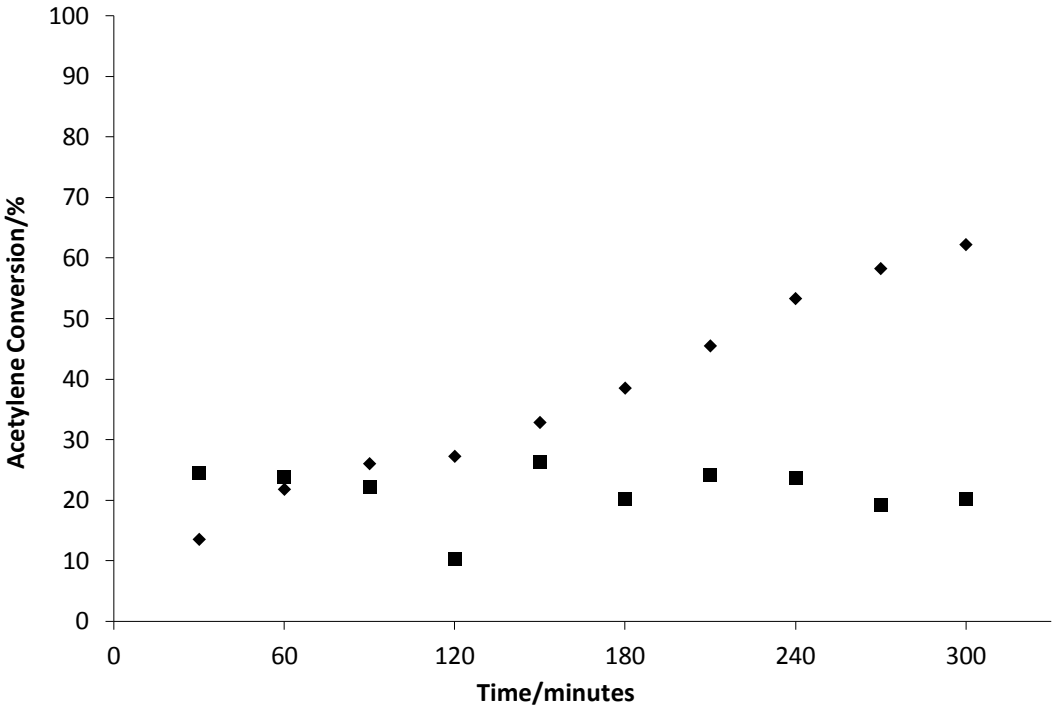

Figure 4.35: Activity of catalysts prepared in HNO_3 (◆) and prepared in water on an acid treated carbon support (■)

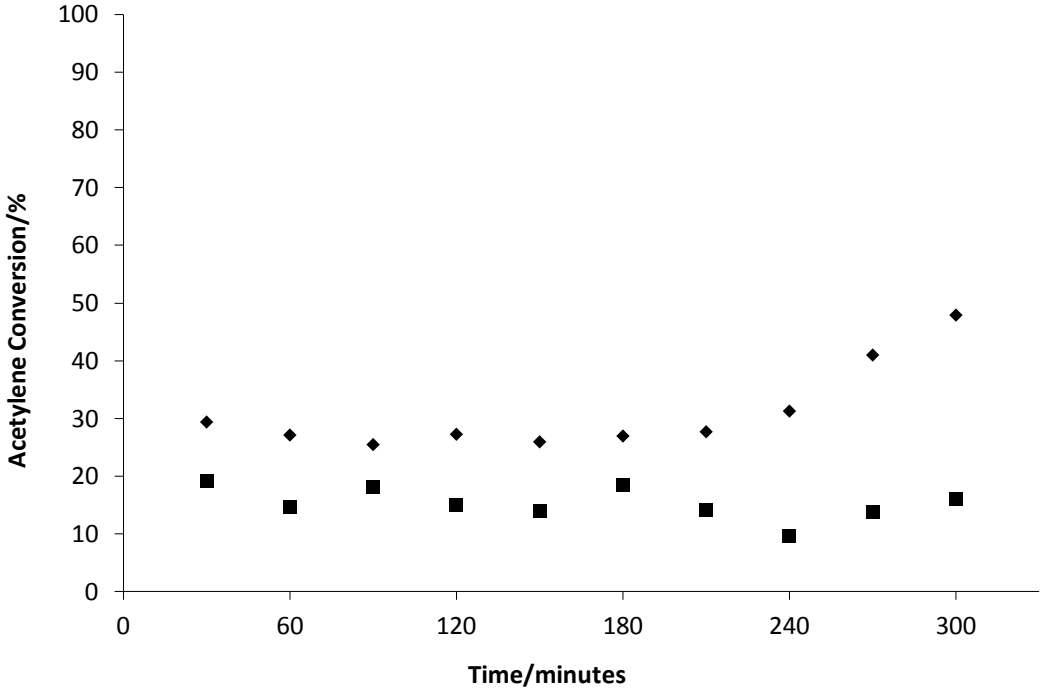

Figure 4.36: Activity of catalysts prepared in HCl (◆) and prepared in water on an acid treated carbon support (■).

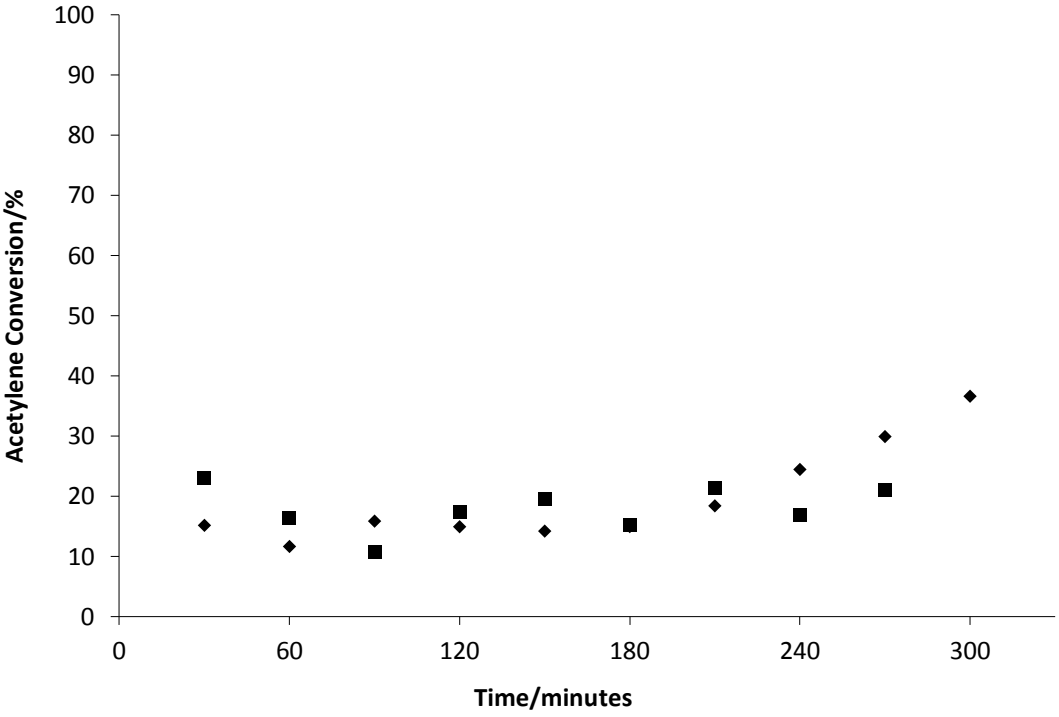

Figure 4.37: Activity of catalysts prepared in *aqua regia* (◆) and prepared in water on an acid treated carbon support (■)

It can be seen that for each of the acids used, both catalysts have a similar level of activity initially, however by the end of the reaction time the catalyst prepared in the acid has a significantly higher activity than the one prepared in water, on the acid treated carbon. The greatest difference in activity is seen for the nitric acid set of catalysts. The activity of the catalysts prepared in water stays roughly constant, whereas the activity of those prepared in acid begins to increase after 2-3 hours reaction time. This shows that although the acid does have a significant effect on the carbon surface, in terms of the functional groups present, while this may be a factor in how the gold interacts with the surface of the catalyst support, it seems that the effect of the acids on the gold itself is the more significant factor in determining the activity of the catalyst.

4.8 Conclusions

Consistent with previous work, it has been demonstrated that 1% Au/C catalysts prepared *via* impregnation of $HAuCl_4$ in an acid solvent contain a significant amount of Au^{3+} and are by far the most active for acetylene hydrochlorination, when compared to catalysts prepared by other commonly used methods.

It has been shown that using *aqua regia* as a solvent in the catalyst preparation produces more active catalysts than either of its constituent acids, nitric acid and hydrochloric acid, alone; this is considered to be due to the combination of the oxidising effect of the nitric acid and the stabilising effect of the chloride from HCl leading to a greater amount of Au^{3+}. The drying temperature used in preparation of catalysts was also found to influence the amount of Au^{3+}, with increasing temperature generally leading to a decrease in the amount of Au^{3+} detected. However, it has been found that there is not a direct correlation between the amount of Au^{3+} present on a catalyst and its activity, leading to the idea that the presence of Au^{3+} alone is insufficient for good activity, but it must also be in the correct chemical environment.

Since a possible mechanism for the reaction may be a redox cycle involving Au^{3+}, characterisation of catalysts was carried out by TPR. This was found to be a useful technique for analysis of Au^{3+} containing Au/C catalysts such as those used in this work, since it is able to provide information on both the Au species and the carbon support. There is a significant amount of information that may be obtained from TPR, for example quantification of reducible species and determination of kinetic parameters for the reduction reactions. TPR results have also shown that the reducibility of the Au^{3+} in these catalysts is a key factor in their activity, since the most easily reducible catalyst (*i.e.* the one for which the reduction of Au^{3+} occurred at the lowest temperature) was also the most active.

The effect of the acid on the carbon support was investigated, and it was found that treatment with acids leads to an increase in the oxygen containing functional groups present on the carbon surface, in particular carboxylic and lactone groups. Of the three acids used, HNO_3 was the most strongly oxidising, followed by *aqua regia* and then HCl, as would be expected. Catalysts were prepared by impregnation in water on each of the acid treated carbons and all were found to have low activity, suggesting that while the acid used in the catalyst preparation does significantly alter the carbon surface, it is the effect on the gold itself that is responsible for the differences in activity observed.

4.9 References

1. G. J. Hutchings, *J. Catal.*, 1985, **96**, 292-295.
2. B. Nkosi, N. J. Coville and G. J. Hutchings, *Appl. Catal.*, 1988, **43**, 33-39.
3. M. Conte, A. F. Carley, G. Attard, A. A. Herzing, C. J. Kiely and G. J. Hutchings, *J. Catal.*, 2008, **257**, 190-198.
4. M. Conte, Cardiff University, 2006.
5. B. NKOSI, N. COVILLE, G. HUTCHINGS, M. ADAMS, J. FRIEDL and F. WAGNER, *J. Catal.*, 1991, **128**, 366-377.
6. M. Conte, A. F. Carley and G. J. Hutchings, *Catal. Lett.*, 2008, **124**, 165-167.
7. J. A. Lopez-Sanchez, N. Dimitratos, C. Hammond, G. L. Brett, L. Kesavan, S. White, P. Miedziak, R. Tiruvalam, R. L. Jenkins, A. F. Carley, D. Knight, C. J. Kiely and G. J. Hutchings, *Nat. Chem.*, 2011, **3**, 551-556.
8. G. Hutchings, *Cat. Sci. Tech.*, 2012.
9. R. C. Tiruvalam, J. C. Pritchard, N. Dimitratos, J. A. Lopez-Sanchez, J. K. Edwards, A. F. Carley, G. J. Hutchings and C. J. Kiely, *Faraday Discussions*, 2011, **152**, 63-86.
10. P. R. Shukla, S. Wang, H. Sun, H. M. Ang and M. Tadé, *Applied Catalysis B: Environmental*, 2010, **100**, 529-534.
11. S. Wang and G. Q. Lu, *Carbon*, 1998, **36**, 283-292.
12. H. S. Oh, J. H. Yang, C. K. Costello, Y. M. Wang, S. R. Bare, H. H. Kung and M. C. Kung, *J. Catal.*, 2002, **210**, 375-386.
13. D. Lozano-Castelló, J. M. Calo, D. Cazorla-Amorós and A. Linares-Solano, *Carbon*, 2007, **45**, 2529-2536.
14. J. M. Calo, D. Cazorla-Amorós, A. Linares-Solano, M. C. Román-Martínez and C. S.-M. De Lecea, *Carbon*, 1997, **35**, 543-554.
15. C. Baatz, N. Decker and U. Pruesse, *J. Catal.*, 2008, **258**, 165-169.
16. S. Gil, L. Munoz, L. Sanchez-Silva, A. Romero and J. L. Valverde, *Chem. Eng. J.*, 2011, **172**, 418-429.
17. G. Bond, *Gold Bull.*, 2010, **43**, 88-93.
18. J. M. Calo, D. CazorlaAmoros, A. LinaresSolano, M. C. RomanMartinez and C. S. M. DeLecea, *Carbon*, 1997, **35**, 543-554.
19. G. Goncalves, P. A. A. P. Marques, C. M. Granadeiro, H. I. S. Nogueira, M. K. Singh and J. Gracio, *Chem. Mater.*, 2009, **21**, 4796-4802.
20. J. L. Figueiredo, M. F. R. Pereira, M. M. A. Freitas and J. J. M. Orfao, *Carbon*, 1999, **37**, 1379-1389.
21. P. Serp and J. L. Figueiredo, *Carbon Materials for Catalysis*, Wiley, 2009.
22. J. Filik, *Spectrosc. Eur.*, 2005, **17**, 10-17.
23. A. Manivannan, M. Chirila, N. C. Giles and M. S. Seehra, *Carbon*, 1999, **37**, 1741-1747.
24. H. P. Boehm, W. Heck, R. Sappok and E. Diehl, *Angew. Chem. Int. Ed.*, 1964, **3**, 669-&.

5 The Significance of Au^{3+} in the Hydrochlorination of Acetylene

5.1 Introduction

It was concluded in previous work that Au^{3+} is most likely to be the active site for the acetylene hydrochlorination reaction using carbon-supported Au catalysts, since catalyst deactivation occurs with reduction of Au^{3+} to Au^{0} [1]. However, the results obtained so far suggest that Au^{3+} may not be the only species responsible for the observed activity, since catalysts containing metallic gold only have also shown higher activity for this reaction than the carbon support alone (see chapter 3, effect of preparation method). It was also observed that catalysts containing the most Au^{3+} were not the most active (see Chapter 4). It has been suggested that a redox cycle between gold in different oxidation states (Au^{3+}, Au^{+}, Au^{0}) could be a possible mechanism for this reaction[2]. With a view to improving catalyst design, some systematic oxidation and reduction studies of various Au/C catalysts have been carried out in an attempt to determine the true importance of the Au^{3+} species.

5.2 Nitric Oxide Oxidation Treatments

Previous work on catalyst reactivation has shown that addition of nitric oxide (NO) to the reactant gas stream can regenerate catalyst activity for the acetylene hydrochlorination reaction[2]. This is illustrated in figure 5.1. It can be seen that there is a steady decrease in activity without the NO, then when it is added to the reactant gas stream there is a steady increase in activity, although the original HCl % conversion is not reached during the two hour time period of exposure to NO. This increase in activity is thought to be due to oxidation of metallic gold to Au^{3+} by the nitric oxide, and so XPS was used to investigate this hypothesis. Experiments were then carried out in which the nitrogen diluent was switched to a NO/N_2 mixture during the reaction, to investigate the possibility of *in-situ* oxidation of the catalyst. Pre-treatment of the catalyst with NO was also investigated.

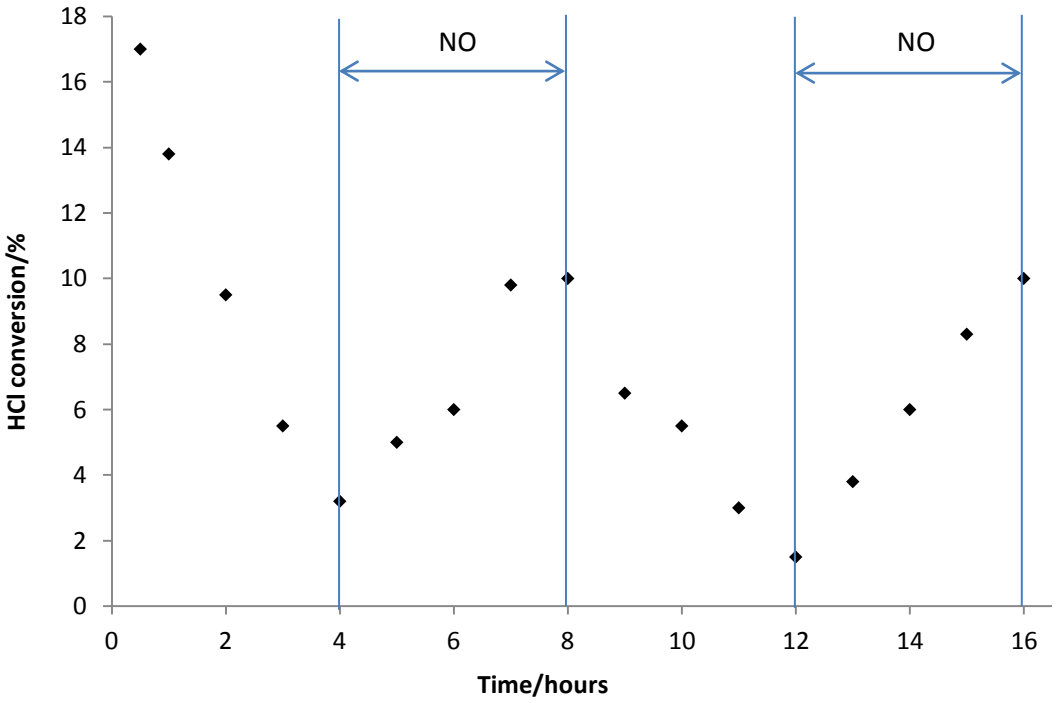

Figure 5.1: Time on line data for acetylene hydrochlorination to show the effect of addition of NO to the reactant gas stream[2].

5.2.1 XPS of catalysts in a nitric oxide atmosphere

A catalyst sample provided by Johnson Matthey, Au/C-JM, was exposed to an atmosphere of dilute NO in nitrogen (500 ppm) and XPS spectra recorded after exposure at room temperature of 30 minutes and 1 hour, also at a temperature of 150°C after 1 hour. These spectra can be seen in Figure 5.2. It is important to note that to use the sample in the XPS cell, it was necessary to form it into a disc. This was to avoid disturbance of a powder sample both when the vacuum was applied and then when the gas atmosphere (in this case the NO) was added. The only method by which a suitable disc could be made was to grind the sample to a powder, and then mix it with graphite, to act as a binding agent and prevent the disc falling apart after pressing. However, it is known from XPS analysis that this catalyst contains a greater amount of Au^{3+} than Au^{+0}, yet only metallic gold was detected in the Au 4f region of the XPS spectrum of the disc. Therefore it appears that the cationic gold was reduced

to metallic gold on the surface of the disc *via* the above process. The XPS spectrum of a mixture of ground catalyst and graphite shows that Au^{3+} is still present, so the reduction of the gold is most likely to occur due to the pressing of the disc, rather than solely the addition of graphite, although it is known that carbon is able to act as a reducing agent[3].

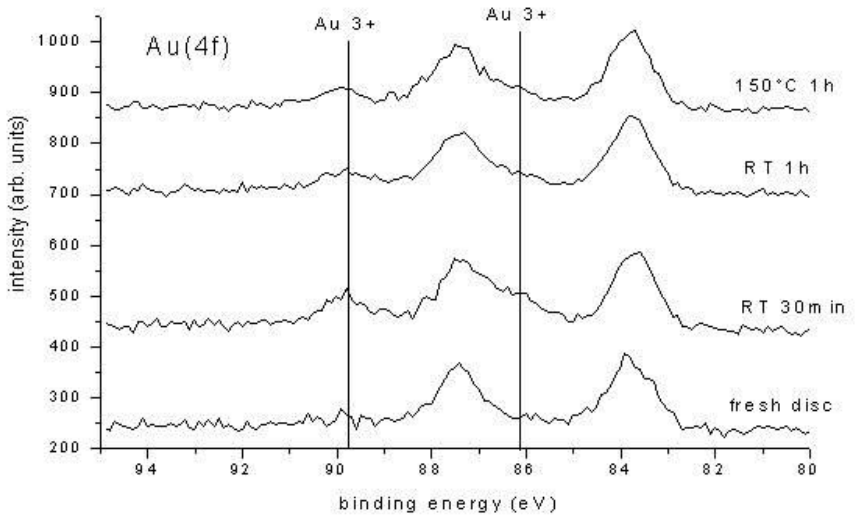

Figure 5.2: XPS spectra of Au/C catalyst after exposure to NO.

After exposure to NO, however, around 20% of the original amount of Au^{3+} was detected. This was found to be independent of both the duration of the exposure time and the temperature of the sample, since a similar amount of Au^{3+} was detected after thirty minutes and one hour, both at room temperature and after heating to 150°C. This XPS analysis of the catalyst shows that NO is indeed capable of oxidising Au^{0} to Au^{3+}, and that this is likely to be the cause of the regeneration of activity as described previously.

5.2.2 Reactions using nitric oxide in the reactant gas stream

Since it has been shown in principle that an oxidising agent such as NO is able to regenerate a significant amount of the original Au^{3+} of a catalyst after it has been reduced, this was then applied under reaction conditions. In order to try and improve catalytic activity by *in-situ* addition of an oxidising agent, reactions were carried out where the nitrogen diluent in the reactant gas stream was switched for a dilute (500 ppm) NO/nitrogen mixture between two and four hours reaction time. Initially the switching experiment was done using the Au/C-JM catalyst; the results are shown in figure 5.3. No significant enhancement in activity was observed during the addition of the NO and so a higher concentration NO gas mixture was used, since the first one (500ppm) was a lower concentration than that used in the previous work. A 4200ppm mixture was used, to be consistent with the experiment described in the previous work, and similar results to the 500ppm mixture were obtained.

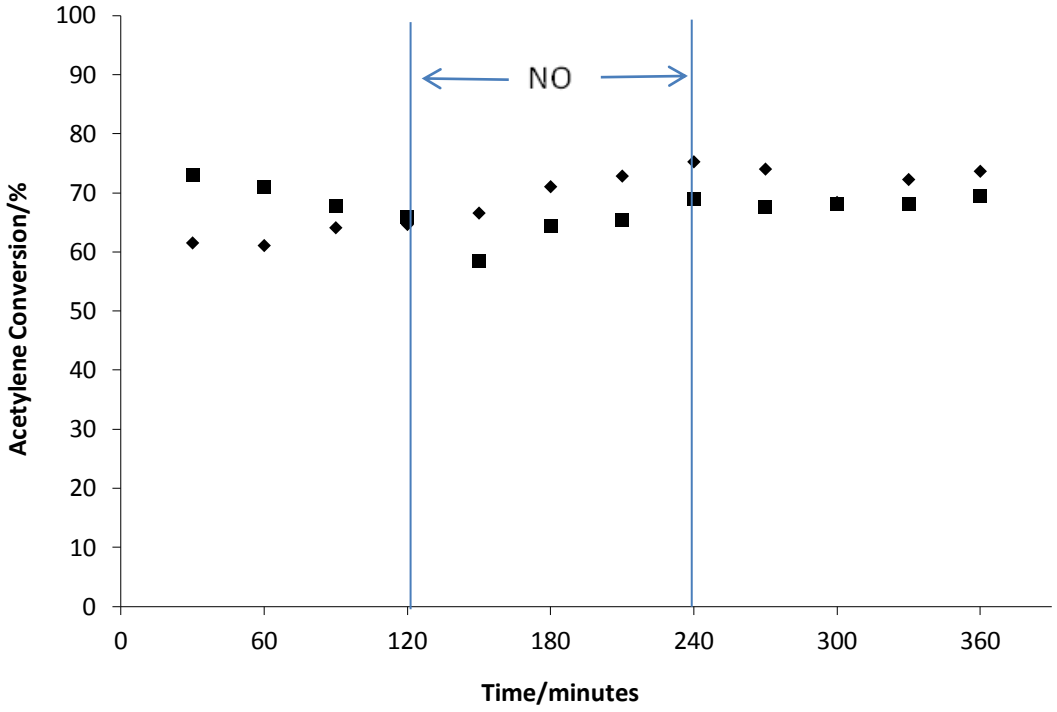

Figure 5.3: Au/C-JM, NO switching reactions using 500ppm (◆) and 4200ppm (■) NO/N_2.

It was thought that this lack of effect could be due to the catalyst already containing a large amount (approximately 59%) of Au^{3+} on the surface (as observed from XPS) and therefore the oxidising effect of the NO not making a large enough difference to the amount of Au^{3+} present. To investigate this, catalysts known to contain only metallic gold were tested with the addition of NO for part of the reaction, as before. The catalyst prepared by sol immobilisation also showed no significant enhancement in activity due to NO addition, for both the concentrations of NO used (500 and 4200 ppm), these results compared to activity under standard conditions can be seen in figure 5.4.

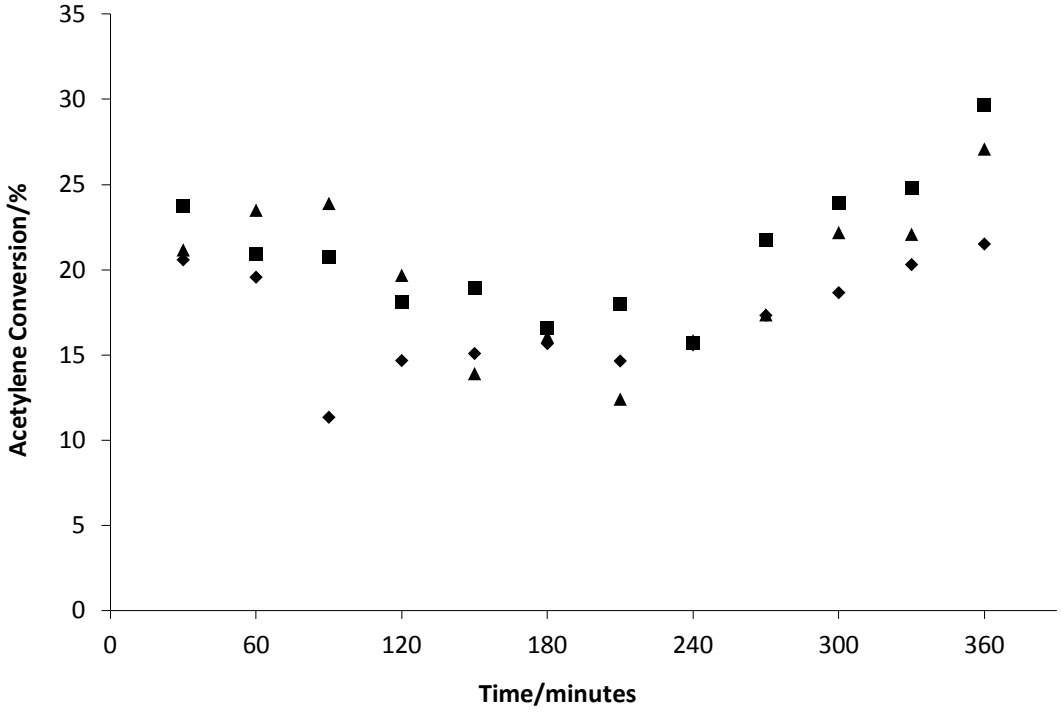

Figure 5.4: 1% Au/C Sol Immobilisation tested under standard conditions (▲), and switching reactions using 500ppm (◆) and 4200ppm (■) NO/N_2.

However, the Au nanoparticles on such catalysts have a layer of protecting PVA ligands, which may inhibit the reaction of the NO with the gold particles - it has been shown that stabilisation of gold nanoparticles with various ligands can reduce their catalytic activity[4], and that gold catalysts prepared *via* the sol immobilisation method

can display an increase in activity for a number of reactions when their stabilising ligands are removed[5]. Therefore catalysts prepared *via* DP and IMP methods were also tested (using only the 4200 ppm NO/N_2 mixture), since these are known to have metallic Au particles with exposed surfaces. These results are shown in figures 5.5 and 5.6 respectively. However, yet again, no significant enhancement in activity is observed.

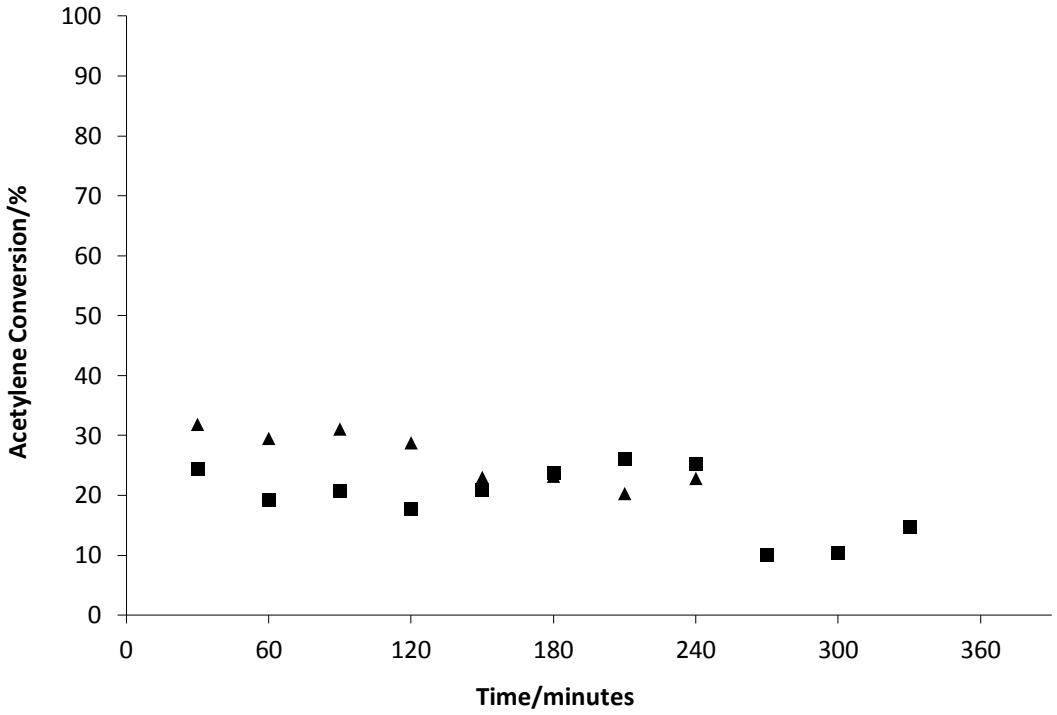

Figure 5.5: 1% Au/C DP, under standard conditions (▲) and switching reaction using 4200 ppm NO/N_2 (■).

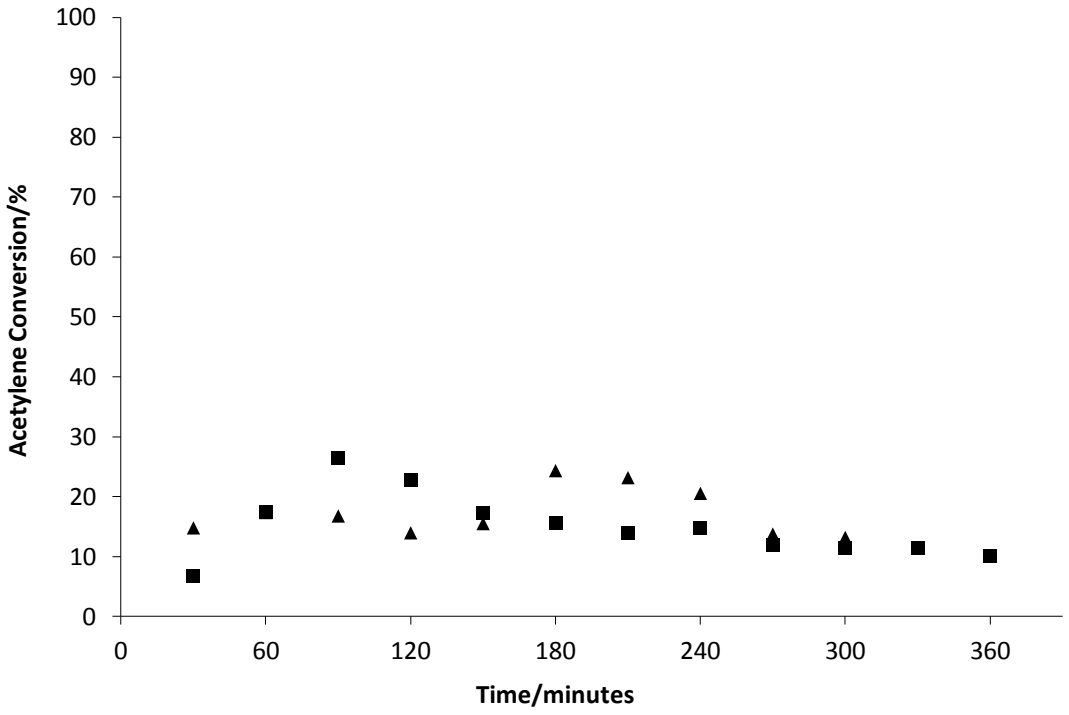

Figure 5.6: 1% Au/C IMP under standard conditions (▲) and switching experiment using 4200ppm NO/N_2 (■).

Whilst no significant improvement is seen in the activity of any of the above catalysts when NO is added to the gas stream, it is important to note that in the original work the increase in activity is from approximately 2 – 10% HCl conversion. This is a lower activity than is observed for the catalysts used in the above experiments. In addition an increase in activity this small may not be noticeable within the experimental error. Another important factor to be considered at this point is the difference in the set-up of the reactors used for the previous NO work and this project, in particular the control of gas flow. Whereas electronic mass flow controllers are now used (with the exception of the HCl, due to the likelihood of damage to the equipment caused by corrosion), previously needle valves would have been used which may have led to the possibility of an initial 'blast' of NO which could have a different effect to a steadily controlled gas flow. Whilst this effect may be small, it is nevertheless significant that there is a large difference in the reactor set-up and that this could contribute to the differences in the results obtained.

5.2.3 Reactions using a nitric oxide pre-treatment of the catalyst

The experiments involving switching the nitrogen diluent in the reactant gas stream for a NO/N_2 mixture did not show the increase in activity that might be expected, and one possible explanation for this is that perhaps competitive adsorption with the reactant gases present may be preventing the NO from having the desired effect on the gold particles. Therefore, NO pre-treatment of catalysts before reaction was also used. This means that the catalyst was subjected to similar conditions to those after which the oxidation of Au^0 to Au^{3+} was observed by XPS, *i.e.* exposed to an atmosphere of NO/N_2 only. In addition, a similar sample to that used in the XPS was used: The catalyst Au/C-JM was ground to a powder, mixed with graphite and pressed into a disc, then this disc was re-ground to a powder and tested for acetylene hydrochlorination. Another sample prepared in the same way was tested but with an NO pretreatment. The catalyst was heated to 185°C under a flow of NO/N_2 (500ppm, 10 mL/min) for 2 hours, then the hydrochlorination reaction carried out as normal. The results are shown in figure 5.7.

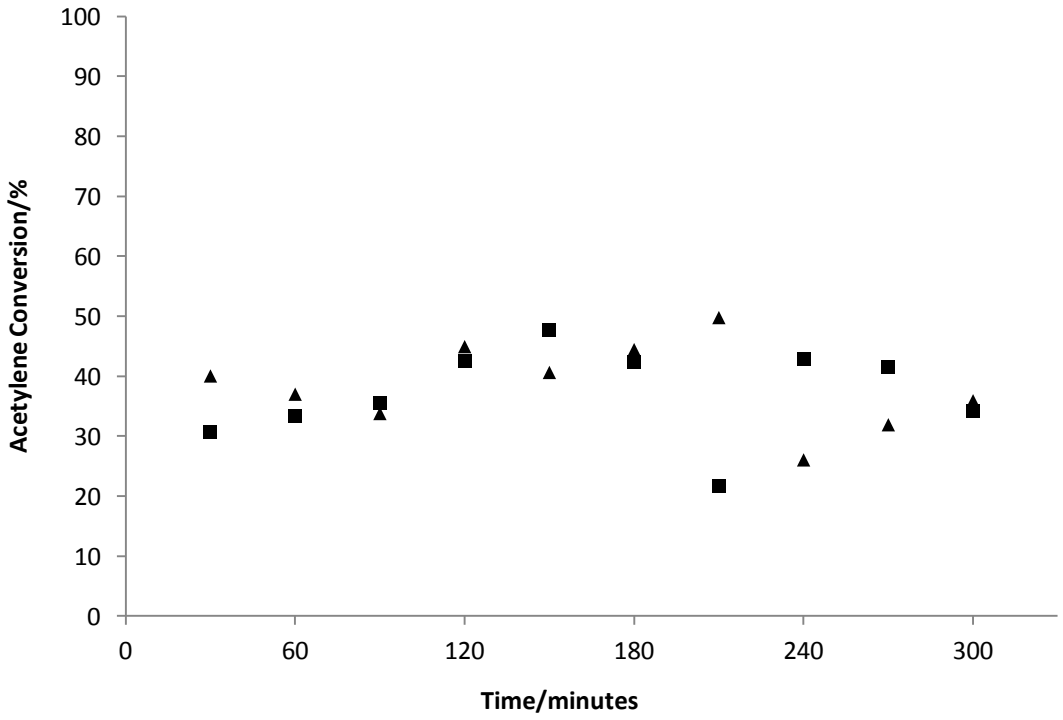

Figure 5.7: Activity of a mixture of Au/C-JM and graphite that had been pressed into a disc, under standard conditions (▲) and with a NO pretreatment (■).

No significant enhancement in activity was seen due to the NO pre-treatment. The activity of each of the samples is quite similar, in places where there is a large variation in activity this is most likely to be due to fluctuation of HCl pressure, which occasionally occurs and can affect the activity – it has been shown previously that an excess of HCl increases the activity of similar catalysts whereas an excess of acetylene decreases the activity[6]. The TPR profiles of the catalyst/graphite mixture before and after pressing into a disc and then grinding the sample back to powder are shown in figure 5.8.

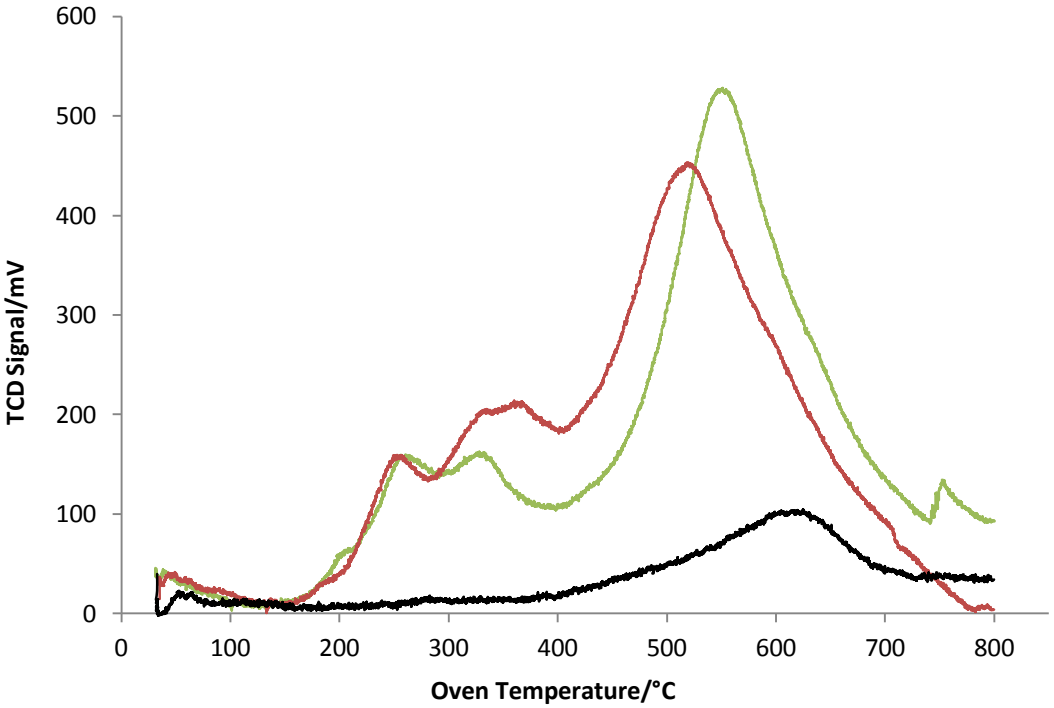

Figure 5.8: TPR profiles of catalyst Au/C-JM mixed with graphite, before (green line) and after (red line) pressing into a disc, and of graphite (black line).

The TPR of the sample after pressing is very similar to that of the catalyst itself, with a more pronounced feature at around 350 °C. This shows that the sample after mixing with graphite and pressing does in fact still contain Au^{3+}, which suggests that the complete reduction as observed by XPS only occurred on the surface of the disc. The TPR profile of graphite alone shows that this extra feature does not come from the

graphite, which has a similar profile to that of the carbon support, with only a small reduction feature at around 600°C.

Overall, despite showing that in principle NO may be used to oxidise Au^0 to Au^{3+}, attempts to utilise this to increase catalyst activity have been unsuccessful. This may be due to the interaction of the NO with the catalyst under the reaction conditions used. Au based catalysts have been used in the reduction of NO, which is an important aspect of exhaust cleansing[7-9], so it is known that NO will adsorb and interact with Au nanoparticles. Investigations into the adsorption of NO on Au have therefore been carried out, for example Bukhtiyarov *et al.* found that decomposition of NO occurs on steps and defects of Au particles, but not on a clean (111) plane, and that these adsorbed N atoms may be stable up to temperatures of 470K[10], which is equivalent to 197°C and therefore similar to the reaction temperature of 185°C used for acetylene hydrochlorination. It could therefore be the case that the NO does oxidise the gold, but the effects are counteracted by blocking of the active sites by NO or derived species. Carbon materials have also been used for reduction of NO[11], so another possibility is that the NO could be reacting with the carbon support, rather than (or as well as) the gold particles and so the effect on the gold is lessened.

5.3 Cerium (IV) Sulphate treatments

As a clear oxidising effect of NO on the reduced surface of the catalyst disc used for XPS analysis was observed, yet did not produce the expected increase in activity when used in the testing of catalysts, other oxidation methods were investigated in order to determine whether simple oxidation treatments of Au/C catalysts before use may increase activity for acetylene hydrochlorination. Cerium (IV) is widely used in aqueous solutions as an oxidant in quantitative analysis[3] and so was considered a good choice for oxidation treatment of catalysts. The cerium (IV) sulphate ($Ce(SO_4)_2$) salt was used. Initially, a catalyst prepared by impregnation in *aqua regia* and dried at 110°C was treated with cerium sulphate and then tested under the standard conditions for acetylene hydrochlorination. To carry out this oxidation treatment, a

portion of the catalyst was stirred in a saturated solution of $Ce(SO_4)_2$ for 1h, then filtered under vacuum, washed with deionised water and dried overnight (16h) at 110°C. Figure 5.9 shows the activity for the treated and untreated catalysts, there is a clear consistent increase in activity after the oxidation treatment, with the treated catalyst giving an additional *ca.* 40% acetylene conversion.

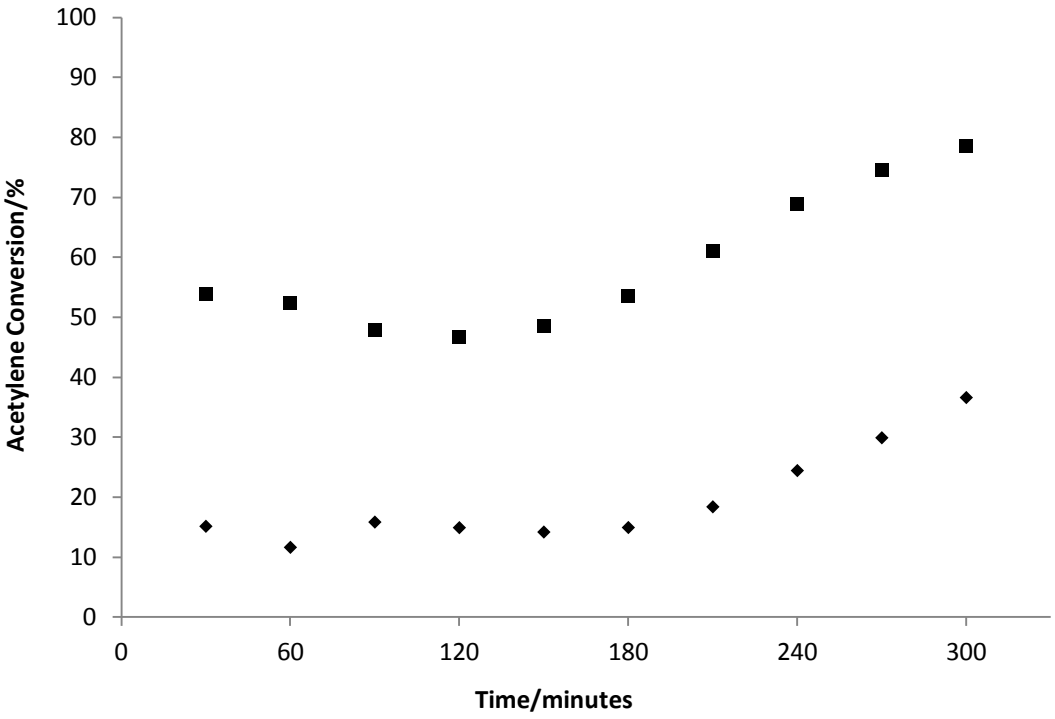

Figure 5.9: 1% Au/C catalyst before (◆) and after (■) cerium (IV) sulphate oxidation treatment.

TPR of the catalyst after oxidation treatment with cerium (IV) sulphate (figure 5.10) shows additional sharp reduction peaks at higher temperature. These are most likely to be due to reductions of cerium species, and indicate that there are some residual cerium containing species on the catalyst even after washing. XPS of the oxidised catalyst confirms that cerium species are present on the surface, since signals at binding energies of around 885 eV were observed after the oxidation treatment and these are in the Ce 3d region. In addition, the reductions attributed to functional groups on the carbon are altered, with the reduction at 450°C disappearing and the reduction at 550°C increasing in intensity, indicating that the treatment has affected the carbon. Changes to the reduction attributed to gold are also observed, with a double peak now being seen where the first peak maximum occurs at a lower

temperature than for the untreated sample: 226°C compared to 265°C. XPS analysis of the Au4f region is shown in figure 5.11 and the presence of Au^{3+} is observed. However, the intensity of the signal is perhaps the opposite of what would be expected: it indicates that there is now less Au^{3+} present compared to the amount of metallic gold. This suggests that the increase in activity does not arise from an increase in the amount of Au^{3+} present due to oxidation by the cerium sulphate. It may be due instead to the observed increase in reducibility of the Au^{3+}, which was found in the previous chapter to be of importance.

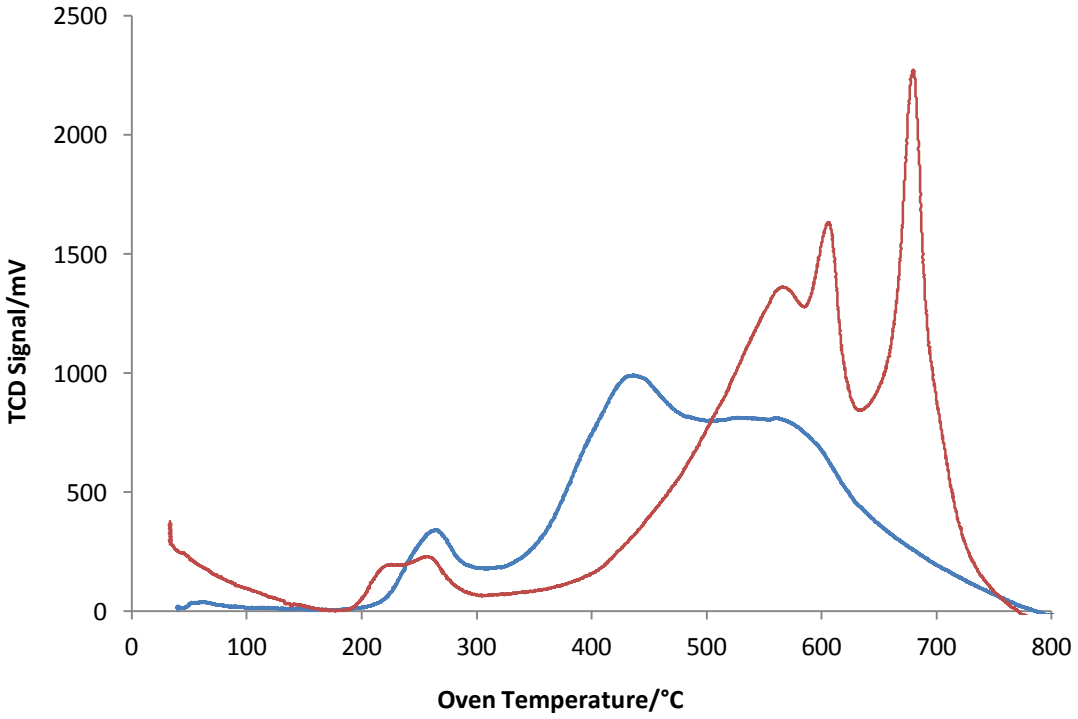

Figure 5.10: TPR profile of 1% Au/C catalyst before (blue line) and after (red line) oxidation treatment with cerium (IV) sulphate.

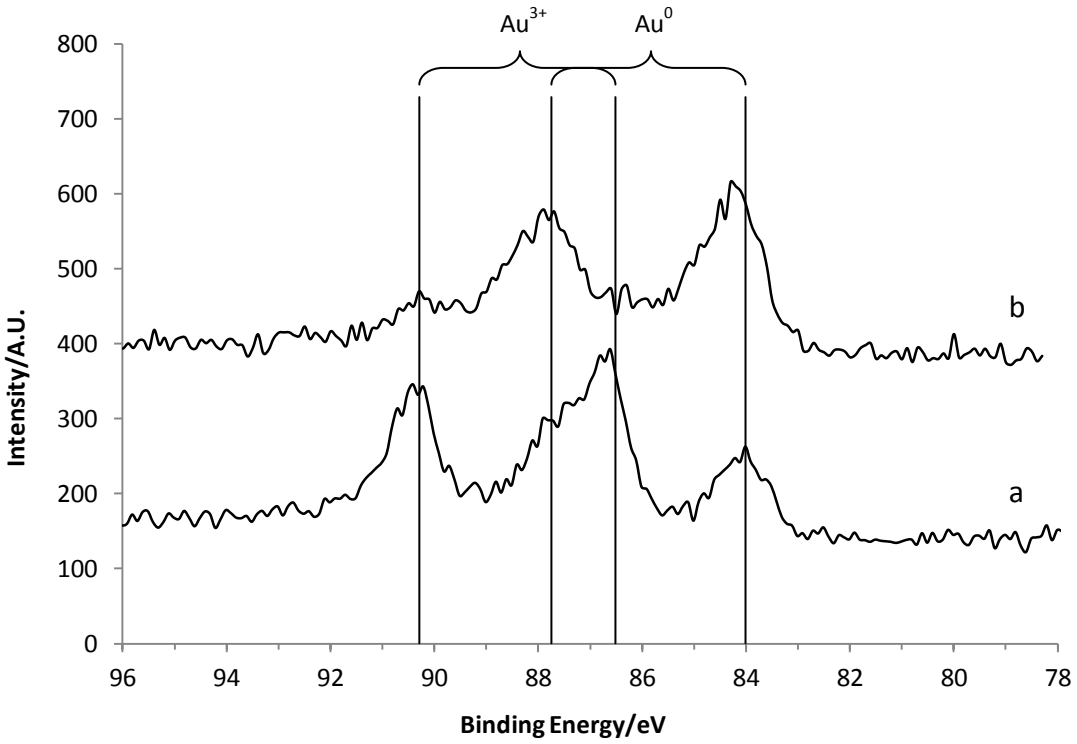

Figure 5.11: XPS spectra of 1% Au/C catalyst a) before and b) after oxidation treatment with cerium sulphate.

Since treatment with cerium sulphate proved successful, in that the activity of the catalyst was greatly increased after treatment, the same treatment was used on other catalysts: one prepared by impregnation in water (IMP), one prepared by impregnation in *aqua regia* then subjected to a reduction treatment (heating under hydrogen) and the standard catalyst, Au/C-JM. This was in order to investigate the difference in the effect of the cerium sulphate on catalysts which contain different amounts of cationic/metallic gold. Figures 5.12 – 5.14 show the TPR profiles of each of these cerium sulphate samples compared to those of the original, untreated catalysts.

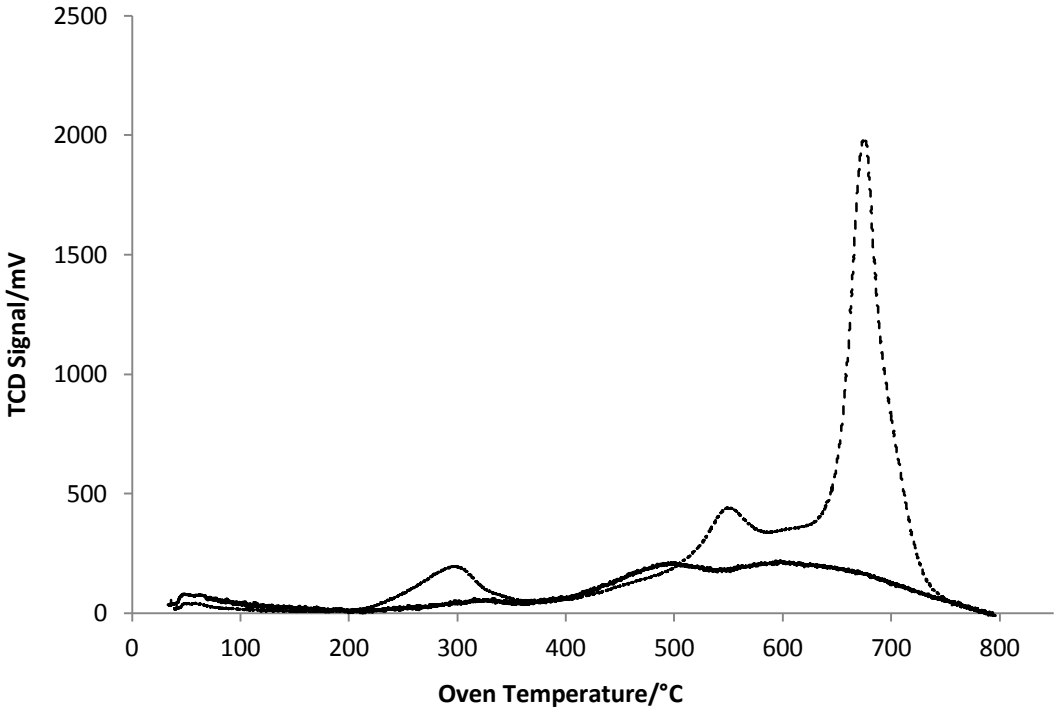

Figure 5.12: TPR profile of 1% Au/C catalyst prepared by IMP in water, before (solid line) and after (dashed line) cerium sulphate treatment.

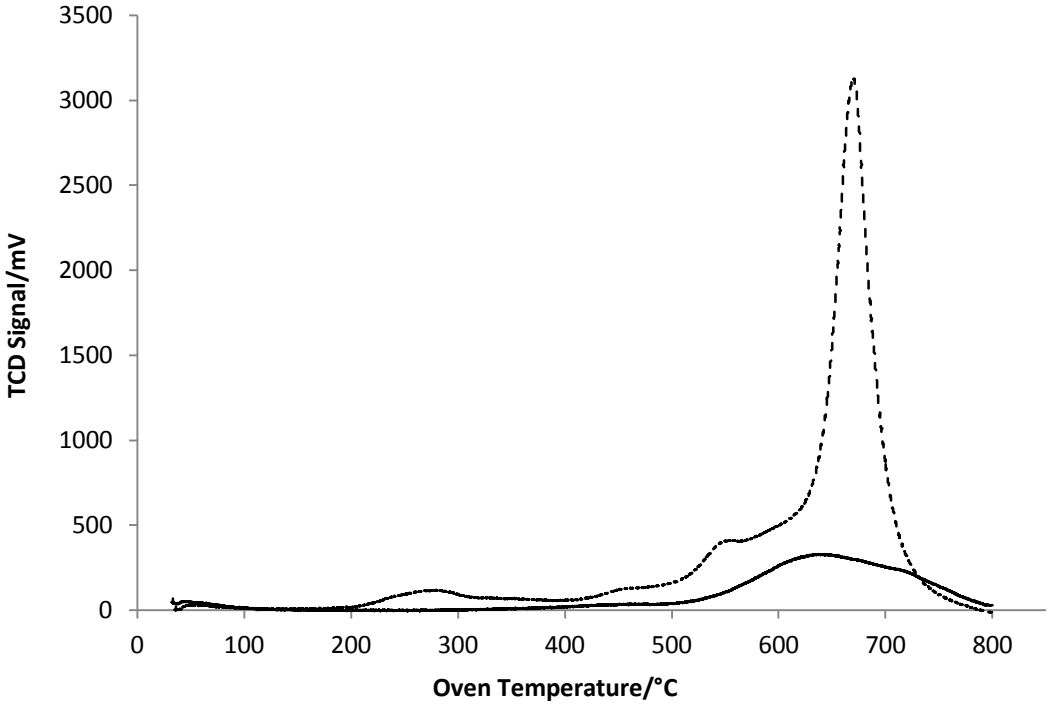

Figure 5.13: TPR profile of 1% Au/C catalyst prepared by IMP in *aqua regia* then reduced by heating under hydrogen, before (solid line) and after (dashed line) cerium sulphate treatment.

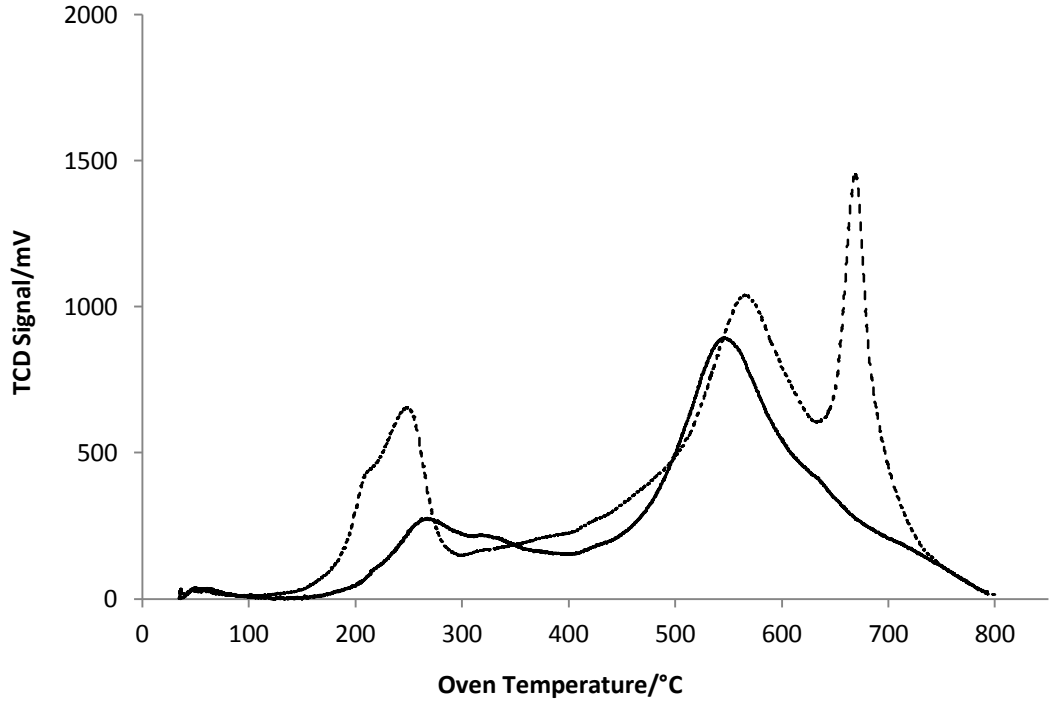

Figure 5.14: TPR profile of Au/C-JM catalyst, before (solid line) and after (dashed line) cerium sulphate treatment.

It can be seen in each case that the cerium sulphate treatment has a significant effect on the catalysts. For all three samples an additional sharp reduction is seen at around 700°C. Reductions around 750°C are known to occur due to bulk ceria, CeO_2[12], and so this feature may be due to reduction of Ce^{4+} species. There is also a larger reduction feature at around 550°C, which corresponds with the reduction peaks attributed to functional groups on the carbon support, indicating that the cerium sulphate treatment may be creating these groups. Reductions at this temperature have been attributed to surface reduction of capping oxygen[12], which fits with these reductions being due to oxygen containing functional groups on the carbon surface. For both the IMP and reduced catalysts a reduction at a temperature of just below 300°C is introduced, indicating that oxidation of gold has occurred. For the Au/C-JM catalyst, which already had a reduction due to gold present, this reduction now occurs at a lower temperature, indicating that the gold is more easily reducible. For comparison

with the TPR profiles of the cerium sulphate treated catalysts, the TPR profile of the cerium sulphate salt itself is shown in figure 5.15.

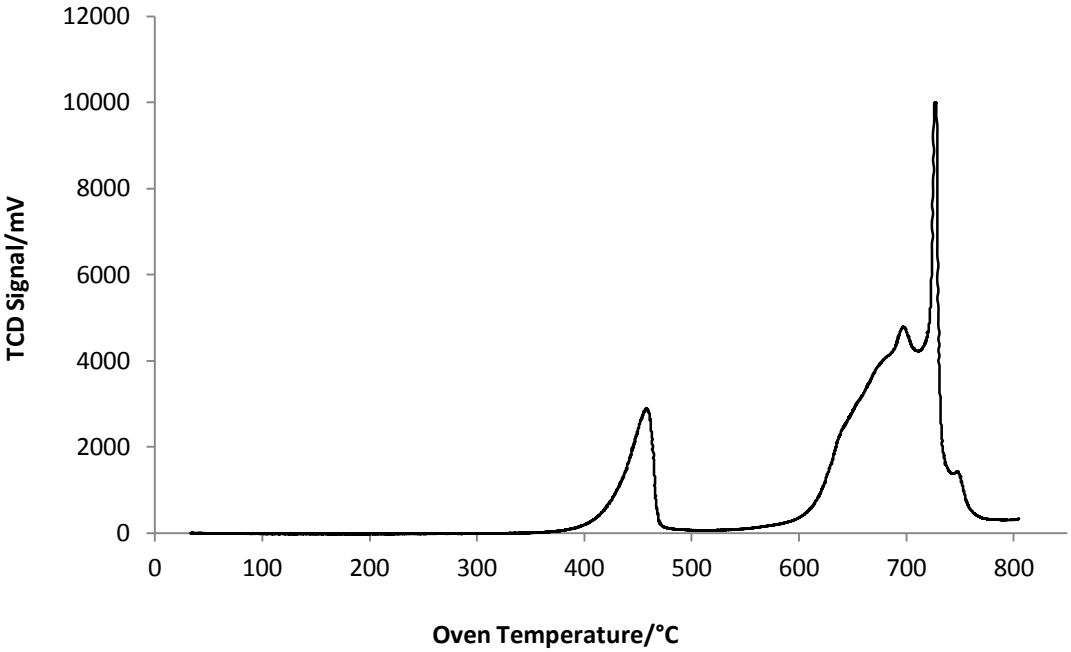

Figure 5.15: TPR profile of cerium (IV) sulphate salt, $Ce(SO_4)_2$.

There is a peak at 700°C which corresponds with the sharp reduction feature in the treated catalysts, although the signal intensity is much lower for these samples. This is consistent with features at this temperature being due to the reduction of Ce^{4+} as it would be expected for a lot less of this reducible species to be present on the treated catalyst, compared to the cerium sulphate salt. There are also reduction features in the TPR of the cerium sulphate salt which are no longer present in the treated catalyst samples, those at *ca.* 450°C and 750°C. It is therefore likely that the species leading to these reduction features are those that are reduced in the oxidation of the catalyst.

These other cerium sulphate treated samples have not been tested for acetylene hydrochlorination so it is difficult to determine which of the effects the treatment has is responsible for the increase in activity observed. It is possible that the changes to

the oxidation state/reducibility of the gold, the oxidation of the carbon support or the presence of residual cerium species may be involved. Many metals are able to catalyse the acetylene hydrochlorination reaction[13]; however, the standard electrode potential for the reduction of Ce^{3+} (-2.336) is lower than that of Au^{3+} (1.498)[14] and so it should not be as active. However, the standard electrode potential for the reduction of Ce^{4+} to Ce^{3+} has a value of 1.72 which is higher than for the gold and therefore it could be expected that the presence of Ce^{4+} may lead to an increase in activity, as observed.

5.4 Catalyst Regeneration *via* oxidation by acids

In previous studies on catalyst reactivation for the acetylene hydrochlorination reaction it has been shown that activity of a 1% Au/C catalyst which has deactivated during the reaction can be restored to an extent by boiling in *aqua regia*[15] . It was decided to further investigate acid treatments of reduced catalysts, as a simple way of regenerating catalyst activity by oxidation to form Au^{3+} species.

A catalyst prepared in *aqua regia* and dried overnight at 140°C was heated at 550°C for 3h in a 5% H_2/Ar flow at a ramp rate of 10°C/min. Figure 5.16 shows the activity for the fresh and reduced catalysts. The fresh catalyst shows the usual activity profile, with a steady increase in acetylene conversion to around 70%, however the reduced catalyst shows a much lower activity of around 10-20% conversion, similar to that of the carbon support alone. The TPR of both these catalysts can be seen in figure 5.17 and shows that after reduction both the gold species and the carbon surface functional groups have been reduced. The XPS spectra of the Au 4f region of the fresh and reduced catalysts are shown in figure 5.18 and confirm that Au^{3+} has been reduced to Au^0.

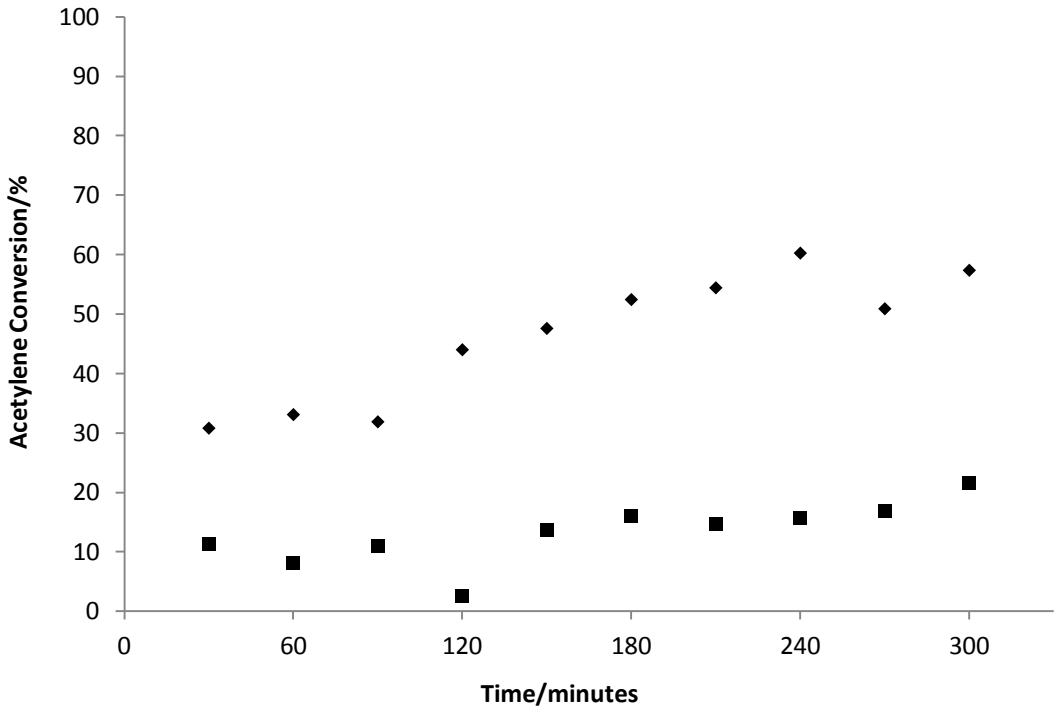

Figure 5.16: catalytic activity of an Au/C catalyst prepared by impregnation in *aqua regia*, before (◆) and after (■) reduction treatment.

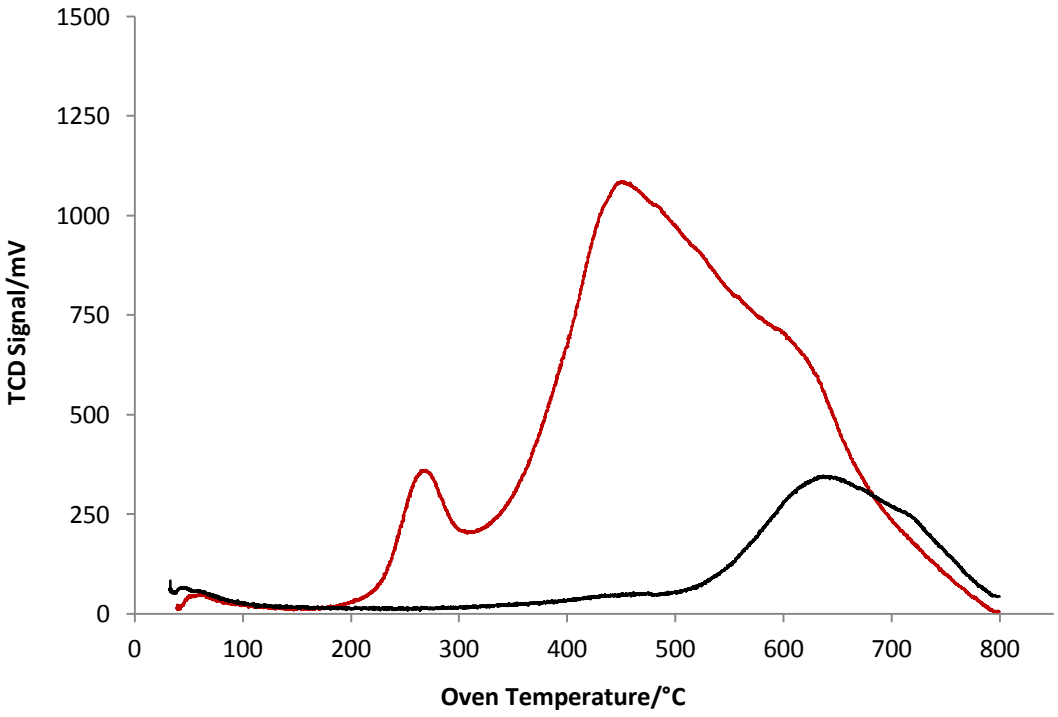

Figure 5.17: TPR profiles of an Au/C catalyst prepared by impregnation in *aqua regia*, before (red line) and after (black line) reduction treatment.

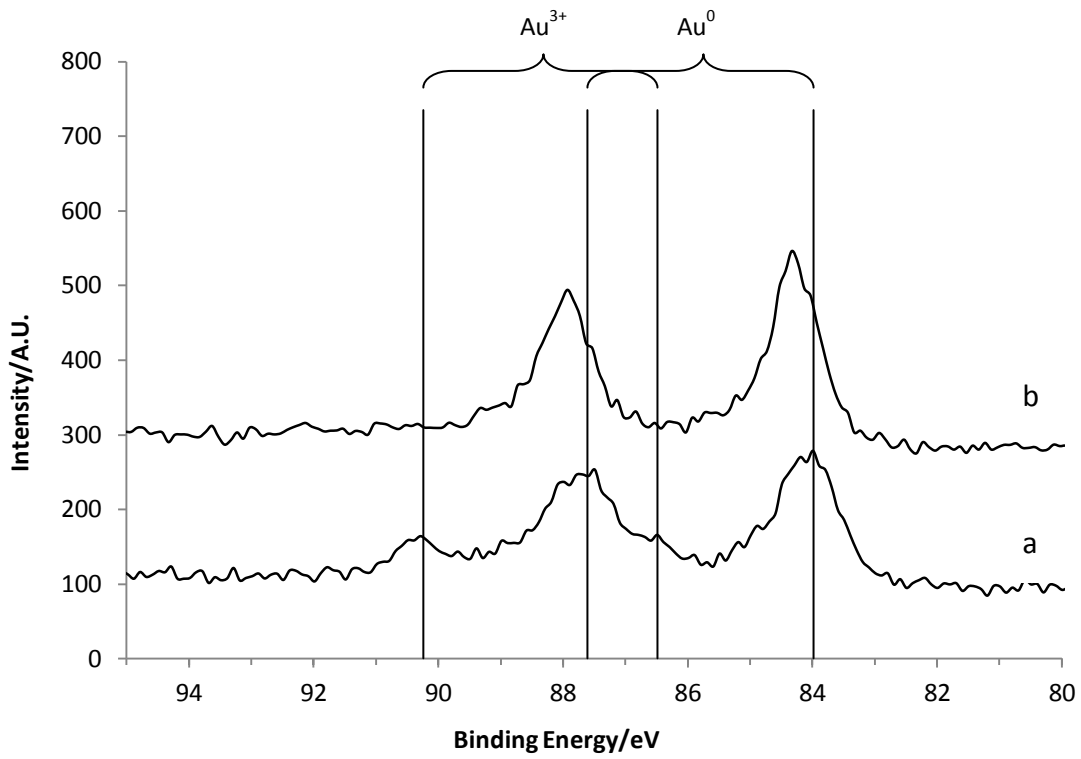

Figure 5.18: XPS spectra of a) 1% Au/C catalyst prepared by impregnation and dried at 140°C and b) the same catalyst, after reduction treatment.

The reduced catalyst was then split into three portions, each of which was treated with one of the acids HCl, HNO_3 and *aqua regia*, by stirring in the concentrated acid at room temperature for 10 minutes (*i.e.* until production of NO_x had subsided), then drying overnight (16 h) at 140°C. These catalysts were then tested for acetylene hydrochlorination and the results are shown in figure 5.19. Following each of the acid treatments, catalyst activity has been regenerated, with activity of around 60% conversion attained by all three after 5h reaction time. The TPR profiles of these catalysts, shown in figure 5.20, show that in each case the acid treatment has re-oxidised both the gold and the carbon support. The nitric acid is the most strongly oxidising of the set of acids used, followed by *aqua regia*, then hydrochloric acid, as would be expected and this can be seen from the size of the reduction features at 500 - 600°C, attributed to reductions of surface functional groups on the carbon support. The reduction due to Au^{3+}, at around 250°C is at a slightly higher temperature for the samples treated by HCl and *aqua regia*, this is likely to be due to stabilisation of the

oxidised gold species by the Cl^- ions which are present in these two acids, but not the nitric acid. The Au 4f XPS spectra of the three catalysts treated with acid after reduction are shown in figure 5.21. The signals due to metallic gold are clearly visible, however no significant increase in the signal due to Au^{3+} is observed. The high activity obtained by catalysts which appear to have virtually no Au^{3+} from XPS analysis, although reductions attributed to this species are present in the corresponding TPR profiles, again indicate that whilst the presence of Au^{3+} generally leads to good catalytic activity, there is not a direct link between the amount of cationic gold present on a catalyst's surface and its activity.

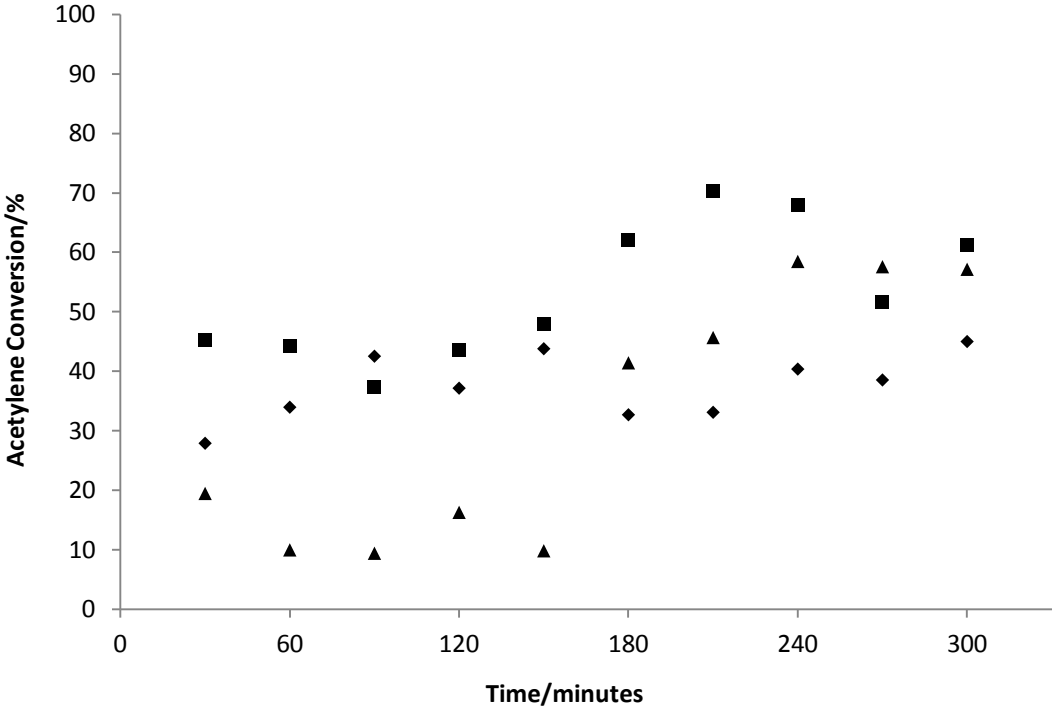

Figure 5.19: Catalytic activity of catalysts treated with HCl (▲), HNO_3 (◆) and *aqua regia* (■) after reduction treatment.

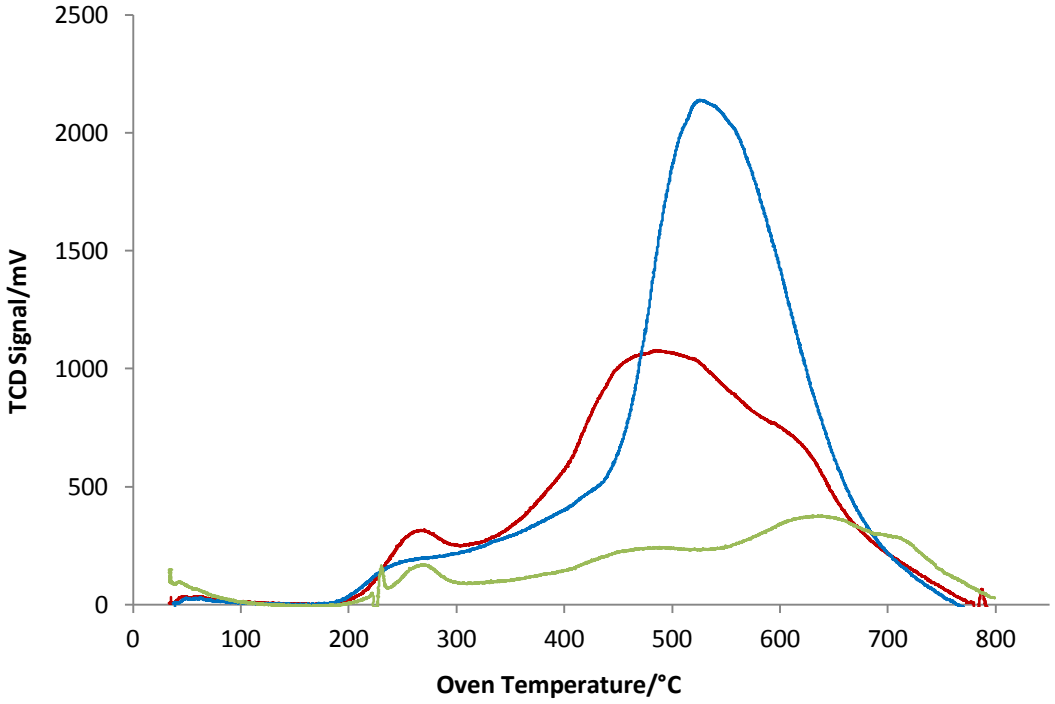

Figure 5.20: TPR profiles of catalysts treated with HCl (green), HNO_3 (blue) and *aqua regia* (red) after reduction treatment.

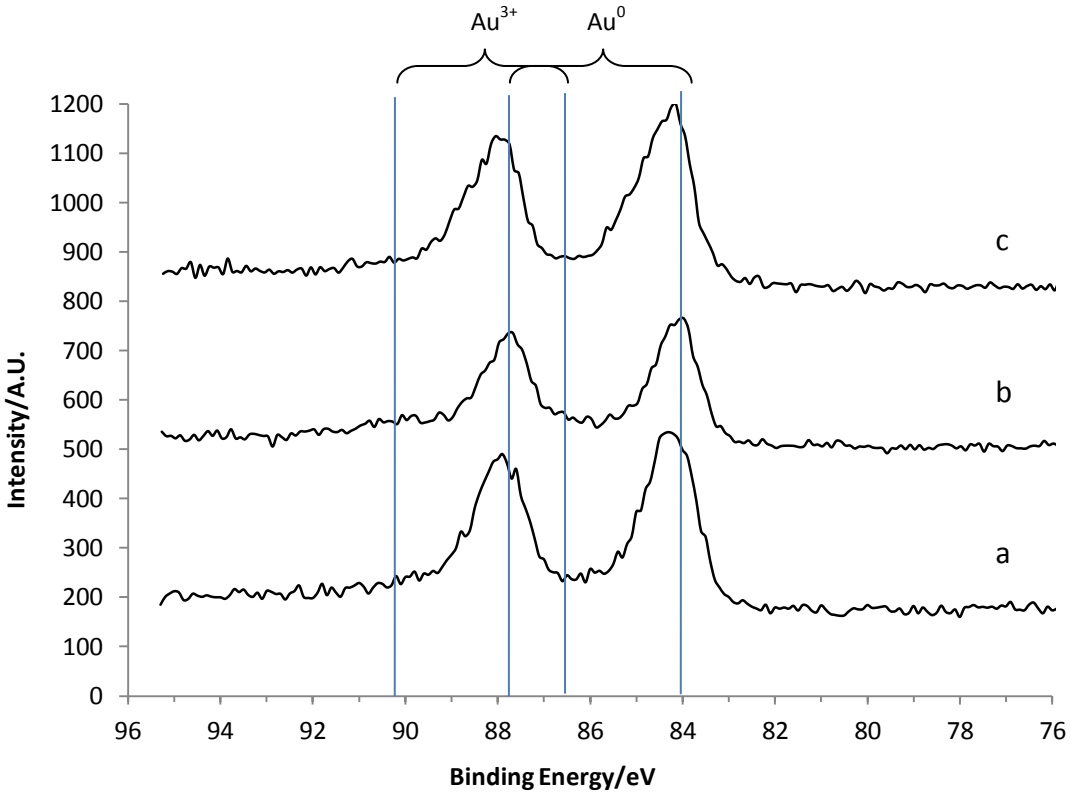

Figure 5.21: XPS spectra of the Au 4f region for the reduced 1% Au/C catalyst, after treatment with a) aqua regia, b) HCl and c) HNO_3.

5.5 Sequential oxidation/reduction treatments

A catalyst prepared by impregnation in *aqua regia* and dried at 140°C was subjected to sequential reduction and oxidation treatments. Reduction treatment consisted of heating the sample at 550°C for 3h (ramp rate 10°C/min) under a flow of 5% H_2/Ar. Oxidation treatment was stirring in a minimum amount of *aqua regia* (3:1 HCl:HNO_3 by volume) at ambient temperature for 10 minutes (*i.e.* until NO_x production subsided) followed by drying overnight at 140°C. A number of reduction and oxidation treatments were carried out, producing the catalysts labelled F (fresh), R, R/O, R/O/R, R/O/R/O and R/O/R/O/R, where O indicates an oxidation treatment and R a reduction treatment, as described above. Testing data for these catalysts is shown in figure 5.22. The fresh and oxidised samples all show a similar activity profile, with an initial low activity which then gradually increases and then stabilises at a good activity of approximately 60% after 5 hours reaction time, although the increase in activity during reaction occurs at a different time for each. All of the reduced catalysts have a low, stable activity of around 10%.

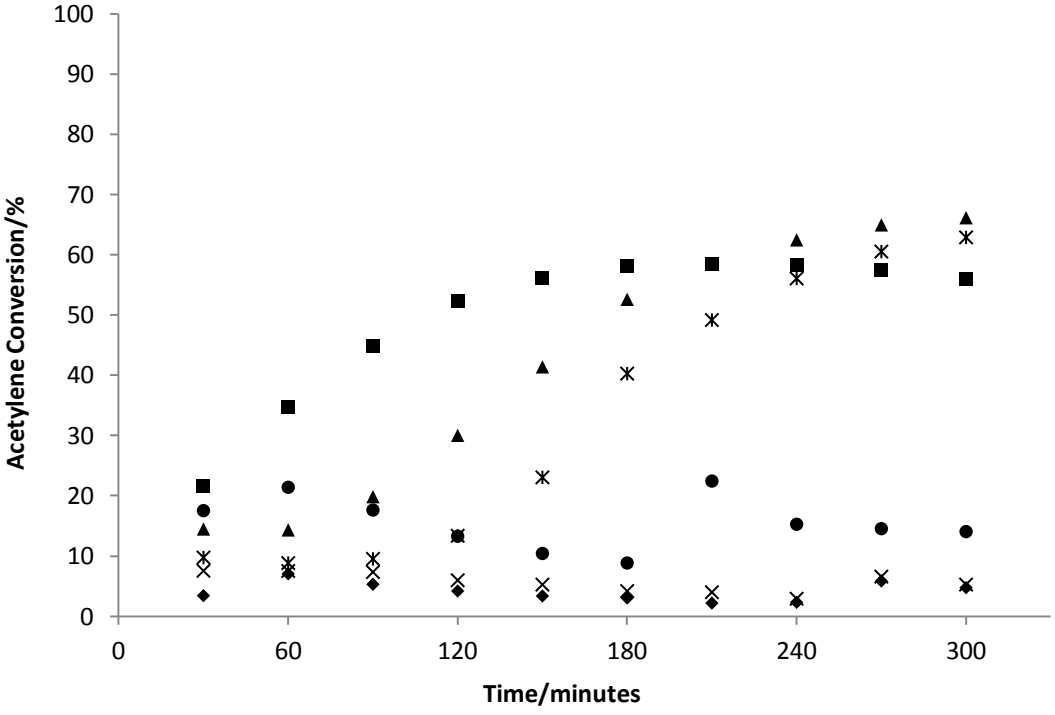

Figure 5.22: Catalytic activity of a series of Au/C catalysts following sequential reduction/oxidation treatments: fresh (▲), R (×), R/O (✳), R/O/R (●), R/O/R/O (■) and R/O/R/O/R (◆).

TPR profiles for each of the catalysts are shown in figure 5.23. The profile shapes are similar for the fresh and oxidised samples, and for the reduced samples, showing that both the gold and carbon support are oxidised after oxidation treatments, and reduced after reduction treatments, and that this is repeatable. This can be considered to be further experimental evidence of the correlation between oxidation state and activity in Au based catalysts for the hydrochlorination of acetylene.

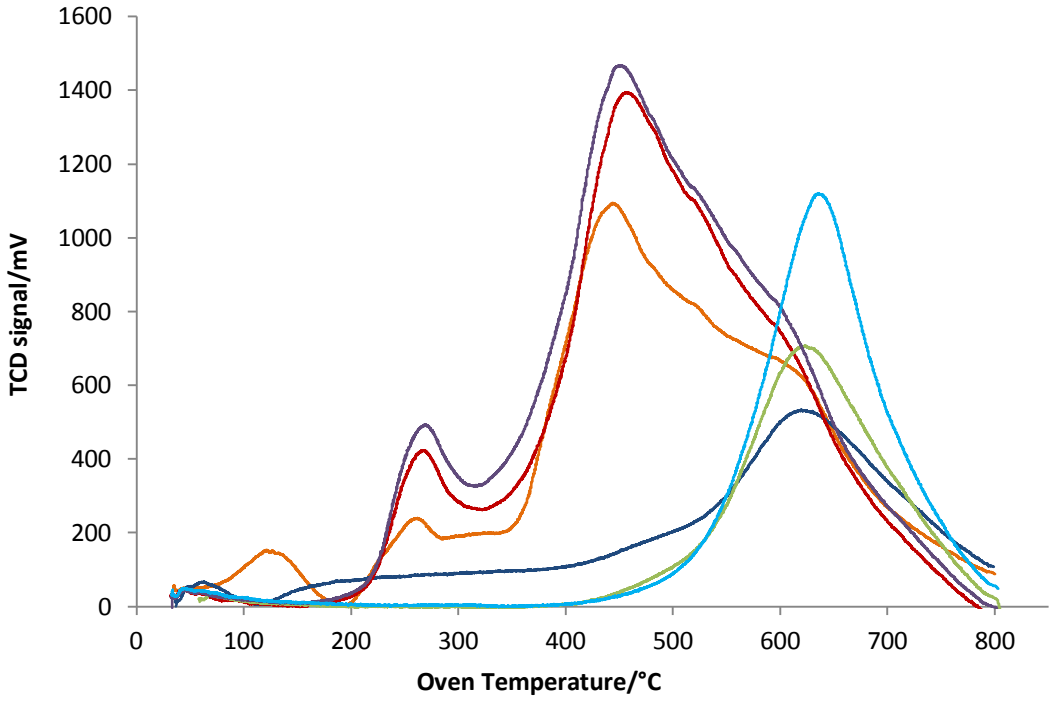

Figure 5.23: TPR profiles of a series of Au/C catalysts following sequential reduction/oxidation treatments: fresh (orange),R (dark blue), R/O (red), R/O/R (green), R/O/R/O (purple) and R/O/R/O/R (light blue).

In order to have a more accurate picture of this effect the samples were also analysed by XPS. The XPS spectra of the Au 4f region of these samples are shown in figure 5.24. It appears initially that all samples contain only metallic gold, with the doublet at the typical binding energies of 84 and 87.7 eV, however on closer inspection of the fresh and oxidised samples, a small amount of Au^{3+} is visible, at binding energies of 86.5 and 90.2 eV, this is shown in figure 5.25.

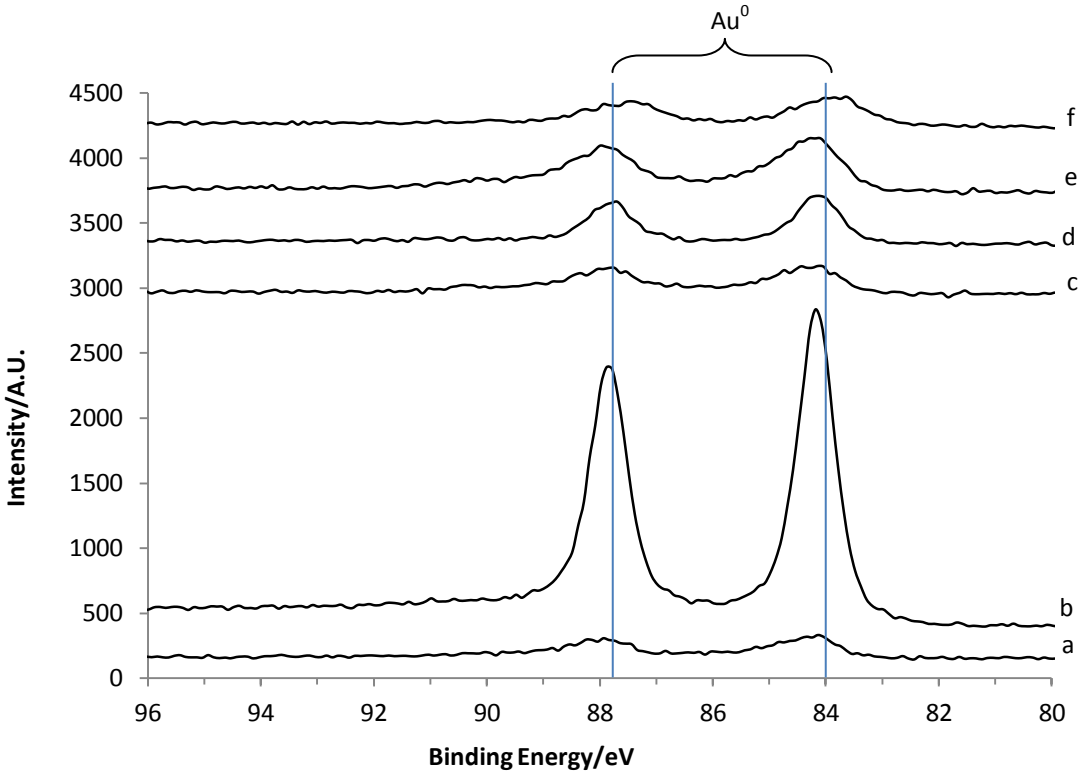

Figure 5.24: XPS spectra of Au/C catalysts, fresh and subjected to a sequence of oxidation and reduction treatments: a) fresh, b) R, c) RO, d) ROR, e) RORO, f) ROROR.

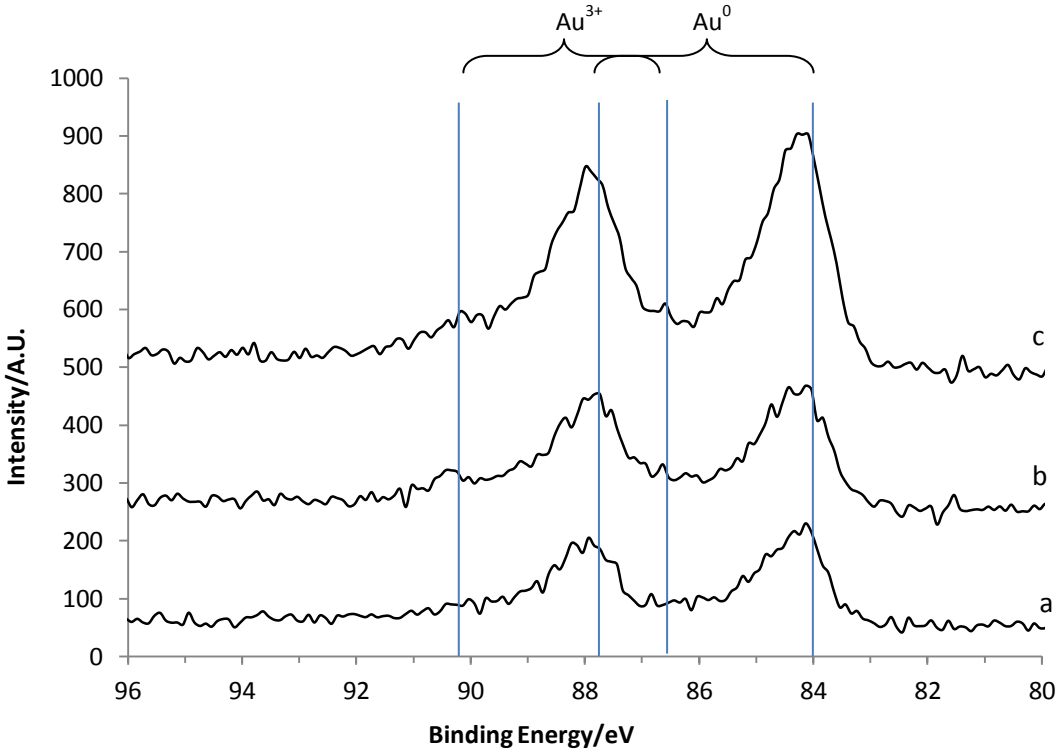

Figure 5.25: XPS spectrum of the Au4f region of the fresh catalyst and those after oxidation treatments: a) fresh, b) RO, c) RORO.

The XPS analysis correlates with the TPR profiles for these catalysts, showing that the oxidation treatments do oxidise metallic gold to Au^{3+}, although only a small amount. However, a fairly high activity of around 60% acetylene conversion is seen for these catalysts after 5h reaction time, although the initial activity is low and this does increase during the course of the reaction. These data are important because they show that despite the correlation between reduction/oxidation and activity, *i.e.* that the presence of Au^{3+} is important in order to have good activity, only a very small amount of Au^{3+} is sufficient. Therefore it is likely to be the dispersion and location of the Au^{3+} that is important in determining activity, rather than the presence of the species alone.

5.6 Conclusions

The aim of this chapter was to investigate the effect of oxidation and reduction treatments on Au/C catalysts, in an attempt to further the understanding of the source of the activity of these catalysts, with a view to improving the catalyst design. The premise of Au^{3+} being the most active site for the reaction is supported by the results obtained, with catalysts after oxidation treatments repeatedly showing higher activities for the acetylene hydrochlorination reaction and reduction treatments lowering the activity of the catalysts to a similar level as that observed from the carbon support alone. Presence of Au^{3+} after oxidation was confirmed by TPR and XPS analysis, whilst TPR also showed that the surface of the carbon support was oxidised.

In-situ oxidation by co-feeding NO in the reactor did not show a significant increase in catalytic activity as has been reported previously, although the theory that the NO oxidises the Au^0 to Au^{3+} has been confirmed by XPS. Treatment of catalysts pre-reaction by heating under a NO/N_2 gas flow also did not lead to any significant increase in their activity. Therefore although it has been successfully used before, *in-situ* oxidation of catalysts cannot be seen to be an effective method of enhancing catalyst activity using the current reactor design.

Oxidation treatments of catalysts outside of the reactor, however, have been shown to be an extremely effective way of enhancing catalyst activity. Treatment with cerium sulphate was particularly successful in increasing activity for this reaction, with approximately an additional 40% of acetylene conversion observed. Although whilst the oxidation of Au^{0} to Au^{3+} due to the treatment was observed, the effect of the residual cerium species on the catalyst is not fully known at this point. Simple treatments at room temperature with concentrated acids were able to regenerate the activity of catalysts which had been subjected to a reduction treatment, it was observed that this acid treatment had re-oxidised a small amount of gold to the 3+ oxidation state.

The results described in this chapter show that the presence of Au^{3+} is indeed important in order to have a good catalyst activity. However, as suggested in the previous chapter, the presence of Au^{3+} alone is not responsible for this activity, since catalysts with a very small amount of the oxidised species have displayed a higher activity than catalysts containing a larger amount of it. As observed again from the TPR, the reducibility of the oxidised species is also a key factor, with catalysts containing more easily reducible species giving higher activity. In addition, it could be that the location and dispersion of the oxidised species is important.

Another observation is that oxidation of the gold species is accompanied by oxidation of the carbon support, and the effect of this on activity is currently unknown. Since the carbon support itself shows some activity for acetylene hydrochlorination, its contribution to the overall catalyst activity merits further investigation. Likewise, the effect of the residual cerium on catalysts after oxidation treatment would be worth investigating in more detail as it may provide a route to a new, more active catalyst.

5.7 References

1. B. Nkosi, N. J. Coville, G. J. Hutchings, M. D. Adams, J. Friedl and F. E. Wagner, *J. Catal.*, 1991, **128**, 366-377.
2. B. Nkosi, M. D. Adams, N. J. Coville and G. J. Hutchings, *J. Catal.*, 1991, **128**, 378-386.
3. N. N. Greenwood and A. Earnshaw, *Chemistry of the Elements*, 2nd edn., Reed Educational and Professional Publishing Ltd, 1997.
4. M. Biswas, E. Dinda, M. H. Rashid and T. K. Mandal, *J. Colloid Interface Sci.*, 2012, **368**, 77-85.
5. J. A. Lopez-Sanchez, N. Dimitratos, C. Hammond, G. L. Brett, L. Kesavan, S. White, P. Miedziak, R. Tiruvalam, R. L. Jenkins, A. F. Carley, D. Knight, C. J. Kiely and G. J. Hutchings, *Nat. Chem.*, 2011, **3**, 551-556.
6. M. Conte, A. F. Carley, C. Heirene, D. J. Willock, P. Johnston, A. A. Herzing, C. J. Kiely and G. J. Hutchings, *J. Catal.*, 2007, **250**, 231-239.
7. A. F. Carley, P. R. Davies, G. J. Hutchings and M. S. Spencer, *Surface Chemistry and Catalysis*, Kluwer Academic/Plenum Publishers, 2002.
8. A. Ueda and M. Haruta, *Applied Catalysis B - Environmental*, 1998, **18**, 115-121.
9. Y. L. Zhang, R. W. Cattrall, I. D. McKelvie and S. D. Kolev, *Gold Bull.*, 2011, **44**, 145-153.
10. A. V. Bukhtiyarov, R. I. Kvon, A. V. Nartova, I. P. Prosvirin and V. I. Bukhtiyarov, *Surf. Sci.*, 2012, **606**, 559-563.
11. P. Serp and J. L. Figueiredo, *Carbon Materials for Catalysis*, Wiley, 2009.
12. E. N. Ndifor, T. Garcia, B. Solsona and S. H. Taylor, *Applied Catalysis B - Environmental*, 2007, **76**, 248-256.
13. G. J. Hutchings, *J. Catal.*, 1985, **96**, 292-295.
14. *CRC Handbook of Chemistry and Physics*, 77 edn., CRC Press, 1996-1997.
15. M. Conte, A. F. Carley and G. J. Hutchings, *Catal. Lett.*, 2008, **124**, 165-167.

6 Conclusions

6.1 Data obtained using the initial reactor set-up

Catalyst testing for acetylene hydrochlorination was initially carried out on a reactor set-up which used technical grade HCl. Under these conditions, testing of catalysts prepared by methods other than impregnation in acid gave unusual activity profiles: the initial activity increased steadily and then stabilised after around three hours reaction time. Most notably, the SI catalyst was actually more active than Au/C-JM after 3 hours of reaction due to the deactivation of the latter. Characterisation by XPS and XRD showed that the SI, DP and IMP catalysts contained only metallic gold, which is thought to be inactive for this reaction, and that there is some correlation between activity and Au particle size. Due to the corrosive nature of HCl in the presence of moisture, however, it was necessary to change to using electronic grade HCl, due to its higher purity and consequent lower moisture content.

During this initial testing phase, two key discoveries were made:

- The effect of the purity of reactant gases on the catalyst activity
- The activity of the activated carbon catalyst support

The use of higher purity HCl gas changed the activity of the Au/C-JM catalyst in two ways: there was an increase in % acetylene conversion and the steady deactivation during the course of the reaction was no longer observed. Comparison of the impurities in the HCl gases used led to the consideration that the difference in the hydrogen impurity was most likely to be the cause of the deactivation due to the possibility of it reducing the Au^{3+}, which has been shown to be the cause of deactivation at the reaction temperature used[1]. However, this cannot be the sole reason for the observed change in activity since an excess of hydrogen compared to the amount from the impurity was added to the reaction and whilst a lower activity was observed, the deactivation as observed previously did not occur. Changing the purity of the gas also affected the activity observed for catalysts prepared by other

methods, *i.e.* SI, DP and IMP, with a fairly steady level of conversion obtained compared to the previous initial increase and then stabilisation. The conversion at the end of the reaction time was similar in both cases for the SI catalyst, but significantly enhanced for the DP and IMP catalysts.

The activity of the carbon support alone was found to be around 10 – 15% acetylene conversion, which constitutes a significant contribution to the activity of the Au/C catalysts. The cause of this activity is not understood, although it is thought that it could be the result of trace metal impurities, which are often present in such materials, acting as a catalyst. Another possibility is that functional groups on the surface of the carbon may be active sites for the reaction. Activated carbon can be used as a catalyst for a number of reactions, for example the oxidative dehydrogenation of ethylbenzene (ODE), dehydration of alcohols, SOx and NOx oxidations and various hydrogen peroxide reactions, and it is often the surface functionality that is the source of the activity[2]. In fact it has been shown that for a Norit ROX 0.8 carbon catalyst, which is of the same type and supplier as the support used in this project, the active sites for the ODE reaction are carbonyl and quinone functional groups on the surface[3].

6.2 Chemistry of Aqua Regia and its influence in the preparation of Au/C Catalysts

Since catalysts prepared by the typical method of impregnation in acid were found to be the most active, the preparation method was investigated in some detail. The use of different acids (aqua regia, HCl and HNO_3) as impregnation solvent as well as variations in the drying temperature were found to affect the amount of gold present in the 3+ oxidation state, however it was found that this did not directly correlate with the observed activity, suggesting that perhaps formation of gold particles of sufficient size is necessary to provide the right chemical environment in order for the cationic gold to function as an active site. However, if the extent of the gold reduction is too

great i.e. larger gold particles are formed and further Au^{3+} is reduced, the activity is poor.

The aqua regia catalyst dried at 140°C was found to be the most active of all those tested, so catalysts dried at this temperature were investigated further. A series of catalysts was prepared using different HCl: HNO_3 ratios and it was found that mixtures of the two acids lead to catalysts containing more Au^{3+} than either acid individually – this is likely to be a result of the ability of HNO_3 to oxidise gold, forming Au^{3+} species, whilst the chloride present due to the HCl is able to stabilise them.

Although it has not been commonly used in previous work on this topic, TPR was used as a technique to investigate the reduction properties of Au/C catalysts, since this has been shown to be a key factor in the deactivation of catalysts used for acetylene hydrochlorination. A large amount of information was able to be obtained from this technique, about both the gold and the carbon support, including kinetic parameters for the reduction reactions taking place. These results enabled the reducibility of the Au^{3+} species to be highlighted as a factor in determining the activity of catalysts, which further supports the idea of a redox mechanism.

Analysis via a range of methods illustrated that the acid used in the impregnation modifies the surface of the carbon by creating oxygen containing functional groups, these were determined to be carboxylic acid and lactone groups. However, testing of catalysts which were prepared by impregnation in water on acid-treated carbons indicated that it is the effect of the acid on the gold, rather than the carbon surface, that is more important in determining a catalyst's activity.

6.3 The Significance of Au^{3+}: Oxidation and Reduction Treatments of Au/C Catalysts

A number of studies involving oxidation and reduction treatments of Au/C catalysts were carried out and the results provided further evidence that the presence of Au^{3+} is

required for catalysts to have good activity. Reduced catalysts consistently showed a low activity of around 10% acetylene conversion, comparable to that of the support alone, while simple oxidation treatments with concentrated acids were able to regenerate the previously observed activity. Characterisation by XPS and TPR correlated this activity with the presence of Au^{3+}. However, these treatments also oxidised the carbon surface leading to the presence of oxygen containing functional groups. The effect of such groups on activity has not been investigated in detail, although results from the previous chapter suggest that the effect of the acid on the gold rather than the carbon is more significant during the catalyst preparation so it is reasonable that the same would apply in this case.

Oxidation using cerium (IV) sulphate was also found to be an effective way of enhancing catalyst activity, with characterisation by TPR and XPS suggesting that this is likely to be due to an increase in the reducibility of the Au^{3+}. However, the presence of residual cerium species on the catalyst surface was also detected and the effect of this is as yet unknown.

Oxidation of a catalyst *in-situ* by addition of NO to the reaction, however, did not prove successful, neither did exposure of a catalyst to NO prior to reaction, despite NO being reported to regenerate catalyst activity previously[4]. XPS studies were able to show that exposure to NO did in fact increase the amount of Au^{3+} present on a catalyst surface, however, it could be that this Au^{3+} is not in the right location to be an active site, as the other results obtained and discussed here suggest is necessary.

6.4 Summary

Overall, it has been demonstrated that the previously stated theory of Au^{3+} being the active site for Au/C catalysed acetylene hydrochlorination holds true. The use of aqua regia in catalyst preparation is thought to produce the best catalysts due to the combination of the oxidation properties of HNO_3 with the ability of chloride supplied by the HCl to stabilise the cationic species. However, it is not a simple relationship

whereby a catalyst which contains a greater amount of this species is more active. Indeed, catalysts in which the majority of the gold (65%) was found to be in the 3+ oxidation state were less active than others in which it was only around 40%. Extensive characterisation by TPR has suggested that the reducibility of the Au^{3+} is also a key factor governing the activity, indicating that the location of the Au^{3+} on gold nanoparticles, rather than merely its presence, is important. The carbon support is also of significance, as it has been shown to be active itself, with around 10% conversion observed.

The sensitivity of this reaction to the reactor set-up used has also been demonstrated, with an increase in the purity of a reactant gas leading to a great difference in the results obtained. In addition, reproduction of previously published work has been attempted with different results obtained, this may be in some part due to differences between the reactors and methods used.

6.5 Future Work

The work done in this project could be continued in a number of ways, in order to provide further insight into the activity of Au/C catalysts for acetylene hydrochlorination:

6.5.1 Chapter 3

The underlying cause of the difference in activity observed using different purities of HCl gas was not determined. Whilst hydrogen is likely to contribute to the effect, due to its reducing nature, adding an excess relative to the original impurity back into the reactant gas stream did not reverse the changes as might be expected. However, TPR characterisation of catalysts shows that reduction of Au^{3+} in hydrogen occurs at temperatures of around 250 – 300°C, supporting the idea that it is not the hydrogen that is responsible for the changes observed. Other significant differences in impurities were oxygen and moisture; whilst the effect of moisture is not suitable for

investigation due to the corrosive nature of HCl in the presence of water, the effect of oxygen could be investigated, for example by replacing the nitrogen diluent with air. Also of note is that the nitrogen used as a diluent was not of as high a purity as the other gases used, and although molecular sieve traps were used to eliminate as much moisture as possible, the effect of these potential impurities is unknown and could be of interest, given that the amount used is greater than that of the HCl.

The source of the activity of the carbon support is also uncertain; experiments could be carried out to ascertain this, for example by acid washing to remove metal impurities which may be acting as a catalyst, or by treating the carbon in a number of other ways to modify the surface functionalities present which may also have an effect.

6.5.2 Chapter 4

Whilst a combination of XPS, XRD and TPR have been useful tools for characterising Au/C catalysts in terms of the amount of Au^{3+} present and relative gold particle sizes on different catalysts, utilising microscopic techniques such as TEM could also provide valuable information. Since it has been shown that not only the presence of Au^{3+} is important, but also its location, it would be of great interest to investigate the particle size, shape and dispersion in more detail, and this would be achievable using such techniques.

A number of alternative solvents were used in the catalyst preparation by impregnation, none of which gave a catalyst with activity as good as that obtained by HNO_3/HCl/*aqua regia*. However, it is thought that it is the contribution of oxidising and stabilising properties of the nitric and hydrochloric acids that lead to sufficient amounts of Au^{3+}, so it could be of interest to experiment with combinations of these solvents to see if the amount or reducibility of the Au^{3+} may be improved, for example by using different oxidising agents or sources of chloride.

The effect of the acids on the carbon surface was investigated, however, whilst it was shown that the effect of the acid on the gold is more important in determining a catalyst's activity, the effect of the carbon surface functional groups on activity was not investigated. The different acid treated carbons could be tested for comparison with the untreated carbon, this also ties in with further investigations to determine the source of the carbon's activity as mentioned for the previous chapter.

6.5.3 Chapter 5

The treatment of a catalyst with cerium sulphate led to a significant enhancement of its activity, with approximately an additional 40% acetylene conversion observed. Since this was the most effective of any of the treatments, it warrants further investigation. From the results presented it appears that the enhancement may be due to the treatment facilitating reduction of the cationic gold species, as observed by TPR analysis. In addition, for catalysts where no cationic gold was observable prior to the treatment, it was detectable after indicating that the oxidation treatment can generate Au^{3+}. Unfortunately these catalysts were unable to be tested so it would be of interest to do so, in order to ascertain the activity of the Au^{3+} created by the cerium sulphate treatment. However, it is also clear that there is some residual cerium present on the catalyst surface after treatment and as yet the contribution of this to the observed effect is unknown. It has been shown that when ceria, CeO_2, is used as a support for Au catalysts prepared by sol immobilisation, cationic gold species are present on the surface and these catalysts have an enhanced selectivity in liquid phase oxidation reactions[5]. If, as suggested, the ceria is capable of stabilising the Au^{3+} it could be interesting to test Au/CeO_2 catalysts for acetylene hydrochlorination. Furthermore, similar observations have been made for Au/La_2O_3 materials, which were also shown to stabilise cationic gold[6] so investigating other similar (i.e. lanthanide series) metal oxide supports may be of interest.

In addition, Au/C catalysts such as those used in this project could be investigated for other alkyne substrates, for example phenylacetylene, with a view to use in the fine

chemicals industry. Other types of substrates could also be investigated, for example catalytic hydrochlorination of glycerol to produce dichloropropanols is of interest[7] and Au/C catalysts are able to catalyse other glycerol oxidation reactions[8].

6.6 References

1. B. Nkosi, N. J. Coville, G. J. Hutchings, M. D. Adams, J. Friedl and F. E. Wagner, *J. Catal.*, 1991, **128**, 366-377.
2. P. Serp and J. L. Figueiredo, *Carbon Materials for Catalysis*, Wiley, 2009.
3. M. F. R. Pereira, J. J. M. Órfão and J. L. Figueiredo, *Appl. Catal. A:Gen.*, 1999, **184**, 153-160.
4. B. Nkosi, M. D. Adams, N. J. Coville and G. J. Hutchings, *J. Catal.*, 1991, **128**, 378-386.
5. G. L. Brett, P. J. Miedziak, N. Dimitratos, J. A. Lopez-Sanchez, N. F. Dummer, R. Tiruvalam, C. J. Kiely, D. W. Knight, S. H. Taylor, D. J. Morgan, A. F. Carleya and G. J. Hutchings, *Cat. Sci. Tech.*, 2012, **2**, 97-104.
6. A. Goguet, M. Ace, Y. Saih, J. Sa, J. Kavanagh and C. Hardacre, *Chem. Commun.*, 2009, 4889-4891.
7. W. M. Pazdzioch and E. Milchert, *Oxid. Commun.*, 2010, **33**, 132-146.
8. M. Sankar, N. Dimitratos, D. W. Knight, A. F. Carley, R. Tiruvalam, C. J. Kiely, D. Thomas and G. J. Hutchings, *ChemSusChem*, 2009, **2**, 1145-1151.

Appendix 1: TPR data for determination of activation energy of Au^{3+} reduction

The catalysts for which activation energy was determined using the Kissinger method as described in Chapter 2 are:

- Impregnation in HCl, dried at 110, 140, 185°C
- Impregnation in HNO_3, dried at 110, 140, 185°C
- Impregnation in aqua regia, dried at 110, 140, 185°C
- Impregnation in aqua regia, dried at 110°C, after oxidation treatment using $Ce(SO_4)_2$
- Catalyst provided by Johnson Matthey, M07565

All of the above are 1% Au/C. The TPR profiles used and Kissinger plots obtained are shown below, with the exception of the JM catalyst as this data can be found as an example in Chapter 3.

Impregnation in HCl

Drying Temperature 110°C

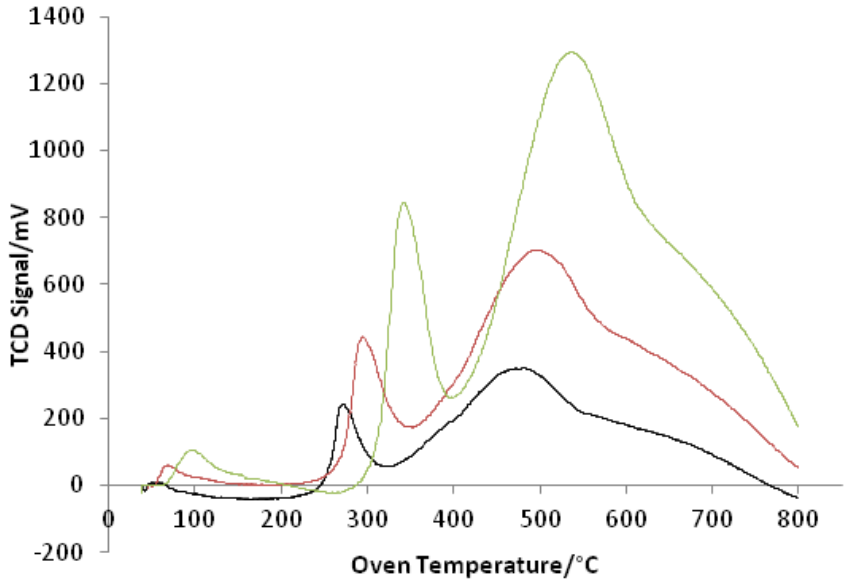

Figure 26: TPR profiles run at heating ramps of 5 (black), 10 (red) and 20 (green) °C/min.

Ramp rate (β)	Temperature of peak max./°C	Temperature of peak max./K (T)	ln (β/T^2)	1/T
5	272	545	-10.99	0.001835
10	295	568	-10.38	0.001761
20	343	616	-9.85	0.001623

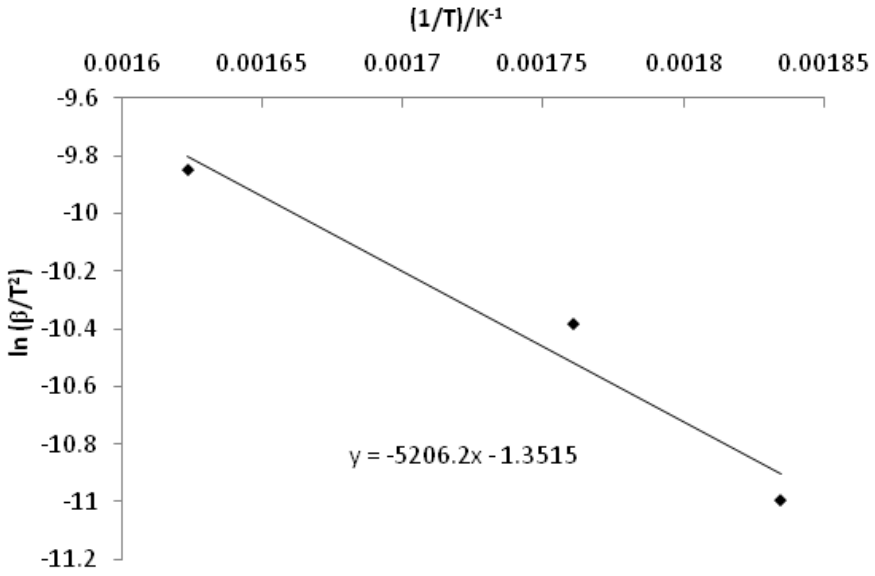

Figure 27: Kissinger plot for catalyst prepared by impregnation in HCl, dried at 110°C.

Gradient = -5206.2 = $-E_a/R$ $\therefore$ E_a = 43284 J/mol

Intercept = -1.3515 = ln (AR/E_a) $\therefore$ A = 1347.6

Drying Temperature 140°C

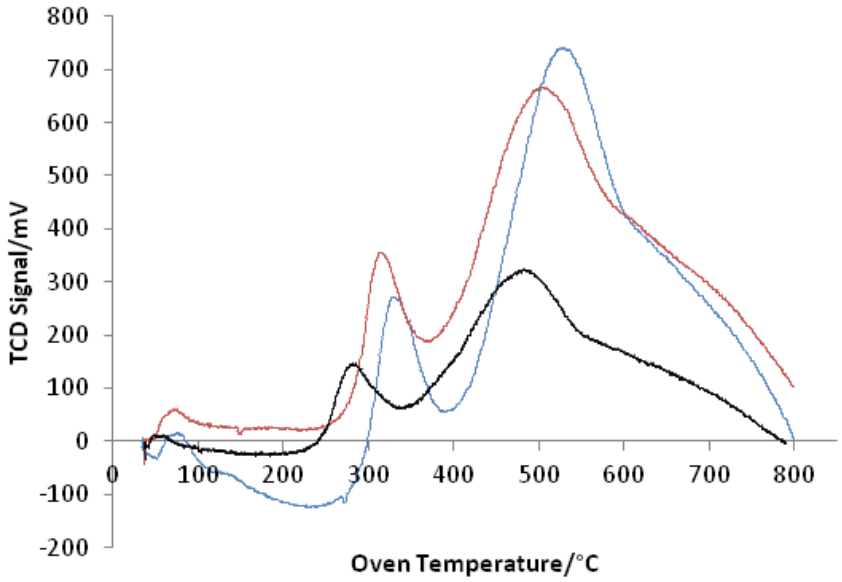

Figure 28: TPR profiles run at heating ramps of 5 (black), 10 (red) and 15 (blue) °C/min.

Ramp rate (β)	Temperature of peak max./°C	Temperature of peak max./K (T)	ln (β/T²)	1/T
5	281	554	-11.02	0.001805
10	314	587	-10.45	0.001704
15	328	601	-10.09	0.001664

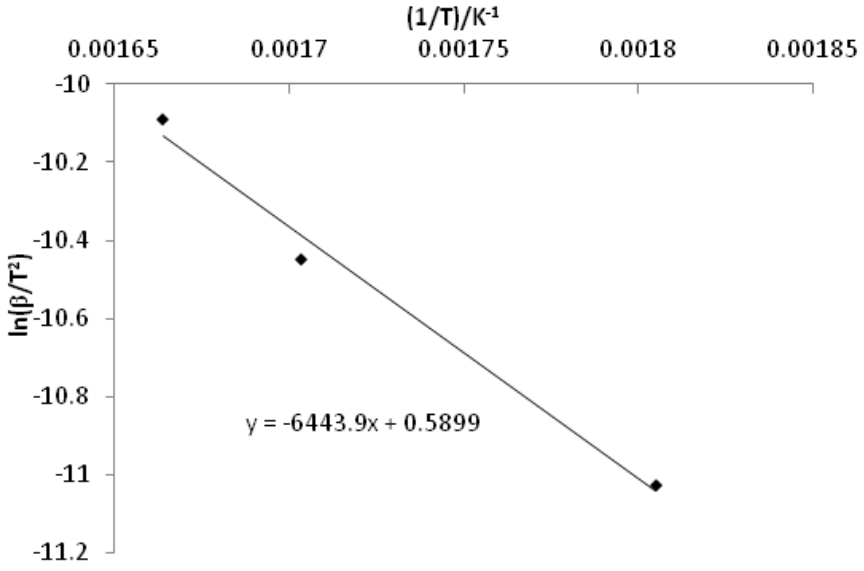

Figure 29: Kissinger plot for catalyst prepared by impregnation in HCl, dried at 140°C.

Gradient = -6443.9 = $-E_a/R$ ∴ E_a = 53575 J/mol

Intercept = 0.5899 = ln (AR/E_a) ∴ A = 11624

Drying Temperature 185°C

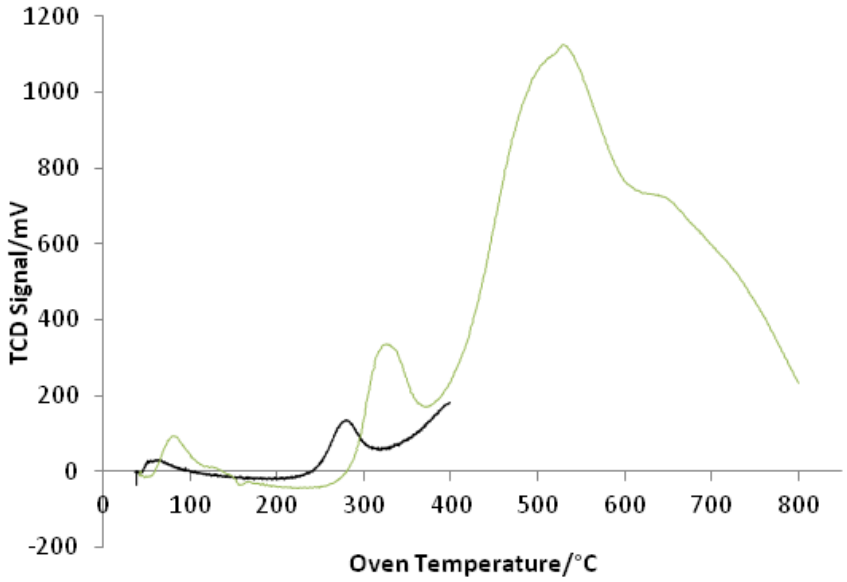

Figure 30: TPR profiles run at heating ramps of 5 (black) and 20 (green) °C/min.

Ramp rate (β)	Temperature of peak max./°C	Temperature of peak max./K (T)	ln (β/T^2)	1/T
5	280	553	-11.02	0.001808
20	327	600	-9.80	0.001667

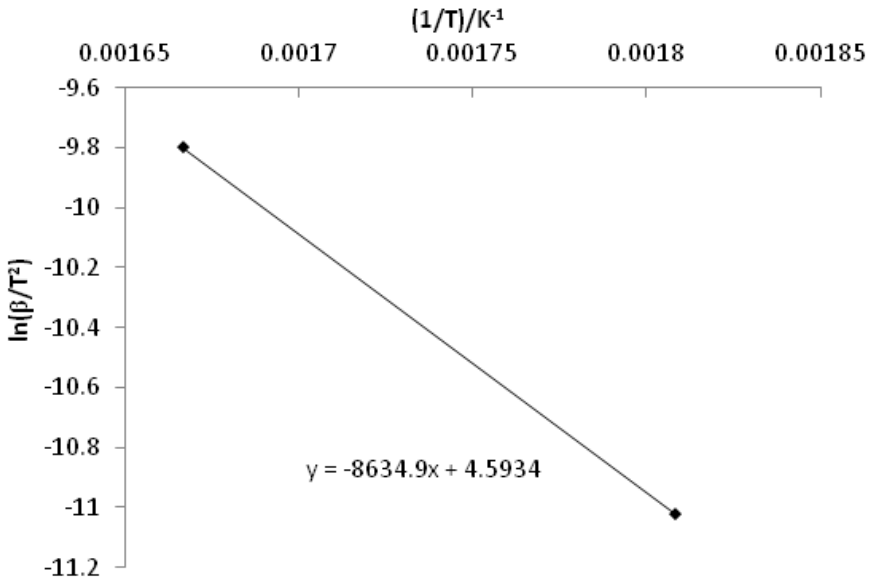

Figure 31: Kissinger plot for catalyst prepared by impregnation in HCl, dried at 185°C.

Gradient = -8634.9 = $-E_a/R$ ∴ E_a = 71791 J/mol

Intercept = 4.5934 = ln (AR/E_a) ∴ A = 853390

Impregnation in HNO_3

Drying Temperature 110°C

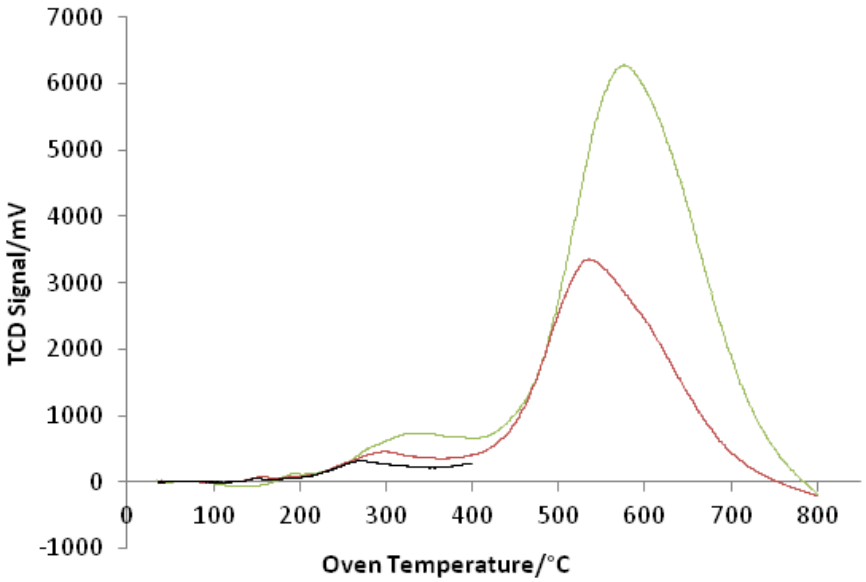

Figure 32: TPR profiles run at heating ramps of 5 (black), 10 (red) and 20 (green) °C/min.

Ramp rate (β)	Temperature of peak max./°C	Temperature of peak max./K (T)	ln (β/T^2)	1/T
5	271	544	-10.99	0.001838
10	300	573	-10.40	0.001745
20	344	617	-9.85	0.001621

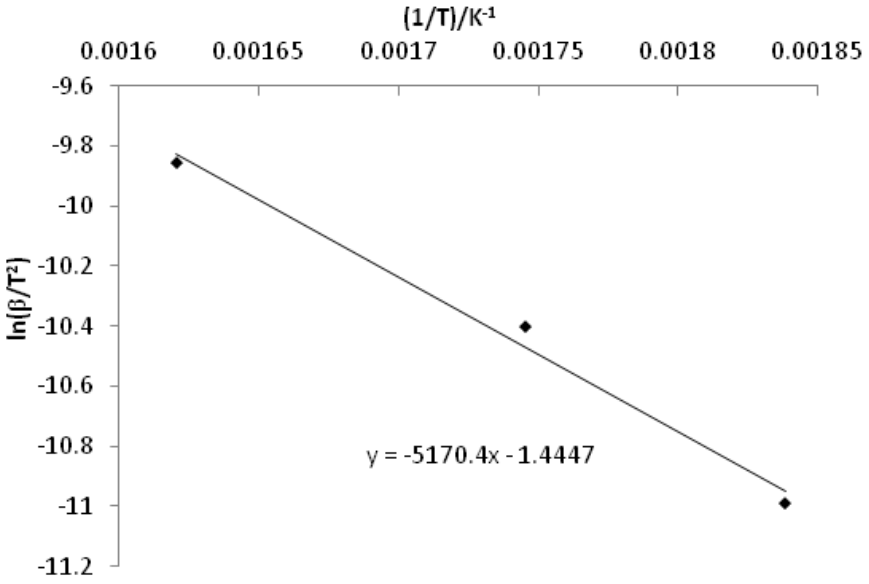

Figure 33: Kissinger plot for catalyst prepared by impregnation in HNO_3, dried at 110°C.

Gradient = -5170.4 = $-E_a/R$ ∴ E_a = 42986.71 J/mol

Intercept = -1.4447 = ln (AR/E_a) ∴ A = 1219.267

Drying Temperature 140°C

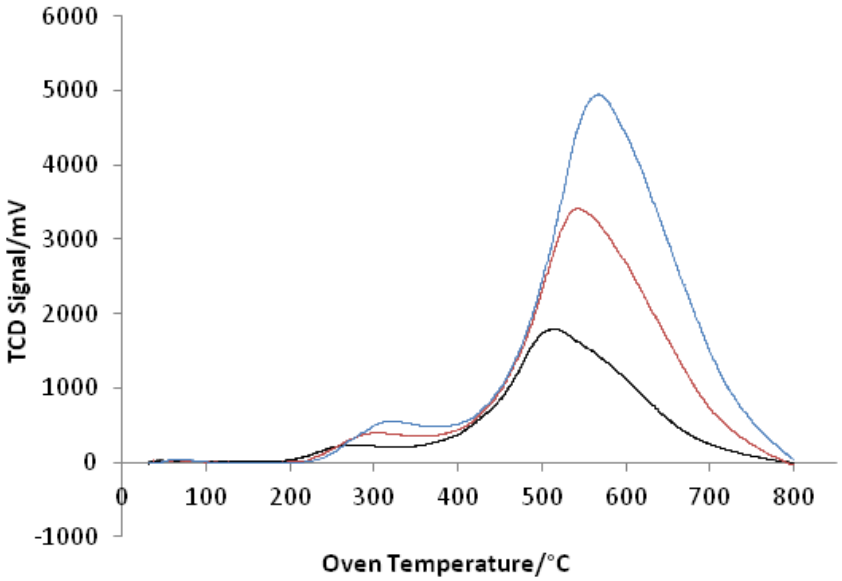

Figure 34: TPR profiles run at heating ramps of 5 (black), 10 (red) and 15(blue) °C/min.

Ramp rate (β)	Temperature of peak max./°C	Temperature of peak max./K (T)	ln (β/T^2)	1/T
5	275	548	-11.00	0.001825
10	302	575	-10.41	0.001739
15	322	595	-10.07	0.001681

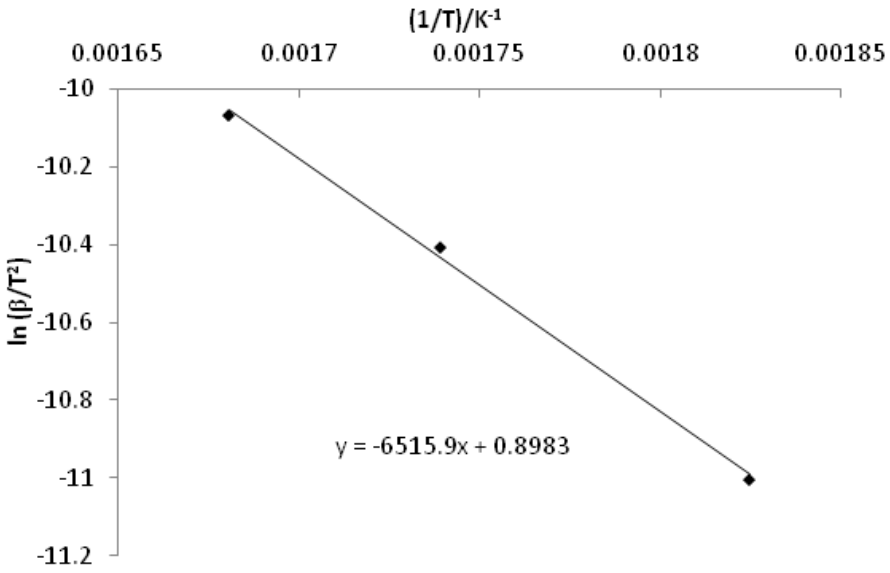

Figure 35: Kissinger plot for catalyst prepared by impregnation in HNO_3, dried at 140°C.

Gradient = -6515.9= $-E_a/R$ ∴ E_a = 54173.19 J/mol

Intercept = 0.8983 = ln (AR/E_a) ∴ A = 15999.31

Drying Temperature 185°C

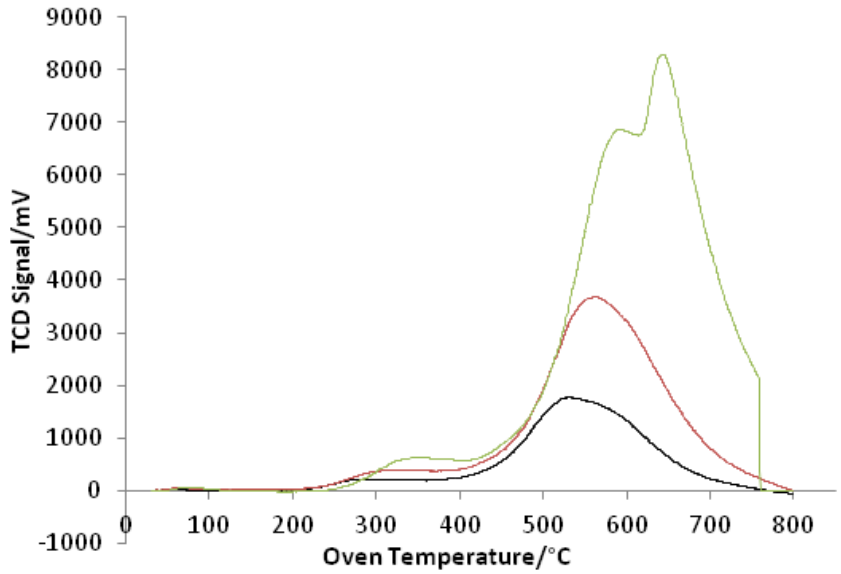

Figure 36: TPR profiles run at heating ramps of 5 (black), 10 (red) and 20 (green) °C/min.

Ramp rate (β)	Temperature of peak max./°C	Temperature of peak max./K (T)	ln (β/T^2)	1/T
5	278	551	-11.01	0.001815
10	316	589	-10.45	0.001698
20	350	623	-9.87	0.001605

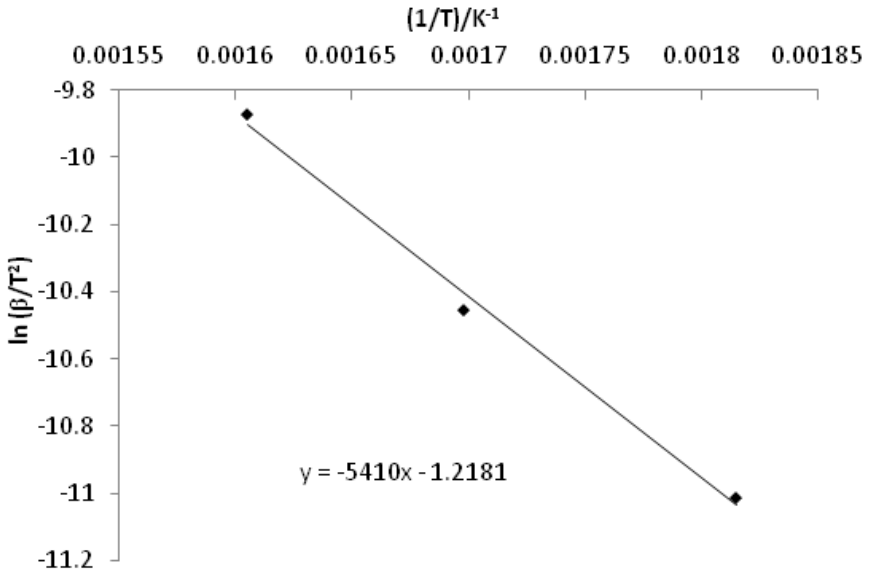

Figure 37: Kissinger plot for catalyst prepared by impregnation in HNO_3, dried at 185°C.

Gradient = -5410 = $-E_a/R$ ∴ E_a = 44978.74 J/mol

Intercept = -1.2181 = ln (AR/E_a) ∴ A = 1600.233

Impregnation in Aqua Regia

Drying Temperature 110°C

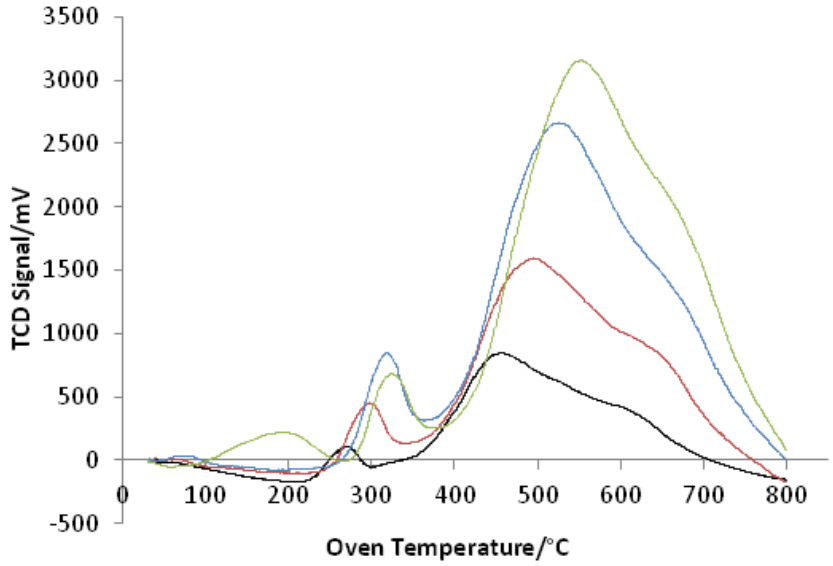

Figure 38: TPR profiles run at heating ramps of 5 (black), 10 (red), 15 (blue) and 20(green) °C/min.

Ramp rate (β)	Temperature of peak max./°C	Temperature of peak max./K (T)	ln (β/T^2)	1/T
5	270	543	-10.98	0.001842
10	300	573	-10.40	0.001745
20	324	597	-9.79	0.001675
15	318	591	-10.06	0.001692

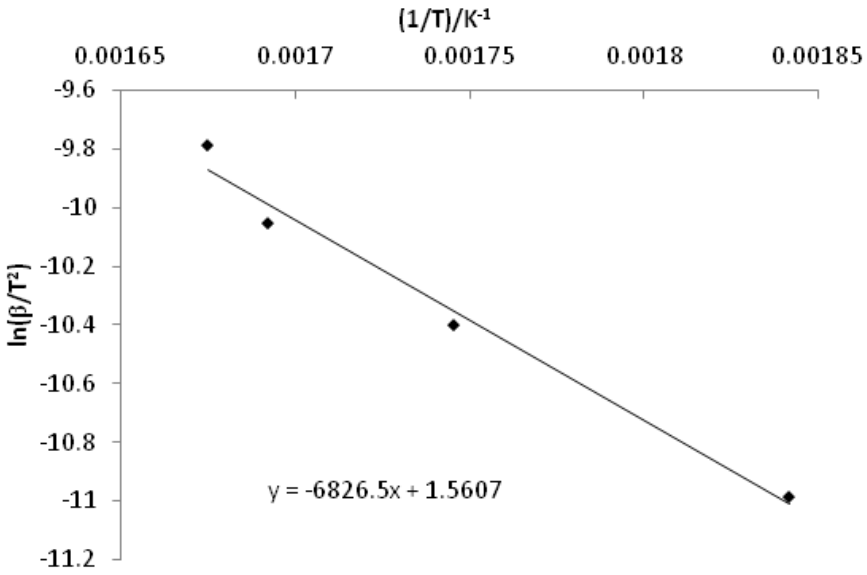

Figure 39: Kissinger plot for catalyst prepared by impregnation in aqua regia, dried at 110°C.

Gradient = -6826.5 = $-E_a/R$ ∴ E_a = 56755.521 J/mol

Intercept = 1.5607 = ln (AR/E_a) ∴ A = 32508.84

Drying Temperature 110°C, Cerium (IV) Sulphate treated

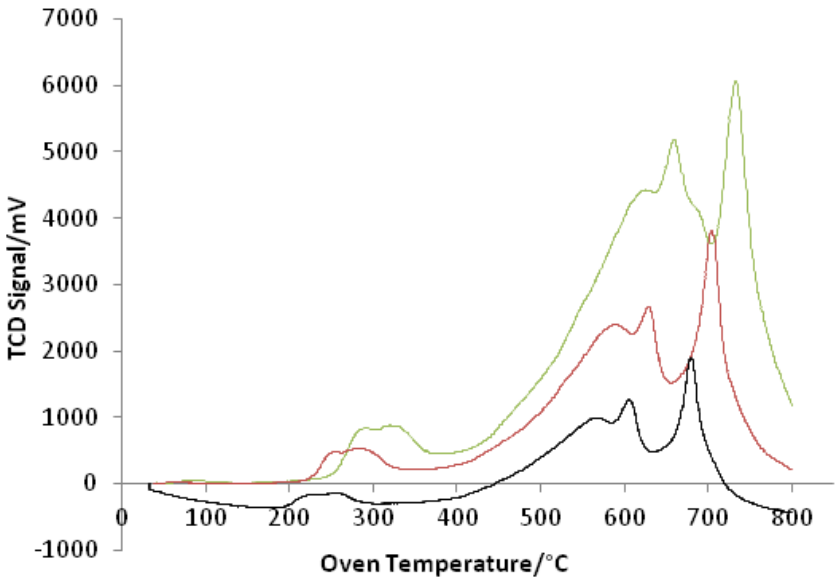

Figure 40: TPR profiles run at heating ramps of 5 (black), 10 (red) and 20 (green) °C/min.

Ramp rate (β)	Temperature of peak max./°C	Temperature of peak max./K (T)	ln ($β/T^2$)	1/T
5	258	531	-10.94	0.001883
10	284	557	-10.34	0.001795
20	321	594	-9.78	0.001684

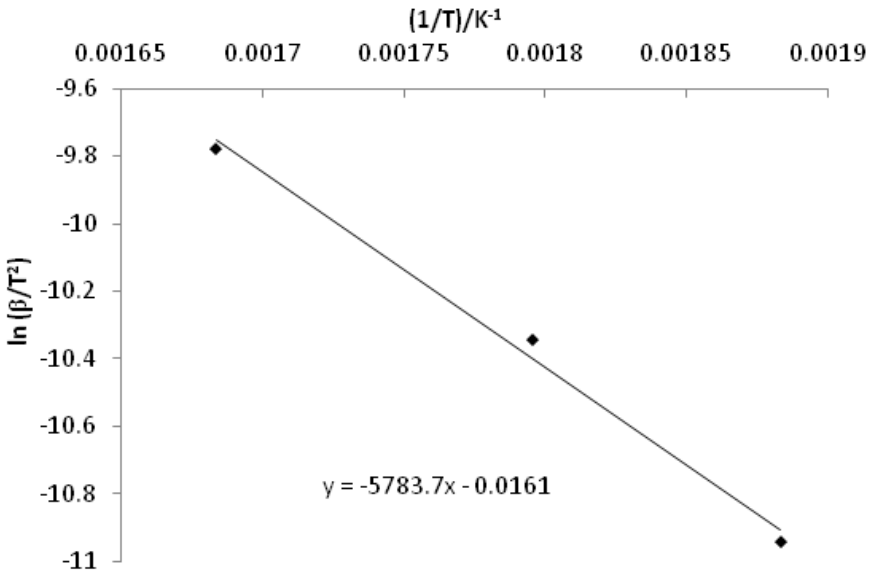

Figure 41: Kissinger plot for catalyst prepared by impregnation in aqua regia, dried at 110°C, treated with cerium sulphate.

Gradient = -5783.7 = $-E_a/R$ ∴ E_a = 48085.68 J/mol

Intercept = -0.0161 = ln (AR/E_a) ∴ A = 5691.328

Drying Temperature 140°C

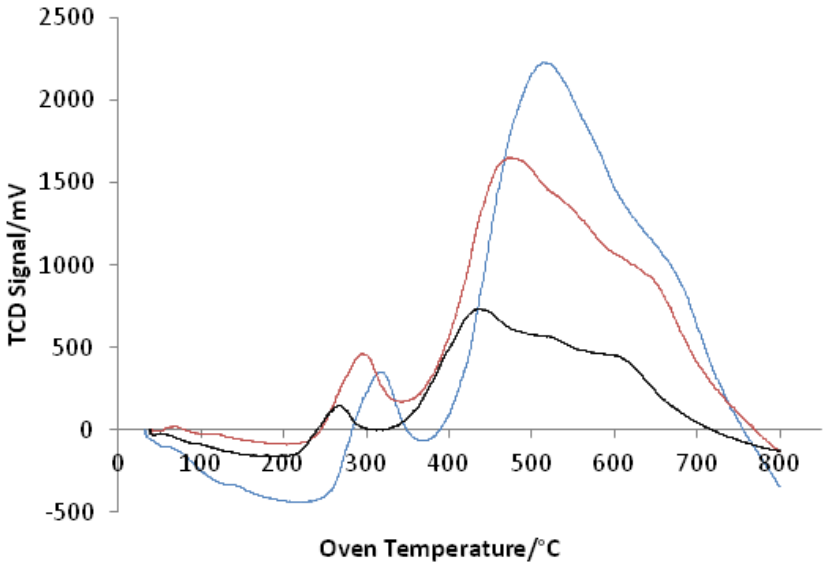

Figure 42: TPR profiles run at heating ramps of 5 (black), 10 (red) and 15 (blue) °C/min.

Ramp rate (β)	Temperature of peak max./°C	Temperature of peak max./K (T)	ln (β/T^2)	1/T
5	268	541	-10.9774	0.001848
10	296	569	-10.3852	0.001757
15	317	590	-10.0522	0.001695

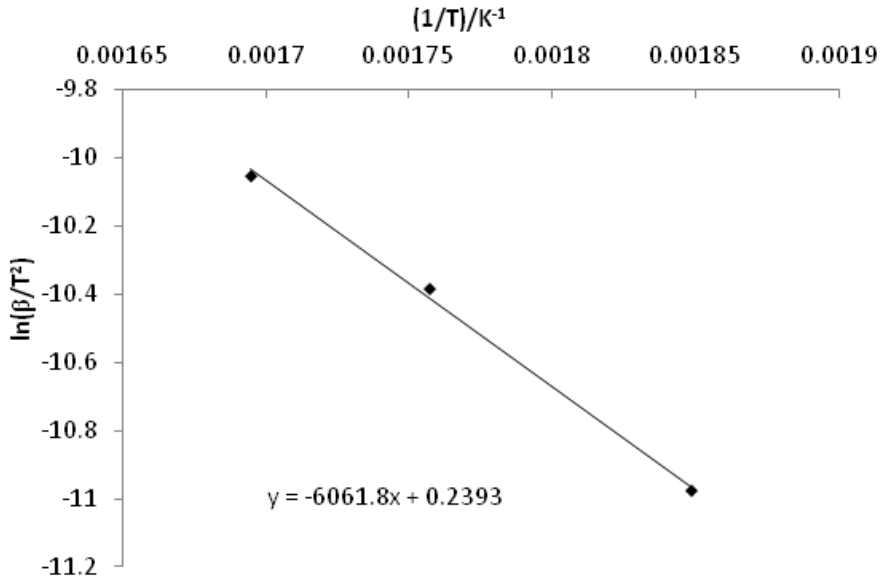

Figure 43: Kissinger plot for catalyst prepared by impregnation in aqua regia, dried at 140°C.

Gradient = -6061.8 = $-E_a/R$ ∴ E_a = 50397.81 J/mol

Intercept = 0.2393 = ln (AR/E_a) ∴ A = 7700.666

Drying Temperature 185°C

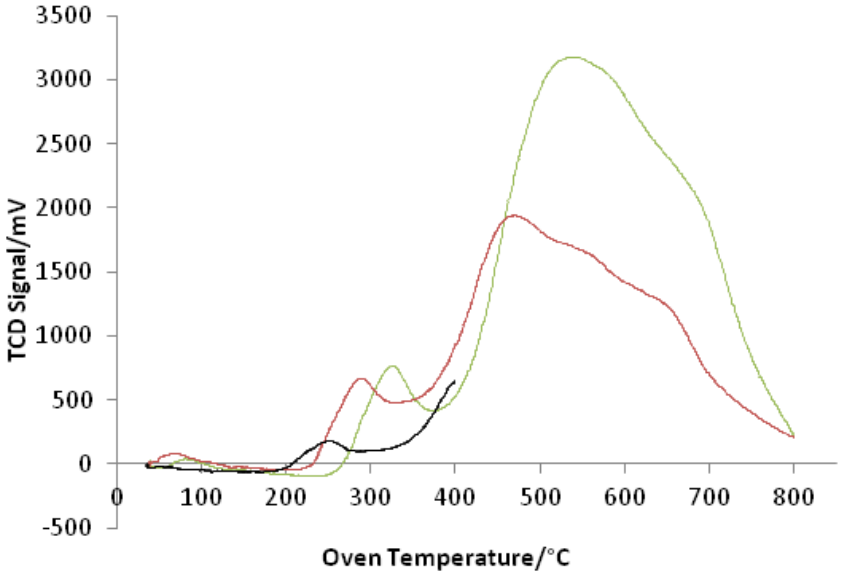

Figure 44: TPR profiles run at heating ramps of 5 (black), 10 (red) and 20(green) °C/min.

Ramp rate (β)	Temperature of peak max./°C	Temperature of peak max./K (T)	ln (β/T^2)	1/T
5	252	525	-10.9174	0.001905
10	288	561	-10.3569	0.001783
20	326	599	-9.79479	0.001669

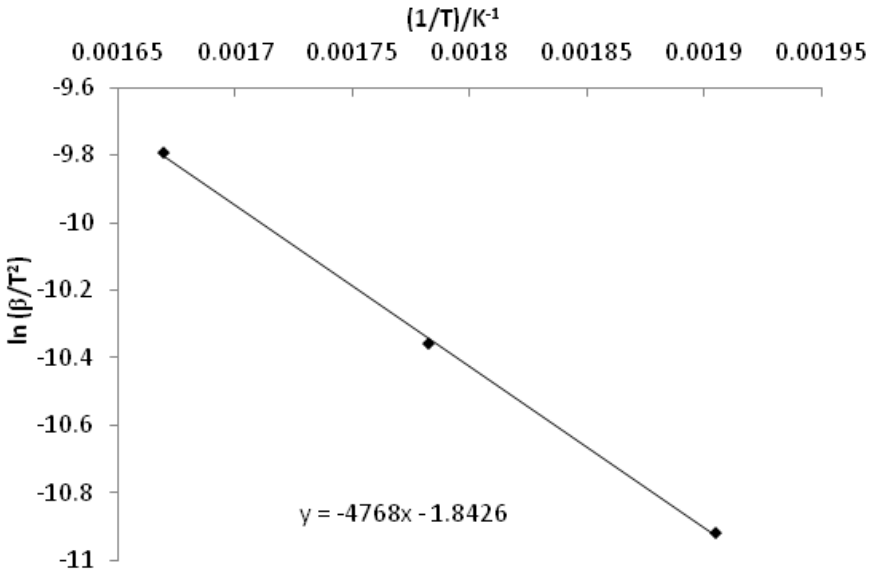

Figure 45: Kissinger plot for catalyst prepared by impregnation in aqua regia, dried at 185°C.

Gradient = -4768 = $-E_a/R$ $\therefore$ E_a = 39641.15 J/mol

Intercept = -1.8426 = ln (AR/E_a) $\therefore$ A = 755.2752